KATHARINA HOLSTEIN

MULTISITE PHOSPHORYLATION IN (BIO-) CHEMICAL REACTION NETWORKS: MULTISTATIONARITY AND ROBUSTNESS

MULTISITE PHOSPHORYLATION IN (BIO-) CHEMICAL REACTION NETWORKS: MULTISTATIONARITY AND ROBUSTNESS

Dissertation

zur Erlangung des akademischen Grades

Doktoringenieurin (Dr.-Ing.)

von Dipl.-Ing. Katharina Holstein

geb. am 30. Januar 1984 in Burg
genehmigt durch die
Fakultät für Elektro- und Informationstechnik
der
Otto-von-Guericke-Universität Magdeburg

Gutachter: Prof. Dr. rer. nat. Dietrich Flockerzi
Prof. Dr.-Ing. Rolf Findeisen
Prof. Dr.-Ing. Jörg Raisch

Promotionskolloqium am: 17. Juni 2014

To my mother.

Don't sacrifice your dreams for the illusion of security.
There is no security.
Realize there is no security
and become comfortable with that.
It will free you up to do what you really need to do.

— David Mack

ABSTRACT

The topic of multistationarity in multisite phosphorylation networks is exploited in this thesis. A distributive, sequential phosphorylation network with n phosphorylation sites is introduced and extended by several different network setups. Multistationarity is established for the distributive, sequential network setup and $n \geqslant 2$. For extended network setups including synthesis and degradation of the enzymes and the (phosphorylated) protein in various forms multistationarity is established for two phosphorylation steps. For network setups allowing compartmentalization, i. e., two phosphorylation networks of size n with distinct transport reactions being coupled, multistationarity can be established under certain restrictions for arbitrary $n \geqslant 2$. Furthermore, a parametrization of the multistationarity region for the n-times distributive, sequential phosphorylation network is provided and analyzed. A random walk is applied to the distributive, sequential phosphorylation network to test the robustness towards parameter variations of the multiple steady states in parameter space.

ZUSAMMENFASSUNG

Die vorliegende Promotion betrachtet das Thema mehrfach stationärer Zustände in distributiven, sequentiellen Phosphorylierungsnetzwerken mit n Phosphorylierungsstufen. Netzwerke unterschiedlicher Komplexität werden analysiert. Mehrfach stationäre Ruhelagen können für ein distributives, sequentielles n-fach Phosphorylierungsnetzwerk und $n \geqslant 2$ nachgewiesen werden und eine Parametrisierung der mehrfach stationären Ruhelagen erfolgt. Für Phosphorylierungsnetzwerke, die auch Auf- und Abbau von (phosphorylierten) Proteinen und Enzymen erlauben, werden mehrfach stationäre Ruhelagen für $n = 2$ nachgewiesen. Durch das Koppeln zweier n-fach Phosphorylierungsnetzwerke mit Transportreaktionen zwischen diesen beiden Netzerken wird ein Reaktionsnetzwerk auf Basis von Kompartmentalisierung erzeugt. Für dieses kann für $n \geqslant 2$ und unter bestimmten Voraussetzungen Mehrfachstationarität nachgewiesen und eine Parametrisierung der Ruhelagen angegeben werden. Weiterhin wird die Robustheit des distributiven, sequentiellen n-fach Phosphorylierungsnetzwerkes in seiner einfachsten Form untersucht.

PUBLICATIONS

Some ideas and figures have been published previously or are on their way to publication in:

[P1] K. Holstein, D. Flockerzi, and C. Conradi: Multistationarity in Sequential Distributed Multisite Phosphorylation Networks, *Bulletin of Mathematical Biology*, 75(11):2028–2058, published November 2013

[P2] D. Flockerzi, K. Holstein, and C. Conradi: N-site phosphorylation systems with $2N - 1$ steady states, *Bulletin of Mathematical Biology*, accepted June 2014

[P3] K. Holstein, D. Flockerzi, and C. Conradi: State and Parameter Regions of Multistationarity in Multisite Phosphorylation Networks, *Journal of Computational Biology*, in preparation

[P4] C. Conradi, K. Holstein, and D. Flockerzi: Multistationarity in mass-action networks by degree two polynomial inequalities, *Journal of Mathematical Biology*, in preparation

[P5] K. Holstein, D. Flockerzi, and C. Conradi: Double Phosphorylation of Proteins with Synthesis and Degradation: Existence of Multistationarity, *Plos Computational Biology*, in preparation

[P6] K. Holstein, D. Flockerzi, and C. Conradi: Bistability and Compartmentalization Can Induce Oscillations, *Journal of Theoretical Biology*, in preparation

Additionally, the following publication is a result of this thesis:

[P7] V. Ssemaganda, K. Holstein, and G. Warnecke: Uniqueness of steady-state solutions for thermodynamically consistent Becker-Döring models. *Journal of Mathematical Physics*, 52 (8): 1–28, 2011

Parts of [P5] have been presented at:

[S1] K. Holstein, D. Flockerzi, and C. Conradi: Multistationarity in Double Phosphorylation Networks with Protein Synthesis and Degradation, *International Symposium on Mathematical Theory of Networks and Systems*, Melbourne, Australia, July 2012

You need to believe in things that aren't true –
how else can they become?

— Terry Pratchett

ACKNOWLEDGMENTS

A thesis is not only the sum of thoughts of several years fixed on paper. It also reflects the ideas, support and encouragement of various people.

Foremost, I like to thank my advisory Prof. Dr. Dietrich Flockerzi, who had always time for the strangest questions, found answers to those and is a source of constant inspiration.

Besides him, I like to thank Dr. Carsten Conradi who supervised me already during the time of my diploma thesis and made this thesis possible at all.

Thanks goes also to Prof. Dr. Jörg Raisch and Prof. Dr. Rolf Findeisen for letting me finish this thesis at the university of Magdeburg.

To reflect on the encouragement, I thank all members of the lab S3.18 (at various points in time) for time, support, discussions, coffee breaks and a cake-lovers friendly environment: Boris, Robert, Berni, Anke and Phil. But also Andi, Janine, Maayan and Astrid as noninhabitants of the office but also part of this community. I'd also like to thank my diligent proof readers: Astrid and Boris (from above) and, from a different spatial list of friends, my most favorite ex-roommate Günni and my most favorite Canadian Dave.

For his love and support till the very end (and only thus rendering this work possible) I'd like to thank my Steintülling André.

But most of all, I'd like to thank my father: obwohl du vermutlich wenig von dem lesen wirst, was in dieser Arbeit geschrieben steht, so hast du sie erst durch deine konstante Unterstützung, Weisheit und Zuversicht ermöglicht. Danke.

CONTENTS

LIST OF FIGURES

LIST OF TABLES

LIST OF ABBREVIATIONS

BIOLOGICAL TERMS

ATP	adenosin triphosphate
Cdc	cell division cycle protein
Cdk	cyclin-dependent kinase, found in cell cycle regulation
Ck	casein kinase
Clb	B-type cyclin
Cln	cyclin proteins in *S. cerevisiae*
Cyc	cyclin protein
ERK	extracellular signal-regulated kinases (unphosphorylated)
ERK2/pY	extracellular signal-regulated kinase, phosphorylated on tyrosine-185
ERK2/pT	extracellular signal-regulated kinase, phosphorylated on threonine-183
ERK2/pTpY	extracellular signal-regulated kinase, phosphorylated on both residues
DNA	deoxyribonucleic acid
G1 phase	first gap phase during cell cycle
G2 phase	second gap phase during cell cycle
GSK	glycogen synthase kinase
IKK	*IκB* kinase
IκBα	nuclear factor of kappa light poylpeptide gene enhancer in B-cells inhibitor, alpha (inhibits *NFκB*)
JNK1	mitogen-activated protein kinase 8
MAPK	mitogen-activated protein kinase
MEK	mitogen-activated protein kinase; extracellular signal-regulated protein kinase kinase
MKP	mitogen-activated protein kinase phosphatase
NES	nuclear export signal
NFAT	nuclear factor of activated T-cells, found in immune response
NFκB	nuclear factor kappa-light-chain-enhancer of activated B cells
NLS	nuclear localization signal
PP2A	protein phosphatase 2
RAS	protein family belonging to hydrolyze guanosine triphosphate
RNA	ribonucleic acid
S phase	synthesis phase during cell cycle
S. cerevisiae	budding yeast *Saccharomyces cerevisiae*
S. pombe	fission yeast *Schizosaccharomyces pombe*

Sic1	stoichiometric inhibitor protein of *Cdk1-Clb* in *S. cerevisiae*
SP motif	serine and proline-rich region
SRR-1 motif	serine-rich region
Swe1	protein kinase in *S. cerevisiae*, homologue of *Wee1*
VHR	vaccinia H1-related phosphatase
Wee1	protein kinase in *S. pombe*

FURTHER ABBREVIATIONS

add. dep.	additional dependencies
con	convergence
CRNT	chemical reaction network theory
H	Hopf bifurcation
LP	limit point
nd	no data
nmss	no multiple steady states
PM	phosphorylation mechanism
RW	random walk
TB	toolbox

A	substrate of the network
K	kinase of the network
P	phosphatase of the network
n	number of phosphorylation steps, also number of species in the network
i	index addressing phosphorylation step, vector and matrix elements
x	concentration vector of substances in networks
k	vector of rate constants
r	number of reactions in a network, also number of educt complexes in the network
v	vector of reaction rates
y	vector of educt complexes in the network
$\tilde{y}$	vector of complexes in the network
m	number of complexes in the network; later maximum number of variation steps during random walk
N	stoichiometric matrix
s	rank of stoichiometric matrix; later $s \in \mathrm{im}(N)$ with $s = b - a$
E	basis for right nullspace of stoichiometric matrix, referred to as cone
W	basis for left nullspace of stoichiometric matrix, referred to as weight matrix
c	vector of total concentration in network
Y	rate exponent matrix
U	basis for right nullspace of rate exponent matrix
$\tilde{Y}$	complex matrix
I_A	incidence matrix
$\mathcal{M}$, $\mathcal{S}$, $\mathcal{U}$	linear subspaces, their corresponding bases M, W and U respectively
l	number of linkage classes in a network
t	time
a, b	steady states of the system
μ	$\ln(b/a)$
$\varkappa$	$\ln(v/\lambda)$
$E^{\mathcal{M}}$, $E^{\mathcal{S}}$	matrices of generators for cones
λ, v, α, β	parameters defining ratios of basis vectors of their respective cones E, $E^{\mathcal{M}}$ and $E^{\mathcal{S}}$
p, q	size of α and β, respectively
δ	sign vector (signature of sign structure)

Δ	matrix of sign vectors
σ	sign pattern
Σ	matrix of sign patterns
ϑ	deficiency of the reaction network
M	linear solution set to μ
Q	nonlinear inequality set for positivity of λ
q, r	elements of Q
K	matrix of sign constraints posed by Q
$\mathcal{K}$	set of sign constraints
δk, Δk	directed vector and step size for random walk
r	biased vector to adjust step size
R	number of initial steady states of k
m	maximum number of variation steps
$\bar{I}$, I_{min}, I_{max}	mean, minimal and maximal exit number

The creation of a single world
comes from a huge number
of fragments and chaos.

— Hayao Miyazaki

1 INTRODUCTION

Multisite phosphorylation is an often found feature in (bio-) chemical reaction networks. The size of the phosphorylation network can vary from two phosphorylation steps, for example, in the layers of the *mitogen activaded protein kinases* (*MAPK*), [69], up to very large numbers of more than 150 sites, [101]. They are not only restricted to procaryotics, but can be found in intracellular processes of eucaryotics. These intracellular processes include among others signal transduction, check point control in the cell cycle, and information processing. For example, signal transduction is achieved via the cascades of the *MAPK*s, [69]. Check point control in the cell cycle is achieved by various proteins, for example the *stoichiometric inhibitor protein*, (*Sic1*), with nine phosphorylation sites, the *cell division cycle protein* 25, (*CDC25*), with probably more than fourteen phosphorylation sites and *Wee1* with more than five sites, [82]. For signal transduction, information is processed in one compartment of the cell. Information processing is used for transition of information between different cells or cell compartments. For example, the proteins of the *nuclear factor of activated T-cells* family, (*NFAT*), are activated in the cytoplasm and enable gene transcription for immune response in the nucleus. These proteins posses at least 21 phosphorylation sites, [64].

The important feature of, for example, cell cycle control is the ability of the underlying reaction to exhibit a switch-like response curve. This switch-like curve cannot only be achieved by a uni-valued function, but also by a multi-valued function, e. g., an s-shaped function, with underlying multistationarity, [16, 106]. Networks also display dynamic properties like oscillations, [104]. Higher-level network structures, such as positive or double negative feedback loops, are used to create models with multiple steady states displaying bistability, oscillations or limit cycles. These feedback loops were seen as a prerequisite for a bistable response curve in (bio-) chemical reaction networks, [69]. But analysis on multisite phosphorylation networks showed, networks with multisite phosphorylation can already exhibit multiple steady states without the need of higher-level network structures, see for example [22]. N. I. Markevich et al. were the first to demonstrate the possibility of multistationarity in a single cascade level of *MAPK*. Further work followed by J. Gunawardena and, for example, L. Wang and E. D. Sontag on the number of steady states a multisite phosphorylation network could exhibit. These studies so far only brought answers to general "yes-or-no" questions, i. e., multiple steady states exist or not, or found exactly one explicit pair of steady states, such providing only one explicit solution. An overview of these works is discussed briefly in chapter 4, after a discussion on the theoretical and experimental aspects of multisite phosphorylation and multistationarity in chapters 2 and 3, respectively.

C. Conradi then provided an algorithm based on the work of M. Feinberg as well as [31], that not only answered the question of multistationarity but

also provided a parametrization of the multistationarity region. This algorithm was then exploited in the diploma thesis, [49], of the author. These results are summarized and extended in chapter 5. Here, a multisite phosphorylation process with a distributive, sequential mechanism is introduced, referred to as the standard phosphorylation network. Multistationarity can be established for a multisite phosphorylation network of size $n \geqslant 2$. The parametrization of the multistationarity region provides also rate constants and steady states. Thus, a parametrization for the multistationarity region is provided with explicit solutions of not only one pair but for the whole region. The parameter space as well as region of steady states is then analyzed. And a parametrization yielding steady states in biological relevant regions is achieved in the same chapter.

As the phosphorylation network discussed in chapter 5 does not represent all (bio-) chemical network setups of multisite phosphorylation processes, further setups are considered as well. Often the phosphorylated protein is bound to further reactions. It can be actively degradated or inactivated by the phosphorylation process or compartmentalization. Thus the introduced multisite phosphorylation is extended by additional reactions. These allow synthesis and/or degradation of the protein as well as its phosphorylation forms, but also synthesis and/or degradation of the enzymes. Examples for these networks can again be found in the cell cycle. Degradation of the protein *Sic1* by an ubiquitinase is the trigger for transition from *G1* to *S* phase in cell cycle, [24]. Compartmentalization by sequestration is present in the deactivation of the protein *Cdc25*, [38]. And hyper-phosphorylation can be seen in *Swe1*, an analogon of *Wee1*, [115]. Such phosphorylation networks with additional reactions are discussed in chapter 6. The provided solution algorithm for these multisite phosphorylation networks with additional synthesis and/or degradation only discusses double phosphorylation networks. Multistationarity can be established for some of the arising network setups resulting as well in a parametrization. Larger phosphorylation networks are considered as well, but no explicit solution is provided: The reaction network is analyzed in a reduced form instead of considering the actual number of states and rates. The double phosphorylation network is a simple translation of an n-times phosphorylation network in a reduced form. Here, the unphosphorylated form of the protein in the reduced model corresponds to the actual unphosphorylated protein of the large model. The double phosphorylated form of the protein in the reduced model corresponds to the fully phosphorylated protein. And the single-phosphorylated protein in the reduced model corresponds to all in between phosphorylation forms. This reduction of reactions is often found in (bio-) chemical reaction networks, see for example [39]. It is also used in the next chapter on compartmentalization.

As (bio-) chemical reaction networks often display some sort of compartmentalization, chapter 7 discusses two coupled phosphorylation networks and existence of multiple steady states. The de-/phosphorylation of the protein *NFAT* in cytoplasm and nucleus is taken as an example for these kind of mechanisms. Again, multistationarity is established for $n \geqslant 2$. A parametrization for rate constants together with steady states is provided for arbitrary n and an explicit example is given for a reduced model of two phosphorylation steps.

Besides the existence of multiple steady states in multisite phosphorylation network, this thesis also considers the robustness of these steady states in terms of variations of parameters. If parameters in (bio-) chemical reac-

tion network change, the property of multistationarity could be lost due to sensitive behavior of the reaction network towards these changes. On the other hand, robustness of the reaction network might preserve the property of multistationarity. The work of S. Herold on robustness towards variation in parameter space is extended in this thesis and discussed in chapter 8. A random walk in parameter space is applied to test the robustness of the multistationarity. Here the robustness of the multisite phosphorylation network increases with the step size n up to four to six phosphorylation steps and decreases afterwards. Thus larger phosphorylation networks show a less robust behavior in numerical simulation towards variation in parameter space.

For reasons of readability large matrices and proofs can be found in the appendices. They are organized as follows: Appendix A contains proofs and further algorithms of chapter 5 and 7. Large matrices of chapter 5 and further results of chapter 6 can be found in appendix B. Appendix C contains some more figures and tables from chapters 3, 7 and 8.

The thesis establishes mutlistationarity for different multisite phosphorylation networks: multistationarity of an n-times phosphorylation network, of double phosphorylation networks with synthesis and/or degradation, as well as of networks with compartmentalization. Furthermore, it provides a parametrization for the multistationarity region. Thus higher-level network setups are not needed any more to establish multiple steady states in these forms of (bio-) chemical reaction networks. And dynamic properties, such as switching, oscillations or limit cycles, can be established by these small networks.

Over thinking, over analyzing separates the body from the mind.
Withering my intuition, missing opportunities and I must
feed my will to feel my moment drawing way outside the lines.

— Justin Chancellor

2 MODELING BIOLOGICAL SYSTEMS

This chapter covers conceptual basics needed to get a start. Included are nomenclature and some standard approaches in systems biology. Not covered however are basics in systems biology and control theory. The interested reader not familiar with the topic at hand is advised to follow the work of E. Klipp, et al. for an introduction in systems biology in general and to A. Cornish-Bowden for a more detailed introduction in enzyme kinetics. For an introduction to control theory the work of D. G. Luenberger is recommended.

Furthermore, this thesis makes use of some standard mathematical concepts from stochastics and bifurcation theory. Again it is assumed that the reader is familiar with these or might follow standard literature, see for example [7, 46, 72] and [112] for the first, and [41] and [62] for bifurcation theory.

2.1 KEY TERMS AND DEFINITIONS

This work makes extensive use of matrices and vectors. To achieve a distinct nomenclature the following terms are used:

$\mathbb{R}^n$	the n-dimensional Euclidean space
$\mathbb{R}^n_{>0}$	the positive orthant of $\mathbb{R}^n$
$\mathbb{R}^n_{\geqslant 0}$	the nonnegative orthant of $\mathbb{R}^n$
$\mathbb{R}^{n\times m}$	set of $n \times m$ matrix with real entries
$q \in \mathbb{R}^n$	a column vector of length n
$\mathcal{A}$	uppercase calligraphic letters denote sets
A^T	transpose of a matrix or a vector, often used to denote column vectors as transposed row vectors
$q^\perp$	orthogonal complement of q
$\lvert a\rvert$	absolute value of a variable a
$\lVert q\rVert$	L2-norm of a vector $q \in \mathbb{R}^n$ with $\lVert q\rVert = \sqrt{q_1^2 + \cdots + q_n^2}$, also denoted as $\lVert q\rVert_2$
$\exp(a)$	exponential function for basis e and exponent a, a real number, also denoted as e^a

To describe the standard scalar product in $\mathbb{R}^n$:

$$\langle p\, q\rangle = \sum p_i\, q_i = q^T\, p.$$

Subscripts i and j are used to denote either rows, columns or elements of matrices and vectors respectively. A bracketed superscript denotes the phosphorylation step considered. For a time series or an analysis over several steps (j) is used to denote the current step. Furthermore, the following standard forms are used:

I	identity matrix
0	matrix of zeros
$\underline{0}$	vector of zeros
e_n	unit vector of length n
e_i	unit vector of suitable dimension with a one at the ith entry

Mathematical notations for parameters $p \in \mathbb{R}$ and vectors $x \in \mathbb{R}^n$:

$$
\begin{aligned}
x &= \begin{bmatrix} x_1 \\ \vdots \\ x_n \end{bmatrix} = [x_1, \ldots, x_n]^T, \\
x > 0 \quad &\Leftrightarrow \quad x_1 > 0, \ldots, x_n > 0, \\
x^{-1} &= \frac{1}{x} = \left[\frac{1}{x_1}, \ldots, \frac{1}{x_n}\right]^T, \\
\ln x &= [\ln x_1, \ldots, \ln x_n]^T, \; x > 0, \\
\exp(x) &= e^x = [e^{x_1}, \ldots e^{x_n}]^T, \\
p \cdot x &= [p \cdot x_1, \ldots, p \cdot x_n]^T.
\end{aligned}
$$

Furthermore, x^y with $x, y \in \mathbb{R}^m_{\geqslant 0}$ is defined as:

$$x^y = x_1^{y_1} x_2^{y_2} \cdots x_n^{y_n} = \prod_{i=1}^{n} x_i^{y_i}$$

The expression col is used to denote the existence of sub-vectors in a vector. Consider a column vector of length n, the vector can be displayed as an $p(q+1)$ dimensional column vector with

$$x = \left[x_{(10)}, \ldots, x_{(p0)}, x_{(11)}, \ldots, x_{(p1)}, \ldots, x_{(1q)}, \ldots, x_{(pq)}\right]^T$$

by

$$x = \operatorname{col}\left(x_{(0)}, \ldots, x_{(q)}\right) \in \mathbb{R}^{p(q+1)},$$

where $x_{(i)}$ with $0 \leqslant i \leqslant q$ denotes the i-th sub-vector of x.

In addition to the biological abbreviations given on page xix, abbreviations are used in the following sense:

tot	refers to the total sum of an entity (for example total concentration)
diag	denoting an $n \times n$ diagonal matrix
ker	nullspace of a matrix
$[A]$	image of a matrix A, also $\operatorname{im}(A)$, or concentration of a substance A in the reaction network
sgn	sign pattern describing sign of each entry of a vector
orth	orthonormal basis of image of a matrix

supp	closure or support of a vector, i.e., set of indices where the vector has nonzero elements
span	span of a set
rand	random number in associated probability distribution
length	length of a vector
size	size of a matrix
rank	rank of a matrix

2.2 ORDINARY DIFFERENTIAL EQUATIONS ARISING FROM (BIO-) CHEMICAL REACTION NETWORKS

In this section the notation of reoccurring network matrices is introduced. A simple (bio-) chemical reaction network can be given by the following example

$$\begin{aligned} &2A + B \rightleftharpoons A_2B \longrightarrow C + B, \\ &C \longrightarrow D + E, \\ &A + D \rightleftharpoons E, \end{aligned} \tag{$\mathcal{N}$2.1}$$

where B may describe an enzyme catalyzing the first reaction. Arrows point from consumed species, called educts, to produced species, called products. The network consists of six species. The number of species in a network will be given by n. If the system is open, i. e., a species can enter and/or leave the system at any time, a zero element is used in the following form:

$$\text{species} \rightleftharpoons 0$$

Every species can be described by its concentration $x \in \mathbb{R}^n$:

$$\begin{aligned} &x_1 = [A], && x_2 = [B], && x_3 = [A_2B], \\ &x_4 = [C], && x_5 = [D], && x_6 = [E]. \end{aligned}$$

Furthermore, the network is described by reactions and associated rate constants $k \in \mathbb{R}^{r=6}$:

$$\begin{aligned} &\overset{x_1}{2A} + \overset{x_2}{B} \underset{k_2}{\overset{k_1}{\rightleftharpoons}} \overset{x_3}{A_2B} \xrightarrow{k_3} \overset{x_4}{C} + \overset{x_2}{B}, \\ &\overset{x_4}{C} \xrightarrow{k_4} \overset{x_5}{D} + \overset{x_6}{E}, \\ &\overset{x_1}{A} + \overset{x_5}{D} \underset{k_6}{\overset{k_5}{\rightleftharpoons}} \overset{x_6}{E}. \end{aligned}$$

Assumption 2.1. All reactions are irreversible.

The network can also be analyzed in terms of graph-theory, see for example the work of M. Feinberg. Here, only nodes or complexes of the network but not individual substances are considered. Network ($\mathcal{N}$2.1) consists of seven complexes $\tilde{y}$:

$$\begin{aligned} &\tilde{y}_1 \rightleftharpoons \tilde{y}_2 \longrightarrow \tilde{y}_3 \\ &\tilde{y}_4 \longrightarrow \tilde{y}_5 \\ &\tilde{y}_6 \rightleftharpoons \tilde{y}_7 \end{aligned} \tag{$\mathcal{N}$2.2}$$

The number of complexes of a system will be described by m thus $\tilde{y} \in \mathbb{R}^m$, here $m = 7$. Some complexes $\tilde{y}$ appear only as educt complexes y in the network,e. g., $\tilde{y}_4$. Whereas other complexes appear only as products in the network, e. g., $\tilde{y}_5$ or even as both, e. g., $\tilde{y}_1$. To differ between educts and educt complexes, the variable $\tilde{y}$ refers to all complexes and the variable y to educt complexes. The number of educt complexes in a network is equal to the number of reactions, as each reaction is based on an educt.

Network matrices are used to describe, in a compact form, the reaction network itself. These matrices enable a structural interpretation of the network as no quantitative values are used. The structure of a reaction network can, for example, be described by the stoichiometric matrix $N \in \mathbb{R}^{n\times r}$, the complex matrix $\tilde{Y} \in \mathbb{R}^{n\times m}$, or the rate exponent matrix $Y \in \mathbb{R}^{n\times r}$, also known as educt complex matrix.

The stoichiometric matrix is composed of rate constants describing column and species describing row elements. Each rate constants describes synthesis or degradation of a species, where the sign is set by the type of consumption in the network itself:

$$N = \begin{array}{c} \\ x_1 \\ x_2 \\ x_3 \\ x_4 \\ x_5 \\ x_6 \end{array} \begin{array}{c} \begin{array}{cccccc} k_1 & k_2 & k_3 & k_4 & k_5 & k_6 \end{array} \\ \begin{bmatrix} -1 & 1 & 0 & 0 & -1 & 1 \\ -1 & 1 & 1 & 0 & 0 & 0 \\ 1 & -1 & -1 & 0 & 0 & 0 \\ 0 & 0 & 1 & -1 & 0 & 0 \\ 0 & 0 & 0 & 1 & -1 & 1 \\ 0 & 0 & 0 & 1 & 1 & -1 \end{bmatrix} \end{array}.$$

For network (N2.1), the stoichiometric matrix $N \in \mathbb{R}^{6\times 6}$.

The complex matrix $\tilde{Y} \in \mathbb{R}^{n\times m}$ describes each node of the network in a simple ascending manner. Each node describes the contribution of a species in the network towards this node in terms of unit vectors of length n with a contributing factor at the appropriate position of the species:

$$\begin{aligned} \tilde{y}_1 &= 2e_1 + e_2, & \tilde{y}_2 &= e_3, \\ \tilde{y}_3 &= e_2 + e_4, & \tilde{y}_4 &= e_4, \\ \tilde{y}_5 &= e_5 + e_6, & \tilde{y}_6 &= e_1 + e_5, \\ \tilde{y}_7 &= e_6. \end{aligned}$$

Thus $\tilde{Y}$ can be given by

$$\tilde{Y} = \begin{bmatrix} \tilde{y}_1 & \tilde{y}_2 & \tilde{y}_3 & \tilde{y}_4 & \tilde{y}_5 & \tilde{y}_6 & \tilde{y}_7 \end{bmatrix}$$

with $\tilde{Y} \in \mathbb{R}^{6\times 7}$ for network (N2.1). Collecting all educt complexes in the network yields the rate exponent matrix Y. This matrix describes all educt complexes y of the reaction network in the same ascending manner of ordered entries:

$$Y = \begin{bmatrix} \tilde{y}_1 & \tilde{y}_2 & \tilde{y}_2 & \tilde{y}_4 & \tilde{y}_6 & \tilde{y}_7 \end{bmatrix}$$

with $Y \in \mathbb{R}^{6\times 6}$ or in general $Y \in \mathbb{R}^{n\times r}$.

If in- or outflow of certain species as educts is allowed, corresponding zero columns in Y can be found. To differ between all complexes and educt complexes in the reaction network, $\tilde{y}$ always refers to elements of the complex matrix $\tilde{Y}$ and y refers to elements of the rate exponent matrix Y.

The graph of the reaction network itself is represented by the incidence matrix I_A. Columns of I_A correspond to rate constants k and rows to complexes $\tilde{y}$. Thus, each column contains only nonzero entries for synthesis and degradation of a complex:

$$I_A = \begin{array}{c} \\ \tilde{y}_1 \\ \tilde{y}_2 \\ \tilde{y}_3 \\ \tilde{y}_4 \\ \tilde{y}_5 \\ \tilde{y}_6 \\ \tilde{y}_7 \end{array} \begin{array}{c} \begin{array}{cccccc} k_1 & k_2 & k_3 & k_4 & k_5 & k_6 \end{array} \\ \begin{bmatrix} -1 & 1 & 0 & 0 & 0 & 0 \\ 1 & -1 & -1 & 0 & 0 & 0 \\ 0 & 0 & -1 & 0 & 0 & 0 \\ 0 & 0 & 0 & -1 & 0 & 0 \\ 0 & 0 & 0 & 1 & 0 & 0 \\ 0 & 0 & 0 & 0 & -1 & 1 \\ 0 & 0 & 0 & 0 & 1 & -1 \end{bmatrix} \end{array}$$

with $I_A \in \mathbb{R}^{7\times 6}$ or in general $I_A \in \mathbb{R}^{m\times r}$. Note that

$$N = \tilde{Y} I_A.$$

To describe the network in terms of ordinary differential equations a further assumption is made:

Assumption 2.2. The mass action law holds for all reactions, i. e., the reaction rate ν is proportional to the product of the concentrations of the educts.

With the rate ν being proportional to the product of educt concentration and the rate exponent matrix describing coupling of educts, the elements of the educt complex matrix Y can be used to describe, in a short form, each individual reaction rate ν:

$$\nu_i = k_i \prod_j^r x^{y_j}$$

$$\nu = \left[k_1 x_1^2 x_2,\ k_2 x_3,\ k_3 x_3,\ k_4 x_4,\ k_5 x_1 x_5,\ , k_6 x_6\right]^T.$$

Thus, the proportional coefficient is given by the rate constant k, and the exponents of the monomials yield the contribution of each educt. This product is also referred to as:

$$\nu(k, x) = \operatorname{diag}(k)\,\Phi(x) \tag{2.1}$$

with the monomial vector Φ defined by

$$\Phi(x) := \begin{bmatrix} x^{y_1} & \dots & x^{y_r} \end{bmatrix}^T. \tag{2.2}$$

Following the law in its simplest form thus yields ordinary differential equations composed of proportional rates (amount of species) of contributing educts. This correlation can be used to describe the change of concentration of substrates over time. The result are ordinary differential equations for the single substances:

$$\begin{aligned} \dot{x}_1 &= -k_1 x_1^2 x_2 + k_2 x_3 - k_5 x_1 x_5 + k_6 x_6, \\ \dot{x}_2 &= -k_1 x_1^2 x_2 + k_2 x_3 + k_3 x_3, \\ \dot{x}_3 &= k_1 x_1^2 x_2 - k_2 x_3 - k_3 x_3, \\ \dot{x}_4 &= k_3 x_3 - k_4 x_4, \\ \dot{x}_5 &= k_4 x_4 - k_5 x_1 x_5 + k_6 x_6, \\ \dot{x}_6 &= k_4 x_4 + k_5 x_1 x_5 - k_6 x_6. \end{aligned} \tag{2.3}$$

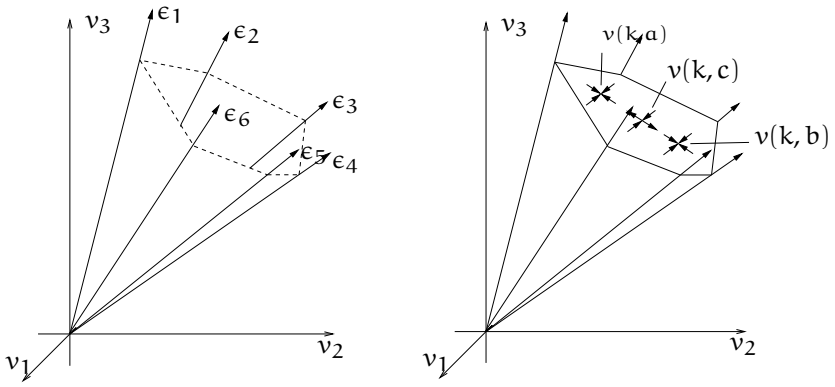

Figure 2.1: *Left hand side: example of a pointed polyhedral cone in* $\mathbb{R}^3$ *and its generators* $\epsilon_1, \epsilon_2, \ldots$ *described by solid lines, [58, 78]. Note that this sketch does not describe the given example network or any network in this thesis. Right hand side: "appearance" of steady states* a *and* b*, outer stable ones, and a third unstable steady state,* c*, in their middle.*

The sign of individual terms is negative, if a substrate is consumed or positive, if it is produced. As this sign is also displayed in the stoichiometric matrix, the ordinary differential equations can be given in a short form using the stoichiometric matrix N and the vector of reaction rates v:

$$\frac{dx(t)}{dt} = N\,v(k, x(t)) \tag{2.4}$$

In general, the stoichiometric matrix N does not have full row rank s. The number of species is in most cases smaller than the number of reactions. Often, so called conservation relations can be found, describing the conservation of sums of species in the reaction network. Thus, s is usually smaller then the number of species. Given the stoichiometric subspace $\mathcal{S} = \mathrm{im}(N)$ a matrix $W \in \mathbb{R}^{(n-s)\times n}$ can be given by

$$W^T N = 0$$

whose rows yield the conservation relation of the reaction network:

$$W^T x(t) = \text{constant} = c,\ \forall t \tag{2.5}$$

The matrix W is referred to as a weight matrix.

This can be seen from a (bio-) chemical point of view: while conservation of substances is present, the network operates in a closed environment, see for example [28]. If not all substances are conserved, some species might enter or leave the system, for example proteins moving into or out of the cell nucleus. Thus, equations (2.5) are referred to as conservation relations of the reaction networks.

The number of ordinary differential equations can be reduced by the number of present conservation relations. Only $\mathrm{rank}(N)$ equations have to be solved. In the given network example (N2.1), $n - s = 6 - 4 = 2$ conservation relations can be found:

$$x_1 + x_3 = \text{constant} \qquad \text{and} \qquad x_2 + x_3 = \text{constant},$$

thus only four equations have to be solved.

Interesting points of such (bio-) chemical reaction networks are steady states of the network as these translate, for example, to certain stable cell

states. For example, the four phases in the cell cycle are associated with steady states of the underlying reaction networks, for example, see the work of J. J. Tyson. The reaction network is in steady state, if equation (2.4)

$$N\,v(k, x) = 0. \tag{2.6}$$

For chemical reaction networks only positive x are meaningful. Furthermore, with irreversible reactions all rate constants in k are positive. Thus, solutions to equation (2.6) lie in the cone $\ker(N) \cap \mathbb{R}^{n\times r}_{\geqslant 0}$, a pointed polyhedral cone, see for example the arbitrary cone in figure 2.1. The stoichiometric matrix of reaction networks discussed in this work show cones E, whose columns form also a basis for the right nullspace of the stoichiometric matrix, see the proof in appendix A.1 for an n-times phosphorylation network:

$$N\,E = 0 \quad \text{with } E \in \mathbb{R}^{n\times q}_{\geqslant 0}. \tag{2.7}$$

Note, this is not the case for all reaction networks, i. e., the number of generators for the cone E in the positive subspace is usually larger then the number of basis vectors of the right nullspace of N.

For reaction network (N2.1) the cone E can be given by

$$E^T = \begin{bmatrix} 1 & 1 & 0 & 0 & 0 & 0 \\ 0 & 0 & 0 & 0 & 1 & 1 \end{bmatrix}.$$

Remark 2.3. [Biological Interpretation.] Extreme rays of the pointed polyhedral cone E can be interpreted in a biological way. Each column describes a minimal set of rates in v. In this biological sense the steady state is interpreted as a steady state, where rates are balanced and $N\,v$ is zero. The columns of E are then interpreted as a flux or extreme pathway through the reaction network. For example, see the work of [57, 79, 87, 89, 97] and [105] on metabolic flux analysis.

In general, (bio-) chemical reaction networks have at least one steady state in one set $x_0(t) + \operatorname{im}(N)$, where for a certain given initial concentration the following

$$W^T x(t) \equiv W^T x(0) \Leftrightarrow x(t) - x(0) \in \operatorname{im}(N)$$

holds for any such steady state.

Certain (bio-) chemical reaction networks can not only exhibit one steady state in one set but several ones in the same set. For example, the phosphorylation network of *ERK* in the *MAPK* cascade can exhibit multiple steady states, [69]. Furthermore, the single phases of the cell cycle are associated with multiple steady states. Here, each phase can exhibit at least two stable steady states in the same set enabling switching between different phases, see [109] for a model of the cell cycle and the associated switching.

Definition 2.4. [Multistationarity.] *Assume that a system can at least exhibit two distinct steady states* a *and* b *in the same coset with* $x_0(t) + \operatorname{im}(N)$. *The polynomial system in equation* (2.4) *has to hold for both steady states with*

$$N\,v(k, a) = 0 = N\,v(k, b), \tag{2.8a}$$

referred to as the polynomial condition.

Furthermore, as equation (2.4) *holds and if a left kernel of* N *can be found, the following holds for the steady states in the system*

$$W^T a = c = W^T b \Leftrightarrow b - a \in \operatorname{im}(N), \tag{2.8b}$$

referred to as the coset condition for multistationarity.

In figure 2.1 the two corresponding rates of the steady states a and b are represented by the outer stable ones.

Remark 2.5. [The Generators of the Cone E.] Considering $E\,\lambda$ different approaches can be used to generate λ. In a first approach, one would assign each generator the same value λ. This can be interpreted in terms of the reaction network as well. As each generator corresponds to a flux in the network, the same value is assigned to each contributing reaction. Thus, every reaction has the same efficiency and thus same quantitative meaning in the network, see for example [57]. On the other hand, if different values are assigned to generators, i. e., $\lambda_i \neq \lambda_j$, reactions in the network are weighted differently. Here, different effects of single reactions are taken into account. For example, the efficiency of certain fluxes could be higher. With this second approach, a quantitative analysis of fluxes can be done, [91].

After all the world is indeed beautiful
and if we were any other creature than man
we might be continuously happy in it.

Sebastian Barry

3 MULTISITE PHOSPHORYLATION AS AN IMPORTANT INTRACELLULAR PROCESS

Throughout this thesis, chemical reaction networks are restricted to phosphorylation networks, where a protein is phosphorylated by an enzyme and dephosphorylated by another enzyme. The binding of enzymes enables de-/coupling of phosphate groups to and from the protein or conformational changes of the protein itself. The phosphorylation of the protein itself triggers further processes, such as degradation of the protein or further reactions as ubiquitination. Furthermore, phosphorylation often limits the movement of proteins, e. g., bounded phosphate groups increase the volume of the molecule and phosphorylated proteins thus might not be able to pass the cell membrane. Even energy carrier in the cell such as *ATP* can be generated via phosphorylation, for example, see [36, 80, 103]. The number of phosphorylation sites depends on the considered protein. Short phosphorylation processes of only two steps are possible and can be found, for example, as phosphorylation of the proteins in the layers of the *MAPK* cascades. Proteins can exhibit more than one or two phosphorylation sites, for example, phosphorylation of *Sic1* with nine phosphorylation sites, [24], or proteins of the *NFAT* family with 21 sites or even more, where 14 are considered important for its biological function, [13, 24].

This chapter gives a brief overview on phosphorylation itself with examples provided for experimental or theoretical results of three types of phosphorylation processes, namely a double phosphorylation of the protein *MAPK*, nine times phosphorylation of *Sic1*, and fourteen times phosphorylation of *NFAT*.

3.1 MULTISTATIONARITY, ENZYME KINETICS AND RATE THEORIES

The single phosphorylation of a protein can be described by the following process: an enzyme E binds to a protein A. This catalytic binding enables phosphorylation at one site by a phosphate group, yielding a single phosphorylated protein A_{1P}. In general, an enzyme driven reaction can be given by:

$$\overset{x_1}{E} + \overset{x_2}{S} \underset{k_2}{\overset{k_1}{\rightleftharpoons}} \overset{x_3}{ES} \xrightarrow{k_3} \overset{x_1}{E} + \overset{x_4}{P} \tag{$\mathcal{N}$3.1}$$

Where S describes the substrate, E describes the enzyme, and P describes the product. Rates are defined as the association rate k_1 and the dissociation rate k_2.[1] In terms of phosphorylation networks rate k_3 describes the phosphorylation of the enzyme-substrate complex ES.

3.1 Note that $\frac{k_2}{k_1}$ is also sometimes referred to as dissociation rate in literature.

The mechanism (N3.1) describes a general mechanism. If a phosphorylation of a protein is described, two such enzymatic reactions would be needed, one describing phosphorylation and one describing dephosphorylation. Referring to de-/phosphorylation processes, the substrate is given by A and the product by its phosphorylated form A_P:

$$\begin{aligned} K + A &\rightleftharpoons KA \longrightarrow K + A_P \\ P + A_P &\rightleftharpoons PA_P \longrightarrow P + A \end{aligned} \tag{N3.2}$$

The forward process of phosphorylation is catalyzed by an enzyme called kinase, K. The backward process of dephosphorylation is catalyzed by a different enzyme, the phosphatase P. The phosphorylation step will be indicated by an index iP up to the maximum number of nP phosphorylation steps. The first phosphorylation step will be referred to as $\{\}_P$.

In accordance to network (N3.2) the following assumptions are made and hold throughout this thesis:

Assumption 3.1. Both, phosphorylation and dephosphorylation follow a distributive mechanism, i. e., the enzyme-substrate complex enables allocation of one phosphate.

Different mechanisms would be possible, where more than one phosphate group could be allocated or first the allocation happens before the complex falls apart, also known as a processive phosphorylation. The latter ones do not exhibit multiple steady states and are thus not of interest, see for example [17]. Furthermore, the binding of the phosphate group can follow several mechanisms:

Assumption 3.2. Phosphorylation and dephosphorylation follow a sequential mechanism, i. e., no difference is made between individual phosphorylation sites of a protein.

The kind of mechanism plays only a role for networks with a larger number of phosphorylation sites. If a network has only one phosphorylation site, the number of possible states of the sequential and random mechanisms are equal. It changes for higher number of sites. A strictly sequential mechanism, e. g., phosphorylation of *serine/theronine* ($S/T-X-X-X-S/T$) sites at *CKI*, can be given in the following form with $n+1$ different phosphorylation states:

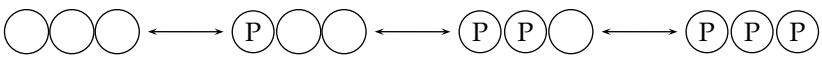

The number of sequences needed to achieve full phosphorylation is exactly one. If each phosphorylation site of a protein is regarded individually, and the order of de-/phosphorylation is not fixed, like before, a random mechanism is present:

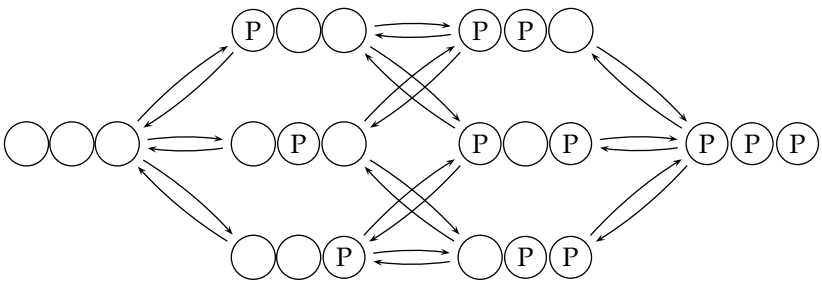

Here, 2^n different phosphorylation states for the protein can be found. The number of sequences to achieve full phosphorylation is $n!$.

Of course, mixed mechanisms can be found as well. E. g., phosphorylation could follow a random mechanism and dephosphorylation a sequential one. See for example the work of [85] and [86].

If synthesis and/or degradation reactions are not present, the total concentration is constant for certain species in the network, see also the previous chapter on conservation of species and the left nullspace of the stoichiometric matrix on page 10. For network (N3.1) total concentration of the enzymes is constant with:

$$E_{tot} = c = [E] + [ES].$$

Values for total concentrations are known in in-vitro experiments. But values for concentrations of individual substances are hard to provide even in small phosphorylation networks. For one, reactions can take place in a millisecond and thus are hard to measure, furthermore intermediate phosphoforms, i. e., $A_P, \ldots, A_{n-1}P$, usually cannot be dissolved other than in qualitative degree, e. g., the gel electrophoresis method. If only product synthesis is of interest in network (N3.1)

$$S \longrightarrow P,$$

assumptions are made on ratios of substrate-enzyme concentrations as well as on phosphorylation rates, allowing to provide rate laws for this explicit product synthesis, [21]. To describe product synthesis the Michaelis-Menten constant

$$k_M = \frac{k_2 + k_3}{k_1}, \tag{3.1}$$

with a unit of mol/l and the maximal velocity

$$v_{max} = k_3\, c$$

of mol/s are often used as a simple measure in the reaction network. The Michaelis-Menten constant k_M describes the affinity of an enzyme to its substrate, or in more general terms, it is a measurement for effective catalysis of the enzyme dependent on substrate concentration. The reaction rate v describes the rate of product synthesis. And, the maximal velocity v_{max} describes the maximal rate achievable by complete enzyme saturation for product synthesis, thus describes a limiting rate for the network, [59]. Furthermore, the turn-over number

$$k_{cat} = \frac{v_{max}}{c}, \qquad \text{here } = k_3 \tag{3.2}$$

with a unit of $1/s$ is the maximal number of molecules of substrates being converted, [21]. Here, the turn over number can be reduced to k_3. The Michealis-Menten kinetic is used as a simplification of the mass action law in enzyme kinetics. The rate law for k_M in equation (3.1) can be derived by a quasi steady state approximation in the respective system of ordinary differential equations, see [21] for a derivation. Using Michaelis-Menten kinetics reduces the number of ordinary differential equations in the system and thus enables an easier handling of the underlying network due to the simplification. For example, it is often applied, where only speed of substrate consumption is of interest, see left hand side of figure 3.1. To be

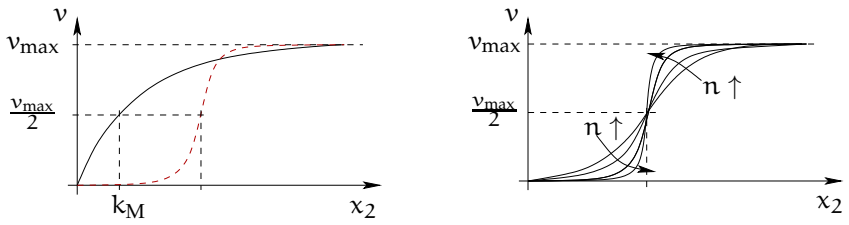

Figure 3.1: *Both sides: Rate v of product synthesis dependent on substrate concentration $[S] = x_2$. Left hand side: The black, solid curve describes the standard Michaelis-Menten mechanism with a saturation response curve for network (N3.1). The red, dashed curve describes a Hill mechanism. Right hand side: A Hill mechanism as described by (N3.3). If the number of substrates molecules (here $n > 2$) binding to the enzyme increases, the curve steepens.*

able to derive explicit solutions to the system of ordinary differential, rate constants for each enzyme reaction in a network have to be known. If the reaction network rises in size, e. g., double or triple phosphorylation exists, different approaches have to be used, to model reactions correctly. Further rate laws exist besides the mass action law and Michaelis-Menten kinetics, describing various effects, e. g., allosteric effects, enzyme inhibition and so on.

But different kinetic rate laws do not only describe the network in a different way, e. g., in a simplified manner, they also define results beforehand. Michaelis-Menten kinetics result in a saturation curve, due to the initial assumption of saturation in the network. This assumption is often valid in-vitro experiments but might fail in-vivo due to, for example, cell compartmentalization. Furthermore, if these kinetics are used for small networks, e. g., (N3.1), without higher-level reactions like feedback loops as present in *MAPK* cascades, they cannot describe switch like response curve for a phosphorylation mechanism.[2] If higher phosphorylation steps are assumed, they can only achieve a strictly monotone response curve like other mechanism, for example Hill-kinetics, e. g., compare the A. Goldbeter and D. E. Koshland model.

The reaction mechanism is then often reduced in such a way, that the intermediate substrate forms are not considered anymore, but the mechanism takes place in only one reaction step. The Hill-mechanism can be given in such a way:

$$E + nS \underset{k_2}{\overset{k_1}{\rightleftharpoons}} ES_n \xrightarrow{k_3} E + nP. \tag{N3.3}$$

If a large reaction network is used, a second approach besides lumping the network as in (N3.3) is possible. A simplified Michaelis-Menten mechanism can be applied for reaction networks of n steps, where each reaction part $i = 1, \dots, n$ is considered individually:

$$\begin{aligned} E + S &\underset{k_2}{\overset{k_1}{\rightleftharpoons}} ES \xrightarrow{k_3} E + S_1 \underset{k_5}{\overset{k_4}{\rightleftharpoons}} \cdots \\ &\xrightarrow{k_{3n-3}} E + S_{n-1} \underset{k_{3n-1}}{\overset{k_{3n-2}}{\rightleftharpoons}} ES_{n-1} \xrightarrow{k_{3n}} E + nP, \end{aligned} \tag{N3.4}$$

3.2 This thesis uses the term strictly monotone if the response curve is uni-valued and at most shows a very steep gain. In contrast the term "s-shaped" response curve is used, if the curve is multi-valued and actually "binds over".

where the final product describes either full substrate conversion to nP after n steps. In terms of the single phosphorylation network depicted in (N3.2) network (N3.4) can be given in terms of

$$\begin{aligned} K + A &\rightleftharpoons AK \longrightarrow \cdots \rightleftharpoons A_{n-1}PK \longrightarrow K + A_{nP}, \\ P + A_{nP} &\rightleftharpoons A_{nP}P \longrightarrow \cdots \rightleftharpoons A_{P}P \longrightarrow P + A. \end{aligned} \tag{N3.5}$$

See network (N3.2) on page 14 for notation. For these large reaction networks a Michaelis-Menten constant can be introduced for each step disregarding former or latter steps:

$$\tilde{k}_{M,i} = \frac{k_{3i} + k_{3i-1}}{k_{3i-2}}, \text{ with } i = 1, \ldots, n, \tag{3.3}$$

where k_{3i} and k_{3i-1} describe the phosphorylation and dissociation, respectively. And k_{3i-2} describes the association rate. This corresponds to the standard Michaelis-Menten rate constants for $i = 1$.

The next section will take a closer look at actual values of rate constants and concentrations of substances.

3.1.1 *Ranges for Rate Constants*

Reaction constants often cannot simply be measured in experiments, as the reaction time is quite small, e. g., range of milliseconds for the dissociation rate. Different theories exist to describe transition from one state of a substance, e. g., inactive, unphosphorylated or unbound, to another state, e. g., active, phosphorylated or bound to another substance.

These theories take into account the probability of two substances meeting or how their orientation to one another has to be in order to bind. For a good overview on theories for rate constants see the work of Huan-Xiang Zhou.

The dissociation and phosphorylation rate constants describe two fairly simple rate constants. By dissociating, a complex simply falls apart. Whereas the phosphorylation step (or in more general terms the last step to build the product) describes a simple change in the structure of the protein, e. g., a conformational change, in the substrate structure. Thus, these rates can be modeled by intramolecular transition, [124]. For reaction networks of various phosphorylation steps as given by network (N3.4), the rates are given usually in the range of

$$k_2 \in [10^{-3}, 10^{1}]\,1/s \qquad \text{and} \qquad k_3 \in [10^{-3}, 10^{1}]\,1/s.$$

These ranges hold also for higher phosphorylation steps, as k_{3i-1} describes the dissociation, e. g., k_2, k5 and so on, and k_{3i} the phosphorylation rate constant.

The association rate constant k_1 is far more complicated as two molecules have to meet at the right position in order to bind. This rate is thus limited by the diffusion rate of protein-protein interaction. The theory behind diffusion rates is motivated by the Brownian motion of particles. In the case of association rates educts have to meet in order to react to their corresponding product. But diffusion can only take place in an open or free space. The cell is not an open space, e. g., cell compartmentalization by the endoplasmic reticulum, where substances can move freely, as required by Brownian motion. The cell compartments hinder the free motion of molecules in the cell. Furthermore, after meeting, the orientation of the reactants has to be

right for the substances to react to a complex, also known as the transition complex. Both, the meeting of the reactants through diffusion as well as the conformational rearrangement can be the limiting factor in the association rate. If the first one is limiting, the mechanism is diffusion controlled, if the latter is limiting, the process is called activation controlled, [124].

An upper bound on association rate constants motivated by free diffusion and transition complex theory is in the order of $[10^9, 10^{10}]\,1/(\mathrm{mol\,s})$, see for example [98, 75, 124]. Usually, these values can not be achieved as they arise from purely probabilistic models. In this model, multiple of the probability of correct alignment of reactants together with their probability of random collision are used to compute association rates. As these neglect, for example, cell compartmentalization, the provided value for the association rate is far too optimistic. The transition complex state theory, see for example [88], was proposed to account for limiting factors in the association rates of proteins. For example, it takes into account that energy barriers or side-chain freezing during complex formation might arise, [88]. Thus, protein-protein interactions are rather in the order of $[10^2, 10^7]\,1/(\mathrm{mol\,s})$ depending on the proteins. Here $[10^4, 10^6]\,1/(\mathrm{mol\,s})$ seems to mark the crucial range for the limiting factor described in the former paragraph, [1, 88, 113]. Rates higher than $10^5\,1/(\mathrm{mol\,s})$, [124], are enhanced, for example by electrostatic enhancement, and are thus diffusion controlled. These can be found for example at *RNA*-protein interactions. Association rates are lower when the interaction is activation controlled. Comparing different protein-protein interactions the association rate is in the range of

$$k_1 \in [10^3, 10^5]\,1/(\mathrm{mol\,s}) \qquad \text{and} \qquad [10^5, 10^7]\,1/(\mathrm{mol\,s})$$

for unbiased diffusion and enhanced biased diffusion, respectively. For some examples, see tables C.1 and C.2 and various tables in [60, 88]. The range for the first case, diffusion controlled, is chosen as the range for the association rate in this work. This range is more realistic for in-vivo reactions where the diffusion is indeed the limiting factor, for example, due to cell compartmentalization.

For a more detailed overview on rate theories and experimental results for proteins see the work by H.-X. Zhou and [44, 54, 56, 60, 61, 102, 123] and references therein.

3.1.2 *Concentration Range for Substances*

Ranges for substrates and enzymes are needed for simulation, and comparison with actual biological networks of multisite phosphorylation processes. Literature data can be found in table C.1 for phosphorylation and in table C.2 for dephosphorylation, respectively.

With a single phosphorylation process given in network (N3.2), the following ranges are chosen for an unphosphorylated protein and its enzymes:

$$\begin{aligned} [K] &\in [10^{-9}, 10^{-3}]\,\mathrm{mol/l}, \\ [A] &\in [10^{-9}, 10^{-5}]\,\mathrm{mol/l}, \\ [P] &\in [10^{-9}, 10^{-3}]\,\mathrm{mol/l}. \end{aligned} \tag{3.4}$$

For the i-times phosphorylated protein, with $i = 1, \ldots, n$, and bounded enzyme-protein forms smaller ranges are chosen. See again network (N3.5) for the overall reaction. This is motivated by the models given by [20, 69], as

the bounded forms in general only form intermediate complexes, compare also the Michaelis-Menten approach discussed above:

$$\begin{aligned}[A_{(i-1)P}K] &\in [10^{-9}, 10^{-5}]\,\text{mol/l},\\ [A_{iP}] &\in [10^{-9}, 10^{-5}]\,\text{mol/l},\\ [A_{iP}P] &\in [10^{-9}, 10^{-5}]\,\text{mol/l}.\end{aligned} \tag{3.5}$$

If steady states are present in the system, concentrations lie in the range as given by equations (3.4) and (3.5). Furthermore, restricting concentrations of enzyme complexes and phosphorylated proteins to these intervals does not pose such a large restriction on the network as, for example, Michaelis-Menten assumptions would pose. Note that later on concentrations and rate constants will be given in units in the region of nmol/l. This rescaling accounts for numerical issues, as, e. g., multiplication of $x_1\,x_2$ would already yield values below the floating point precision.

3.2 MULTISTATIONARITY IN INTRACELLULAR PROCESSES

3.2.1 *Multistationarity in Signal Transduction Networks*

To depict an example for a small scale phosphorylation network, the double phosphorylation of the *MAPK ERK* by *MEK* and dephosphorylation by *MKP3* is described by N. I. Markevich et al., [69], This reaction network is present in signal transduction cascades in the cell, for an overview of its functions see [122]. [69] describe a model of a sequential, distributive double phosphorylation of *MAPK*, exhibiting a bistability region not only in a hypothetical region but actually in a realistic region for parameter combinations received from experimental data. Total concentration of the protein $[A]_{tot}$, as well as the enzymes $[K]_{tot}$ and $[P]_{tot}$ are given by 500 nmol/l. Referring furthermore to the nomenclature for rate constants used later on in this thesis the following rates can be given[3]

$$\begin{aligned} k_1 &= 0.02\,\text{l/(nmol s)}, & k_2 &= 1\,\text{1/s}, & k_3 &= 0.01\,\text{1/s},\\ k_4 &= 0.045\,\text{l/(nmol s)}, & k_5 &= 1\,\text{1/s}, & k_6 &= 1\,\text{1/s},\\ k_7 &= 0.032\,\text{l/(nmol s)}, & k_8 &= 1\,\text{1/s}, & k_9 &= 15\,\text{1/s},\\ k_{10} &= 0.01\,\text{l/(nmol s)}, & k_{11} &= 1\,\text{1/s}, & k_{12} &= 0.5\,\text{1/s}. \end{aligned}$$

Furthermore, concerning the aforementioned Michaelis-Menten rate laws, see equation (3.1) and equation (3.2), values can be given by:

$$\begin{aligned} k_{cat,1} &= 0.01\,\text{1/s}, & k_{M,1} &= 50\,\text{nmol/l},\\ k_{cat,2} &= 15\,\text{1/s}, & k_{M,2} &= 500\,\text{nmol/l},\\ k_{cat,3} &= 0.084\,\text{1/s}, & k_{M,3} &= 22\,\text{nmol/l},\\ k_{cat,4} &= 0.06\,\text{1/s}, & k_{M,4} &= 18\,\text{nmol/l}, \end{aligned}$$

where the first two turn-over numbers, see equation (3.2), correspond to k_3 and k_9, the phosphorylation rate constant of the first and second phosphorylation step, respectively. See network (N3.5) for $n = 2$. The first two

3.3 Nomenclature for higher phosphorylation steps will be introduced in chapter 5. For the network see (N5.1) on page 36. Note that k_4, k_5 and k_6 describe the dephosphorylation process. Thus, the next phosphorylation step (from the single phosphorylated form to the double phosphorylated one) starts with k_7.

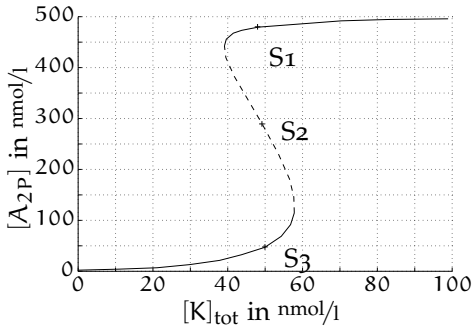

$[K]_{tot} \sim 50\,\text{nmol/l}$
S1: $[A_{2P}] \sim 480\,\text{nmol/l}$
S2: $[A_{2P}] \sim 288\,\text{nmol/l}$
S3: $[A_{2P}] \sim 46\,\text{nmol/l}$

Figure 3.2: *Graphic adapted from [69]: Bifurcation analysis resulting in two stable steady states, S1 and S3, as well as an unstable one, S2, for phosphorylation of the fully phosphorylated protein* $[MAPK_{2P}] \mathrel{\widehat{=}} [A_{2P}]$ *over* $[K]_{tot}$.

Michaelis-Menten rate constants can be given as Michaelis-Menten rate constants for individual phosphorylation steps via

$$k_{M,1} \mathrel{\widehat{=}} \frac{k_2 + k_3}{k_1} \qquad \text{and} \qquad k_{M,2} \mathrel{\widehat{=}} \frac{k_8 + k_9}{k_7},$$

see equation (3.3). Conversion of remaining rates is possible but not of interest for the following chapters and thus omitted. Indeed, here a region of multistable states can be found. Bifurcation analysis was performed for change in $[K]_{tot}$. The resulting steady state curve of the concentration of the double phosphorylated protein $[A_{2P}]$ can be found in figure 3.2.

Concentration of the double phosphorylated protein, $[A_{2P}]$, is stable for low total kinase concentration, $[K]_{tot}$. It is furthermore stable for a high total kinase concentration. Changing the total kinase concentration leads to switching in the network between these two stable concentrations. Thus, bistable regions for substrates in phosphorylation networks can appear already in small networks of double phosphorylation for realistic parameter combinations without the need of positive feedback loops or further feedback mechanisms.

3.2.2 *Multistationarity in Cell Cycle Control*

Phosphorylation is possible up to quite large n. In the cell cycle transition of *Saccharomyces cerevisiae* from *G1* to *S* phase, phosphorylation networks with larger n can be found: *Cdc6* with four sites, *Cln2* with seven sites, and *Sic1* with nine phosphorylation sites, [3]. Here, the phosphorylation process is used for cell cycle control, [52]. The cell cycle itself is associated with different stable states: *G1*-phase, *S*-phase, *G2*-phase and *Mitosis*. The cell switches through the single cell states by changing certain concentrations. Between different cell state a so called checkpoint is used to control correct timing in the cell cycle, see figure 3.3 and, for example, work of [53]. These checkpoints are usually concentrations of certain proteins ensuring that the cell is actually ready to move on in the cell cycle, e. g., is large enough to split, or chromosome replication is correct. See [108], where an online model can be found allowing simulation of the cell cycle and its various steps.

Figure 3.3 describes progression through the cell cycle dependent on different kinase and phosphatase concentrations. Depicting just one example, transition from *G1*- to *S*-phase is, in a nutshell, enabled by a change in the concentration of the protein *Sic1*. *Sic1* is *de-novo* synthesized in late *Anna*-phase, a part of *Mitosis*. It is then phosphorylated at the end of *G1* by the

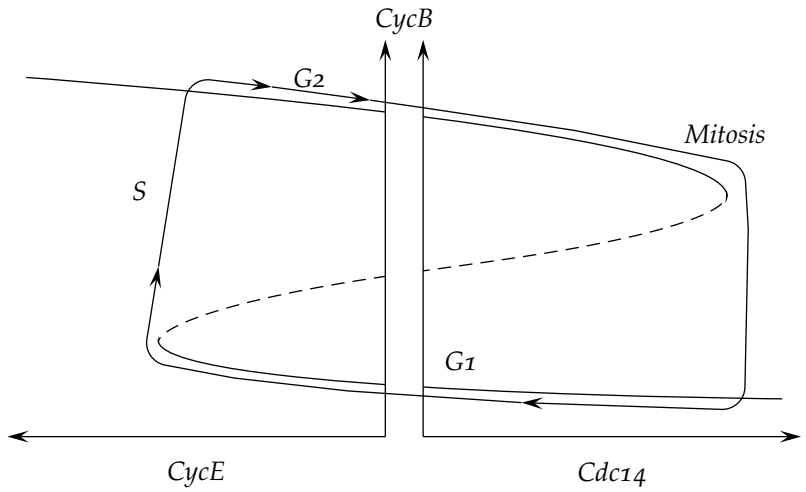

Figure 3.3: *Transition through the cell cycle as posed by [107], see also [110]: changing kinase, CycE, or phosphatase, Cdc14, concentration enables the cell to move through the cell cycle phases, where each phase is represented by a steady state. Arrowheads describe check points between individual cycles. Bifurcation curve itself describes qualitative concentration levels of CycB throughout the cell cycle with the dashed line describing the unstable area. The cell cycle starts in G1 phase with a newborn cell and a low concentration of Cdc14. This low concentration leads to phosphorylation of the corresponding protein Sic1 followed by its ubiquitination and thus transition to S phase. Kinase concentration in final S phase is high. As CycB down-regulates the kinase CycE the cell moves on to G2 phase. Finally the phosphatase Cdc14 down-regulates CycB resulting in a move towards Mitosis and in a final roundup closing of the cell cycle. See also the work of Tyson, for example in [111].*

kinase *Cdc28* in high amounts. *Sic1* exhibits nine equal phosphorylation sites, [14]. After phosphorylation of six of the nine phosphorylation sites an ubiquitinase binds to *Sic1*, [24], enabling degradation of the six-times phosphorylated form of *Sic1*. This results finally in a low concentration of *Sic1* as a result of its phosphorylation and subsequent degradation. The low concentration of *Sic1* triggers transition from *G1* to *S* phase in the cell cycle. The protein can be dephosphorylated by the phosphatase *Cdc14*. Transition through the cell cycle is usually depicted via this phosphatase and the kinase *CycE*, regulating different phosphorylation processes further on through the cell cycle. Concentration of the phosphatase *Cdc14* at the end of *G1* phase is low with an antagonistic mechanism down regulating its concentration by *CycB*, another important player in the cell cycle. With a low concentration of the phosphatase *Cdc14* the concentration of the unphosphorylated form of *Sic1* is very low over the process, resulting in the cycle as described above with stable *Sic1* concentrations for stable *Cdc28* concentrations, [3]. Figure 3.4 describes oscillations of *Sic1* and its corresponding phosphatase concentration.

Thus, with degradation being an important feature of this reaction network, phosphorylation of *Sic1* does not only describe a process of a larger phosphorylation network, but also of an extended network mechanism. The network introduced in (ℕ3.2) cannot only be extended to higher phosphorylation steps, as described by network (ℕ3.5), but also by additional synthesis and degradation reactions of the (phosphorylated) protein and enzymes.

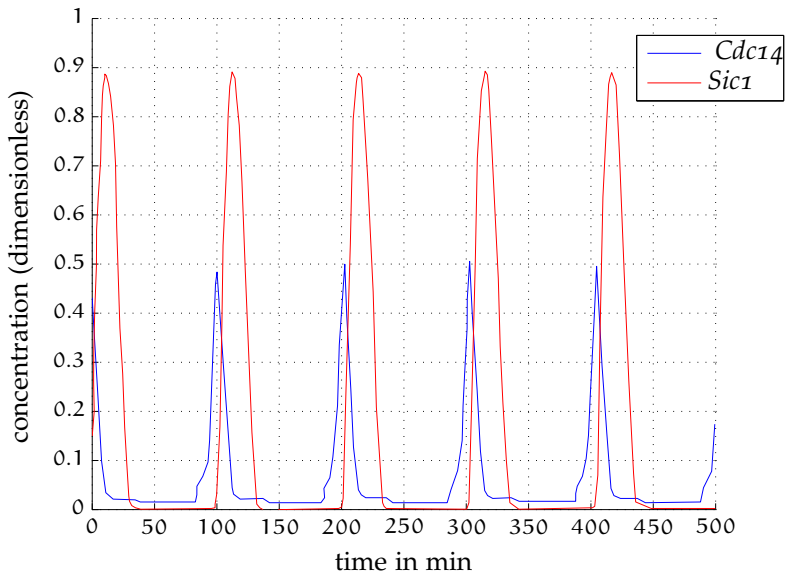

Figure 3.4: *Adaptation from the online model provided by [108]: Oscillation of Sic1 and its phosphatase Cdc14 throughout the cell cycle. Each oscillation peak in concentration of Sic1 describes progression from S phase to G1 phase.*

Recently, it has been proposed by M. Kõivomägi, [51], that phosphorylation of *Sic1* itself follows a processive mechanism. Whereas [2, 24, 73, 97, 115] and [117] postulate a distributive mechanism. A purely processive mechanism as proposed by M. Kõivomägi would not allow multiple steady states. Higher-level reactions, like positive or double-negative feedback loops, would be needed to produce multiple steady states as desired for the cell cycle mechanism. This is not in agreement with measurement data found in literature, see also M. Kõivomägi et al.'s work in [116]: measurements provided by [51] can as well be explained by a mathematical model based on a distributive mechanism, as they highlight themselves in their supplementary work in [51]. This mathematical model of a distributive mechanism corresponds to others already used in literature, see for example [42, 85] and [115] and parameters therein.

Problems arise while determining rate constants and concentrations in multisite phosphorylation systems. E. g., to provide exact values, cells have to be at the exact same timing and state. Furthermore, stoichiometric mechanisms and recovery of only picomole quantities complicate the measurement process. To identify various phosphorylation states of a protein, different methods exist, e. g., electro-spray mass spectrometry, [2, 14, 73, 97, 117] . In gels, different phosphorylation states can be recovered. Here, various phosphorylation states of *Sic1* can be recovered, see [38, 73, 115] and measurements by [51]. Thus, phosphorylation of *Sic1* cannot follow a purely processive mechanism. An at least partly distributive mechanism should be present. The distributive mechanism could then account for the observed switch-like changes and the sharp threshold, [38].

The switch in the cell state at *G1/S* transition is possibly not only enabled by a strictly monotone function, see figure 3.1. *Sic1* can indeed exhibit at least two distinct stable states, as described by a distributive phosphorylation mechanism, [106]. For example, concentration of *Sic1* is stable at two distinct steady states based on the medium, [5, 23]: in poor medium with

a low carbon source (e. g., ethanol) small daughter cells with an elongated *G1* phase are born whereas their mother cells are larger and show a shorter *G1* phase. The elongated *G1* phase is due to a high *Sic1* concentration. If the cells are grown in rich medium, e. g., high carbon source like glucose, large amounts of *Sic1* are phosphorylated resulting in degradation of the phosphorylated form, thus growth between mother and daughter cells is comparable, with a short *G1* phase due to very low *Sic1* concentrations.

As the cell cycle model described above is available online, no data is provided here, but rates can be found for a reduced model on the website, [108].

Large phosphorylation networks do not only exist in the cell cycle. They can be found in various other cell processes. Furthermore, synthesis and degradation of substances is not the only network variation possible in multisite phosphorylation networks. The next section covers a further possible variation found in the cell: compartmentalization.

3.2.3 *Multistationarity in Multisite Phosphorylation Processes with Compartmentalization*

Phosphorylation networks with more phosphorylation sites exist, for example, in the phosphorylation process of proteins of the *NFAT* family with at least 21 phosphorylation sites. Fourteen of these 21 sites are important during immune response, [48]. This network shows a further complex structure as a compartmentalization of the phosphorylation process exists: part of the protein is phosphorylated and dephosphorylated in cytoplasm, and part of it in nucleus.

The protein family has a broad range of diverse functions like bone maintenance, memory formation, and is present in immune response and in cell differentiation, [20]. For example, high level of expression of nuclear *NFATc1* can be found in pancreatic carcinomas, high expression of *NFATc2* and *NFAT5* are found in tumor breast cells. Thus, the *calcineurin*/*NFAT* pathway is considered as a potential target for therapy, see for example [70] and [39]. In total five members of the protein of the *NFAT* family exist, denoted by *NFATc1*, ..., *NFATc4*, and *NFAT5*. The first four are regulated by the phosphatase *calcineurin* whereas the last one is regulated via osmotic stress, [67]. These proteins are found in the expression of the immune system except for *NFATc4*, which can be found in neurons of vertebrates.

In this thesis, the unphosphorylated protein is described simply by *NFAT* and its fully phosphorylated form by $NFAT_{fP}$. This short notation though only covers the first four groups of *NFAT*. *NFAT5* is not considered in this thesis.

The protein itself allows gene transcription via a signaling cascade, see figure 3.5 for an overview: *NFAT* is phosphorylated in resting T-cells on at least 21 serine residues. Eighteen of these are located in the regulatory domain, the so called N-terminal. Fourteen of these eighteen are a conserved sequence motif in the *NFAT* family.

In a nutshell, during immune response, the concentration of Ca^{2+} rises caused by opening of pores in T-cells. These ions then activate the Ca^{2+} sensor *calmodulin*, which then activates in turn the phosphatase *calcineurin* in cytoplasm of T-cells.[4] The phosphatase *calcineurin* dephosphorylates thirteen phosphorylation sites of *NFAT*, [37] , thus a decrease in the concentration of

3.4 Note, concentrations of *calcineurin* are not measured usually. Instead, the reaction network is controlled via changes of concentrations in Ca^{2+} resulting in changes of *calcineurin* concentration.

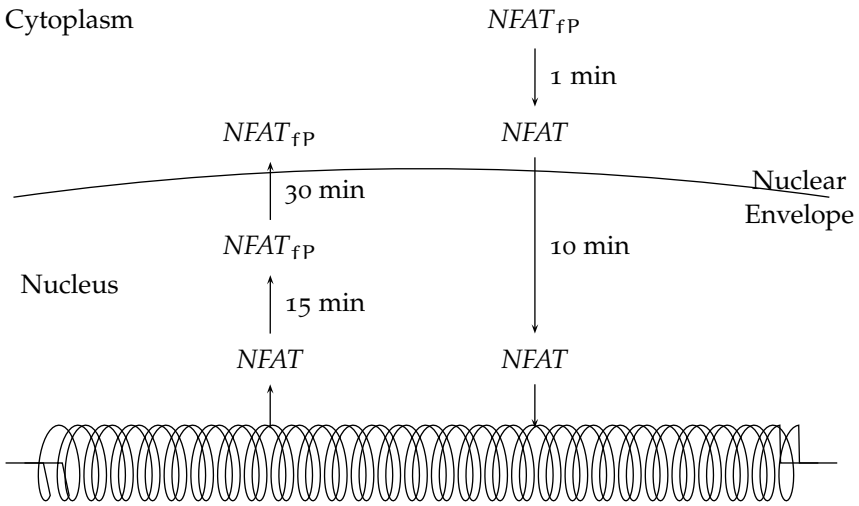

Figure 3.5: *Schematic description of dephosphorylation and transport of NFAT into the nucleus and further gene transcription and rephosphorylation of NFAT, and transport of $NFAT_{fP}$ into the cytoplasm. Kinetics and thus exact parameters for NFAT de-/phosphorylation and nuclear translocation vary with cell type and stimulation conditions, [25]. Still qualitative kinetics can be provided for general transport mechanisms during NFAT activation. Transport and reaction times given here are a summary of the work of [20, 47, 64, 94] and [100].*

unphosphorylated *NFAT* can be found. Dephosphorylation of these thirteen sites results in exposure of a nuclear localization signal in the regulatory domain and mask of a nuclear export sequence. With exposure of the nuclear localization signal and unphosphorylation of thirteen sites, the protein is in its maximum state of transcriptional activity. It is then transported into the nucleus where it binds to specific *DNA* response elements to regulate gene transcription of *Interleukin-2*, e. g. [12]. After gene transcription *NFAT* decouples from the *DNA* and is phosphorylated by *CK1* and *GSK3*, [77]. These two kinases synergize for rephosphorylation of *NFAT* resulting in exposure of the nuclear export sequence. The kinase *CK1* phosphorylates proteins located at the *SRR-1* motif, the region of the nuclear translocation signal, and *GSK3* phosphorylates the protein on its *SP* motif, the region of the nuclear export signal, [84]. Thus, if only the second kinase is present, the protein stays in nucleus as the nuclear localization signal is not masked, see again work in [77] on fine tuning of *NFAT* functions via phosphorylation by different kinases. The two forms of *NFAT* enable a conformational switch. After the nuclear export signal is exposed and the nuclear localization one masked, nuclear export of the fully phosphorylated form of the protein takes place. Furthermore, the phosphatase *calcineurin* can enter the nucleus via nuclear pores prolonging the stay of *NFAT* in nucleus, [39, 95]. For an overview on the phosphorylation process as well as transition times between the single states see figure 3.5.

To validate the range of values for rate constants and concentrations, different literature values are used and described quantitatively in figure 3.5. Dephosphorylation of *NFAT* takes place in about 1 minute [64]. In literature, data can be found to show that *NFAT* rests in the nucleus for about one hour and nuclear translocation takes about 10 minutes, [64]. Transport from the nucleus into the cytoplasm takes about 30 minutes, [65]. Phosphorylation in the nucleus takes about 15 minutes, [65]. Furthermore by stimulating

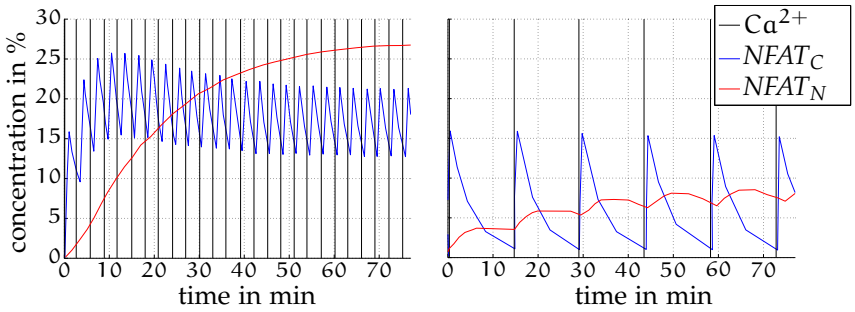

Figure 3.6: *Reproduction of modelling data by [104] describing translocation of NFAT via Ca^{2+} oscillations. High frequency in three minute intervals lead to nuclear translocation of dephosphorylated NFAT whereas low frequencies of fifteen minute intervals result only in slight nuclear translocation of NFAT together with periodic dephosphorylation of cytosolic NFAT followed by nuclear translocation. Note that Ca^{2+} pulses correspond to 100 % concentration in the figures given. They result in calcineurin oscillations (not shown here).*

NFAT periodically, its activity signal will be averaged by the import and export kinetics, [47, 93].

This process is considered as the activation of *NFAT* as it leads to immune response. It follows a rather complicated mechanism of distinct *calcineurin* activation. Brief activation of Ca^{2+} and thus brief increase of *calcineurin* concentration results only in degradation of mast cells, [37]. Usually, levels of Ca^{2+} are elevated for several hours after initial contact of T-cells with antigen pulsed B-cells. But a simple increase of Ca^{2+} levels is not sufficient for *NFAT* activation. The progression of the increase is of importance as well: for example a transient high spike of Ca^{2+} results in activation of *NFκB* and *JNK1*. Whereas a prolonged low increase in Ca^{2+} activates *NFAT*.

Modeling results with oscillating phosphatase concentrations indicate already a more complex reaction scheme, see figure 3.6 adapted from [104]: oscillations of Ca^{2+} as initial inducer of *calcineurin* activity cause oscillations of cytosolic *NFAT*. Thus, cytosolic *NFAT* is actually able to respond in an oscillatory way. In response to these oscillations, nuclear *NFAT* may or may not oscillate: high frequencies of Ca^{2+} impulses do not yield oscillations of nuclear *NFAT*. Low frequencies, on the other hand, induce indeed oscillations of nuclear *NFAT* with a low amplitude.

These findings, based on experimental results and reproduced via mathematical models, give rise to several questions. First, one might ask whether the oscillations of nuclear *NFAT* is actually the result of *calcineurin* oscillations, i. e., in engineering terms, whether *NFAT* oscillation is a forced oscillation. Or is the underlying system of *NFAT* phosphorylation able to produce oscillations on its own. Finally, one might ask whether the response curves of *NFAT* concentrations, i. e., linear or oscillating with small frequencies, are actually a result of an averaged response stabilizing over time, i. e., the expected high frequency in figure 3.6 cannot be resolved at all by experiments. Or, whether it could be resolved correctly, displaying a distinct complex response curve resulting from multiple states.

Furthermore, oscillations of Ca^{2+} can either yield oscillatory responses of cytosolic *NFAT*, see figure 3.6 Or they can lead to a higher activation concentration of *calcineurin* without *calcineurin* oscillating itself, [26]. Spikes of lower concentrations of Ca^{2+} evoke only a transient nuclear translocation of *NFAT*, where approximately half of the present *NFAT* proteins returned to the cytoplasm after Ca^{2+} returned to the baseline concentration, [26], and

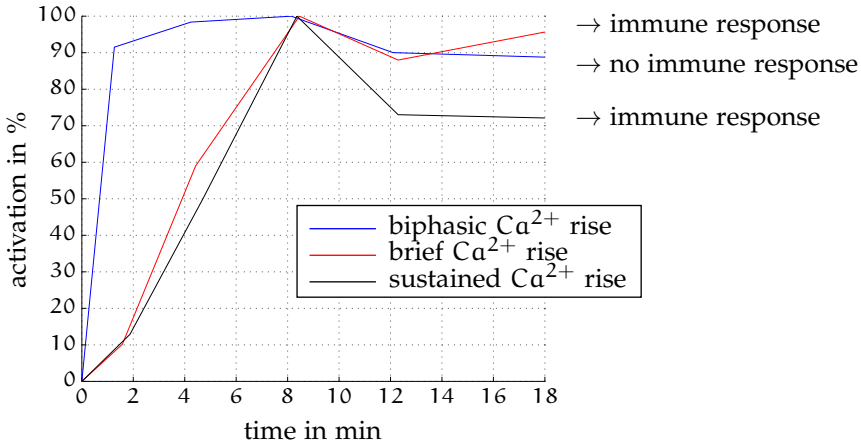

Figure 3.7: *Reproduction of measurement data in [26]: Activation of NFAT as a response to different concentration levels of Ca^{2+} activation. Depicted are always responses of cytosolic NFAT: the blue curve describes the response towards a biphasic Ca^{2+} rise resulting in cytosolic NFAT activation but only a transient translocation into the nucleus. A high spike of Ca^{2+}, response in red curve, as well as a sustained rise in Ca^{2+}, response in black curve, results in a sustained NFAT translocation into the nucleus. Though both the red and black curve result nuclear translocation and final immune response, they show different levels of activation.*

the remaining half staying in the nucleus. Same experimental results can be found, if concentration of Ca^{2+} and thus activator of *calcineurin* returns to baseline: half of the activated *NFAT* returns to the cytoplasm while the rest remains active in the nucleus resulting in multistationarity, see as well figure 3.7.

A condensed model of *NFAT* cycling can be found for example in [39] with a reduced model of only two phosphorylation states: unphosphorylated *NFAT* and fully phosphorylated $NFAT_{fP}$. Rates as well as concentrations for this reduced model are provided. Rates are given in terms of Michaelis-Menten like rate constant, where the ratio of rate constants is given in terms of the rate constant of nuclear translocation of *NFAT* over activation rate constant of calcineurin, [20], i. e., the association rate constant in equation (3.3):

$$k_M = 535\,\text{nmol/l}.$$

In general the following ranges for concentrations can be found in literature together with the quantitative data provided in figure 3.5, see for example [20] as well as [96] for further work on *NFAT* together with the already mentioned work above:

$$\begin{aligned}[NFAT]_{tot} &\in [2.0,\ 1000]\ \mu\text{mol/l},\\ \textit{calcineurin} &\in [1,\ 1000]\ \mu\text{mol/l},\\ Ca^{2+} &\in [2.0,\ 60]\ \text{nmol/l}.\end{aligned}$$

As the focus of the thesis lies on multisite phosphorylation processes, only the phosphorylation process of the *calcineurin*/*NFAT* network will be considered. For an overview on the reaction network see work by F. Macian as well as the extensive work of Ch. Loh, et al., and H. Okamura.

Although the phosphorylation network of *NFAT* is highly complex and, up until now, not completely understood the interesting question is again,

whether a very small part of it can exhibit multistable states, or if the process is, by itself without higher-level reactions, only able to show a stable response curve based on a single steady state.

Before discussing these different phosphorylation networks, i. e., the standard network of n-times phosphorylation, networks allowing additionally synthesis and/or degradation of (phosphorylated) proteins and/or enzymes, and networks with compartmentalization, theoretical findings from literature on multisite phosphorylation networks are discussed.

The writing of some men
is like a vast bridge
that carries you over
the many things
that claw and tear.

— Charles Bukowski

4

KNOWN THEORETICAL RESULTS FOR MULTISITE PHOSPHORYLATION NETWORKS AND CHEMICAL REACTION NETWORKS IN GENERAL

(Bio-) chemical reaction networks and in particular multisite phosphorylation processes have been subject to study for quite a long time. With multisite phosphorylation processes appearing in a variety of cellular processes not only the reaction network itself, but also its dynamics have been of interest. This chapter introduces related literature to the work at hand. Though considerably more literature exists, the focus is set on three works, and the interested reader is advised to follow literature given here or in the work of the cited authors.

Starting with the work of J. Gunawardena, and comparable work by C. Salazar and T. Höfer, a multisite phosphorylation process is introduced yielding steady states and insight on the properties of networks exhibiting switch like response curves. This introduction is followed by the prediction of a higher number of steady states as introduced by the work of M. Feinberg on chemical reaction network theory. It builds the basis of this thesis, as it gives rise to the idea, that not only single steady states can reveal a switch like response curve, but also multiple steady states resulting in rather s-shaped curves than strictly monotone functions of sharp steps. It is then rounded off by the work of L. Wang and E. D. Sontag on upper and lower bounds on the number of steady states in distributive phosphorylation processes.

4.1 A GOOD THRESHOLD BUT POOR SWITCH BY MULTISITE PHOSPHORYLATION

In this thesis, a multisite phosphorylation process with a distributive mechanism is analyzed. Work already exists on this topic, but the focus lies on arising dynamics to achieve a switch like response curve based on univalued response curves and not on s-shaped response curves.

Whereas J. Gunarwardena, see [42], considers only a distributive, sequential phosphorylation the work of C. Salazar and T. Höfer, see for example [85], covers different mechanisms (sequential, random and various cyclic mechanisms). Both papers are based on the same reaction network with an initial sequential, distributive phosphorylation network, that can also be translated into the networks used throughout this thesis.

To derive rate laws for the reaction mechanism they assume Michaelis-Menten mechanism to hold, see equation (3.1) on page 15. They justify this approach, by assuming that low enzyme concentrations are present

compared to substrate concentration , i. e., $[A] \gg [K]$, $[A] \gg [P]$, compare network (N3.2). This results in fast reaction constants, e. g., $k_1 \gg k_3$, see network (N3.1). Making furthermore a rapid-equilibrium approximation, e. g., $d[AK]/dt = 0$, $d[A_PP]/dt = 0$, reduces the number of reactions rates enabling numerical analysis. They reduce the derived system of ordinary differential equations further, compare equation (2.3), by merging variables, e. g., considering $[A] + [AK] + [AP]$ instead of individual variables.

Having simplified the ordinary differential equations for the network this far, they provide solutions for the steady state response curve at a phosphorylation step $i = 1, \ldots, n$, i. e., $([A_{iP}] + [A_{iP}K] + [A_{i-1P}P]/([A]_{tot} + [K]_{tot} + [P]_{tot})$ over $[K]_{tot}/[P]_{tot}$), and the transition time of the system can be given, i. e., the time needed for changes in concentration of the fully phosphorylated protein. Results are summarized briefly for each reaction mechanism considered. For detailed analysis of the reaction network see the cited papers. The following conclusions are drawn in terms of response curves towards changes in $[K]_{tot}/[P]_{tot}$:

SEQUENTIAL MECHANISM With an increasing n the steady state response curve resembles a step function. For $n = 1$ the curve corresponds to a standard Michaelis-Menten steady state response curve. The step function gives rise to a more threshold like response for changes in the activity of the two enzymes. But the fully de-/phosphorylated forms can only be achieved for extreme values of $[K]_{tot}/[P]_{tot}$.

RANDOM MECHANISM The response curve is less steep than for the sequential mechanism. A clear step shape appears way later for this mechanism than for the sequential one. As there are more intermediate states of the phosphorylated substrate, more partially phosphorylated substrates can be found for moderate values of $[K]_{tot}/[P]_{tot}$. Even larger values than for the sequential mechanism are needed to achieve a fully de-/phosphorylated form.

CYCLIC MECHANISM The steady state response curve is even less steep than the one for the random mechanism.[1]

Overall, at most step functions can be found but no s-shaped or multivalued curves, a consequence of the assumptions made on kinetics, i. e., quasi steady state and fast phosphorylation reaction. Thus, switching in the network is here only enabled via the step functions.

Furthermore, C. Salazar and T. Höfer compute effective Hill coefficient n_H for each mechanism, a measure for the sensitivity of the network. I. e., cooperative binding of a protein already bound to an enzyme is increased ($n_H > 1$) or decreased ($n_H < 1$), compare also figure 3.1 on page 16. They find two cases yielding a switch like response curve based on step functions in phosphorylation networks:

1. Enzyme concentration in the network is very low and enzyme binding shows a negative cooperativity.
2. Enzyme concentration is high and enzyme binding shows a positive cooperativity.

The first case is described as zero-order ultra sensitivity and does not depend on multiple phosphorylation sites but can be found at proteins with one phosphorylation site.

4.1 A cyclic mechanism corresponds to a sequential mechanism, but dephosphorylation follows inverse order of protein de-binding than phosphorylation.

Combining cooperativity for catalytic rate constants, e. g., k_3, with the two necessities above, the system can exhibit a bistable response curve. This bistable curve then results in a switch like response of the system. As the initial assumptions, i. e., quasi steady state and fast phosphorylation reaction, are quite strict on the reaction networks, they conclude that only strict conditions on the network enable multistability:

- Efficient competition between unphosphorylated and phosphorylated targets for binding to enzymes.
- Total enzyme concentration must be low enough for competition.
- The unphosphorylated protein must be phosphorylated slowly. The fully phosphorylated protein must be dephosphorylated slowly.

Concentration of substances and rate constants are not the only values influencing the shape of the response curve. An additional degree of freedom can be found by the order of phosphorylation, i. e., sequential vs. cyclic vs. random mechanism. Having a fixed order for the sequential mechanism, a sharp steady state response curve can be found. The random and cyclic mechanism show flatter response curves than the sequential one. Furthermore, the concentrations of the partially phosphorylated states of the cyclic and random mechanisms are higher than for the sequential. This difference is even more pronounced for higher networks with higher phosphorylation steps due to the growing number of intermediate states. Due to this number, they conclude that a higher ratio of kinase activity to phosphatase concentration is needed to achieve full phosphorylation of the protein.

These results corresponds to the work of J. Gunarwardena, as he makes the same assumptions for reactions and concentrations in the network.[2] He concludes, that multisite protein phosphorylation can make a good threshold but a poor switch, [42].

A lot of assumptions on the concentrations in the system are made. They are indeed valid for invitro (bio-) chemical reaction networks. But invivo reaction networks are subject to cell compartmentalization resulting in, for example, different concentration levels, or restrictions in reaction rates, see 3.1.1 on page 17. Thus, assumptions made above might not be valid for all reaction networks. Furthermore, networks showing an actual multistable response curve are known, see 3.2. The question arises whether networks can be constructed showing at least a bistable response curve with less restrictions on the phosphorylation network itself then the ones above. For example, C. Conradi constructs such a network with less assumptions than C. Salazar and T. Höfer. This network shows response curves with an s-shaped response curve. As the work of C. Conradi is the overall basis of this thesis, an excursion towards chemical reaction network theory follows presenting the fundamental ideas behind his work.

4.2 ESTABLISHING BISTABILITY IN CHEMICAL REACTION NETWORKS

Solving ordinary differential equations based on (bio-) chemical reaction networks (with mass action kinetics) is not always an easy task, because often a large number of species and unknown rate constants are present.

4.2 Note that the phosphorylation process used in this thesis can be completely translated into the system described by C. Salazar and T. Höfer, and thus yields under the same restrictions the same results.

Thus, instead of solving the arising system of ordinary differential equations, prediction on the properties is welcomed. Already in 1987, M. Feinberg introduced a method guaranteeing existence and uniqueness of steady states in (bio-) chemical reaction networks under certain restrictions, see also [31, 32, 33, 35]. For more recent work see [16, 27, 81].

The structure of the (bio-) chemical reaction network allows already to draw conclusions about the existence and uniqueness of (multiple) steady state of the underlying reaction network. The theory is based on an index called deficiency ϑ. Besides the already introduced number of species of a network, n, the number of reactions, r, the number of complexes, m, and the rank s of the stoichiometric matrix N, see section 2.2, a further variable is introduced: The network is divided into complexes that are linked together. For network (N2.1) on page 7 three groups of these linked complexes, the so called linkage classes of the network, can be found:

$$\{2A + B,\ A_2B,\ C + B\};\ \{C,\ D + E\};\ \{A + D,\ E\}.$$

The number of linkage classes l can be used to compute the deficiency ϑ of the network:

$$\vartheta = m - l - s.$$

Thus, for the given example network in (N3.1): $n = 6$, $m = 7$, and $s = 4$, and $l = 3$, the deficiency can be given by $\vartheta = 0$. The Deficiency Zero Theorem allows to draw conclusions on the existence of steady states if the deficiency is zero:[3]

- If the network is not weakly reversible,[4] the ordinary differential equations of the network cannot admit a positive steady state for any kinetics applied and any rate constants endowed to the system.
- If the network is weakly reversible, then exactly one asymptotically stable steady state exists in every coset $(x_0(t) + \mathrm{im}(S)) \cap \mathbb{R}^r_{\geqslant 0}$ for mass action kinetics.

As the given example network (N2.1) has $\vartheta = 0$ and is indeed not weakly reversible, the first statement holds true and any further analysis of the network concerning qualitative analysis is not necessary.

To address a broader class of reaction networks, the Deficiency Zero Theorem is extended in [30] by the Deficiency One Theorem. The reader is advised to follow detailed work in [22, 31, 32] and [33]. Reaction networks of deficiency zero build a subset of reaction networks, where the Deficiency One Theorem holds. For reaction networks of deficiency zero, the deficiency of each linkage class is zero and the deficiency of the entire network is equal to the sum of the deficiencies of the individual linkage classes, [30]. For reaction networks of deficiency one the deficiency of individual linkage classes can be no greater than one. If each linkage class of the reaction network contains just one terminal strong linkage class, the deficiency of the linkage classes is not greater than one and the sum of the deficiencies of the linkage classes is equal to the deficiency of the entire reaction network, then:

4.3 More conclusions can be drawn, but only necessary ones building the background of this thesis are provided.

4.4 Reaction networks are reversible, if each reaction is accompanied by its reverse reaction. They are weakly reversible, if there is a direct pathway from one complex to another, even via further complexes. Reaction network (N2.1) is not (weakly) reversible. If additional reactions from $C + B$ back to A_2B, and from $D + E$ back to C would be included, the network would become reversible.

- Ordinary differential equations based on mass action kinetics can admit no more than one stable steady state with positive rate constants k under some restrictions on the reaction network.

- And, if furthermore, the network is weakly reversible, then differential equations based on mass action kinetics admit exactly one positive steady state for a given vector of rate constants.

As an extension to the Deficiency Zero and One Theorems, the Advanced Deficiency Algorithm allows to draw further conclusions.

- For networks having exactly one linkage class, $l = 1$, with $\vartheta \geqslant 1$ (and further restrictions), the ordinary differential equations based on mass action kinetics can admit multiple steady states for a given k.

Thus, without solving the ordinary differential equations, conclusions can be drawn on the number of steady states the network can exhibit. Further work exists for networks not fulfilling these conditions, for example [8] and [27], extending the work of M. Feinberg. A toolbox based on the chemical reaction network theory exists, [34], allowing to draw conclusions in a simple manner. Here, only the reaction network has to be inserted. The toolbox provides an answer whether the network exhibits multiple steady states in the same coset and provides exactly one parameter set in case these exists.

Nonetheless, the deficiency theorems themselves only provide qualitative answers. Using the toolbox, they provide, if possible, exactly one pair of solutions. The theorems give rise to an algorithm introduced in [15] by C. Conradi, to check whether multiple steady states exist in the same coset in a double phosphorylation network of multisite phosphorylation. This algorithm furthermore provides a parametrization of rate constants and concentrations, see for example the thesis of C. Conradi and consecutive work. This algorithm will be exploited in chapter 5 for n site multisite phosphorylation networks. Variations thereof are introduced in chapter 6 and 7 providing solutions for further networks. An algorithm is provided to check if a mass action network can exhibit at least two positive steady states for a certain parameter vector k in the same coset. The algorithm is only dependent on the network structure itself and not inherently on the differential equations stated by the network or further strict assumptions like quasi steady states and fast phosphorylation reactions. Further, it allows the computation of the actual steady states to the system.

4.3 BOUNDS FOR THE NUMBER OF STEADY STATES IN MULTISITE PHOSPHORYLATION NETWORKS

The work of L. Wang and E. D. Sontag conjectures an upper bound for the number of steady states an n-site sequential, distributive phosphorylation network can exhibit in the same coset. Ordinary differential equations describing the network are provided, assuming that the mass action law holds. A system of $3n + 3$ ordinary differential equations arises, see section 5.1 for a description of the state space. The system is reduced by a transformation of coordinates. Only two equations remain. Instead of solving a system of $3n$ ordinary differential equations ($3n + 3$ ordinary differential equations - 3 conservation relations) to find multiple steady states, the problem is shifted to solve only two polynomials by finding their positive roots corresponding

to steady states. The interested reader is referred to [119] and the solution algorithm therein for finding these positive roots.

The question of the number of steady states a sequential, distributive multisite phosphorylation system can exhibit is coupled to properties of the rate constants as biological parameters. If rate constants are close to Michaelis-Menten conditions, $[S]_{tot} \gg [E]_{tot}$, they proof a lower bound for the number of steady states by $n+1$ for even phosphorylation steps n, and n for odd n in their first theorem. They proof furthermore an upper bound of $2n-1$ positive steady states for rate constants of mass action in their third theorem. This upper bound is fine tuned late on, where they proof an upper bound under Michaelis-Menten conditions and an additional condition of at most $n+1$ positive steady states in the fourth theorem. Furthermore, for conditions far from Michaelis-Menten, they proof that at most one positive steady state can be found in their fifth theorem. As they expect the number of steady states to change continuously and bounds coincide under some restrictions, they conjecture that there are at most $n+1$ (n) steady states for n even (or odd) phosphorylation steps under any conditions, .

Thus, only lower and upper bounds on the number of steady states can be given, though it is indeed remarkable, that bounds can be provided at. Nonetheless, a parametrization of states is still missing. The work at hand closes the gap between these different works and provides a parametrization for various phosphorylation network setups in the following chapters and find answers on the existence of multistable states in sequential, distributive phosphorylation networks.

But I come with a dream in my eyes tonight,
And I knock with a rose at the hopeless gate of your heart –
Open to me!
For I will show you the places Nobody knows,
And, if you like,
The perfect places of Sleep.

You are tired, (I think) — E. E. Cummings

5 MULTISTATIONARITY IN MULTISITE PHOSPHORYLATION NETWORKS

To introduce the used nomenclature and algorithm of this thesis, the work by C. Conradi on double-phosphorylation networks and the diploma thesis, [49], of the author on n-times phosphorylation networks are given for an overview. This mechanism of n-times phosphorylation is analyzed and standard nomenclature is introduced. Work therein is extended, and a novel theorem and proof of the result are presented. Furthermore a novum algorithm is introduced to provide the multistable region. The chapter is rounded off by an analysis of parameter values in the multistationarity region and its relevance towards actual biological data.

5.1 MULTISITE PHOSPHORYLATION OF PROTEINS IN N STEPS

A phosphorylation/dephosphorylation process in n steps is analyzed, see figure 5.1: the phosphorylation is catalyzed by an enzyme, a kinase K, and is described by the upper branch. The dephosphorylation is catalyzed by a different enzyme, a phosphatase P, and is described by the lower branch. The substrate and its phosphorylated form is represented by an A and a corresponding subscript nP, where n describes the order of phosphorylation and i the current phosphorylation step $1 \leqslant i \leqslant n$. For a double phosphorylation with $n = 2$ this network represents a single layer of the Mitogen-activated protein kinase (*MAPK*) cascade. Especially considering the mammalian extracellular signal-regulated protein kinase (*ERK*) cascade the substrate represents the protein *ERK*. The kinase describes *RAS* and the phosphatase *Clb*, [92].

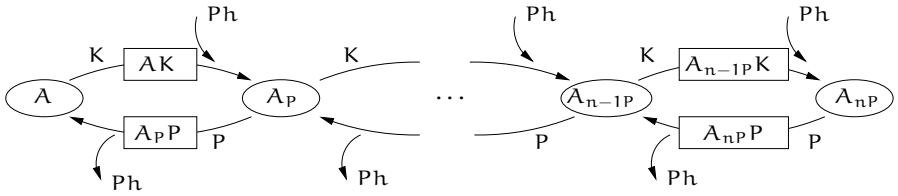

Figure 5.1: *Simplified reaction model of a distributive phosphorylation process in n steps. The catalytic active enzymes are denoted by K and P for kinase and phosphatase, respectively, the (phosphorylated) proteins by A and a corresponding subscript. The phosphate group attaching to the substrate is denoted by Ph.*

Different phosphorylation processes exist in nature. For example, the order of phosphorylation, i. e., order of binding phosphate groups to individual regions on proteins, can follow a random, a sequential or a mixed

mechanism. The phosphorylation process itself can follow a processive or distributive mechanism. As given by assumption 3.2 and 3.1 on page 14, here only networks following a sequential, distributive mechanism are analyzed. Furthermore, in phosphorylation networks a varying number of enzymes can be found, de-/phosphorylating the individual phosphate groups attached to the protein:

Assumption 5.1. Throughout this thesis each branch is catalyzed by just one enzyme form, K and P, respectively.

This assumption is valid as a simplification. Often the exact number and the principle behind phosphorylation by a kinase are not known in detail, and phosphorylation is only modeled in a reduced way assuming existence of a certain number of kinases phosphorylating the protein together. This phosphorylation mechanism of sequential, distributive phosphorylation with one kinase and phosphatase forms is referred to as the standard phosphorylation mechanism.

To model the underlying mechanism of the de-/phosphorylation network the concentration of substances is described by a vector x with $x_i \geqslant 0$, $x \in \mathbb{R}^n_{\geqslant 0}$. Rate constants are denoted by a vector k with $k_i \geqslant 0$, $k \in \mathbb{R}^r_{\geqslant 0}$. Following assumption 2.1, all rates are irreversible. Thus, each reaction is labeled separately. Against standard notation (labeling one substance after another, starting with the upper branch in figure 5.1 and finishing with the lower branch and thus the complex A_nP) a stepwise nomenclature is introduced: each substance is labeled according to its appearance in the network. I. e., each phosphorylation step introduces new species in the network, thus they are labeled after the species and rates of the former step are described: the concentration of the unphosphorylated protein [A] and the enzymes [K] and [P] are described by x_2, x_1 and x_3 respectively. In the second step the concentration of the single phosphorylated protein [A_P] and arising enzyme complexes, [AK] and [AP], are described by x_5, x_4 and x_6 respectively. This formalism is continued for all steps up to n and yields finally $[A_{i-1P}] = x_{3i-1}$ for $i = 1, \ldots, n+1$ (or $[A_{iP}] = x_{3i+2}$ for $i = 2, \ldots, n$), and $[A_{i-1P}K] = x_{3i+1}$ and $[A_{iP}P] = x_{3i+3}$ for $i = 1, \ldots, n$. This notation allows a more intuitive handling of the network and enables an easy recognition of each step in the network matrices, and therefore, a more efficient way to solve the posed multistationarity problem. The following network describes the phosphorylation

$$\begin{aligned} &\overset{x_1}{K} + \overset{x_2}{A} \underset{k_2}{\overset{k_1}{\rightleftharpoons}} \overset{x_4}{AK} \xrightarrow{k_3} K + \overset{x_5}{A_P} \underset{k_8}{\overset{k_7}{\rightleftharpoons}} \overset{x_7}{A_PK} \xrightarrow{k_9} \cdots \\ &\xrightarrow{k_{6n-9}} K + \overset{x_{3n-1}}{A_{n-1P}} \underset{k_{6n-4}}{\overset{k_{6n-5}}{\rightleftharpoons}} \overset{x_{3n+1}}{A_{n-1P}K} \xrightarrow{k_{6n-3}} K + \overset{x_{3n+2}}{A_{nP}} \end{aligned} \tag{$\mathcal{N}$5.1a}$$

and dephosphorylation

$$\begin{aligned} &P + \overset{x_{3n+2}}{A_{nP}} \underset{k_{6n-1}}{\overset{k_{6n-2}}{\rightleftharpoons}} \overset{x_{3n+3}}{A_{nP}P} \xrightarrow{k_{6n}} P + A_{n-1P} \underset{k_{6n-7}}{\overset{k_{6n-8}}{\rightleftharpoons}} \cdots \\ &\cdots \underset{k_{11}}{\overset{k_{10}}{\rightleftharpoons}} \overset{x_9}{A_{2P}P} \xrightarrow{k_{12}} P + A_P \underset{k_5}{\overset{k_4}{\rightleftharpoons}} \overset{x_6}{A_PP} \xrightarrow{k_6} \overset{x_3}{P} + A. \end{aligned} \tag{$\mathcal{N}$5.1b}$$

In total $3n + 3$ states x_i described by their concentrations x, and $6n$ rate constants k_i are needed for network ($\mathcal{N}$5.1).

The reaction mechanism can be given in form of ordinary differential equations by assuming that the mass action law holds, see assumption 2.2 on page 9. The stoichiometric matrix $N \in \mathbb{R}^{(3n+3)\times 6n}$ and the vector of reaction rates $v \in \mathbb{R}^{6n}$ are used to describe the network.

$$\frac{dx}{dt} = Nv(k, x). \tag{5.1}$$

Network matrices, among them the stoichiometric matrix N, and the vector of reaction rates v are introduced below.

The aforementioned stepwise nomenclature results in a block structure of the stoichiometric matrix:

$$N^{(1)} = \begin{bmatrix} n_{11} \\ n_{21} \end{bmatrix}, \quad N^{(2)} = \left[\begin{array}{c|c} N^{(1)} & \begin{matrix} n_{12} \\ n_{22} \end{matrix} \\ \hline 0_{3\times 6} & n_{21} \end{array}\right],$$

$$N^{(3)} = \left[\begin{array}{c|c} N^{(2)} & \begin{matrix} n_{12} \\ 0_{3\times 6} \\ n_{22} \end{matrix} \\ \hline 0_{3\times 12} & n_{21} \end{array}\right], \quad \ldots,$$

$$N^{(n)} = \left[\begin{array}{c|c} N^{(n-1)} & \begin{matrix} n_{12} \\ 0_{3(n-2)\times 6} \\ n_{22} \end{matrix} \\ \hline 0_{3\times 6(n-1)} & n_{21} \end{array}\right] \tag{5.2}$$

with the superscript describing the number of phosphorylation steps and

$$n_{11} = \begin{bmatrix} -1 & 1 & 1 & 0 & 0 & 0 \\ -1 & 1 & 0 & 0 & 0 & 1 \\ 0 & 0 & 0 & -1 & 1 & 1 \end{bmatrix},$$

$$n_{12} = \begin{bmatrix} -1 & 1 & 1 & 0 & 0 & 0 \\ 0 & 0 & 0 & 0 & 0 & 0 \\ 0 & 0 & 0 & -1 & 1 & 1 \end{bmatrix},$$

$$n_{21} = \begin{bmatrix} 1 & -1 & -1 & 0 & 0 & 0 \\ 0 & 0 & 1 & -1 & 1 & 0 \\ 0 & 0 & 0 & 1 & -1 & -1 \end{bmatrix},$$

$$n_{22} = \begin{bmatrix} 0 & 0 & 0 & 0 & 0 & 0 \\ -1 & 1 & 0 & 0 & 0 & 1 \\ 0 & 0 & 0 & 0 & 0 & 0 \end{bmatrix}.$$

The stoichiometric matrix neither has full row nor column rank, thus a left and right nullspace can be computed. The matrix $W \in \mathbb{R}^{(3n+3)\times 3}$ is introduced, referred to as the matrix of conservation laws, whose columns form a basis of the left nullspace of the stoichiometric matrix N, see also page 10. The rank of W is three. Thus, one choice of W is given by three independent conservation relations in the network: if the network operates in a closed space, as is so far considered for network (№5.1), the total concentration

of the species is conserved. This is reflected in the following conservation relation:

$$\langle w_j, x\rangle = c_j, \qquad j = 1, 2, 3, \tag{5.3}$$

recall w_j as columns of $W = (w_1, w_2, w_3)$ and c_1 associated with the total concentration of K and its protein-complexes, c_2 with P and its protein-complexes, and c_3 with A and its phosphorylation forms respectively. In a compressed form the matrix can be given by:

$$W^{(n)^T} = \left[\begin{array}{ccc|ccc|c|ccc} 1&0&0&1&0&0&&1&0&0\\ 0&0&1&0&0&1&\cdots&0&0&1\\ 0&1&0&1&1&1&&1&1&1 \end{array}\right]. \tag{5.4}$$

n-times

Later on, different network setups are considered where not always a left nullspace appears.

Besides the left nullspace for $N^{(n)}$, a right nullspace can be found. The columns of the matrix $E^{(n)} \in \mathbb{R}^{6n\times 3n}$ form a basis of this right nullspace:

$$E^{(n)} = \begin{bmatrix} E^{(1)} & & \\ & \ddots & \\ & & E^{(1)} \end{bmatrix} \tag{5.5}$$

with

$$E := E^{(1)} = \begin{bmatrix} 1&0&1\\ 1&0&0\\ 0&0&1\\ 0&1&1\\ 0&1&0\\ 0&0&1 \end{bmatrix}. \tag{5.6}$$

See appendix A.1 on page 137 for a proof on columns of $E^{(n)}$ being generators of $\ker(N^{(n)}) \cap \mathbb{R}^{6n}_{\geqslant 0}$.

The vector of reaction rates shows a reappearing structure due to the network setup and the chosen nomenclature:

$$\begin{aligned} v(k,x) &= \operatorname{diag}(k)\,\Phi(x), \\ &= [k_1 x_2 x_1,\ k_2 x_4,\ k_3 x_4,\ k_4 x_5 x_3,\ k_5 x_6,\ k_6 x_6,\ \ldots,\\ &\quad k_{6i-5}x_{3i-1}x_1,\ k_{6i-4}x_{3i+1},\ k_{6i-3}x_{3i+1},\\ &\quad k_{6i-2}x_{3i+2}x_3,\ k_{6i-1}x_{3i+3},\ k_{6i}x_{3i+3},\ \ldots\\ &\quad k_{6n-5}x_{3n-1}x_1,\ k_{6n-4}x_{3n+1},\ k_{6n-3}x_{3n+1},\\ &\quad k_{6n-2}x_{3n+2}x_3,\ k_{6n-1}x_{3n+3},\ k_{6n}x_{3n+3}]^T, \end{aligned} \tag{5.7}$$

with $i = 1, \ldots, n$ and the monomial vector

$$\Phi(x) := \left[\begin{array}{ccc} x^{y_1} & \cdots & x^{y_{6n}} \end{array}\right]^T, \tag{5.8}$$

and y_i columns of $Y^{(n)}$, see the next paragraph. Recall equation (2.2) on page 9. The vector of reaction rates $v(k,x)$ describes the coupling between

each substance and the single rate constants. Each y_i describes an educt complex of the network. Complexes of the network describe single network nodes, see network (N2.2) on page 7 for an introduction. The tilde is used to differ between elements y as educt complexes and $\tilde{y}$ as complexes of the reaction network. Complexes $\tilde{y}$ of the network are assigned in the same stepwise manner as was done for concentrations and rate constants: for example, for $n = 1$ complexes can be given by $\tilde{y}_1 = x_1 + x_2$, $\tilde{y}_2 = x_4$, $\tilde{y}_3 = x_1 + x_5$, $\tilde{y}_4 = x_3 + x_5$, $\tilde{y}_5 = x_6$ and $\tilde{y}_6 = x_3 + x_5$. The complexes are collected in a stepwise manner in the complex matrix $\tilde{Y}^{(n)} \in \mathbb{R}^{(3n+3)\times(4n+2)}$. Combining furthermore the complexes corresponding to their appearance as educts in the network itself yields the rate exponent matrix $Y^{(n)} \in \mathbb{R}^{(3n+3)\times 6n}$. Assigning each node unit vectors e_i of length $3n+3$, with ones at their ith position, yields its final form:

$$\begin{aligned}\tilde{Y}^{(n)} = [&e_1 + e_2 \;\; e_4 \;\; e_1 + e_5 \;\; e_3 + e_5 \;\; e_6 \;\; e_3 + e_2 \\ &e_7 \;\; e_1 + e_8 \;\; e_3 + e_8 \;\; e_9 \;\; \cdots \\ &e_{3i+1} \;\; e_1 + e_{3i+2} \;\; e_3 + e_{3i+2} \;\; e_{3i+3} \;\; \cdots \\ &e_{3n+1} \;\; e_1 + e_{3n+2} \;\; e_3 + e_{3n+2} \;\; e_{3n+3}]\end{aligned} \tag{5.9}$$

$$\begin{aligned}Y^{(n)} = [&e_1 + e_2 \;\; e_4 \;\; e_4 \;\; e_3 + e_5 \;\; e_6 \;\; e_6 \;\; \cdots \\ &e_1 + e_{3i-1} \;\; e_{3i+1} \;\; e_{3i+1} \;\; e_3 + e_{3i+2} \;\; e_{3i+3} \;\; e_{3i+3} \;\; \cdots \\ &e_1 + e_{3n-1} \;\; e_{3n+1} \;\; e_{3n+1} \;\; e_3 + e_{3n+2} \;\; e_{3n+3} \;\; e_{3n+3}]\end{aligned} \tag{5.10}$$

As the rate exponent matrix $Y^{(n)}$ is used thoroughly throughout this thesis, a different notation is presented as well:

$$Y^{(n)} = \left[\begin{array}{c} Y^{(n-1)} \\ \mathbf{0}_{3\times 6(n-1)} \end{array}\middle|\begin{array}{ccc} e_1 + e_{3n-1} & e_{3n+1} & e_{3n+1} \end{array}\right. \tag{5.11}$$

$$\left.\begin{array}{ccc} e_3 + e_{3n+2} & e_{3n+3} & e_{3n+3} \end{array}\right], \tag{5.12}$$

with

$$Y^{(1)} = \left[\begin{array}{cccccc} e_1 + e_2 & e_4 & e_4 & e_3 + e_5 & e_6 & e_6 \end{array}\right]. \tag{5.13}$$

Here, the stepwise structure can be seen with matrices of the former step $n-1$ appearing in the upper left corner of the matrices of n. The y_i given in equation (5.8) are the columns of $Y^{(n)}$. A representation U for the nullspace of the rate exponent matrix is chosen by $U^{(n)} \in \mathbb{R}^{6n\times(3n-2)}$, with $\operatorname{rank}(Y^{(n)}) = 3n+2$. See section A.2 on page 139 for a proof that columns of U span a basis for the nullspace of $Y^{(n)}$.

5.2 MULTISTATIONARITY IN MULTISITE PHOSPHORYLATION NETWORKS

The phosphorylation network is completely described by the differential equation, see (5.1). Given an initial x_0, the solution of equation (5.1) is confined to

$$W^T x(t) = W^T x_0 =: c.$$

Assuming that the considered network (N5.1) can at least exhibit two distinct steady states a and b with $a \neq b$, the differential equation (5.1) in terms of these two steady states can be given by

$$\begin{aligned} \frac{da}{dt} &= N\nu(k, a) = 0, \\ \frac{db}{dt} &= N\nu(k, b) = 0. \end{aligned} \tag{5.14}$$

This condition is referred to as the polynomial condition for multistationarity, see also definition 2.4 on page 11.

The conservation relation has to hold as well for both steady states yielding the same total concentration for the overall network:

$$\begin{aligned} & \langle w_j, b\rangle = c_j = \langle w_j, a\rangle, \quad \text{with } j = 1, 2, 3, \\ \rightarrow \quad & \langle w_j, b - a\rangle = 0. \end{aligned} \tag{5.15}$$

This condition is referred to as the coset condition for multistationarity, see the second part of definition 2.4.

Thus, (multiple) steady states, a and b, in the phase space of x_0 are defined by (5.14) and (5.15). Solutions for a and b are derived over the next two sections in two consecutive steps. The first one regards the solution of the polynomial condition in equation (5.14), the second one the solution of the coset condition in equation (5.15).

5.2.1 *The Polynomial Condition*

This section considers the arising polynomial of the system of ordinary differential equations given in equation (5.14). To solve this system in terms of two distinct steady states a and b, the polynomial condition is rewritten first.

Only non-negative concentrations $x_i \geqslant 0$ with $x \in \mathbb{R}^{3n+3}_{\geqslant 0}$ and non-negative rate constants $k_i \geqslant 0$ with $k \in \mathbb{R}^{6n}_{\geqslant 0}$ are considered. Thus, the vector of reaction rates ν is non-negative with $\nu_i \geqslant 0$ and $\nu \in \mathbb{R}^{6n}_{\geqslant 0}$, see equation (5.7). Therefore, in steady state the vector $N\nu$ lies in the pointed polyhedral cone, spanned by the cut of $\ker(N)$ and the non-negative orthant $\mathbb{R}^{6n}_{6n}$:

$$\begin{aligned} \nu(k, a) &\in \ker(N^{(n)}) \cap \mathbb{R}^{6n}_{\geqslant 0}, \\ \nu(k, b) &\in \ker(N^{(n)}) \cap \mathbb{R}^{6n}_{\geqslant 0}. \end{aligned} \tag{5.16}$$

This pointed polyhedral cone can be described by positive linear combination of its generators. Of course, in general $\nu(k, x)$ can exhibit arbitrary values, with $k \geqslant 0$ by definition, see assumption 2.1, and x arbitrary in a mathematical sense. But, in a bio-chemical meaningful sense, only positive solutions are of interest. Thus, with $x \geqslant 0$, generators for the pointed polyhedral cone result directly from the network, [99]:

$$\begin{aligned} \nu(k, a) &= E^{(n)}\lambda, \ \ \lambda \in \mathbb{R}^{3n}_{>0} \\ \nu(k, b) &= E^{(n)}\nu, \ \ \nu \in \mathbb{R}^{3n}_{>0}. \end{aligned} \tag{5.17}$$

Recall equation (5.5) for $E^{(n)}$. With ν given in terms of k_i and its corresponding a and b, the two equations in (5.17) can be rewritten using the row vectors ϵ_i of E for $i = 1, \ldots, 6n$:

$$k_i\, a^{y_i} = \epsilon_i\, \lambda \qquad\qquad k_i\, b^{y_i} = \epsilon_i\, \nu$$

Applying furthermore the logarithm and subtracting the first group of terms from the second group yields:

$$\langle \ln \frac{b}{a}, y_i \rangle = \ln \frac{\epsilon_i \nu}{\epsilon_i \lambda}.$$

Introducing

$$\mu_i = \ln(b_i/a_i) \tag{5.18}$$

and

$$\ln \frac{E^{(n)}\nu}{E^{(n)}\lambda} := \begin{bmatrix} \ln \frac{\epsilon_1 \nu}{\epsilon_1 \lambda} & \cdots & \ln \frac{\epsilon_{6n} \nu}{\epsilon_{6n} \lambda} \end{bmatrix}^T \tag{5.19}$$

yields finally

$$Y^{(n)^T} \mu = \ln \frac{E^{(n)} \nu}{E^{(n)} \lambda} \tag{5.20}$$

as a solution to the polynomial condition. To solve this problem, the following two matrices $\Pi^{(n)}$ and $M^{(n)}$ are introduced:

$$\Pi^{(n)} = \begin{bmatrix} \Pi(1) \\ \vdots \\ \Pi(n) \end{bmatrix} \tag{5.21}$$

with

$$\Pi(i) = \begin{bmatrix} (2-i)\underline{1} & (i-1)\underline{1} \end{bmatrix}, \quad i = 1, \ldots, n, \tag{5.22}$$

with $\underline{1}$ a vector of ones of length six. Thus, $\Pi^{(n)} \in \mathbb{R}^{6n \times 2}$. And $M^{(n)}$

$$M^{(n)} = \begin{bmatrix} M(0,n) \\ M(1,n) \\ \vdots \\ M(n,n) \end{bmatrix} \tag{5.23}$$

with

$$M(0,n) = \begin{bmatrix} -1 & -n+1 & n \\ 1 & n & -n \\ -1 & -n+2 & n-1 \end{bmatrix}, \tag{5.24}$$

$$M(i,n) = \begin{bmatrix} 0 & -i+2 & i-1 \\ 1 & n-i & -n+i \\ 0 & -i+2 & i-1 \end{bmatrix} \tag{5.25}$$

for $i = 1, \ldots, n$. Thus, $M^{(n)} \in \mathbb{R}^{(3n+3)\times 3}$. These two matrices are chosen, such that

$$\Pi^{(n)} = Y^{(n)^T} M^{(n)}, \tag{5.26}$$

see the proof in appendix A.3 on page 142 for a construction of these matrices. With M and Π defined, the following can be stated.

Theorem 5.2. [Solutions to the Polynomial Condition.] *See also the theorem in [P1] on page 12.*

Recall the following network matrices for an n-site sequential, distributed phosphorylation network as given by network (N5.1): the stoichiometric matrix $N^{(n)}$ in equation (5.2), the rate exponent matrix $Y^{(n)}$ in equation (5.10), $E^{(n)}$ in (5.5), $\Pi^{(n)}$ in (5.21) and $M^{(n)}$ in (5.23). The following are equivalent:

(A) There exists a vector $k \in \mathbb{R}^{6n}$ and vectors a, $b \in \mathbb{R}^{3n+3}$ with $a \neq b$ satisfying (5.14).

(B) There exist vectors $\mu \in \mathbb{R}^{3n+3}$, $\mu \neq 0$, and ν, $\lambda \in \mathbb{R}^{6n}$ satisfying (5.20)

(C) There exist vectors $\mu \in \mathbb{R}^{3n+3}$, $\xi \in \mathbb{R}^2$ and ν, $\lambda \in \mathbb{R}^{6n}$, with $\mu \neq 0$ such that

a) the vectors μ and ξ satisfy

$$Y^{(n)^T} \mu = \Pi^{(n)} \xi, \tag{5.27}$$

b) and the vectors ν, λ and ξ satisfy

$$\lambda \in \mathbb{R}^{6n}, \quad \textit{free}, \tag{5.28a}$$

and, for $i = 1, \ldots, n$

$$\nu_{3i} = \lambda_{3i}\, e^{(2-i)\xi_1 + (i-1)\xi_2}, \tag{5.28b}$$

$$\nu_{3i-2} = \lambda_{3i-2}\, \frac{\nu_{3i}}{\lambda_{3i}}, \tag{5.28c}$$

$$\nu_{3i-1} = \lambda_{3i-1}\, \frac{\nu_{3i}}{\lambda_{3i}}. \tag{5.28d}$$

(D) There exists a vector $\mu \in \mathbb{R}^{3n+3}$, $\mu \neq 0$ with

$$\mu \in \operatorname{im}\left(M^{(n)}\right) =: \mathcal{M}. \tag{5.29}$$

For a proof of the theorem see appendix A.3 on page 142 or [P1].

Choosing μ according to equation (5.20) then yields a set of steady state vectors by deriving the second steady state b in terms of a and μ:

$$\begin{aligned} a_i &= \bar{a}_i \\ b_i &= \exp(\mu_i)\, a_i, \end{aligned} \tag{5.30}$$

where $\bar{a}_i$ is an arbitrary, but positive value.

Choosing $\lambda > 0$, the vector of rate constants can be given according to equation (5.17):

$$k = \operatorname{diag}\left(\Phi(a^{-1})\right) E^{(n)} \lambda \tag{5.31}$$

Vectors a and b are a solution to polynomial condition in equation (5.14) if k is chosen according to equation (5.31). For multistationarity, a and b have to satisfy additionally the coset condition in equation (5.15). This condition is discussed in the next section.

5.2.2 *The Coset Condition*

This section discusses solutions to the coset condition in equation (5.15). To find these solutions, the coset condition is rewritten

$$\langle w_j, b - a \rangle = 0$$

yielding a vector $s = b - a$. This vector lies in the orthogonal subspace $\mathcal{S}$ to the linear subspace $\mathcal{W}$ spanned by w_j of $W^{(n)}$:

$$\mathcal{S} = \left\{ s \in \mathbb{R}^{3n+3} | \langle w_j, s \rangle = 0, \;\; j = 1, 2, 3 \right\} = \mathrm{im}(N). \tag{5.32}$$

$\mathcal{S}$ is the stoichiometric subspace [30, 33]. To derive solutions for the coset condition, the approach by [19] is used. Instead of finding all pairs a and b satisfying $\ln(b/a) = \mu$ and $b - a = s$, the existence of a and b is linked to the existence of μ and s: there are two steady states $a, b \in \mathbb{R}^{3n+3}$, if and only if $\mu = \ln(b/a) \in \mathcal{M}$ as well as $s = b - a \in \mathcal{S}$ hold. Thus, a and b can be directly computed via μ and s if and only if such a pair exists. Lemma 2 in [19] holds not only for $n = 2$ in [19] but also for arbitrary n as no further restrictions to the network appear: vectors μ and s are only prolonged by three entries per phosphorylation step. See [19, page 114] for a proof of this condition. By lemma 2 of [19] steady states a and b can be found for $n = 2$, if and only if $\mu \in \mathcal{M}$ and $s \in \mathcal{S}$ exist with the same sign pattern:

$$\mathrm{sgn}(\mu) = \mathrm{sgn}(s). \tag{5.33}$$

If the sign of μ and s are equal, they are called valid vectors μ and s, and their signs valid sign vectors. The sign pattern will be given by a sign vector δ as composed elements of $\{+, -, 0\}^{3n+3}$:

$$\mathrm{sgn}(x) = \left\{ \delta \in \{+, -, 0\}^{3n+3} | \;\; \exists x \in \mathbb{R}^{3n+3} \text{ with } \delta = \mathrm{sgn}(x) \right\}. \tag{5.34}$$

There are, at most, 3^{3n+3} possible sign vectors for $\delta \in \{+, -, 0\}$ with $\mathrm{sgn}(\mu) = \mathrm{sgn}(s)$. Assume, that j distinct valid sign vectors $\delta^{(n)} \in \{+, -, 0\}^{3n+3}$ can be found for a given phosphorylation step n, then all valid $\delta^{(n)}$ are collected in a matrix $\Delta^{(n)} \in \{+, -, 0\}^{(3n+3)\times j}$ with

$$\Delta^{(n)} = \mathrm{col}\left(\delta_1^{(n)}; \ldots; \delta_j^{(n)} \right)$$

for $\delta^{(n)} \in \{+, -, 0\}^{3n+3}$ (or $\in \{+, -\}^{3n+3}$). If at least one valid sign vector can be found, a pair (μ, s) can be given. This results in the coset condition being satisfied and multistationarity established (if sign vectors can be found) for the considered reaction network.

Remark 5.3. The approach of solving the polynomial and coset condition is not dependent on the actual network structure, e. g., a sequential, distributive, phosphorylation network, but holds for all (bio-) chemical reaction networks satisfying assumptions 2.2 and 2.1, i. e., the mass action law holds and reactions are irreversible.

The next section discusses the computation of these sign vectors.

5.3 COMPUTATION OF SIGN VECTORS YIELDING MULTIPLE STEADY STATES

Without any information on the underlying structure of the matrices M and W, see equations (5.23) and (5.4) respectively, the sign vector problem

Table 5.1: *Number of valid sign vectors for individual sign vectors* ($\{+,-,0\}$, $\{+,-\}$) *and different phosphorylation steps in* n *satisfying* $\operatorname{sgn}(\mu) = \operatorname{sgn}(s)$. *For the single phosphorylation process no sign vector can be found. Therefore no multiple steady states exist. The rule for the number of valid sign vectors for an arbitrary step* n *and* $\delta \in \{+,-\}$ *is motivated later on in equation* (5.46), *the empirical rule for* $\delta \in \{+,-,0\}$ *is validated up to* $n = 5$.

n	1	2	3	4	5	6	n
$\#\delta \in \{+,-\}$	–	8	20	36	56	80	$2(n-1)(n+2)$
$\#\delta \in \{+,-,0\}$	–	14	46	94	158	no data	emp. $2(4n^2-4n-1)$

can be solved in a very naïve way: there are in total 3^{3n+3} possible sign vectors for $\delta \in \{+,-,0\}$, referred to as the ternary set of sign vector, or 2^{3n+3} for $\delta \in \{+,-\}$, the binary set respectively. One would have to check half of the sign vectors of each set (as the other one can be computed by simple sign conversion of the first half) for valid μ and s, providing in total $\frac{1}{2}(3^{3n+3}-1)$ or $\frac{1}{2}(2^{3n+3}-1)$ possible sign vectors to be checked.[1] The MATLAB function `elmodes_calc` by S. Klamt, [58], or the very powerful MATLAB function `orthi_calc` by M. Uhr, [114], can be used to check for valid sign vectors δ. The first one is suitable for any sign condition and the second one only for the binary set. Note though, that the algorithm by [58] runs only sufficiently fast for very small phosphorylation networks (up to $n = 5$ for the ternary set and $n = 6$ for the binary set). The second one is based on mixed integer linear programming and actually designed to run fast. It can be used to check sign vectors for larger network sizes. It was tested for $n = 2, \ldots, 25$ and even up to $n = 53$ for the binary set. Results of these two algorithms can be found in table 5.1.

As the number of possible sign vectors rises exponentially, it would be tedious to check all possible sign vectors for all n. One could either try until at least one valid sign vector is found for the desired n. One could also take a closer inspection on the underlying network structure and thus structure of the matrices, these might yield some insight to find all valid sign vectors δ for arbitrary n.

5.3.1 *Remarks on the Structure of the Sign vector*

With three elements prolonging the sign vector, the binary set of sign vectors $\{+,-\}$ yields in total eight possible combinations:

$$\left\{\begin{matrix} + & + & + & - & - & + & - & - \\ +, & +, & -, & +, & -, & -, & +, & - \\ + & - & + & + & + & - & - & - \end{matrix}\right\}. \tag{5.35}$$

The ternary set of possible sign vectors yields in total 27 possible combinations to prolong the set of possible sign vectors in each phosphorylation step n:

$$\left\{\begin{matrix} + & + & + & - & - & + & - & - & + & + & 0 & - & + & + & - & 0 & 0 & - & - & 0 \\ +, & +, & -, & +, & -, & -, & +, & -, & +, & 0, & +, & +, & -, & 0, & 0, & +, & -, & -, & 0, & - \\ + & - & + & + & + & - & - & - & 0 & + & + & 0 & 0 & - & + & - & + & 0 & - & - \\ + & 0 & 0 & - & 0 & 0 & 0 \\ 0, & +, & 0, & 0, & -, & 0, & 0 \\ 0 & 0 & + & 0 & 0 & - & 0 \end{matrix}\right\}. \tag{5.36}$$

5.1 These numbers account for half of the set to be checked minus the null vector.

Remark 5.4. Due to the introduced stepwise notation in network (N5.1), each sign vector $\delta^{(n)}$ is prolonged per phosphorylation step by one of the possible sign vectors given above, e. g., $\delta^{(n+1)} = \mathrm{col}(\delta^{(n)}, +, +, +)$.

Remark 5.5. An entry of '0' corresponds to s_i, $\mu_i = 0$ and thus $a_i = b_i$, thus, the ternary set might provide solutions with $a_i = b_i$. The binary set excludes this case in advance.

A sign vector $\delta^{(n)} = \mathrm{sgn}(s) = \mathrm{sgn}(\mu)$ can be composed only of elements of the above range given in (5.35) for the binary set and (5.36) for the ternary set. Thus, the whole valid set of sign patterns for an arbitrary phosphorylation step n can also be regarded in terms of a sign matrix of columns of sign vectors. Introducing column vectors $\delta_{(0)} = [\delta_{10}, \delta_{20}, \delta_{30}]^T$, $\ldots$, $\delta_{(n)} = [\delta_{1n}, \delta_{2n}, \delta_{3n}]^T$ from $\{+, -\}^3$ in case of the binary set, a sign vector $\delta^{(n)}$ can be defined as

$$\delta^{(n)} = \mathrm{col}\,(\delta_0, \ldots, \delta_n) \in \{+, -\}^{3(n+1)} \tag{5.37}$$

and a sign matrix $\Delta^{(n)}$ of the whole set of all valid $\delta^{(n)}$ for a given phosphorylation step n by:

$$\Delta^{(n)} = \left[\delta_1^{(n)}, \cdots, \delta_j^{(n)}\right] \in \{+, -\}^{(3n+3)\times j}. \tag{5.38}$$

Furthermore, define the following sign matrix Δ_0 of elements $\delta_{(i)}$ for $i = 0, \ldots, n$:

$$\Delta_0 = \begin{bmatrix} \delta_{10} & \cdots & \delta_{1n} \\ \delta_{20} & \cdots & \delta_{2n} \\ \delta_{30} & \cdots & \delta_{3n} \end{bmatrix} = \begin{bmatrix} \delta_{(0)} & \ldots & \delta_{(n)} \end{bmatrix} \in \{+, -\}^{3+(n+1)}. \tag{5.39}$$

The given set of possible signs thus reduces to a vector $\delta^{(n)}$ as a composed vector of sub-vector $\delta_0, \ldots, \delta_n$. Thus, defining the following sign vectors

$$\delta_1 := [\ 1,\ \ 1,\ \ 1]^T, \qquad \delta_2 := [\ 1, -1,\ \ 1]^T, \tag{5.40a}$$
$$\delta_3 := [-1, -1, -1]^T = -\delta_1, \qquad \delta_4 := [\ 1, -1, -1]^T, \tag{5.40b}$$
$$\delta_5 := [-1,\ \ 1, -1]^T = -\delta_2, \qquad \delta_6 := [-1,\ \ 1,\ \ 1]^T = -\delta_4, \tag{5.40c}$$
$$\delta_7 := [\ 1,\ \ 1, -1]^T, \qquad \delta_8 := [-1, -1,\ \ 1]^T = \delta_7 \tag{5.40d}$$

allows to rewrite the sign vector $\delta_1^{(2)}$, compare matrix (5.42)

$$\delta_1^{(2)} = [\ 1,\ \ 1,\ \ 1,|\ \ 1, -1,\ \ 1,|-1, -1, -1]^T \tag{5.41}$$

in terms of these sub-vectors

$$\delta_1^{(2)} = \mathrm{col}\,(\delta_1, \delta_2, \delta_3)\,.$$

For small n the sign matrix $\Delta^{(n)}$ can be computed by the algorithms provided by [114] and [58]. Of course, this computation does not yield a proof of having found all valid sign vectors, nor a prediction of all valid sign vectors for the ternary and binary set. In equation (5.42) on page 46 all $\Delta^{(7)}$ are given as computed by the algorithm of [114]. Thus, order of vectors $\delta^{(n)}$ in $\Delta^{(n)}$ follow the order provided by the algorithm. Note, the matrix $\Delta^{(n)}$ also contains all valid $\Delta^{(n)}$ for $n = 2, \ldots, 6$, see also remark 5.4. A color code is used to distinguish between individual solutions: the valid

sign matrix $\Delta^{(7)}$ is not highlighted at all (as it describes the complete matrix in (5.42)). The elements of the sign matrix $\Delta^{(6)}$ are highlighted by a very light gray. Elements of the matrix $\Delta^{(5)}$ are highlighted by light gray. Elements of $\Delta^{(4)}$ are highlighted by a middle gray, elements of $\Delta^{(3)}$ by a light-dark gray, and elements of $\Delta^{(2)}$ by a dark gray:

$$
\Delta^{(7)^{\mathrm{T}}} = \begin{bmatrix}
1&1&1&1&1&1&1&1&1&1&1&1&1&1&1&1&1&1&1&-1&1&-1&-1&-1\\
1&1&1&1&1&1&1&1&1&1&1&1&1&1&1&1&-1&1&1&-1&1&-1&-1&-1\\
1&1&1&1&1&1&1&1&1&1&1&1&1&1&1&1&-1&1&-1&-1&-1&-1&-1&-1\\
1&1&1&1&1&1&1&1&1&1&1&1&1&-1&1&1&-1&1&1&-1&1&-1&-1&-1\\
1&1&1&1&1&1&1&1&1&1&1&1&1&-1&1&1&-1&1&-1&-1&-1&-1&-1&-1\\
1&1&1&1&1&1&1&1&1&1&1&1&1&-1&1&-1&-1&-1&-1&-1&-1&-1&-1&-1\\
1&1&1&1&1&1&1&1&1&1&-1&1&1&-1&1&1&-1&1&1&-1&1&-1&-1&-1\\
1&1&1&1&1&1&1&1&1&1&-1&1&1&-1&1&1&-1&1&-1&-1&-1&-1&-1&-1\\
1&1&1&1&1&1&1&1&1&1&-1&1&1&-1&1&-1&-1&-1&-1&-1&-1&-1&-1&-1\\
1&1&1&1&1&1&1&1&1&1&-1&1&-1&-1&-1&-1&-1&-1&-1&-1&-1&-1&-1&-1\\
1&1&1&1&1&1&1&-1&1&1&-1&1&1&-1&1&1&-1&1&1&-1&1&-1&-1&-1\\
1&1&1&1&1&1&1&-1&1&1&-1&1&1&-1&1&1&-1&1&-1&-1&-1&-1&-1&-1\\
1&1&1&1&1&1&1&-1&1&1&-1&1&1&-1&1&-1&-1&-1&-1&-1&-1&-1&-1&-1\\
1&1&1&1&1&1&1&-1&1&1&-1&1&-1&-1&-1&-1&-1&-1&-1&-1&-1&-1&-1&-1\\
1&1&1&1&1&1&1&-1&1&-1&-1&-1&-1&-1&-1&-1&-1&-1&-1&-1&-1&-1&-1&-1\\
1&1&1&1&-1&1&1&-1&1&1&-1&1&1&-1&1&1&-1&1&1&-1&1&-1&-1&-1\\
1&1&1&1&-1&1&1&-1&1&1&-1&1&1&-1&1&1&-1&1&-1&-1&-1&-1&-1&-1\\
1&1&1&1&-1&1&1&-1&1&1&-1&1&1&-1&1&-1&-1&-1&-1&-1&-1&-1&-1&-1\\
1&1&1&1&-1&1&1&-1&1&1&-1&1&-1&-1&-1&-1&-1&-1&-1&-1&-1&-1&-1&-1\\
1&1&1&1&-1&1&1&-1&1&-1&-1&-1&-1&-1&-1&-1&-1&-1&-1&-1&-1&-1&-1&-1\\
1&1&1&1&-1&1&-1&-1&-1&-1&-1&-1&-1&-1&-1&-1&-1&-1&-1&-1&-1&-1&-1&-1\\
1&-1&1&-1&-1&-1&1&1&1&1&1&1&1&1&1&1&1&1&1&1&1&1&1&1\\
1&-1&1&-1&-1&-1&1&-1&1&1&1&1&1&1&1&1&1&1&1&1&1&1&1&1\\
1&-1&1&-1&-1&-1&1&-1&1&1&-1&1&1&1&1&1&1&1&1&1&1&1&1&1\\
1&-1&1&-1&-1&-1&1&-1&1&1&-1&1&1&-1&1&1&1&1&1&1&1&1&1&1\\
1&-1&1&-1&-1&-1&1&-1&1&1&-1&1&1&-1&1&1&-1&1&1&1&1&1&1&1\\
1&-1&1&-1&-1&-1&1&-1&1&1&-1&1&1&-1&1&1&-1&1&1&-1&1&1&1&1\\
1&-1&1&-1&-1&-1&-1&-1&-1&1&1&1&1&1&1&1&1&1&1&1&1&1&1&1\\
1&-1&1&-1&-1&-1&-1&-1&-1&1&-1&1&1&1&1&1&1&1&1&1&1&1&1&1\\
1&-1&1&-1&-1&-1&-1&-1&-1&1&-1&1&1&-1&1&1&1&1&1&1&1&1&1&1\\
1&-1&1&-1&-1&-1&-1&-1&-1&1&-1&1&1&-1&1&1&-1&1&1&1&1&1&1&1\\
1&-1&1&-1&-1&-1&-1&-1&-1&1&-1&1&1&-1&1&1&-1&1&1&-1&1&1&1&1\\
1&-1&1&-1&-1&-1&-1&-1&-1&-1&-1&-1&1&1&1&1&1&1&1&1&1&1&1&1\\
1&-1&1&-1&-1&-1&-1&-1&-1&-1&-1&-1&1&-1&1&1&1&1&1&1&1&1&1&1\\
1&-1&1&-1&-1&-1&-1&-1&-1&-1&-1&-1&1&-1&1&1&-1&1&1&1&1&1&1&1\\
1&-1&1&-1&-1&-1&-1&-1&-1&-1&-1&-1&1&-1&1&1&-1&1&1&-1&1&1&1&1\\
1&-1&1&-1&-1&-1&-1&-1&-1&-1&-1&-1&-1&-1&-1&1&1&1&1&1&1&1&1&1\\
1&-1&1&-1&-1&-1&-1&-1&-1&-1&-1&-1&-1&-1&-1&1&-1&1&1&1&1&1&1&1\\
1&-1&1&-1&-1&-1&-1&-1&-1&-1&-1&-1&-1&-1&-1&1&-1&1&1&-1&1&1&1&1\\
1&-1&1&-1&-1&-1&-1&-1&-1&-1&-1&-1&-1&-1&-1&-1&-1&-1&1&1&1&1&1&1\\
1&-1&1&-1&-1&-1&-1&-1&-1&-1&-1&-1&-1&-1&-1&-1&-1&-1&1&-1&1&1&1&1\\
1&-1&1&-1&-1&-1&-1&-1&-1&-1&-1&-1&-1&-1&-1&-1&-1&-1&-1&-1&-1&1&1&1\\
1&-1&-1&-1&1&-1&1&1&1&1&1&1&1&1&1&1&1&1&1&1&1&1&1&1\\
1&-1&-1&-1&-1&-1&1&1&1&1&1&1&1&1&1&1&1&1&1&1&1&1&1&1\\
1&-1&-1&-1&-1&-1&-1&1&-1&1&1&1&1&1&1&1&1&1&1&1&1&1&1&1\\
1&-1&-1&-1&-1&-1&-1&-1&-1&1&1&1&1&1&1&1&1&1&1&1&1&1&1&1\\
1&-1&-1&-1&-1&-1&-1&-1&-1&-1&1&-1&1&1&1&1&1&1&1&1&1&1&1&1\\
1&-1&-1&-1&-1&-1&-1&-1&-1&-1&-1&-1&1&1&1&1&1&1&1&1&1&1&1&1\\
1&-1&-1&-1&-1&-1&-1&-1&-1&-1&-1&-1&-1&1&-1&1&1&1&1&1&1&1&1&1\\
1&-1&-1&-1&-1&-1&-1&-1&-1&-1&-1&-1&-1&-1&-1&1&1&1&1&1&1&1&1&1\\
1&-1&-1&-1&-1&-1&-1&-1&-1&-1&-1&-1&-1&-1&-1&-1&1&-1&1&1&1&1&1&1\\
1&-1&-1&-1&-1&-1&-1&-1&-1&-1&-1&-1&-1&-1&-1&-1&-1&-1&1&1&1&1&1&1\\
1&-1&-1&-1&-1&-1&-1&-1&-1&-1&-1&-1&-1&-1&-1&-1&-1&-1&-1&1&-1&1&1&1\\
1&-1&-1&-1&-1&-1&-1&-1&-1&-1&-1&-1&-1&-1&-1&-1&-1&-1&-1&-1&-1&1&1&1
\end{bmatrix}
\qquad (5.42)
$$

The following three points are noteworthy in matrix (5.42) and motivate the next section 5.3.2 for arbitrary $\delta^{(n)}$.

Observation 5.6. As a consequence of remark 5.4, the first n vectors, of size three each, are of the former set of sign vectors. Observe that this set of the former step is unique in the following one, e. g., take the third valid sign vector $\delta_3^{(3)}$ and the first valid sign vector $\delta_1^{(2)}$ in equation (5.42):

$$\begin{aligned} \delta_3^{(3)} &= \operatorname{col}(\delta_1, \delta_2, \delta_3, \delta_3), \\ \delta_1^{(2)} &= \operatorname{col}(\delta_1, \delta_2, \delta_3) \end{aligned} \qquad \rightarrow \delta_3^{(3)} = \operatorname{col}\left(\delta_1^{(2)}, \delta_3\right).$$

Note, $\delta_1^{(2)}$ does not appear again in the first nine elements of any other vector in $\Delta^{(7)}$ in equation (5.42).

Observation 5.7. The color code follows a certain highlighting pattern. This color code enables a kind of prediction of valid sign vectors. This observation motivates the next section. E. g., a colored row in $\Delta^{(7)}$ (the row were $\delta_1^{(2)}$ can be found) enables prediction of valid sign vectors for larger n by simply adding δ_3 of (5.40b):

$$\begin{aligned} \delta_{21}^{(7)} &= \operatorname{col}\left(\delta_{15}^{(6)}, \delta_3\right) = \operatorname{col}\left(\delta_{10}^{(5)}, \delta_3, \delta_3\right) = \operatorname{col}\left(\delta_6^{(4)}, \delta_3, \delta_3, \delta_3\right) \\ &= \operatorname{col}\left(\delta_3^{(3)}, \delta_3, \delta_3, \delta_3, \delta_3\right) = \operatorname{col}\left(\delta_1^{(2)}, \delta_3, \delta_3, \delta_3, \delta_3, \delta_3\right). \end{aligned}$$

The short notation

$$\operatorname{col}\left(\delta_1^{(2)}, \delta_3, \delta_3, \delta_3, \delta_3, \delta_3\right) = \operatorname{col}\left(\delta_1^{(2)}, [\delta_3]_5\right)$$

will be used to describe vectors $\delta^{(n)}$ of reoccurring elements. Furthermore, colored "diagonals" in $\Delta^{(7)}$ (sign vector $\delta_4^{(2)}$ in $\Delta^{(7)}$ and every second vector below it) enable prediction in a similar form, e. g., the number of present δ_3 increases in $\delta^{(n)}$ per phosphorylation step n

$$\begin{aligned} \delta_{54}^{(7)} &= \operatorname{col}(\delta_4, \delta_3, \delta_3, \delta_3, \delta_3, \delta_3, \delta_3, \delta_1) &&= \operatorname{col}(\delta_4, [\delta_3]_6, \delta_1) \\ \delta_{40}^{(6)} &= \operatorname{col}(\delta_4, \delta_3, \delta_3, \delta_3, \delta_3, \delta_3, \delta_1) &&= \operatorname{col}(\delta_4, [\delta_3]_5, \delta_1) \\ \delta_{28}^{(5)} &= \operatorname{col}(\delta_4, \delta_3, \delta_3, \delta_3, \delta_3, \delta_1) &&= \operatorname{col}(\delta_4, [\delta_3]_4, \delta_1) \\ \delta_{18}^{(4)} &= \operatorname{col}(\delta_4, \delta_3, \delta_3, \delta_3, \delta_1) &&= \operatorname{col}(\delta_4, [\delta_3]_3, \delta_1) \\ \delta_{10}^{(3)} &= \operatorname{col}(\delta_4, \delta_3, \delta_3, \delta_1) &&= \operatorname{col}(\delta_4, [\delta_3]_2, \delta_1) \\ \delta_{4}^{(2)} &= \operatorname{col}(\delta_4, \delta_3, \delta_1) &&= \operatorname{col}(\delta_4, \delta_3, \delta_1) \end{aligned}$$

and the number of appearance of δ_1 decreases in the same amount as δ_3 increases in one set of $\delta^{(n)}$ for a fixed n:

$$\begin{aligned} \delta_{44}^{(7)} &= \operatorname{col}(\delta_4, \delta_3, \delta_1, \delta_1, \delta_1, \delta_1, \delta_1, \delta_1) &&= \operatorname{col}(\delta_4, \delta_3, [\delta_1]_6) \\ \delta_{46}^{(7)} &= \operatorname{col}(\delta_4, \delta_3, \delta_3, \delta_1, \delta_1, \delta_1, \delta_1, \delta_1) &&= \operatorname{col}(\delta_4, [\delta_3]_2, [\delta_1]_5) \\ \delta_{48}^{(7)} &= \operatorname{col}(\delta_4, \delta_3, \delta_3, \delta_3, \delta_1, \delta_1, \delta_1, \delta_1) &&= \operatorname{col}(\delta_4, [\delta_3]_3, [\delta_1]_4) \\ \delta_{50}^{(7)} &= \operatorname{col}(\delta_4, \delta_3, \delta_3, \delta_3, \delta_3, \delta_1, \delta_1, \delta_1) &&= \operatorname{col}(\delta_4, [\delta_3]_4, [\delta_1]_3) \\ \delta_{52}^{(7)} &= \operatorname{col}(\delta_4, \delta_3, \delta_3, \delta_3, \delta_3, \delta_3, \delta_1, \delta_1) &&= \operatorname{col}(\delta_4, [\delta_3]_5, [\delta_1]_2) \\ \delta_{54}^{(7)} &= \operatorname{col}(\delta_4, \delta_3, \delta_3, \delta_3, \delta_3, \delta_3, \delta_3, \delta_1) &&= \operatorname{col}(\delta_4, [\delta_3]_6, \delta_1) \end{aligned}$$

Of course, this order is a consequence of the solution algorithm. Using a different solution algorithm, the order would change. Still, as the same solution would be found, only the position of $\delta_i^{(n)}$ in $\Delta^{(n)}$ would change.

Following these two observations and the order presented by the second one, one could assume, that

$$\operatorname{col}\left(\delta_1^{(2)}, [\delta_3]_6\right) \qquad \text{and} \qquad \operatorname{col}\left(\delta_4, [\delta_3]_7, \delta_1\right)$$

are valid sign vectors of $\Delta^{(8)}$, which is indeed the case.[2]

Observation 5.8. The number of valid sign vectors for each phosphorylation step n seems to follow a certain numerical order. This numerical order gives rise to the (empirical) rule for the number of valid sign vectors in each phosphorylation step in table 5.1. A rule for this number together with a theorem providing actual sign vectors in case of $\delta \in \{+, -\}$ will be established in the next section.

5.3.2 *Binary Set of Sign Vectors for Feasibility of the Multistationarity Problem*

Sign vectors can be constructed from the binary set, $\delta \in \{+, -\}$, or ternary set $\delta \in \{+, -, 0\}$. It suffices to show that at least one sign vector exists to prove existence of multistationarity in the corresponding (bio-) chemical reaction network. Nonetheless, all valid sign vectors for the binary set for an arbitrary n are provided later on.

To find valid sign vectors, two subproblems have to be solved. The first subproblem is given by the coset condition: given a δ, find a vector s such that

$$W^{(n)^T} s = 0, \text{ with } \operatorname{sgn}(s) = \delta \in \{+, -\}^{3n+3}. \tag{5.43}$$

This result is applied to the second subproblem, the solution of the polynomial condition: for a given δ and s, find a vector μ such that

$$\mu = M^{(n)}\, \xi \text{ with } \operatorname{sgn}(\mu) = \delta \in \{+, -\}^{3n+3}. \tag{5.44}$$

The subproblem of the coset condition (5.43) reduces to a decoupled problem, where only columns of the matrix of conservation laws have to be considered:

$$\sum_{j=0}^{n} s_{1j} = 0, \tag{5.45a}$$

$$\sum_{j=0}^{n} s_{3j} = 0, \tag{5.45b}$$

$$\sum_{j=0}^{n} s_{2j} = s_{10} + s_{30}. \tag{5.45c}$$

Here the first line corresponds to the decoupled problem arising from the first column of the matrix of conservation laws, the second line corresponds to the second column. The last line is a result of the sum of the first two columns minus the last one. Thus, the following can be stated.

5.2 Here, the first vector is a consequence of the first example in observation 5.7. The second vector describes the arising vector as a consequence of the second example: its first $3n$ elements would not be part of $\Delta^{(7)}$, compare $\delta_{54}^{(7)}$.

Lemma 5.9. [Sign Vectors Satisfying the Coset Condition.] *See also Lemma 4.9 in [P1]. For a given sign vector matrix*

$$\Delta_0 = \begin{bmatrix} \delta_{(0)} & \cdots & \delta_{(n)} \end{bmatrix} = \begin{bmatrix} \delta_{10} & \cdots & \delta_{1n} \\ \delta_{20} & \cdots & \delta_{2n} \\ \delta_{30} & \cdots & \delta_{3n} \end{bmatrix} \in \{+, -\}^{3\times n+1}$$

as given by equation (5.39) and its sign vector $\delta^{(n)} \in \{+, -\}^{3n+3}$*, the subproblem*

$$W^{(n)^T} s = 0, \text{ with } \operatorname{sgn}(s) = \delta^{(n)}$$

in (5.43) is not feasible if and only if Δ_0 *has one of the following three properties:*

(1) The elements of its first row are all of the same sign δ_{10}*, cf. (5.45a).*

(2) The elements of its third row are all of the same sign δ_{30}*, cf. (5.45b).*

(3) The elements of its second row are all of the same sign δ_{20} *with* $\delta_{20}\,\delta_{10} < 0$*, and* $\delta_{20}\,\delta_{30} < 0$*, cf. (5.45c).*

These restrictions are already a very good reduction of the set of possible sign vectors. They reduce the whole set to one, that does fulfill equation (5.43) and fulfills (5.44). Thus, no in-depth solution is necessary. On the contrary only sign changes with respect to Lemma 5.9 have to be considered. Only sign vectors defined in equations (5.40a)–(5.40c) but not in equation (5.40d) yield valid signs such that elements of the composed vector $\delta^{(n)} \in \{-, +\}^{3n+3}$ satisfy equation (5.44) in the following combinations:

Theorem 5.10. [Valid Sign Vectors of the Binary Set.] *See also the corresponding theorem in [P1]. The linear feasibility problem in equation (5.43) and (5.44) with a sign vector* $\delta^{(n)} \in \{+, -\}^{3n+3}$*, is feasible with a non-empty* $M^{(n)}$*, if and only if* $\delta^{(n)}$ *is of one of the following sign vectors (or its sign inverse):*

- *For* $n \geqslant 2$*:*

$$\delta = \operatorname{col}\left(\delta_1, [\delta_2]_{i_1}, [\delta_3]_{i_2}\right) \text{ with } i_1, i_2 \geqslant 1 \text{ and } i_1 + i_2 = n, \tag{5.Δ_b1}$$

$$\delta = \operatorname{col}\left(\delta_2, [\delta_3]_{i_1}, [\delta_1]_{i_1}\right) \text{ with } i_1, i_2 \geqslant 1 \text{ and } i_1 + i_2 = n, \tag{5.Δ_b2}$$

$$\delta = \operatorname{col}\left(\delta_4, [\delta_5]_{i_1}, [\delta_1]_{i_2}\right) \text{ with } i_1 = 1, i_2 \geqslant 1 \text{ and } i_1 + i_2 = n, \tag{5.Δ_b3}$$

$$\delta = \operatorname{col}\left(\delta_4, [\delta_3]_{i_1}, [\delta_1]_{i_2}\right) \text{ with } i_1, i_2 \geqslant 1 \text{ and } i_1 + i_2 = n. \tag{5.Δ_b4}$$

- *And additionally for* $n \geqslant 3$*:*

$$\delta = \operatorname{col}\left(\delta_1, [\delta_1]_{i_1}, [\delta_2]_{i_2}, [\delta_3]_{i_3}\right) \text{ with } i_1, i_2, i_3 \geqslant 1 \text{ and } i_1 + i_2 + i_3 = n, \tag{5.Δ_b5}$$

$$\delta = \operatorname{col}\left(\delta_2, [\delta_3]_{i_1}, [\delta_2]_{i_2}, [\delta_1]_{i_3}\right) \text{ with } i_1, i_2, i_3 \geqslant 1 \text{ and } i_1 + i_2 + i_3 = n, \tag{5.Δ_b6}$$

$$\delta = \operatorname{col}\left(\delta_4, [\delta_3]_{i_1}, [\delta_5]_{i_2}, [\delta_1]_{i_3}\right) \text{ with } i_1, i_3 \geqslant 1, i_2 = 1 \text{ and } i_1 + i_2 + i_3 = n. \tag{5.Δ_b7}$$

The proof has been moved to A.4, see also [P1].

Note, to refer to explicit $\delta_i^{(n)}$ in $\Delta^{(n)}$ and a given continuation, e. g., equation (5.41), the expression $\delta_2^{(1)}$ is used for $\Delta^{(n)}$ with $n = 2$ and its second valid vector with $\delta^{(n)} \in \{+, -\}$, i. e., equation (5.$\Delta_b$1) with a continuation $i_1 = 1$ and $i_2 = 1$, compare also matrix (5.51) given later on page 54.

Corollary 5.11. *Theorem 5.10 together with proof A.4 forms an independent proof, that for $n \geqslant 2$ a sign vector δ can be found, defining a linear system (5.43)–(5.44), and thus parameterizing steady states a and b, see Remark 5.14 on page 54.*

Example 5.12. The rules in Theorem 5.10 pose a simple integer problem to generate valid sign vectors. For the first arising sign vector $\delta_1^{(2)}$ given as in equation (5.41) the following pattern generates all possible signs, that can be generated from ($5.\Delta_b 1$):

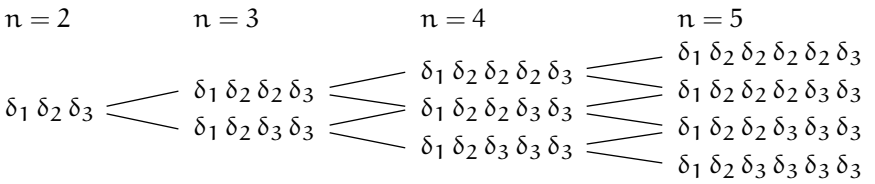

The arising path in the tree like pattern is of course not unique in terms of generating sign vectors. Taking first the upper and then lower branch from $\delta^{(2)}$ to $\delta^{(4)}$ yields the same sign vector $\mathrm{col}(\delta_1\ \delta_2\ \delta_2\ \delta_3\ \delta_3)$, as taking first the lower and then the upper branch. The sign vectors themselves are, of course, unique. One has to account for these "double" generated sign vectors using the tree like pattern by comparing generated sign vectors to generate a valid unique set.

The total number of valid sign vectors per phosphorylation step n can thus be computed by solving the integer partition problem posed by Theorem 5.10.

Example 5.13. For $2 \leqslant n \leqslant 5$ rule ($5.\Delta_b 1$) poses an integer partition problem of an integer n into a sum of two integers i_1 and i_2. Taking order into account the following partitions per step n are possible:

$$\begin{aligned}
2 &= 1+1 && \to \{(1,1)\},\\
3 &= 1+2 && \to \{(1,2),\ (2,1)\},\\
4 &= 1+3 = 2+2 && \to \{(2,2),\ (1,3),\ (3,1)\},\\
5 &= 1+4 = 2+3 && \to \{(1,4),\ (4,1),\ (2,3),\ (3,2)\}.
\end{aligned}$$

There are in total $n-1$ possible partitions of the integer n per step n. Thus ($5.\Delta_b 1$) yields per phosphorylation step $n-1$ valid sign vectors.

The solution to the integer partition problem posed by Theorem 5.10 can be given by counting solutions to rules ($5.\Delta_b$). Counting is possible here, as the problem is quite small. Solving the integer partition problem at hand for a general problem would be possible as well. By solving first the posed partition problem, i. e., partition of an integer n as sum of two integers q and r: $p(n|2) = q+r$, or as sum of three integers q, r and s: $p(n|3) = q+r+s$, for unique solutions (not taking ordering into account), and then by permuting arising solutions, accounting for all possible orders, the correct number can be given.

Counting possible partitions, a general form is given first. The partition of an integer n as a sum of two positive variables, $p(n|2) = r+q$, taking order into account, can be given by:

$$n = (n-1)+1 = (n-2)+2 = \cdots = (n-(n-1))+(n-1).$$

There are in total $n-1$ possible ways to partition n into the sum of two. This partition gives already rise to the solution of $p(n|3) = r+q+s$ with r, q, $s > 0$. If zero would be taken into account, the partition above would already be valid for sums of three elements with the third integer set to zero. Moving one integer further, the above partition is already valid for two of the three integers:

$$
\begin{aligned}
&n = (n-2)+1+1 = (n-3)+1+2 = \cdots = (n-(n-1))+1+(n-2)\\
&\to n-2 \text{ ways,}\\
&\quad = (n-3)+2+1 = (n-4)+2+2 = \cdots = (n-(n-1))+2+(n-3)\\
&\to n-3 \text{ ways,}\\
&\quad \vdots\\
&\quad = (n-i)+(i-1)+1 = \cdots = (n-i-(n-1))+(i-1)+(n-i)\\
&\to n-i \text{ ways,}\\
&\quad \vdots\\
&\quad = 1+(n-2)+1\\
&\to 1 \text{ way.}
\end{aligned}
$$

Thus, there are in total

$$\sum_{i=2}^{n-2} i-1 = \frac{1}{2}(n-2)(n-1)$$

possible integer partitions for $p(n|3)$. To compute the total number of valid sign vectors per phosphorylation step n, the numbers of integer partitions per ($5.\Delta_b$) have to be summed to compute the total number of valid sign vectors $\delta^{(n)}$ per phosphorylation step n:

$$\underbrace{(n-2)(n-1)}_{(5.\Delta_b5)\ \&\ (5.\Delta_b6)} + \underbrace{3(n-1)}_{(5.\Delta_b1),\ (5.\Delta_b2)\ \&\ (5.\Delta_b4)} + \underbrace{(n-2)}_{(5.\Delta_b7)} + \underbrace{(\ 1\ )}_{(5.\Delta_b3)} = (n-1)(n+2). \tag{5.46}$$

Recall, table 5.1 considers the whole solution set of $\delta^{(n)} \in \{+,-,\}$ whereas equation ($5.\Delta_b$) considers only half of the set. The remaining sign vectors can be computed by sign inverting the set of ($5.\Delta_b$).

5.3.3 *The Ternary Set of Sign Vectors*

The former section considers only the binary set of sign vectors. A solution for all $n \geqslant 2$ is provided. This yields valid sets of steady states a and b and is already sufficient for the cause of proving existence of multiple steady states for networks (№5.1). Nonetheless, it would be nice to have rules like ($5.\Delta_b$) for the ternary set of sign vectors $\delta \in \{+,-,0\}^{3n+3}$ for cases where also a zero sign, i. e., $a_i = b_i$, would be of interest for some i.

Per phosphorylation step n 27 possible sign vectors δ_i can prolong the existing set of sign vectors, as given in equation (5.36). Half of this set would have to be checked in a similar manner as in the former section. With a possible zero sign, i. e., $s_i = 0$ as well as $\mu_i = 0$, the three items in Lemma 5.9 still hold: no matter if a zero emerges or not, a sign change has to appear for equations (5.45).

The new arising sign sub-vectors, omitting the negative form for sake of brevity, are given by:

$$\delta_9 := [\ 1,\ \ 1,\ \ 0]^T, \qquad \delta_{10} := [\ 1,\ \ 0,\ \ 1]^T, \tag{5.47a}$$
$$\delta_{11} := [\ 0,\ \ 1,\ \ 1]^T, \qquad \delta_{12} := [\ 1,\ \ 0,\ \ 0]^T, \tag{5.47b}$$
$$\delta_{13} := [\ 0,\ \ 1,\ \ 0]^T, \qquad \delta_{14} := [\ 0,\ \ 0,\ \ 1]^T, \tag{5.47c}$$
$$\delta_{15} := [\ 1,\ -1,\ \ 0]^T, \qquad \delta_{16} := [\ 1,\ \ 0,\ -1]^T, \tag{5.47d}$$
$$\delta_{17} := [\ 0,\ \ 1,\ -1]^T, \qquad \delta_{18} := [\ 0,\ \ 0,\ \ 0]^T. \tag{5.47e}$$

Note, the null vector $\delta^{(n)} = \mathrm{col}([\delta_{18}]_{n+1})$ would correspond to $a = b$ and thus just one steady state.

The binary set of valid sign vectors is contained in the ternary. Thus, its valid sign vectors are valid for the ternary set $\delta \in \{+, -, 0\}^{3n+3}$. These vectors do not have to be checked again for validity. Only new arising sign vectors containing one of the above δ_i in equation (5.47) have to be tested.

The number of all possible sign vectors is of course larger. With the Theorem 5.10 being a consequence of the observations on the structure of the binary sign vectors, similar observations for the ternary sign vectors would be of help. But, as they are only known up to $n = 5$, recall section 5.3 on page 5.3, such observations could not be made so far. Nonetheless rules can be given, tested up to $n = 5$, for additionally valid sign vectors of $\delta \in \{+, -, 0\}^{3n+3}$ satisfying equations (5.43) and (5.44):

- For $2 \leqslant n \leqslant 5$:

$$\delta = \mathrm{col}\left(-\delta_{15}, [\delta_3]_{i_1}, [\delta_{18}]_{i_2}, [\delta_1]_{i_3}\right) \text{ with } i_1, i_3 \geqslant 1,\ i_2 = 0, 1 \text{ and } i_1 + i_2 + i_3 = n, \tag{5.Δ_t1}$$
$$\delta = \mathrm{col}\left(\delta_4, \delta_3, [\delta_3]_{i_1}, -\delta_{10}, [\delta_1]_{i_2}\right) \text{ with } i_1, i_2 \geqslant 1 \text{ and } i_1 + i_2 = n, \tag{5.Δ_t2}$$
$$\delta = \mathrm{col}\left(\delta_{11}, \delta_1, [\delta_1]_{i_1}, \delta_2, [\delta_3]_{i_2}\right) \text{ with } i_1, i_2 \geqslant 1 \text{ and } i_1 + i_2 = n. \tag{5.Δ_t3}$$

- Additionally for $3 \leqslant n \leqslant 5$

$$\delta = \mathrm{col}\left(\delta_4, [\delta_3]_{i_1}, \delta_{13}, [\delta_1]_{i_2}\right) \text{ with } i_1, i_2 \geqslant 1 \text{ and } i_1 + i_2 = n - 1, \tag{5.Δ_t4}$$
$$\delta = \mathrm{col}\left(\delta_8, \delta_1, [\delta_1]_{i_1}, \delta_{10}, -\delta_{13}, [\delta_3]_{i_2}\right) \text{ with } i_1, i_2 \geqslant 1 \text{ and } i_1 + i_2 = n - 1, \tag{5.Δ_t5}$$
$$\delta = \mathrm{col}\left([\delta_1]_{i_1}, [\delta_2]_{i_2}, -\delta_{13}, [\delta_3]_{i_3}\right) \text{ with } i_1, i_2, i_3 \geqslant 1 \text{ and } i_1 + i_2 + i_3 = n, \tag{5.Δ_t6}$$
$$\delta = \mathrm{col}\left([\delta_1]_{i_1}, \delta_{10}, [\delta_2]_{i_2}, [\delta_3]_{i_3}\right) \text{ with } i_1, i_2, i_3 \geqslant 1 \text{ and } i_1 + i_2 + i_3 = n, \tag{5.Δ_t7}$$
$$\delta = \mathrm{col}\left(\delta_2, [\delta_3]_{i_1}, -\delta_{13}, [\delta_2]_{i_2}, [\delta_{10}]_{i_3}, [\delta_1]_{i_4}\right) \text{ with } i_1, i_4 \geqslant 1,\ i_2, i_3 = 0, 1,\ i_2 + i_3 \leqslant 1 \text{ and } i_1 + i_2 + i_3 + i_4 = n - 1, \tag{5.Δ_t8}$$
$$\delta = \mathrm{col}\left(\delta_2, [\delta_3]_{i_1}, \delta_2, [\delta_2]_{i_2}, \delta_{10}, [\delta_1]_{i_3}\right) \text{ with } i_1, i_2, i_3 \geqslant 1 \text{ and } i_1 + i_2 + i_3 = n. \tag{5.Δ_t9}$$

- Additionally for $4 \leqslant n \leqslant 5$

$$\delta = \mathrm{col}\left([\delta_1]_{i_1}, \delta_{10}, [\delta_2]_{i_2}, -\delta_{13}, [\delta_3]_{i_3}\right) \text{ with } i_1, i_2, i_3 \geqslant 1 \text{ and } i_1 + i_2 + i_3 = n - 1, \tag{5.Δ_t10}$$

$$\delta = \operatorname{col}\left(\delta_2, \delta_1, [\delta_2]_{i_1}, \delta_{10}, [\delta_1]_{i_2}\right) \text{ with } i_1 = 0, 1, i_2 \geqslant 1 \text{ and } i_1 + i_2 = n - 2. \tag{5.Δ_t11}$$

- And additionally for $n = 5$

$$\delta = \operatorname{col}\left(\delta_2, [\delta_1]_2, -\delta_{13}, [\delta_{10}]_{i_1}, [\delta_2]_{i_2}, [\delta_1]_{i_3}\right) \text{ with } i_1, i_2 = 0, 1, i_1 + i_2 = 1, i_3 \geqslant 1 \text{ and } i_1 + i_2 + i_3 = n - 3. \tag{5.Δ_t12}$$

Until now, no further results for $\delta^{(n)} \in \{+, -, 0\}$ and $n > 5$ can be provided.

The multisite phosphorylation network in (N5.1) exhibits multiple steady states, see Corollary 5.11. But states themselves are not discussed so far. The next section takes a closer look at steady states and provides examples.

5.4 EXPLICIT FORMULATION FOR MULTISTATIONARITY

Sign vectors in either the binary or ternary set are defined in equations (5.Δ_b) for arbitrary $n \geqslant 2$ and (5.Δ_t) for $2 \leqslant n \leqslant 5$, respectively. These sign vectors can be used to provide a description for μ and s: the solution space $\mathcal{D}$ with $\sigma(\mu) = \sigma(s)$ is given by a cut of the corresponding linear subspaces $\mathcal{M}$, $\mathcal{S}$ with $\mathbb{R}^{3n+3}_\delta$:

$$\mathcal{D} := \{\delta \in \{+, -, 0\}^{3n+3} \mid \mathcal{M} \cap \mathbb{R}^{3n+3}_\delta \neq 0 \text{ and } \mathcal{S} \cap \mathbb{R}^{3n+3}_\delta \neq 0\}. \tag{5.48}$$

Note again, the solution set for the ternary sign vectors contains the one for the binary sign vectors. A short notation for those cuts is used in the following form:

$$\mathcal{M}_\delta = \mathcal{M} \cap \mathbb{R}^{3n+3}_\delta,$$
$$\mathcal{S}_\delta = \mathcal{S} \cap \mathbb{R}^{3n+3}_\delta.$$

Each pointed polyhedral cone can be described by its generators following the notation introduced in section 2.2:

$$E^{\mathcal{S}_\delta} = \begin{bmatrix} \epsilon_1^{\mathcal{S}_\delta} & \dots & \epsilon_{p_{\mathcal{S}_\delta}}^{\mathcal{S}_\delta} \end{bmatrix},$$
$$E^{\mathcal{M}_\delta} = \begin{bmatrix} \epsilon_1^{\mathcal{M}_\delta} & \dots & \epsilon_{q_{\mathcal{M}_\delta}}^{\mathcal{M}_\delta} \end{bmatrix}.$$

Vectors μ and s can be described in terms of nonnegative linear combinations of the basis vectors of the pointed polyhedral cones, see for example figure 2.1 on page 10:

$$\mu = E^{\mathcal{M}_\delta}\alpha, \quad \alpha \in \mathbb{R}^p_{\delta^{(n)}},$$
$$s = E^{\mathcal{S}_\delta}\beta, \quad \beta \in \mathbb{R}^q_{\delta^{(n)}}. \tag{5.49}$$

The pointed polyhedral cones $E^{\mathcal{M}_\delta}$ and $E^{\mathcal{S}_\delta}$ change of course, dependent on the chosen δ. In appendix B.1 cones are given for $E^{\mathcal{M}_\delta}$ for $\delta^{(n)}$ with $n = 2, \dots, 14$ of (5.Δ_b2) and $i_1 = 1$ and $i_2 = n - 1$. Furthermore, $E^{\mathcal{S}_\delta}$ can be found for the same set of sign vectors and $n = 2, \dots, 5$.

With fixed μ and s, the steady states can be given by solving the equations $\mu = \ln \frac{b}{a}$ and $s = b - a$ for a and b:

$$a_i = \begin{cases} \frac{s_i}{\exp(\mu_i) - 1}, & \text{if } \mu_i \neq 0 \\ \bar{a}_i > 0, & \text{if } \mu_i = 0 \end{cases} \tag{5.50}$$
$$b_i = \exp(\mu_i)\, a_i,$$

with $\bar{a}$ again an arbitrary, but fixed, positive value and $i = 1, \dots, 3n + 3$.

Remark 5.14. Theorem 5.10 together with equations (5.31) and (5.50) provide an explicit solution to the multistationarity problem at hand. As every δ generated in (5.Δ_b) yields a valid sign vector for $n \geqslant 2$, i. e., the binary set of sign vectors, phosphorylation networks as defined in (N5.1) exhibit multiple steady states for all $n \geqslant 2$ and the binary set of sign vectors. These sign vectors (5.Δ_b) provide a parametrization for equations (5.50) and (5.31).

To get an idea of the structure of the steady states a and b, a qualitative parametrization is given first. Then the actual "reachable" range, in terms of quantitative data, is discussed in reference to the biological ranges for parameters given in section 3.1.1.

Towards the qualitative setup: half of the sign vectors for $\delta \in \{+, -\}^{3n+3}$ for a double phosphorylation network can be given by:

$$\Delta_b^{(2)^T} = \begin{bmatrix} 1 & 1 & 1 & 1 & -1 & 1 & -1 & -1 & -1 \\ 1 & -1 & 1 & -1 & -1 & -1 & 1 & 1 & 1 \\ 1 & -1 & -1 & -1 & 1 & -1 & 1 & 1 & 1 \\ 1 & -1 & -1 & -1 & -1 & -1 & 1 & 1 & 1 \end{bmatrix} \tag{5.51}$$

and for the ternary set $\delta \in \{+, -, 0\}^{3n+3}$ by:

$$\Delta_t^{(2)^T} = \begin{bmatrix} 1 & 1 & 1 & 1 & -1 & 1 & -1 & -1 & -1 \\ 1 & -1 & 1 & -1 & -1 & -1 & 1 & 1 & 1 \\ 1 & -1 & 0 & -1 & -1 & -1 & 1 & 1 & 1 \\ 1 & -1 & -1 & -1 & 1 & -1 & 1 & 1 & 1 \\ 1 & -1 & -1 & -1 & 0 & -1 & 1 & 1 & 1 \\ 1 & -1 & -1 & -1 & -1 & -1 & 1 & 1 & 1 \\ 0 & 1 & 1 & 1 & -1 & 1 & -1 & -1 & -1 \end{bmatrix} \tag{5.52}$$

These sign matrices define the whole set of sign vectors for a double phosphorylation network yielding multiple steady states.

By choosing, for example, the second of the valid sign vectors in either matrix for a network of two phosphorylation steps:

$$\delta_2^{(2)} = \begin{bmatrix} 1 & -1 & 1 & -1 & -1 & -1 & 1 & 1 & 1 \end{bmatrix}^T,$$

steady states a and b can be given in terms of α and β according to equation (5.49) and (5.50):

$$\begin{aligned} \mu = [&2\alpha_1 + \alpha_2 + \alpha_3,\ -2\alpha_1 - 2\alpha_2 - \alpha_3,\ \alpha_1,\ -\alpha_2,\ -\alpha_1 - \alpha_2,\ -\alpha_2, \\ &\alpha_1 + \alpha_3,\ \alpha_3,\ \alpha_1 + \alpha_3]^T, \\ s = [&\beta_1,\ -\beta_2,\ \beta_3,\ -\beta_1 - \beta_5,\ -\beta_4,\ -\beta_3 - \beta_6,\ \beta_5, \\ &\beta_1 + \beta_2 + \beta_3 + \beta_4,\ \beta_6]^T, \end{aligned}$$

and thus

$$\begin{aligned} a = \Bigg[&\frac{\beta_1}{\exp(d_2) - 1},\ \frac{-\beta_2}{\exp(d_3) - 1},\ \frac{\beta_3}{\exp(\alpha_1) - 1},\ \frac{-\beta_1 - \beta_5}{\exp(-\alpha_2) - 1}, \\ &\frac{-\beta_4}{\exp(d_1) - 1},\ \frac{-\beta_3 - \beta_6}{\exp(-\alpha_2) - 1},\ \frac{\beta_5}{\exp(d_4) - 1},\ \frac{\beta_1 + \beta_2 + \beta_3 + \beta_4}{\exp(\alpha_3) - 1}, \\ &\frac{\beta_6}{\exp(d_4) - 1}\Bigg]^T, \end{aligned}$$

$$b = \Bigg[\frac{\exp(d_2)\,\beta_1}{\exp(d_2)-1}, \frac{-\exp(d_3)\,\beta_2}{\exp(d_3)-1}, \frac{\exp(\alpha_1)\,\beta_3}{\exp(\alpha_1)-1}, \frac{\exp(-\alpha_2)\,f_2}{\exp(-\alpha_2)-1}, \frac{-\exp(d_1)\,\beta_4}{\exp(d_1)-1}, \frac{\exp(-\alpha_2)\,f_3}{\exp(-\alpha_2)-1}, \frac{\exp(d_4)\,\beta_5}{\exp(d_4)-1}, \frac{\exp(\alpha_3)\,f_1}{\exp(\alpha_3)-1}, \frac{\exp(d_4)\,\beta_6}{\exp(d_4)-1}\Bigg]^T,$$

and by (5.31)

$$k = \Bigg[\frac{-(\lambda_1+\lambda_3)\,\beta_1\,\beta_2}{(\exp(d_2)-1)\,(\exp(d_3)-1)}, \frac{\lambda_1\,f_2}{\exp(-\alpha_2)-1}, \frac{\lambda_3\,f_2}{\exp(-\alpha_2)-1}, \frac{-(\lambda_2+\lambda_3)\,\beta_3\,\beta_4}{(\exp(d_1)-1)\,(\exp(\alpha_1)-1)}, \frac{\lambda_2\,f_3}{\exp(-\alpha_2)-1}, \frac{\lambda_3\,f_3}{\exp(-\alpha_2)-1}, \frac{-(\lambda_4+\lambda_6)\,\beta_1\,\beta_4}{(\exp(d_1)-1)\,(\exp(d_2)-1)}, \frac{\lambda_4\,\beta_5}{\exp(d_4)-1}, \frac{\lambda_6\,\beta_5}{\exp(d_4)-1}, \frac{(\lambda_5+\lambda_6)\,\beta_3\,f_1}{(\exp(\alpha_1)-1)\,(\exp(\alpha_3)-1)}, \frac{\lambda_5\,\beta_6}{\exp(d_4)-1}, \frac{\lambda_6\,\beta_6}{\exp(d_4)-1}\Bigg]^T,$$

with

$$\begin{aligned} d_1 &= -\alpha_1-\alpha_2, & d_2 &= 2\alpha_1+\alpha_2+\alpha_3,\\ d_3 &= -2\alpha_1-2\alpha_2-\alpha_3, & d_4 &= -\alpha_1+\alpha_3,\\ f_1 &= \beta_1+\beta_2+\beta_3+\beta_4, & f_2 &= -\beta_1-\beta_5,\\ f_3 &= -\beta_3-\beta_6. \end{aligned}$$

5.4.1 *Quantitative Approach towards Steady State Parametrization*

Steady states as defined by equation (5.50) can be given in a quantitative way by using uniformly distributed pseudo random numbers in the interval of zero to one, $\mathcal{U}(0,1)$, for components of λ in equation (5.31), and α and β in equation (5.49). Furthermore, with the rule for generating sign vectors given in Theorem 5.10, choosing one sign vector out of the seven possible ones and one path of continuation, compare example 5.12, also enables comparison between results of different phosphorylation steps as the sign vector is the same in its corresponding step length n. The signs of μ and s are maintained while generating α and β as uniformly distributed pseudo random numbers, compare equation (5.49). Elements α_i, β_i and λ_i define the ratio of basis vectors of their respective cones $E^{\mathcal{M}}$, $E^{\mathcal{S}}$ and E. Thus $(0,1)$ is chosen as their range.[3] Choosing a different, positive range for these random numbers would only correspond to a shift of the spanned plane of the basis vector, see also [19, page 122]. MATLAB 7.5.0 is used to generate pseudo random numbers and steady states are computed following equations (5.49)–(5.50).

In total 100 parameter sets per phosphorylation step n with $n = 2, \ldots, 14$ are generated, varying in α, β, and λ.[4] So far, the parametrization is purely chosen for visualization. Thus, no units, e. g., nmol/l for x_i and $1/s$ for k_{3i}, for concentrations and reaction rates can be provided.

As an initial sign vector

$$\delta_2^{(2)} = \begin{bmatrix} 1 & -1 & 1 & -1 & -1 & -1 & 1 & 1 & 1 \end{bmatrix}^T,$$

5.3 Note, the actual value of zero for μ is not allowed due to the form of equation (5.50). Here a new random parameter in α is chosen, if such a case should occur.

5.4 The maximal phosphorylation step of fourteen is chosen, as MatCont 4p2 is used for later numerical analysis of steady states. This program is only able to perform numerical analysis up to fourteen phosphorylation steps due to the increasing number of parameters.

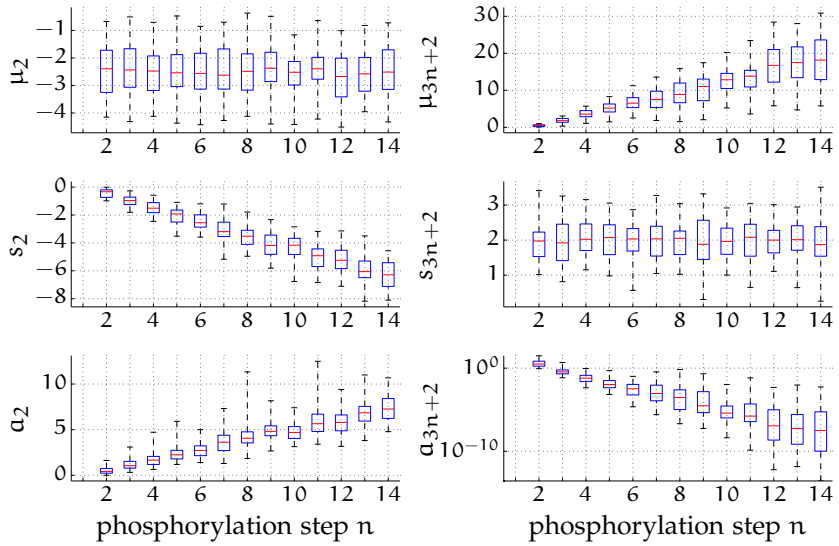

Figure 5.2: *Parameter region for* μ, s *and steady state* a*: given are only the corresponding parameters to the unphosphorylated protein* $a_2 = [A]$*, and the fully phosphorylated protein* $a_{3n+2} = [A_nP]$*. Remaining parameters and steady state can be found in the same intervals. Given is the median over all* 100 *generated values in a red line, first and third quartiles of these values are given by the blue box, black whiskers provide the ninth and* 91*th percentile and red crosses mark outliers.*

of the binary sign set of $\delta \in \{+, -\}$ in (5.51) is chosen. This sign vector is prolonged by rule (5.Δ_b2) with δ_1 or δ_3 and $i_1 = 1$ and $i_2 = n - 1$ for higher phosphorylation steps n. Figures 5.2 and 5.3 illustrate results for some μ, s and steady states a. Here, $a_2 = [A]$ and $a_{3n+2} = [A_nP]$ and their corresponding μ and s are chosen. Furthermore, an overview on rate constants is given, where rate constants are grouped according to their function in the reaction network. Solutions to the random parameters α, β and λ are displayed in terms of the median over all 100 generated values, first and third quartiles of these values. Whiskers provide the ninth and 91th percentile and crosses mark outliers.

Besides rate constants k_i, a Michaelis-Menten like $k_{M,i}$, see as well equation (3.3), can be computed for individual phosphorylation steps, not taking into account the consecutive phosphorylation steps:

$$k_{M,i} = \frac{k_{3i} + k_{3i-1}}{k_{3i-2}}$$

for $i = 1, \ldots, 2n$. Where k_{3i} describes the de-/phosphorylation step, k_{3i-1} describes the breaking of the enzyme-protein complex and k_{3i-2} describes the building of the enzyme-protein complex.

The concentration of the unphosphorylated protein increases with a rising phosphorylation step. In comparison, the concentration of the fully phosphorylated protein decreases significantly with the phosphorylation step. Furthermore, the rate constants increase as well over a significant interval with the phosphorylation step. This de-/increase appears over different intervals. The concentration of the unphosphorylated protein x_2 can be found in an interval $[0.1, 10]$, whereas the concentration of the fully phosphorylated protein is given by approximately $[10^{-10}, 10^{0}]$. Even though no units are used, this de-/increase over such large intervals cannot be reflected by actual biological data from (bio-) chemical reaction networks. These cover

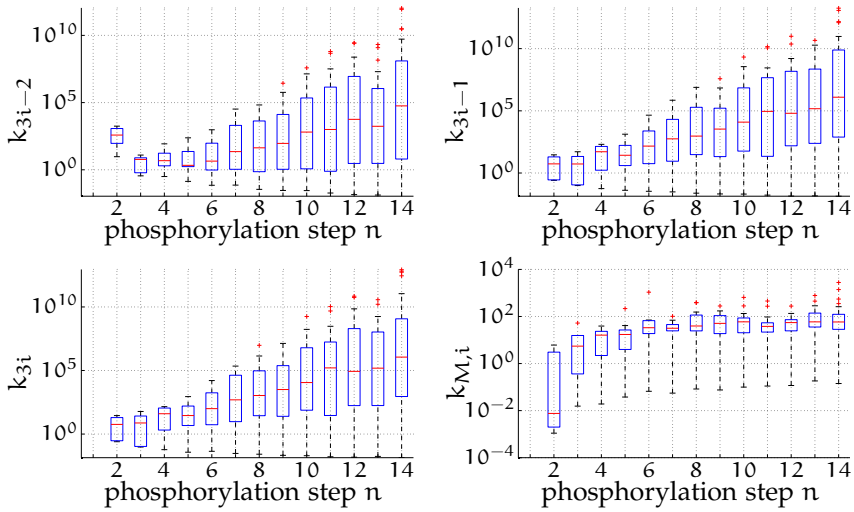

Figure 5.3: *Parameter region for* k_{3i-2}*, corresponding to the association rate,* k_{3i-1}*, corresponding to the dissociation rate,* k_{3i}*, corresponding to de-/phosphorylation rate and pseudo Michaelis-Menten like constant* $k_{M,i}$ *for different phosphorylation steps* $n = 2, \dots, 14$*. Given is the median over all* 100 *generated values in a red line, first and third quartiles of these values are given by the blue box, black whiskers provide the ninth and* 91*th percentile and red crosses mark outliers.*

usually only small ranges, e. g., concentration of all proteins is somewhere in $[10^0, 10^4]$ nmol/l, see section 3.1.2 on page 18. A similar behavior can be found for ranges of the rate constants, see 3.1.1 on page 17 for appropriate ranges.

This de-/increase is due to steady state a being a function of the inverse of $\exp(\mu)$, see equation (5.50), and k being a function of the inverse of a, see equation (5.31). It is independent on the chosen sign vector and due to the increasing or decreasing (depending on the chosen sign vector), elements in $E^{\mathcal{M}}$ and de-/increasing quantity of ones for certain rows in $E^{\mathcal{S}}$, see appendix B.1 on page 149. This results in the described behavior of coverage of very large intervals for concentrations and reaction rates.

But, the large intervals do not pose the only problem. A second problem arises from missing units. Without units, comparison with actual data from (bio-) chemical reaction networks is not possible.

To provide actual biological meaningful values a parametrization of α, β, and λ can be used, to compute scaled variables a, b, and k with given units in a biological sense, compare also section 3.1. This parametrization should also be used to overcome the rise in entries in $E^{\mathcal{M}}$ dependent on the step size n, e. g., compare elements for $n = 2$ of $E^{\mathcal{M}}$ on page 149 with elements for $n = 6$.

5.4.2 *Parametrization of Steady States and Rate Constants*

Data from experiments as well as mathematical models can be used to provide ranges for concentrations and rate constants. See the discussion in section 3.1 as well as tables C.1-C.2 in appendix C.3 for a summary of literature data.

For the unphosphorylated protein and unbounded enzyme forms the following ranges are chosen:

$$\begin{aligned}[K] = x_1 &\in [10^{-9}, 10^{-3}]\,\text{mol/l} = [10^{0}, 10^{6}]\,\text{nmol/l}\\ [A] = x_2 &\in [10^{-9}, 10^{-5}]\,\text{mol/l} = [10^{0}, 10^{4}]\,\text{nmol/l}\\ [P] = x_3 &\in [10^{-9}, 10^{-3}]\,\text{mol/l} = [10^{0}, 10^{6}]\,\text{nmol/l},\end{aligned} \tag{5.53}$$

see also section 3.1.2 and tables in appendix C.3. For phosphorylated proteins as well as bounded enzyme-protein forms smaller ranges are chosen. This is motivated by the models given by [20, 69], as the bounded forms in general only form intermediate complexes:

$$\begin{aligned}[A_{(i-1)P}E_1] = x_{3i+1} &\in [10^{-9}, 10^{-5}]\,\text{mol/l} = [10^{0}, 10^{4}]\,\text{nmol/l},\\ [A_{iP}] = x_{3i+2} &\in [10^{-9}, 10^{-5}]\,\text{mol/l} = [10^{0}, 10^{4}]\,\text{nmol/l},\\ [A_{iP}E_2] = x_{3i+3} &\in [10^{-9}, 10^{-5}]\,\text{mol/l} = [10^{0}, 10^{4}]\,\text{nmol/l},\end{aligned} \tag{5.54}$$

for $i = 1, \dots, n$. These ranges hold of course for both steady states a and b as they lie in the same parameter space.[5]

For rate constants the following ranges are chosen:

$$\begin{aligned}k_{3i-2} &\in [10^{3}, 10^{5}]\,1/(\text{mol s})\\ k_{3i-1} &\in [10^{-3}, 10^{1}]\,1/\text{s}\\ k_{3i} &\in [10^{-3}, 10^{1}]\,1/\text{s}\end{aligned}$$

with again $k = \operatorname{col}(k_{3i-2}, k_{3i-1}, k_{3i})$ for association, dissociation, and de-/phosphorylation, respectively, and $k \in \mathbb{R}^{6n}_{>0}$ and, here, $i = 1, \dots, 2n$. See section 3.1.1 and tables in appendix 3.1.2.

Remark 5.15. With the parametrization provided for steady states a and b in equation (5.50) and for rate constants in equation (5.31), see also Remark 5.14, and the approach presented in this section, a parametrization for arbitrary sequential, distributive phosphorylation networks can be given to compute values in a biological meaningful sense.

To provide a parametrization for rate constants k, the steady state a is regarded fixed in the above given range. The parameter λ is then fixed accounting for k in equation (5.31) and thus shifting k to the desired interval. In a second step, parameters α and β are fixed to generate a and b in a desired interval by accounting for structures in $E^{\mathcal{M}}$ and E^{S}, see equation (5.49) and examples of $E^{\mathcal{M}}$ and E^{S} in appendix B.1 on page 149.

Choosing the Parameter λ

In a first step the parameter λ is fixed. Instead of generating uniformly distributed pseudo random numbers in $(0, 1)$, the parameter is shifted towards its desired range by multiplication with a coefficient. The choice of this coefficient is motivated next.

5.5 Note, ranges are chosen in nmol/l instead of mol/l due to the computational effort.

As computation of k is dependent on the first steady state a and λ, equation (5.31) for k on page 42 is rearranged with $i = 1, dots, n$:

$$k_{6i-5} = \frac{\lambda_{3i-2} + \lambda_{3i}}{a_1\, a_{3i-1}} \in [10^3, 10^5]\, 1/(\mathrm{mol\,s}) \tag{5.55a}$$

$$k_{6i-4} = \frac{\lambda_{3i-2}}{a_{3i+1}} \in [10^{-3}, 10^1]\, 1/\mathrm{s} \tag{5.55b}$$

$$k_{6i-3} = \frac{\lambda_{3i}}{a_{3i+1}} \in [10^{-3}, 10^1]\, 1/\mathrm{s} \tag{5.55c}$$

$$k_{6i-2} = \frac{\lambda_{3i-1} + \lambda_{3i}}{a_3\, a_{3i+2}} \in [10^3, 10^5]\, 1/(\mathrm{mol\,s}) \tag{5.55d}$$

$$k_{6i-1} = \frac{\lambda_{3i-1}}{a_{3i+3}} \in [10^{-3}, 10^1]\, 1/\mathrm{s} \tag{5.55e}$$

$$k_{6i} = \frac{\lambda_{3i}}{a_{3i+3}} \in [10^{-3}, 10^1]\, 1/\mathrm{s} \tag{5.55f}$$

Note again, k_{6i-5} corresponds to k_{6i-2}, as they both correspond to the association rates. k_{6i-4} corresponds to k_{6i-1}, the dissociation rate constants. And k_{6i-3} corresponds to k_{6i}, the phosphorylation and dephosphorylation rate constants, respectively.

Equations (5.55b) and (5.55e) are considered first to provide expressions for λ_{3i-2} and λ_{3i-1}. Rearranging these two yields

$$[10^{-3}, 10^1]\, 1/\mathrm{s} \ni \frac{\lambda_{3i-2}}{a_{3i+1}}, \frac{\lambda_{3i-1}}{a_{3i+3}}.$$

Using interval arithmetic, see for example [50], expressions for λ_{3i-2} and λ_{3i-1} can be found. Units are omitted for sake of clarity. Furthermore, for sake of argument, lets assume the following:

$$\lambda_{3i-2}, \lambda_{3i-1} \in [10^{-3}, 10^1] \times [10^{-9}, 10^{-7}].$$

By interval arithmetic the multiplication rule has to be obeyed: the minimum and the maximum of the combinations of the two given intervals can be given by

$$\lambda_{3i-1}, \lambda_{3i-2} \in [10^{-12}, 10^{-6}]. \tag{5.56}$$

Next, equations(5.55c) and (5.55f) are analyzed to provide an expression for λ_{3i}:

$$[10^{-3}, 10^1]\, 1/(\mathrm{mol\,s}) \ni \frac{\lambda_{3i}}{a_{3i+1}}, \frac{\lambda_{3i}}{a_{3i+3}},$$

yielding of course the same result with

$$\lambda_{3i} \in [10^{-3}, 10^1] \times [10^{-9}, 10^{-7}]$$
$$\rightarrow \lambda_{3i} \in [10^{-12}, 10^{-6}].$$

Note, this range holds only for k in $\mathrm{mol/l}$. If the desired unit is $\mathrm{nmol/l}$, the range has to be shifted by 10^{-9} with k_{3i-2} given in $1/(\mathrm{nmol\,s})$.

Thus equation (5.55a) and (5.55d) remain. As the former equations fix already the intervals for λ, the range for the steady state a might be affected, to provide association rate constants in the desired interval. Note, using λ in the given intervals might result in association rate constants in too large intervals. To account for this, equation (5.55a) and (5.55d) are used:

$$[10^3, 10^5]\, 1/(\mathrm{mol\,s}) \ni \frac{\lambda_{3i-2} + \lambda_{3i}}{a_1 a_{3i-1}}, \frac{\lambda_{3i-1} + \lambda_{3i}}{a_3 a_{3i+2}}.$$

To minimize ranges for a_1, a_3, a_{3i-1} and a_{3i+2} choose:

$$a_1\, a_{3i-1},\ \ a_3\, a_{3i+2} \in \frac{[10^{-12}, 10^{-6}]}{[10^3, 10^5]}\ \mathrm{mol^2/l^2}.$$

By interval arithmetic the minimum and maximum of combinations of these two intervals is computed, yielding

$$a_1\, a_{3i-1},\ \ a_3\, a_{3i+2} \in [10^{-17}, 10^{-9}]\ \mathrm{mol^2/l^2}.$$

The range for unbounded enzymes is fixed in a larger interval than the one of phosphorylated proteins. Keeping this in mind, choose:

$$\begin{aligned} a_1,\, a_3 &\in [10^{-9}, 10^{-4}]\ \mathrm{mol/l},\\ a_{3i-1},\, a_{3i+2} &\in [10^{-8}, 10^{-5}]\ \mathrm{mol/l}. \end{aligned}$$

Note again, by multiplication the minimum and maximum of combinations of these intervals yield expressions for the combined interval. Note also, x_{3i-1} corresponds to x_{3i+2} for the consecutive phosphorylation step. These ranges are included in the ranges given in table C.1-C.2 for real experimental data and are in accordance with the former chosen ranges in equations (3.4) and (3.5) and (5.53) and (5.54)

Adjusting Parameters α and β

As not only rate constants show a shifting behavior in figure 5.3 but also concentrations for steady states in figure 5.2, parameters α and β have to be adjusted as well. This adjustment should also account for the intervals of x_1, x_3, x_{3i-1} and x_{3i+2}.

The parameter α is adjusted first. With $M^{(n)} \in \mathbb{R}^{(3n+3)\times 3}$, there are only three free α independent of the phosphorylation step n. Furthermore, as α directly translates to μ and thus via steady state a also to the second steady state b, α cannot be changed too much, as this would shift the second steady state towards undesired intervals.

The increase in μ, see figure 5.2, is addressed such that values for μ do not increase over time but are uniformly distributed in an interval corresponding mainly to the one of $n = 2, 3$, and 4, i. e., values between $(-5, 5)$ are desired. Furthermore, steady states a and b are restricted by the argument in the former section. For the sake of the argument let

$$a,\, b \in [10^1, 10^5]\ \mathrm{nmol/l}$$

to cover all intervals given (and adjust them later on in the actual algorithm accordingly). Choose

$$\exp(\mu) \approx 1,$$

to provide a and b in the same interval while taking care that $\mu_i \neq 0$, see equation (5.50). Thus, $\exp(\mu_i) \neq 1$. Furthermore as the sign of μ is fixed by δ, negative values are allowed for μ as well. Thus the interval for $\exp(\mu)$ is relaxed, to account for the sign conditions posed by sign vectors in δ. Orienting at the first intervals given for $n = 2, 3, 4$ in figure 5.2 results in the upper and lower limits of

$$\max(\mu) = \frac{1}{2}\cdot 10^1 \qquad \text{and} \qquad \min(\mu) = -\frac{1}{2}\cdot 10^1$$

resulting in

$$\exp(\mu) \in [10^{-7}, 10^{2}].$$

To shift μ towards these intervals choose an $\alpha \in \left[10^{-2}, 10^{0}\right]$. Note, at most sums of three α multiplied by approximately n appear in $E^{\mathcal{M}}$, see equation (B.1) in appendix B.1 on page 149. Thus, choosing the given interval accounts for increase or decrease of elements in $E^{\mathcal{M}}$ and shift μ at the same time to the desired interval. Note, very small values (close to zero) are not desirable for μ, as this would only yield $a_i = b_i$, not desired for numerical analysis later on.

In the next step the parameter β is adjusted to counteract generated large intervals by $1/\exp(\mu)$ via s. I. e., choosing β is not a trivial task as the dimension of the cone E^{S} rises significantly with an increasing n, see B.1 where cones for various phosphorylation steps are given. Here, α is always $\mathbb{R}^3$, see equation (5.49) on page 53. But length of β increases with increasing n. Still a certain structure of rows of sums of (minus) ones as well as diagonal elements of ones can be found in all E^{S}. β is adjusted accordingly by grouping it to the given structure in the cone, see the next paragraph for an example.

Concentrations for steady states a and b as well as rate constants k are then computed using equation (5.50) and (5.31). Choosing parameters in this range for different phosphorylation steps $n = 2, \ldots, 14$ yields not only adjusted parameters in biological meaningful ranges but the slope (in the position of box plots per step n) is also significantly different, see figures 5.4-5.5. Concentrations in a no longer de-/increase with rising phosphorylation steps but can be found in approximately the same range.

Parameter Regions for Adjusted Steady States and Rate Constants

With the given parametrization above steady states a and b as well as rate constants k can be computed for different phosphorylation networks $n = 2, \ldots, 14$. The following parametrization is chosen:

$$\alpha_i \in \begin{cases} n \cdot \mathcal{U}(0,1) & \text{if } n = 2 \\ n \cdot 10^{-0.5} \cdot \mathcal{U}(0,1) & \text{if } n = 3, 4 \\ n \cdot 10^{-1} \cdot \mathcal{U}(0,1) & \text{if } n = 5, 6, 7 \\ n \cdot 10^{-1.5} \cdot \mathcal{U}(0,1) & \text{if } n = 8, 9, 10 \\ n \cdot 10^{-1.75} \cdot \mathcal{U}(0,1) & \text{if } n = 11, 12, 13, 14 \end{cases}$$

The parameter β is adjusted in the aforementioned form to account for the structure arising in the cone E^{S}. Note, this structure only holds for the chosen sign vector, as a different sign vector yields a different cone. Choosing δ_2 of rule ($5.\Delta_b 2$) with $i_1 = 1$ and $i_2 + n - 1$, β is of dimension $6n - 6$, (5.49). To account for the structure the whole vector is adjusted first, depending on the phosphorylation step n:

$$\beta_{1:2n-2} \in \begin{cases} 10^{1.5} \cdot \mathcal{U}(0,1) & \text{for } n = 2, 4, 7, 10, 11, 13, 14 \\ 10^{1} \cdot \mathcal{U}(0,1) & \text{for } n = 3, 5, 6, 8, 9 \\ 10^{2} \cdot \mathcal{U}(0,1) & \text{for } n = 12 \end{cases}$$

$$\beta_{2n-1:6n-6} \in \begin{cases} 10^{1.5} \cdot \mathcal{U}(0,1) & \text{for } n = 2, 4, 10, 11, 13, 14 \\ 10^{1} \cdot \mathcal{U}(0,1) & \text{for } n = 3, 5, 6, 7, 8, 9, 12 \end{cases}$$

Then, certain rows are substituted for $n \geqslant 3$ by

$$\beta_{2n-1} \in \begin{cases} 10^1 \cdot \mathcal{U}(0,1) & \text{for } n = 3, 5, 6, 7, 8, 10, 11, 12 \\ 10^{1.5} \cdot \mathcal{U}(0,1) & \text{for } n = 4, 9, 13, 14 \end{cases}$$

$$\beta_{2n+1} \in \begin{cases} 10^1 \cdot \mathcal{U}(0,1) & \text{for } n = 3, 5, 6, 7, 8, 10, 11, 12 \\ 10^{1.5} \cdot \mathcal{U}(0,1) & \text{for } n = 4, 9, 13, 14 \end{cases}$$

and for $n \geqslant 4$ by:

$$\beta_{2n+3:3n} \in \begin{cases} 10^{1.5} \cdot \mathcal{U}(0,1) & \text{for } n = 4, 9, 13, 14 \\ 10^1 \cdot \mathcal{U}(0,1) & \text{for } n = 5, 6, 7, 8, 10, 11, 12 \end{cases}$$

$$\beta_{4n-1:5n-4} \in \begin{cases} 10^{1.5} \cdot \mathcal{U}(0,1) & \text{for } n = 4, 9, 13, 14 \\ 10^1 \cdot \mathcal{U}(0,1) & \text{for } n = 5, 6, 7, 8, 10, 11, 12 \end{cases}$$

This row-wise replacement is motivated by the structure of the cone E^S where sums of elements of β appear via the first and third row of the cone. For example, for $n = 1$ and $n = 3$

$$s_1 = \beta_1.$$

For $n = 4$

$$s_1 = \beta_7 + \beta_{11} + \beta_{12},$$

whereas for $n = 10$

$$s_1 = \beta_{21} + \sum_{i=25}^{33} \beta_i.$$

Thus, the range is shifted to still guarantee acceptable values for the steady state a to counteract those sums, compare again the matrices given in appendix B.1.

In the last step λ_i is adjusted for $i = 1, \ldots, 14$ with $\lambda \in \mathbb{R}^{3n}_{\geqslant 0}$. Values are generated as a function of n and $\mathcal{U}(0,1)$ and fixed in $\left[10^{-3}, 10^3\right]$:

$$\begin{aligned} \lambda_{1:6} &\in 10^{-1} \cdot \mathcal{U}(0,1), & \lambda_{4:9} &\in 10^{-1} \cdot \mathcal{U}(0,1), \\ \lambda_{7:12} &\in 10^{-2} \cdot \mathcal{U}(0,1), & \lambda_{13:15} &\in 10^{-2} \cdot \mathcal{U}(0,1), \\ \lambda_{16:18} &\in 10^{-2} \cdot \mathcal{U}(0,1), & \lambda_{19:21} &\in 10^{-3} \cdot \mathcal{U}(0,1), \\ \lambda_{22:24} &\in 10^{-2} \cdot \mathcal{U}(0,1), & \lambda_{25:27} &\in 10^{-2} \cdot \mathcal{U}(0,1), \\ \lambda_{28:30} &\in 10^{0} \cdot \mathcal{U}(0,1), & \lambda_{31:33} &\in 10^{0} \cdot \mathcal{U}(0,1), \\ \lambda_{34:36} &\in 10^{2} \cdot \mathcal{U}(0,1), & \lambda_{37:39} &\in 10^{-2} \cdot \mathcal{U}(0,1), \\ \lambda_{40:42} &\in 10^{-2} \cdot \mathcal{U}(0,1), \end{aligned}$$

where length of λ depends on the phosphorylation step n.

Concentrations for steady states a and b and rate constants k are then computed using equation (5.50) and (5.31) by MATLAB 7.5.0 and generating again 100 random variables per phosphorylation step in α, β and λ. See figure 5.4 and 5.5 for an overview in form of box plots, compare results in section 5.4.1 on page 55 with figures 5.2-5.3.

Choosing parameters in this range for different phosphorylation steps $n = 2, \ldots, 14$ yields not only adjusted parameters in biological meaningful ranges but also a different slope of box plot positions throughout the

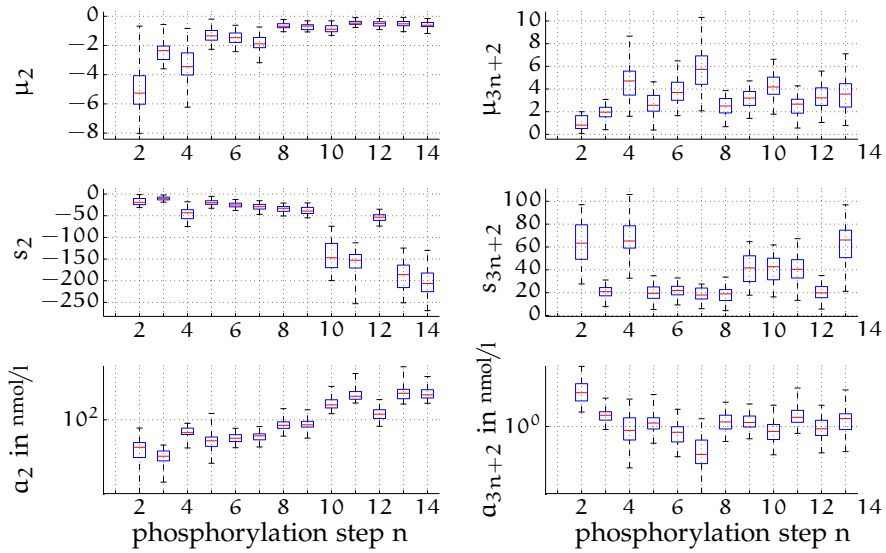

Figure 5.4: *Exemplary parameter regions for* μ, s *and steady state* a. *Given are concentrations of the unphosphorylated protein* $a_2 = [A]$ *and the fully phosphorylated protein* $a_{3n+2} = [A_nP]$ *and their corresponding adjusted variables in* μ *and* s *for different phosphorylation steps* $n = 2, \ldots, 14$.

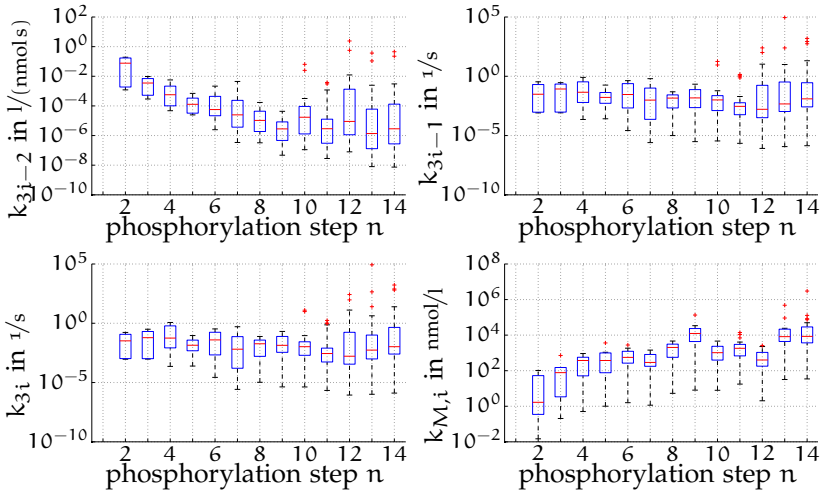

Figure 5.5: *Parameter regions for* k_{3i-2}, *the association rate,* k_{3i-1}, *the dissociation rate,* k_{3i}, *the phosphorylation rate, and a pseudo Michaelis-Menten constant* $k_{M,i}$ *for adjusted variables in* α, β *and* λ *for different phosphorylation steps* $n = 2, \ldots, 14$.

figures. Concentrations in a no longer de-/increase with rising phosphorylation steps but can be found in approximately the same range. Note, values for $a_2 = [A]$ increase in a small interval over the phosphorylation step accounting for higher concentrations of the protein in larger networks, [20]. Furthermore, rate constants follow the given range by [124] for phosphorylation as well as protein binding and breakdown. Also, the Michaelis-Menten like constant $k_{M,i}$, equation (3.3) on page 17, increases per phosphorylation step from 10^0 nmol/l to 10^4 nmol/l. Its deviation stays in the range of 10^1 nmol/l. This corresponds to actual biological data as proteins in networks of higher phosphorylation steps n possess, of course, more binding sites. Thus, for non-fully phosphorylated proteins binding happens first faster and slows down towards saturation as more and more sites are occupied, [42].

Depicting just one example of the generated data with $\alpha = n \cdot \mathcal{U}(0,1)$ and $\beta = 10^{1.5} \cdot \mathcal{U}(0,1)$ for the sign vector $\delta_2^{(2)}$ of (5.Δ_b2) with $i_1 = 1$ and $i_2 = n-1$:

$$\alpha = [1.5025,\ 0.5102,\ 1.0119]^T,$$
$$\beta = [22.1067,\ 28.1728,\ 30.3355,\ 17.3045,\ 4.3837,\ 4.7211]^T,$$

results in

$$\mu = [4.5272,\ -5.0374,\ 1.5025,\ -0.5102,\ -2.0127,\ -0.5102,\ 2.5144,\ 1.0119,\ 2.5144]^T,$$
$$s = [22.1067,\ -28.1728,\ 30.3355,\ -26.4904,\ -17.3045,\ -35.0565,\ 4.3837,\ 97.9195,\ 4.7211]^T.$$

Steady states can be given by:

$$a = [0.2416,\ 28.3569,\ 8.6845,\ 66.2893,\ 19.9734,\ 87.7250,\ 0.3859,\ 55.9265,\ 0.4156]^T \text{ nmol/l},$$
$$b = [22.3484,\ 0.1841,\ 39.0200,\ 39.7989,\ 2.6689,\ 52.6685,\ 4.7696,\ 153.8460,\ 5.1367]^T \text{ nmol/l},$$

and total concentration, recall equation (5.3), by:

$$c = [66.9168,\ 96.8251,\ 259.0726]^T \text{ nmol/l}.$$

Furthermore adjusting λ to the given values in the former section of $\lambda \in 10^{-1} \cdot \mathcal{U}(0,1)$ yields:

$$\lambda = [0.0258,\ 0.0841,\ 0.0254,\ 0.0814,\ 0.0244,\ 0.0929]^T,$$

and rate constants in the following form:

$$k = \left[0.0075,\ 3.892 \cdot 10^{-4},\ 3.832 \cdot 10^{-4},\ 6.312 \cdot 10^{-4},\ 9.587 \cdot 10^{-4},\ 2.895 \cdot 10^{-4},\ 0.0361,\ 0.2109,\ 0.2407,\ 2.415 \cdot 10^{-4},\ 0.0587,\ 0.2235\right]^T.$$

Here, rate constants for association rates are given in $1/(\text{nmol s})$ and remaining rates are given in $1/s$.

Bifurcation Analysis for Various Network Sizes

Besides the range for concentrations and rate constants further points are of interest in the region of steady states a and b. E. g., can the parameters of the (bio-) chemical reaction network be found in a biological meaningful region and, does the switch also lie in a biological meaningful region. Or, whether this region exhibits only one steady state and the other lies somewhere else, where it is not of interest to experimenters.

For bifurcation analysis different parameters can be chosen as the bifurcation parameter. The software MatCont 4p2 for MATLAB is chosen for this analysis. The parameter c_2, the total concentration of the phosphatase P and its bounded forms, e. g., A_P, is chosen as bifurcation parameter for numerical analysis. A sample of values is taken from the initial values generated for section 5.4.1 (for general values) and for section 5.4.2 (for adjusted

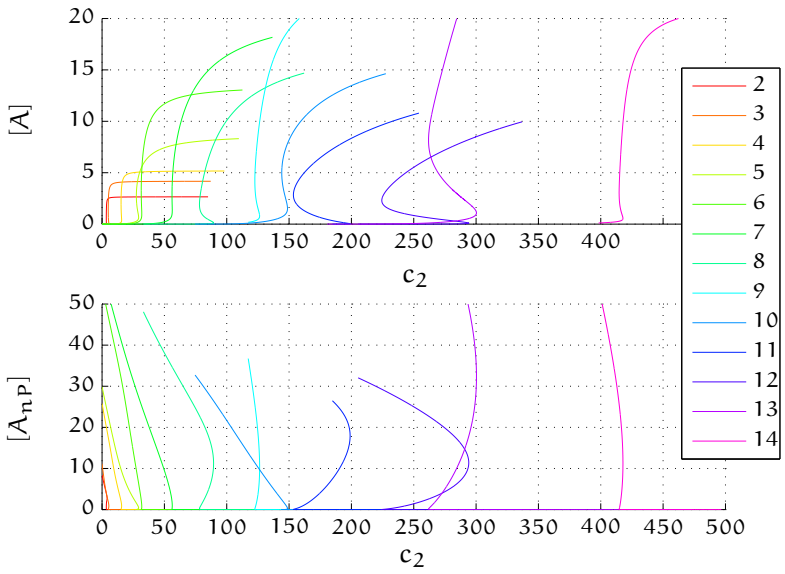

Figure 5.6: *Bifurcation analysis of change in total phosphatase concentration. Given are unphosphorylated protein concentration* $x_2 = [A]$ *(top) and* n*-times phosphorylated protein* $x_{3n+2} = [A_{nP}]$ *(bottom) over concentration* c_2 *(total phosphatase concentration) for various network sizes* $n = 2, \ldots, 14$.

values). Here, only the first 50 generated variables, i. e., generated α, β and λ, are chosen for bifurcation, due to computational costs. All remaining values are fixed. Thus, c_1 and c_3, compare equation (5.3), and rate constant k, equation (5.31) are kept constant. This corresponds to shifting the affine solution plane in the coset. And thus, corresponds to variations, where steady states are born or disappear.

If vectors α, β and λ are not adjusted, the appearance of the bifurcation curves changes with curves becoming thinner in total concentration range and higher in substrate range, see figure 5.6. The step width (width of s-shape) decreases for higher networks of higher phosphorylation steps n for the chosen concentrations, but can be seen in bifurcation curves for concentrations of remaining phosphorylated proteins over c_2. Whereas the step heights (heights of the s) increases with rising step size for the chosen substances. This translates to a more pronounced difference in the concentration of the different steady states, e. g., $a_2 \gg b_2$. But, the range where switching between steady states appears, becomes quite small with a rising phosphorylation step n. This corresponds to a poor switch, compare also section 4.1, as already small changes in the total concentration of the phosphatase would result in a switching behavior.

Performing bifurcation analysis on the adjusted parameter set yields a different behavior. Here, the s-curves are more pronounced. The width of the step increases in terms of the total concentration c_2 with the phosphorylation step n. This is in accordance to actual biological data, compare for example total concentration for *MAPK* systems and *NFAT* systems: e. g. [69] for a double phosphorylation system, where $c_2 = 500\,\mathrm{nmol/l}$, and [20] for a 14-times phosphorylation with $c_2 = 6\,\mu\mathrm{mol/l}$. This makes the switch itself more pronounced, i. e., a bigger change has to be applied to result in actual switching. Thus, the network allows for switching, but is more robust towards very small variations in comparison to the unadjusted case. Fur-

thermore, the height of the step, the height of the s-curve, rises with a rising phosphorylation step n. Thus networks of higher phosphorylation steps seem to actually make a good switch as the step is more pronounced with higher phosphorylation steps n.

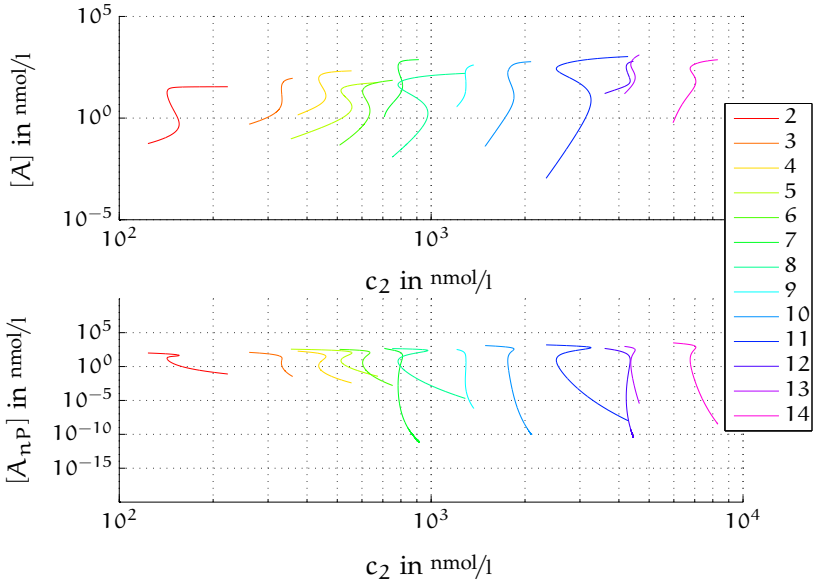

Figure 5.7: *Bifurcation analysis for adjusted parameters: unphosphorylated protein concentration, $x_2 = [A]$, (top) and fully phosphorylated protein concentration, $x_{3n+2} = [A_{nP}]$, (bottom) over total concentration c_2 (total phosphatase concentration) for various network sizes $n = 2, \ldots, 14$.*

Step heights for all results of bifurcation for phosphorylation networks of $n = 2, \ldots, 5$ as well as the thirteen given in figure 5.7 were compared. No significant difference between different networks of phosphorylation sizes could be found. Thus, no conclusions can be drawn, whether the two extrema in the s-shape increase, translating to a greater difference in concentration of the two steady states with an increasing step size n.

5.5 SUMMARY AND OPEN QUESTIONS

This chapter covers the general question of existence of multistationarity in a distributive, sequential multisite phosphorylation network ($\mathcal{N}5.1$) of n steps. (Bio-) Chemical reaction networks of this kind indeed exhibit multiple steady states for any $n \geqslant 2$ phosphorylation sites. A parametrization for the multistationarity region is provided dependent on a sign vector δ. All δ are provided for the binary sign structure of $\{+, -\}$ and all δ for $n = 2, \ldots, 5$ are provided for the ternary set $\{+, -, 0\}$. Thus, a parametrization for steady states using the binary sign structure can be given for any n and for the ternary one for $2 \leqslant n \leqslant 5$, where the ternary one includes all solutions of the binary one.

Though results seem rather theoretical with the provided sign vectors δ, a parametrization of the steady state region can be provided and explicit examples for values of concentrations and rate constants can be given. These values can not only be found in an arbitrary region, but a parametrization of a biological meaningful sense is given. I. e., parameters and concentrations

of the multistationarity region are found in realistic intervals corresponding to actual biological data of phosphorylation networks.

Furthermore, the sign vector δ can be translated in a biological context. First of all, δ and $-\delta$ correspond to the same set of steady states, where the negative sign vector simply yields the results in a sign inverse form, i. e., $a_\delta = b_{-\delta}$ and $b_\delta = a_{-\delta}$. This simply means, that concentrations for steady states are switched if the opposite sign is use. Second, a zero element in the sign vector corresponds to $a_i = b_i$. As the sign vectors of the binary set (for all n) and for ternary set (for $n = 2, \ldots, 5$) always ends with $\{+, +, +\}$ (or $\{-, -, -\}$), the last three components of b are always greater (or smaller) than those of a. Third, with first and third rows of $M(i, n)$, the determining matrix of ratios of a and b, being equal, the ratio of the steady state concentrations of the kinase-substrate complexes is equal to the ratio of the phosphatase-substrate complexes, i. e., $\mu_{3i+1} = \mu_{3i+3}$, see also the discussion in [P1] and fact 6.1 in [P2]. Thus, if a certain ratio is known, remaining ratios can be reconstructed and by further knowledge of concentrations, the corresponding steady state can be reconstructed, e. g., $(b_1/a_1)/(b_3/a_3) = (b_{3i+1}/a_{3i+1})/(b_{3i-2}/a_{3i-2})$. Note, [P2] exploits the idea of L. Wang and E. D. Sontag on bounds on the number of steady states. [P2] studies a scalar determining equation and presents exact solutions for a sequential, distributive phosphorylation network of $n = 2$, 3 and 4 with $2n - 1$ steady states. By doing so, counterexamples to the conjecture of L. Wang and E. D. Sontag are given.

Besides the given biological interpretation, further meaning of sign vectors is of interest. First of all, the question arises, how sign vectors and their corresponding steady state reflect response curves in the multistationarity region. Furthermore, if sign vectors are allowed to be prolonged only in a certain way, i. e., $\{+, +, +\}$ or $\{-, -, -\}$, does this reflect somehow on the robustness of the reaction network? Are thus certain sign vectors more robust than others? Also, switching in reaction networks might attributed to some values being always greater (smaller) than others, compare also the figures by J. Gunawardena and C. Salazar and T. Höfer. In these publications, the steady state concentration of sums of substances of intermediate steps,e. g., $[A_P] + [AK] + [A_PP]$, over total concentration of these sums, $[A]_{tot} + [K]_{tot} + [P]_{tot}$, is plotted versus total concentration of the kinase over total concentration of the phosphatase, $[K]_{tot}/[P]_{tot}$. Thus, if certain ratios are always the same, recall the short example in the previous paragraph, the response curves always have to be the same if plotted in such a way. Further biological interpretations of the sign vectors remain unclear.

The function of the phosphorylation network can, so far, not be derived from the sign vector. I. e., though knowing signs vectors, one still needs to compute an exact parametrization and perform bifurcation analysis to get an insight on the response curve. Here, it would be interesting whether a certain sign vector predetermines the response curve in the reaction network. If such an association would be possible, knowing all possible results for sign vectors would correspond to knowing all functions of a phosphorylation network.

As this chapter covers only multisite phosphorylation networks with a distributive, sequential mechanism, different network setups should be considered as well. First, synthesis and degradation of the proteins and/or enzymes could be considered. This will be covered in the next chapter. Second, a higher number of enzymes catalyzing de-/phosphorylation can indeed be found in (bio-) chemical reaction networks, often several kinases

phosphorylate a single protein. But as the exact number of kinases or sites they can phosphorylate are usually unknown, this topic is not covered here. Furthermore, different (mixed) mechanisms, e. g., purely random de-/phosphorylation or random phosphorylation and distributive dephosphorylation, should be considered as well as they can be found in (bio-) chemical reaction networks. Here, again, the question arises, whether these multisite phosphorylation networks can exhibit multiple steady states at all. And last, with respect to [P2], it would be of interest, whether an exact solution for the number steady states can be provided.

Man muss noch Chaos in sich haben,
um einen tanzenden Stern gebären zu können.

— Friedrich Nietsche [74]

6 EFFECT OF SYNTHESIS AND DEGRADATION OF PROTEINS AND ENZYMES IN MULTISITE PHOSPHORYLATION NETWORKS

The previous chapter discusses phosphorylation and dephosphorylation of a protein in arbitrary steps n. Multiple steady states can be computed for these systems entailing complex dynamical behavior. But recalling section 3.2.2 these simple phosphorylation/dephosphorylation networks might not be sufficient to represent actual (bio-) chemical reaction networks. This chapter expands these phosphorylation networks, still in a basic modeling approach, by allowing also synthesis and/or degradation of the protein, its phosphorylated forms and/or the enzymes.

6.1 MODELING A SMALL PHOSPHORYLATION NETWORK WITH SYNTHESIS AND DEGRADATION

Synthesis and degradation exist in phosphorylation networks of various sizes. These processes depict basic network properties in addition to simple synthesis or degradation, like synthesis from other educts, or into nothing, i. e., degradation into its components, for example *Sic1*. Further examples can be given by unavailability via inactivation of a protein through phosphorylation, found in *Swe1*, or compartmentalization through sequestration, found in *Cdc25*, [38].

As the additional reactions of synthesis and/or degradation of the protein and/or enzyme complicate the system, a small network of double phosphorylation with a distributive, sequential mechanism is considered first. This network represents at the same time an n-times phosphorylation network in a reduced form. In this reduced version the unphosphorylated form of the protein in the double phosphorylation network corresponds to a standard unphosphorylated, active protein, like *Sic1*, *Cdc25*, and *Wee1*. The double phosphorylated protein of the small reaction network with $n = 2$ corresponds to the fully or active form (in terms of activation, degradation, etc.) in the large reaction network, e. g., *Sic1-6p*. The single phosphorylated form of the double phosphorylation network corresponds to all intermediate phospho-forms. Such a model describes a reduced form of the intermediate phosphorylation states. By reducing the model in such a way, the complexity of the network is reduced while still being able to qualitatively describe and analyze the underlying network structure.

A phosphorylation process of a protein in two steps with synthesis and/or degradation of the protein and enzymes is considered. The distributive, sequential double phosphorylation

$$\underset{x_1}{\overset{\tilde{y}_1}{K}} + \underset{x_2}{\overset{}{A}} \underset{k_2}{\overset{k_1}{\rightleftharpoons}} \underset{x_4}{\overset{\tilde{y}_2}{AK}} \xrightarrow{k_3} \underset{x_5}{\overset{\tilde{y}_3}{K}} + A_P \underset{k_{11}}{\overset{k_{10}}{\rightleftharpoons}} \underset{x_7}{\overset{\tilde{y}_{10}}{A_PK}} \xrightarrow{k_{12}} \underset{x_8}{\overset{\tilde{y}_{11}}{K}} + A_{PP} \tag{$\mathcal{N}$6.1a}$$

and dephosphorylation

$$P + \underset{x_9}{\overset{\tilde{y}_{12}}{A_{PP}}} \underset{k_{14}}{\overset{k_{13}}{\rightleftharpoons}} \underset{x_9}{\overset{\tilde{y}_{13}}{A_{PP}}}P \xrightarrow{k_{15}} P + \underset{x_6}{\overset{\tilde{y}_4}{A_P}} \underset{k_5}{\overset{k_4}{\rightleftharpoons}} \underset{x_6}{\overset{\tilde{y}_5}{A_P}}P \xrightarrow[x_3]{k_6} \overset{\tilde{y}_6}{P} + A \tag{N6.1b}$$

of a protein A and its kinase K and phosphatase P are extended by several scenarios: The first scenario considers just synthesis and/or degradation of the protein A and its phosphorylated forms:

$$\underset{A}{\overset{\tilde{y}_8}{}} \underset{k_8}{\overset{k_7}{\rightleftharpoons}} \overset{\tilde{y}_7}{0} \qquad \underset{A_P}{\overset{\tilde{y}_9}{}} \xrightarrow{k_9} \overset{\tilde{y}_7}{0} \xleftarrow{k_{16}} \overset{\tilde{y}_{14}}{A_{2P}} \tag{N6.2a1}$$

$$A \rightleftharpoons 0 \qquad 0 \longleftarrow A_{2P} \tag{N6.2a2}$$

$$A \longleftarrow 0 \qquad A_P \longrightarrow 0 \longleftarrow A_{2P} \tag{N6.2a3}$$

$$A \longleftarrow 0 \qquad 0 \longleftarrow A_{2P} \tag{N6.2a4}$$

Each of these networks combined with network (N6.1) yields the considered reaction network, thus, so far four possible reaction networks. In a second scenario synthesis and/or degradation of the protein itself together with synthesis and degradation of the kinase K is considered:

$$A \rightleftharpoons 0 \rightleftharpoons K \qquad A_P \longrightarrow 0 \longleftarrow A_{2P} \tag{N6.2b1}$$

$$A \rightleftharpoons 0 \rightleftharpoons K \qquad 0 \longleftarrow A_{2P} \tag{N6.2b2}$$

$$A \longleftarrow 0 \rightleftharpoons K \qquad A_P \longrightarrow 0 \longleftarrow A_{2P} \tag{N6.2b3}$$

$$A \longleftarrow 0 \rightleftharpoons K \qquad 0 \longleftarrow A_{2P} \tag{N6.2b4}$$

The third scenario considers along scenario one synthesis and degradation of phosphatase P:

$$A \rightleftharpoons 0 \rightleftharpoons P \qquad A_P \longrightarrow 0 \longleftarrow A_{2P} \tag{N6.2c1}$$

$$A \rightleftharpoons 0 \rightleftharpoons P \qquad 0 \longleftarrow A_{2P} \tag{N6.2c2}$$

$$A \longleftarrow 0 \rightleftharpoons P \qquad A_P \longrightarrow 0 \longleftarrow A_{2P} \tag{N6.2c3}$$

$$A \longleftarrow 0 \rightleftharpoons P \qquad 0 \longleftarrow A_{2P} \tag{N6.2c4}$$

Further scenarios are possible as well:

SYNTHESIS OF ENZYMES ALONG WITH SCENARIO ONE Allowing only synthesis but not degradation for both enzymes. These cases are discussed in appendix B.2.4.

NO SYNTHESIS AND DEGRADATION OF THE PROTEIN The last example considers only synthesis and degradation of the enzymes (and the phosphorylated form) but not of the unphosphorylated protein. These cases are discussed in appendix B.2.5.

Combining network (N6.1) with the given scenarios in the networks (N6.2) above yields in total twelve possible reaction networks. As each of these networks is only a small variation of the former one, compare for example network (N6.2a2) to network (N6.2a1), note the missing degradation reaction

k_9, only one network will be analyzed in detail in this chapter. The focus is set on network (N6.2a1). Results are given for all processes in section 6.2.3. Results for remaining network scenarios can be found in appendix B.2.1-B.2.3 for results of networks (N6.2a2)–(N6.2c4), respectively.

The concentration of single substances is described by a state x. Rate constants are described by a parameter k. Elements are noted in a stepwise manner. Putting the emphasis on the phosphorylation process itself, the phosphorylation step is labeled first before synthesis and degradation steps are considered. Thus, the unphosphorylated protein and unbounded enzyme forms are considered first: $x_1 = [K]$, $x_2 = [A]$ and $x_3 = [P]$ with corresponding rate constants. In a second step the single phosphorylated form of the protein and the enzyme complexes are considered: $x_4 = [AK]$, $x_5 = [A_P]$ and $x_6 = [A_P P]$. Then, degradation and synthesis of the phosphate and enzymes are considered as they occur between each step, see rate constants in (N6.1) and (N6.2a1). Finally the next phosphorylation step is considered yielding $x_7 = [A_P K]$, $x_8 = [A_{PP}]$ and $x_9 = [A_{PP} P]$ and corresponding rate constants.

The double phosphorylation as described by equation (N6.1) yields in total $x \in \mathbb{R}^9$. The number of states does not vary with the considered reaction network as no new species arise. But, the number of parameters $k \in \mathbb{R}^r$ changes with the considered form in network (N6.2), for example $r = 16$ for network (N6.1)+(N6.2a1). The number of complexes and educt complexes changes dependent on the reaction network with $\tilde{y} \in \mathbb{R}^{14}$ for network (N6.1)+(N6.2a1). Furthermore, assumptions 2.1 and 2.2 in section 2.2 on page 7 and assumption 5.1 in section 5.1 on page 35 hold.

The system is rewritten using ordinary differential equations:

$$\frac{dx}{dt} = N\,v \tag{6.1}$$

yielding a polynomial system with the stoichiometric matrix $N \in \mathbb{R}^{9\times 16}$ for network (N6.1)+(N6.2a1)

$$N = \begin{array}{c} \\ x_1 \\ x_2 \\ x_3 \\ x_4 \\ x_5 \\ x_6 \\ x_7 \\ x_8 \\ x_9 \end{array} \begin{array}{c} \begin{array}{cccccccccccccccc} k_1 & k_2 & k_3 & k_4 & k_5 & k_6 & k_7 & k_8 & k_9 & k_{10} & k_{11} & k_{12} & k_{13} & k_{14} & k_{15} & k_{16} \end{array} \\ \begin{bmatrix} -1 & 1 & 1 & 0 & 0 & 0 & 0 & 0 & 0 & -1 & 1 & 1 & 0 & 0 & 0 & 0 \\ -1 & 1 & 0 & 0 & 0 & 1 & 1 & -1 & 0 & 0 & 0 & 0 & 0 & 0 & 0 & 0 \\ 0 & 0 & 0 & -1 & 1 & 1 & 0 & 0 & 0 & 0 & 0 & 0 & -1 & 1 & 1 & 0 \\ 1 & -1 & -1 & 0 & 0 & 0 & 0 & 0 & 0 & 0 & 0 & 0 & 0 & 0 & 0 & 0 \\ 0 & 0 & 1 & -1 & 1 & 0 & 0 & 0 & -1 & -1 & 1 & 0 & 0 & 0 & 1 & 0 \\ 0 & 0 & 0 & 1 & -1 & -1 & 0 & 0 & 0 & 0 & 0 & 0 & 0 & 0 & 0 & 0 \\ 0 & 0 & 0 & 0 & 0 & 0 & 0 & 0 & 0 & 1 & -1 & -1 & 0 & 0 & 0 & 0 \\ 0 & 0 & 0 & 0 & 0 & 0 & 0 & 0 & 0 & 0 & 0 & 1 & -1 & 1 & 0 & -1 \\ 0 & 0 & 0 & 0 & 0 & 0 & 0 & 0 & 0 & 0 & 0 & 0 & 1 & -1 & -1 & 0 \end{bmatrix} \end{array}, \tag{6.2}$$

where k_7 describes synthesis of the unphosphorylated protein A and k_8, k_9 and k_{16} degradation of the unphosphorylated, the single phosphorylated and the double phosphorylated protein, respectively.

The vector of reaction rates can be given by:

$$v(k,x) = \operatorname{diag}(k)\,\Phi(x)\,,$$
$$\Phi(x) := \begin{bmatrix} x^{y_1} & \dots & x^{y_r} \end{bmatrix},$$

compare equation (5.8) and see as well equation (2.1) on page 9 for an introduction. Thus, for network (N6.2a1)

$$v(k,x) = [k_1x_1x_2 \;\; k_2x_4 \;\; k_3x_4 \;\; k_4x_3x_5 \;\; k_5x_6 \;\; k_6x_6 \;\; k_7 \;\; k_8x_2 \;\; k_9x_5 \;\; k_{10}x_1x_5 \;\; k_{11}x_7 \;\; k_{12}x_7 \;\; k_{13}x_3x_8 \;\; k_{14}x_9 \;\; k_{15}x_9 \;\; k_{16}x_8]^T .$$

The rate exponent matrix $Y \in \mathbb{R}^{9\times 16}$ for network (N6.1)+(N6.2a1) can be given by

$$Y = \begin{bmatrix} 1&0&0&0&0&0&0&0&0&1&0&0&0&0&0&0\\ 1&0&0&0&0&0&0&1&0&0&0&0&0&0&0&0\\ 0&0&0&1&0&0&0&0&0&0&0&0&1&0&0&0\\ 0&1&1&0&0&0&0&0&0&0&0&0&0&0&0&0\\ 0&0&0&1&0&0&0&0&1&1&0&0&0&0&0&0\\ 0&0&0&0&1&1&0&0&0&0&0&0&0&0&0&0\\ 0&0&0&0&0&0&0&0&0&0&1&1&0&0&0&0\\ 0&0&0&0&0&0&0&0&0&0&0&0&1&0&0&1\\ 0&0&0&0&0&0&0&0&0&0&0&0&0&1&1&0 \end{bmatrix} . \tag{6.3}$$

The number of conservation relations in the network changes between two for the first four reaction networks in (N6.2) and one for the last eight reaction networks. Here, $[K]_{tot}$ and $[P]_{tot}$ are constant for the first four, only $[P]_{tot}$ is constant for the second four, and $[K]_{tot}$ is constant for the last four networks. Thus, for network (N6.1)+(N6.2a1) the conservation relation can be given by:

$$\langle w_j, x\rangle = c_j, \qquad j = 1,2 \tag{6.4a}$$

with

$$w_1 = \begin{bmatrix} 1&0&0&1&0&0&1&0&0 \end{bmatrix}^T , \tag{6.4b}$$

$$w_2 = \begin{bmatrix} 0&0&1&0&0&1&0&0&1 \end{bmatrix}^T . \tag{6.4c}$$

Furthermore, a basis for the right nullspace of the stoichiometric matrix N for network (N6.1)+(N6.2a1) can be given by:

$$E^T = \begin{bmatrix} 1&1&0&0&0&0&0&0&0&0&0&0&0&0&0&0\\ 0&0&0&1&1&0&0&0&0&0&0&0&0&0&0&0\\ 1&0&1&1&0&1&0&0&0&0&0&0&0&0&0&0\\ 0&0&0&0&0&0&1&1&0&0&0&0&0&0&0&0\\ 1&0&1&0&0&0&1&0&1&0&0&0&0&0&0&0\\ 0&0&0&0&0&0&0&0&0&1&1&0&0&0&0&0\\ 0&0&0&0&0&0&0&0&0&0&0&1&1&0&0&0\\ 0&0&0&0&0&0&0&0&0&1&0&1&1&0&1&0\\ 1&0&1&0&0&0&1&0&0&1&0&1&0&0&0&1 \end{bmatrix} . \tag{6.5}$$

Note, the cone E has a similar structure to $E^{(n)}$ of the previous chapter, recall equation (5.5) on page 38. Again, a matrix $E^{(1)}$ can be found on the main diagonal blocks. But here, additional vectors in columns four, five and

Table 6.1: *Prediction of multiple steady states following the chemical reaction network theory by Martin Feinberg, see for example [29]. The deficiency of the whole network is given by ϑ. The deficiency of the individual subnetworks (given by the lower and upper branch of de-/phosphorylation, respectively) is given by ϑ_i, with $i = 1$ describing the phosphorylation, $i = 2$ the dephosphorylation and $i = 3$ additional synthesis and degradation reactions. Furthermore the CRNT toolbox (TB) provides either an explicit pair of steady states if the system exhibits multistationarity (cases with a ✓) or not (cases with a ✗), see [34].*

(N6.1)+	(N6.2a1)	(N6.2a2)	(N6.2a3)	(N6.2a4)
ϑ	4	3	4	3
ϑ_i, $i = 1, 2, 3$	1, 1, 0	1, 1, 0	1, 1, 0	1, 1, 0
$\sum_{i=1}^{3} \vartheta_i$	2	2	2	2
TB	✓	✓	✓	✓
(N6.1)+	(N6.2b1)	(N6.2b2)	(N6.2b3)	(N6.2b4)
ϑ	4	3	4	3
ϑ_i, $i = 1, 2, 3$	1, 1, 0	1, 1, 0	1, 1, 0	1, 1, 0
$\sum_{i=1}^{3} \vartheta_i$	2	2	2	2
TB	✓	✓	✗	✗
(N6.1)+	(N6.2c1)	(N6.2c2)	(N6.2c3)	(N6.2c4)
ϑ	4	3	4	3
ϑ_i, $i = 1, 2, 3$	1, 1, 0	1, 1, 0	1, 1, 0	1, 1, 0
$\sum_{i=1}^{3} \vartheta_i$	2	2	2	2
TB	✓	✓	✓	✓

nine can be found not present in the previous cone. This structure is similar for remaining networks in (N6.1)+(N6.2).

With ordinary differential equations, the rate exponent matrix and the conservation relation given, networks in (N6.1)+(N6.2) can be checked for multistationarity using an algorithm based on the theorem of the previous chapter.

Compared to the underlying network mechanism in the previous chapter, nothing can be said about the possibility of the networks to exhibit multiple steady states beforehand. But, following the approach by M. Feinberg, see table 6.1, the deficiency of the networks can be computed. The deficiency theorems are not applicable here as the deficiency of the network itself is not the same as the sum of the deficiency of the terminal strong linkage classes. Nonetheless, [34] provides a toolbox, that is based on the deficiency theorems and provides answers even if the Deficiency Zero or Deficiency One Theorem do not hold. This toolbox allows to draw conclusions on the ability of the network to exhibit multiple steady states, see table 6.1. As indicated by checkmarks two of the arising twelve networks are not supposed to yield multiple steady states, the remaining ones do.

Though the toolbox does not provide algebraic solutions to the questions of existence of multiple steady states, it provides one explicit set of solutions.

By doing this, it answers indeed the question of existence of multiple steady states. At the same time, this confines the solution set to one given pair.

The previous chapter provides a parametrization for multiple steady states for a distributive, sequential phosphorylation network of n steps. The same or at least a similar approach could provide also solutions for different kind of phosphorylation networks, like the one discussed in this chapter.

With the result given in table 6.1, analysis of network (N6.1) together with (N6.2) becomes quite interesting. Two questions arise: first, is the approach of the previous chapter applicable to (bio-) chemical reaction networks as motivated by section 3.2.2 and second, if so, does the approach presented in the previous chapter exhibit the same solutions as provided by the toolbox. If so, results using the approach of the previous chapter could yield a parametrization for the overall multistationarity region and not just one pair. It might furthermore provide an algorithm applicable to general (bio-) chemical reaction networks, where the previous chapter might not yield solutions, e. g., cases where providing all sign vectors is not possible or further restrictions appear.

6.2 MULTISTATIONARITY

The twelve reaction networks in (N6.1)+(N6.2) give rise to a set of ordinary differential equations, see equation (6.1), and conservation relations, equation (6.4). These networks can now be checked for existence of multiple steady states similar to the approach introduced in the previous chapter and the ones introduced in [19] and [49]. Detailed steps are again given for network (N6.1)+(N6.2a1). A short form of the solution algorithm can be found in appendix B.2 for all remaining networks, results for all twelve networks are presented at the end of this section.

Again, the existence of two distinct steady states a and b is assumed such that the polynomial condition

$$N\,v(k,a) = 0 \qquad N\,v(k,b) = 0$$

and the coset condition in (6.4) from Definition 2.4

$$\langle w_j,\, b-a\rangle = 0, \quad \text{with } j = 1,\, 2 \tag{6.6}$$

hold. In a first step, the polynomial condition will be solved and a general algorithm provided to solve such systems. In a second step, the coset condition is considered.

6.2.1 *Solution Algorithm for the Polynomial Condition*

The theorem of the previous chapter and the solution approach introduced in [19] and [49] are extended to network (N6.1)+(N6.2a1).

Algorithm 6.1. [Solution Algorithm for the Polynomial Condition.] The polynomial condition

$$N\,v(k,a) = 0 \qquad N\,v(k,b) = 0 \tag{6.7}$$

exhibits solutions, if

$$v(k,a) \in \operatorname{int}\left(\ker(N)\cap\mathbb{R}^{16}_{\geqslant 0}\right), \qquad v(k,b) \in \operatorname{int}\left(\ker(N)\cap\mathbb{R}^{16}_{\geqslant 0}\right). \tag{6.8}$$

This system can be rewritten in terms of the elements of the rate exponent matrix with

$$\nu(k, a) = E\,\lambda \qquad \text{and} \qquad \nu(k, b) = E\,\nu, \qquad \lambda, \nu \in \mathbb{R}^9_{>0}, \tag{6.9}$$

and thus

$$k_i\, a^{y_i} = \epsilon_i\,\lambda, \qquad k_i\, b^{y_i} = \epsilon_i\,\nu,$$

with $i = 1, \ldots, 16$ and ϵ_i denoting row vectors of E, see equation (6.5). Thus, by introducing $\mu = \ln \frac{b}{a}$ the following equation can be given:

$$Y^T \mu = \ln \frac{E\,\nu}{E\,\lambda}. \tag{6.10}$$

In contrast to the former chapter, compare equation (5.6) on page 38 with equation (6.5), the cone E is not of a block-diagonal form with zeros in the upper right and lower left corner. Thus, λ_l are constrained in a more complex way then before, see the two examples on page 76. If the λ_l are unconstrained, equation (6.10) yields

$$Y^T \mu = \Pi \varkappa \tag{6.11}$$

$$\rightarrow \mu = M\,\tilde{\varkappa}. \tag{6.12}$$

If they are constrained nonlinear inequalities for linear constraints in λ_l can be given by:

$$Q(\tilde{\varkappa})\,\tilde{\lambda} = 0, \text{ with } \lambda > 0 \text{ for a subvector } \tilde{\lambda} \text{ of } \lambda. \tag{6.13}$$

Solvability of equation (6.13) implies solvability of equation (6.8). Vectors $\varkappa$, $\tilde{\varkappa}$ and $\tilde{\lambda}$ will be motivated on the following pages. If $\tilde{\varkappa} \in \mathcal{K}$ can be found, a homogeneous $Q(\tilde{\varkappa})\,\tilde{\lambda}$ with $\lambda > 0$ can be given and solutions to the polynomial condition 6.7 can be found.

Remark 6.2. Note, the polynomial condition of section 5.2.1 and its solution approach via Theorem 5.2 describes a special case of this algorithm, where no additional linear constraints on λ_l can be found.

Remark 6.3. The solution algorithm provided here is independent of the considered phosphorylation network. It can be applied to arbitrary (bio-) chemical reaction networks, where mass action kinetics are applied.

6.2.2 *Application of the Solution Algorithm to Network* (N6.1)+(N6.2a1)

Equation (6.10) for network (N6.1)+(N6.2a1) can be given by:

$$\mu_1 + \mu_2 = \ln \frac{\nu_1 + \nu_3 + \nu_5 + \nu_9}{\lambda_1 + \lambda_3 + \lambda_5 + \lambda_9} \qquad \mu_4 = \ln \frac{\nu_1}{\lambda_1} \qquad \mu_4 = \ln \frac{\nu_3 + \nu_5 + \nu_9}{\lambda_3 + \lambda_5 + \lambda_9} \tag{6.14a}$$

$$\mu_3 + \mu_5 = \ln \frac{\nu_2 + \nu_3}{\lambda_2 + \lambda_3} \qquad \mu_6 = \ln \frac{\nu_2}{\lambda_2} \qquad \mu_6 = \ln \frac{\nu_3}{\lambda_3} \tag{6.14b}$$

$$0 = \ln \frac{\nu_4 + \nu_5 + \nu_9}{\lambda_4 + \lambda_5 + \lambda_9} \qquad \mu_2 = \ln \frac{\nu_4}{\lambda_4} \qquad \mu_5 = \ln \frac{\nu_5}{\lambda_5} \tag{6.14c}$$

$$\mu_1 + \mu_5 = \ln \frac{\nu_6 + \nu_8 + \nu_9}{\lambda_6 + \lambda_8 + \lambda_9} \qquad \mu_7 = \ln \frac{\nu_6}{\lambda_6} \qquad \mu_7 = \ln \frac{\nu_8 + \nu_9}{\lambda_8 + \lambda_9} \tag{6.14d}$$

$$\mu_3 + \mu_8 = \ln \frac{\nu_7 + \nu_8}{\lambda_7 + \lambda_8} \qquad \mu_9 = \ln \frac{\nu_7}{\lambda_7} \qquad \mu_9 = \ln \frac{\nu_8}{\lambda_8} \tag{6.14e}$$

$$\mu_8 = \ln \frac{\nu_9}{\lambda_9} \tag{6.14f}$$

Due to the structure of these equations, compare again the structure of the cone E in equation (6.5), dependencies occur between individual expressions reducing the number of parameters. E. g., the following linear constraints can be found due to the present $E^{(1)}$ in E at the first main diagonal block for equation (6.14b):

$$\mu_6 = \ln \frac{\nu_2}{\lambda_2} = \ln \frac{\nu_3}{\lambda_3}.$$

Thus,

$$\frac{\nu_2}{\lambda_2} = \frac{\nu_3}{\lambda_3} \qquad \rightarrow \qquad \nu_2 = \frac{\nu_3 \lambda_2}{\lambda_3}$$

yields also

$$\begin{aligned} \ln \frac{\nu_2 + \nu_3}{\lambda_2 + \lambda_3} &= \ln \frac{\frac{\nu_3 \lambda_2}{\lambda_3} + \nu_3}{\lambda_2 + \lambda_3} \\ &= \ln \frac{\nu_3}{\lambda_3} \frac{\lambda_2 + \lambda_3}{\lambda_2 + \lambda_3} = \ln \frac{\nu_3}{\lambda_3} \end{aligned}$$

and thus, the linear constraint in μ can be given by:

$$\mu_6 = \mu_3 + \mu_5$$

reducing the number of variables. The same holds true for the more complex equations, i. e., linear constraints arise due to the additional column vectors at the fourth, fifth and ninth position in E. E. g., equation (6.14a):

$$\begin{aligned} &\mu_4 = \ln \frac{\nu_1}{\lambda_1} = \ln \frac{\nu_3 + \nu_5 + \nu_9}{\lambda_3 + \lambda_5 + \lambda_9} \\ &\rightarrow \ln \frac{\nu_1}{\lambda_1} = \ln \frac{\nu_1 + \nu_3 + \nu_5 + \nu_9}{\lambda_1 + \lambda_3 + \lambda_5 + \lambda_9} \\ &\rightarrow \mu_1 + \mu_2 = \mu_4 \end{aligned}$$

Together with the two remaining equations

$$\begin{aligned} \ln \frac{\nu_6 + \nu_8 + \nu_9}{\lambda_6 + \lambda_8 + \lambda_9} = \ln \frac{\nu_6}{\lambda_6} = \ln \frac{\nu_8 + \nu_9}{\lambda_8 + \lambda_9} \\ \ln \frac{\nu_7 + \nu_8}{\lambda_7 + \lambda_8} = \ln \frac{\nu_7}{\lambda_7} = \ln \frac{\nu_8}{\lambda_8} \end{aligned}$$

the following linear constraints occur:

$$\begin{aligned} &\mu_1 = \mu_4 - \mu_2, && \mu_1 = \mu_7 - \mu_5, \\ &\mu_3 = \mu_6 - \mu_5, && \mu_3 = \mu_9 - \mu_8. \end{aligned}$$

And thus

$$\mu_4 - \mu_2 = \mu_7 - \mu_5, \qquad \mu_6 - \mu_5 = \mu_9 - \mu_8. \tag{6.15}$$

No further constraints of this kind can be found.

To solve equation (6.10) a vector $\varkappa \in \mathbb{R}^7$ is introduced:

$$\varkappa_1 := \ln \frac{\nu_1}{\lambda_1} \tag{6.16a}$$
$$\varkappa_2 := \ln \frac{\nu_2}{\lambda_2} \tag{6.16b}$$
$$\varkappa_3 := \ln \frac{\nu_4}{\lambda_4} \tag{6.16c}$$
$$\varkappa_4 := \ln \frac{\nu_5}{\lambda_5} \tag{6.16d}$$
$$\varkappa_5 := \ln \frac{\nu_6}{\lambda_6} \tag{6.16e}$$
$$\varkappa_6 := \ln \frac{\nu_7}{\lambda_7} \tag{6.16f}$$
$$\varkappa_7 := \ln \frac{\nu_9}{\lambda_9} \tag{6.16g}$$

where due to equation (6.15)

$$\varkappa_5 = \varkappa_1 - \varkappa_3 + \varkappa_4, \qquad \varkappa_7 = -\varkappa_2 + \varkappa_4 + \varkappa_6. \tag{6.17}$$

Thus

$$\begin{aligned}
\nu_1 &= \exp(\varkappa_1)\,\lambda_1 \\
\nu_2 &= \exp(\varkappa_2)\,\lambda_2 & \nu_3 &= \exp(\varkappa_2)\,\lambda_3 \\
\nu_4 &= \exp(\varkappa_3)\,\lambda_4 \\
\nu_5 &= \exp(\varkappa_4)\,\lambda_5 \\
\nu_6 &= \exp(\varkappa_5)\,\lambda_6 & &\to \nu_6 = \exp(\varkappa_1 - \varkappa_3 + \varkappa_4)\,\lambda_6 \\
\nu_7 &= \exp(\varkappa_6)\,\lambda_7 & \nu_8 &= \exp(\varkappa_6)\,\lambda_8 \\
\nu_9 &= \exp(\varkappa_7)\,\lambda_9 & &\to \nu_9 = \exp(-\varkappa_2 + \varkappa_4 + \varkappa_6)\,\lambda_9
\end{aligned} \tag{6.18}$$

Whereas equation (6.14b), (6.14e) and (6.14f) yield independent λ_l, some equations in (6.14) pose constraints on λ_l, e. g., via equation (6.14a):

$$\varkappa_1 = \ln \frac{\nu_3 + \nu_5 + \nu_9}{\lambda_3 + \lambda_5 + \lambda_9}. \tag{6.19a}$$

The same holds for equation (6.14c):

$$0 = \ln \frac{\nu_4 + \nu_5 + \nu_9}{\lambda_4 + \lambda_5 + \lambda_9}, \tag{6.19b}$$

and equation (6.14d):

$$\varkappa_1 - \varkappa_3 + \varkappa_4 = \ln \frac{\nu_8 + \nu_9}{\lambda_8 + \lambda_9}. \tag{6.19c}$$

Using equation (6.18) these three expressions can be rewritten:

$$\begin{aligned}
0 = {} & (\exp(\varkappa_2) - \exp(\varkappa_1))\,\lambda_3 + (\exp(\varkappa_4) - \exp(\varkappa_1))\,\lambda_5 \\
& + (\exp(-\varkappa_2 + \varkappa_4 + \varkappa_6) - \exp(\varkappa_1))\,\lambda_9
\end{aligned} \tag{6.20a}$$
$$\begin{aligned}
0 = {} & (\exp(\varkappa_3) - 1)\,\lambda_4 + (\exp(\varkappa_4) - 1)\,\lambda_5 \\
& + (\exp(-\varkappa_2 + \varkappa_4 + \varkappa_6) - 1)\,\lambda_9
\end{aligned} \tag{6.20b}$$
$$\begin{aligned}
0 = {} & (\exp(\varkappa_6) - \exp(\varkappa_1 - \varkappa_3 + \varkappa_4))\,\lambda_8 \\
& + (\exp(-\varkappa_2 + \varkappa_4 + \varkappa_6) - \exp(\varkappa_1 - \varkappa_3 + \varkappa_4))\,\lambda_9
\end{aligned} \tag{6.20c}$$

Recall, algorithm 6.1 only poses sign conditions on λ_l. Thus, equation (6.20) does not have to be solved for explicit expressions of λ_l. Solutions satisfying $\lambda_l > 0$ are sufficient for algorithm 6.1.

To provide solutions for algorithm 6.1 the independent $\varkappa_k$ and dependent λ_l, i. e., those that do not appear on the left hand side of equation (6.17) and those, that appear in equation (6.20) respectively, are collected in vectors $\tilde{\varkappa} \in \mathbb{R}^5$ and $\tilde{\lambda} \in \mathbb{R}^5_{>0}$:

$$\tilde{\varkappa} = \begin{bmatrix} \varkappa_1 & \varkappa_2 & \varkappa_3 & \varkappa_4 & \varkappa_6 \end{bmatrix}^T, \tag{6.21}$$

$$\tilde{\lambda} = \begin{bmatrix} \lambda_3 & \lambda_4 & \lambda_8 & \lambda_5 & \lambda_9 \end{bmatrix}^T. \tag{6.22}$$

The solution of equation (6.11) to equation (6.10) can be given by:

$$\mu := M\,\tilde{\varkappa}$$

with $M \in \mathbb{R}^{9\times 5}$

$$M = \begin{bmatrix} 1 & 0 & -1 & 0 & 0 \\ 0 & 0 & 1 & 0 & 0 \\ 0 & 1 & 0 & -1 & 0 \\ 1 & 0 & 0 & 0 & 0 \\ 0 & 0 & 0 & 1 & 0 \\ 0 & 1 & 0 & 0 & 0 \\ 1 & 0 & -1 & 1 & 0 \\ 0 & -1 & 0 & 1 & 1 \\ 0 & 0 & 0 & 0 & 1 \end{bmatrix}. \tag{6.23}$$

Note again, vectors and matrices are given for network (N6.1)+(N6.2a1). And solutions for remaining networks (N6.1)+(N6.2) can be found in appendix B.2.

The first part of algorithm 6.1, finding a solution to μ, is done. The remaining part of finding expressions or rather sign conditions on expressions for $\varkappa_k$ in equation (6.20) is discussed now, yielding a solution to equation (6.13).

To derive expressions for $\varkappa_k$ yielding $\lambda_l > 0$, equations in (6.20) are rewritten using a shorter notation. As only positivity of λ_l is required, variables q_{ij} are introduced for each block of $(\exp() - \exp())$ in equation (6.20):

$$0 = q_{11}\,\lambda_3 + q_{12}\,\lambda_5 + q_{13}\,\lambda_9, \tag{6.24a}$$

$$0 = q_{21}\,\lambda_4 + q_{22}\,\lambda_5 + q_{23}\,\lambda_9, \tag{6.24b}$$

$$0 = q_{31}\,\lambda_8 + q_{32}\,\lambda_9, \tag{6.24c}$$

yielding linear equations in λ_l. To compute $\tilde{\lambda}$ while guaranteeing positivity of λ_l, signs of q_{ij} have to be computed, shifting the nonlinear problem of equation (6.13) to a linear inequality problem of sign conditions. For example, if $\lambda_8, \lambda_9 > 0$ is desired for equation (6.24c), then either $q_{31} > 0$, $q_{32} < 0$ or $q_{31} < 0$, $q_{32} > 0$. Thus, the arising system of inequalities has to be solved only in a qualitative manner. Signs are collected in a sign matrix $Q \in \mathbb{R}^{3\times 5}$ of elements q_{ij} in the following form

$$Q = \begin{bmatrix} q_{11} & 0 & 0 & q_{12} & q_{13} \\ 0 & q_{21} & 0 & q_{22} & q_{23} \\ 0 & 0 & q_{31} & 0 & q_{32} \end{bmatrix} \tag{6.25}$$

with

$$Q\,\tilde{\lambda} = 0 \qquad \text{for } \tilde{\lambda} \in \mathbb{R}^5_{>0}. \tag{6.26}$$

Each element q_{ij} of Q can be smaller, equal or larger then zero resulting in a sign pattern $\{+, -, 0\}$ for each q_{ij}.

Without loss of generality, a matrix $K \in \mathbb{R}^{8\times 5}$ of sign patterns is chosen for equation (6.20) and can be given by:

$$K = \begin{bmatrix} -1 & 1 & 0 & 0 & 0 \\ -1 & 0 & 0 & 1 & 0 \\ -1 & -1 & 0 & 1 & 1 \\ 0 & 0 & 1 & 0 & 0 \\ 0 & 0 & 0 & 1 & 0 \\ 0 & -1 & 0 & 1 & 1 \\ -1 & 0 & 1 & -1 & 1 \\ -1 & -1 & 1 & 0 & 1 \end{bmatrix}, \tag{6.27}$$

where elements q_{ij} of Q are such that

$$q_{ij} = K\,\exp(\tilde{x}) \tag{6.28}$$

and

$$\operatorname{sgn}(q) = \operatorname{sgn}(K\,\tilde{x}),$$

with q a vector of composed elements of q_{ij}, with $i = 1, \ldots, n$, $j = 1, \ldots, m$:

$$\begin{aligned} q &= [q_{11} \;\ldots\; q_{1m} \;\ldots\; q_{i1} \;\ldots\; q_{im} \;\ldots\; q_{n1} \;\ldots\; q_{nm}]^T, \\ q &= \operatorname{col}(q_i). \end{aligned} \tag{6.29}$$

The matrix K is referred to as a sign matrix.

Remark 6.4. If Q has more than three entries in one row, compare equation (6.25), no definite solution can be found, as inequalities of sums of at least four elements have to be solved, see as well Lemma 6.6 or section 6.3 further on.

To find all valid signs for Q, the matrix K is examined first row wise, corresponding to a stepwise testing of various sign conditions for positivity of $\tilde{\lambda}$ and thus, corresponding to the three equations in (6.24). In a second step, a column wise inspection of K is done, to check for contradictions that might arise between single equations in (6.24) while choosing q_{ij}.

The stepwise testing is done in the following way: first, composed elements of $\{+, -, 0\}$ are chosen as a sign for q_{ij} in Q. But, as only certain combinations of these signs yield $\tilde{\lambda}_l > 0$, the maximal possible number of patterns is reduced in advance. I. e., if a row q_i of Q contains only two entries q_{ij}, in total a maximum of nine possible sign pattern arise:

$$\begin{Bmatrix} + & + & - & - & 0 & 0 & + & - & 0 \\ +' & -' & +' & -' & +' & -' & 0' & 0' & 0 \end{Bmatrix}.$$

But only three of these nine sign conditions yield $\tilde{\lambda}_l > 0$:

$$\left\{\begin{matrix} + & - & 0 \\ -, & +, & 0 \end{matrix}\right\}.$$

Note, these signs provide $\tilde{\lambda}_l > 0$ for individual rows of Q, but do not check for contradictions between these rows. Also note, if one sign pattern is valid, its sign-inverse is also valid.

If a row q_i contains three entries, e. g., equation (6.24a) or (6.24b), thirteen of the arising 27 sign combinations yield $\tilde{\lambda}_i > 0$, compare also the signs in (5.36) on page 44:

$$\left\{\begin{matrix} + & + & - & - & 0 & 0 & 0 & + & + & + & - & - & - \\ 0, & -, & +, & 0, & +, & -, & 0, & +, & -, & -, & +, & +, & + \\ - & 0 & 0 & + & - & + & 0 & - & + & - & + & - & + \end{matrix}\right\}.$$

To provide all valid sign patterns for Q and K, all possible signs for rows q_i have to be combined.[1] As equations in (6.24) are composed of one equation containing two q_{ij} and two equations contain three, in total $3 \cdot 13^2 = 507$ possible sign patterns have to be checked for network (N6.1)+(N6.2a1).

Testing which sign patterns for q_{ij} may arise, the set of all possible sign patterns is tested and valid ones are collected in a vector $\sigma \in \{+, -, 0\}^8$ with[2]:

$$\operatorname{sgn}(q) = \left\{\sigma \in \{+, -, 0\}^8 \,|\, \exists\, \tilde{\varkappa} \text{ with } \operatorname{sgn}(q(\tilde{\varkappa})) = \operatorname{sgn}(K\,\tilde{\varkappa}) = \sigma\right\}. \tag{6.30}$$

If such a $\sigma = \operatorname{sgn}(q)$ exists, then, each equation defined by a row vector of Q is feasible:

$$Q(i,j)\,\tilde{\lambda} = 0, \qquad \lambda > 0$$

All valid σ are collected in a matrix $\Sigma \in \{+, -, 0\}^{8\times m}$ with

$$\Sigma = [\sigma_1, \ldots, \sigma_m] \tag{6.31}$$

with $0 \leqslant m \leqslant 507$ for network (N6.1)+(N6.2a1). If no valid σ can be found, the network excludes multistationarity.

This concludes the first step of computing all possible sign patterns. In a second step, contradiction between individual signs of q_{ij} fixing the sign of $\varkappa_l$ have to be checked. Up till now, choosing a $\tilde{\varkappa}$ such that $\operatorname{sgn}(K\,\tilde{\varkappa}) = \sigma$ for some $\sigma \in \delta$ generates feasibility of $Q(i,j)\,\tilde{\lambda} = 0$, $\tilde{\lambda} > 0$, but does not have to hold simultaneously for the system $Q\,\tilde{\lambda} = 0$, $\tilde{\lambda} > 0$.

Example 6.5. Additional conditions on $\varkappa_l$ might occur: combining $\{+, +, -\}$ for the first row with either $\{+, -, +\}$ or $\{+, -, -\}$ for the second one in equation (6.24) poses additional restrictions, see example 6.8 and 6.9 later on.

In more general terms, independent of the networks considered in (N6.2) and the structure in Q for network (N6.1)+(N6.2), the following necessary condition can be posed:

6.1 Matrix K in equation (6.27) describes only one possible matrix of sign patterns, various other matrices are possible as well.

6.2 Note, the length of the vector σ corresponds to the number of q_{ij} in Q.

Lemma 6.6. [Computation of Sign Patterns σ.] *A system of equations* $Q\tilde{\lambda} = 0$ *for* $\tilde{\lambda} > 0$ *with*

$$Q = \begin{bmatrix} q_{11} & & & & 0 & 0 & q_{12} & q_{13} \\ & \ddots & & & & & \vdots & \vdots \\ & & q_{i1} & & \vdots & \vdots & q_{i2} & q_{i3} \\ & & & \ddots & & & \vdots & \vdots \\ & & & & q_{(n-1)1} & 0 & q_{(n-1)2} & q_{(n-1)3} \\ 0 & & & & 0 & q_{n1} & 0 & q_{n3} \end{bmatrix}, \tag{6.32}$$

with $i = 1, \ldots, n$ *and* $\tilde{\lambda} = [\lambda_1, \ldots, \lambda_n, \lambda_{p-1}, \lambda_p]^T$ *can be solved if and only if the matrix* Q *of rows* q_i *obeys the following sign conditions:*

(A) In the bilinear case, i.e., $q_i = [q_{i1}\ q_{i3}]^T$ *with* $Q \in \mathbb{R}^{n\times(n+1)}$ *and* $\tilde{\lambda} = [\lambda_1, \ldots, \lambda_n, \lambda_p]^T$ *each row can contain either of the following three sign patterns:*

$$\begin{matrix} q_{i1} \\ q_{i3} \end{matrix} \left\{ \begin{matrix} + & - & 0 \\ -' & +' & 0 \end{matrix} \right\} \tag{6.33}$$

such that

$$\lambda_i\, q_{i1} + \lambda_p\, q_{i3} \stackrel{!}{=} 0. \tag{6.34}$$

has a positive solution λ_i *and* λ_p.

(B) In the trilinear case, i.e., $q_i = [q_{i1}\ q_{i2}\ q_{i3}]^T$ *with* $Q \in \mathbb{R}^{n\times(n+2)}$ *and* $\tilde{\lambda} = [\lambda_1, \ldots, \lambda_n, \lambda_{p-1}, \lambda_p]^T$ *each row can contain either of the following thirteen sign patterns:*

$$\begin{matrix} q_{i1} \\ q_{i2} \\ q_{i3} \end{matrix} \left\{ \begin{matrix} + & + & - & - & 0 & 0 & 0 & + & + & + & - & - & - \\ 0, & -, & +, & 0, & +, & -, & 0, & +, & -, & -, & +, & +, & + \\ - & 0 & 0 & + & - & + & 0 & - & + & - & + & - & + \end{matrix} \right\} \tag{6.35}$$

such that

$$\lambda_i\, q_{i1} + \lambda_{p-1}\, q_{i2} + \lambda_p\, q_{i3} \stackrel{!}{=} 0. \tag{6.36}$$

has a positive solution λ_i, λ_{p-1} *and* λ_p. *The condition* $\tilde{\lambda} > 0$ *yields for each row* q_i *of* Q

$$\frac{1}{q_{i1}} \left[q_{i2}\, \lambda_{p-1} + q_{i3}\, \lambda_p \right] \stackrel{!}{<} 0$$

for $q_{i1} \neq 0$. *Rearranging yields*

$$\begin{aligned} & \frac{\operatorname{sgn}(q_{i1})}{|q_{i1}|} \left[\operatorname{sgn}(q_{i2})\, |q_{i2}|\, \lambda_{p-1} + \operatorname{sgn}(q_{i3})\, |q_{i3}|\, \lambda_p \right] < 0 \\ \rightarrow \quad & \operatorname{sgn}(q_{i1})\operatorname{sgn}(q_{i2})\, \lambda_{p-1} < -\operatorname{sgn}(q_{i1})\operatorname{sgn}(q_{i3}) \frac{|q_{i3}|}{|q_{i2}|} \lambda_p \end{aligned} \tag{6.37}$$

if $q_{i1}, q_{i2} \neq 0$. *Equation* (6.37) *has to hold to guarantee positivity for all* $\tilde{\lambda}$.

(C) For further cases see Remark 6.4.

Remark 6.7. Combining different sign patterns in various ways might yield additional conditions. E. g., having two rows q_i and q_k, with three entries in the i-th row and and two entries in the k-th row, does not yield additional conditions on the q's while choosing the first column of signs of (6.35) for each row q in Q. But combining different sign patterns might. Here, not only combinations within the same column, i. e., the same sign vector of (6.35) for corresponding entries in rows in Q, but also combinations of different columns can yield additional constraints. Two examples are chosen respectively to elucidate the arising constraints.

Example 6.8. Consider in the case of interest of matrix Q in equation (6.25) for network (N6.1)+(N6.2a1) two rows q_i and q_k with $1 \leqslant i \leqslant n-1$, $2 \leqslant k \leqslant n$ and $i \neq k$, containing three and two elements respectively:

$$\begin{bmatrix} q_{i1} & q_{i2} & q_{i3} \\ 0 & q_{k1} & q_{k3} \end{bmatrix}$$

and a corresponding $\tilde{\lambda}$

$$\begin{bmatrix} \lambda_j & \lambda_{p-1} & \lambda_p \end{bmatrix}^T,$$

for $j = 1, \ldots, n$ with the following signs

$$\operatorname{sgn}\left(\begin{bmatrix} q_{i1} & q_{i2} & q_{i3} \end{bmatrix}\right) = \begin{Bmatrix} + & + & - \end{Bmatrix}$$

and

$$\operatorname{sgn}\left(\begin{bmatrix} q_{k1} & q_{k3} \end{bmatrix}\right) = \begin{Bmatrix} + & - \end{Bmatrix}.$$

Thus

$$\begin{aligned} \lambda_j &= -\frac{q_{i2}}{q_{i1}}\lambda_{p-1} + \frac{|q_{i3}|}{q_{i1}}\lambda_p \overset{!}{>} 0 \\ \lambda_{p-1} &= \frac{|q_{k3}|}{q_{k1}}\lambda_p \overset{!}{>} 0 \end{aligned}$$

Thus, the additional sign restriction

$$\frac{q_{i2}\, q_{k3}}{q_{j1}} < q_{i3}$$

for $q_{i1} > 0$ appears.

Example 6.9. Consider the same matrix Q and vector $\tilde{\lambda}$ as in example 6.8 with a different setup of signs

$$\operatorname{sgn}\left(\begin{bmatrix} q_{i1} & q_{i2} & q_{i3} \end{bmatrix}\right) = \begin{Bmatrix} + & + & - \end{Bmatrix}$$

and

$$\operatorname{sgn}\left(\begin{bmatrix} q_{k1} & q_{k3} \end{bmatrix}\right) = \begin{Bmatrix} - & + \end{Bmatrix}.$$

These conditions result in a reversed pattern for final values in q:

$$\frac{q_{i2}\, q_{k3}}{q_{k1}} > q_{i3}$$

for $q_{i1} > 0$ appears.

Recall equation (6.24) and the discussion on page 80 on the number of possible sign patterns. For network (N6.1)+(N6.2a1) in total $13 \cdot 13 \cdot 3 = 507$ possible sign patterns σ can be found. Each σ defines a linear inequality system

$$\operatorname{diag}(\sigma)\, K\, \tilde{x} > 0.$$

All valid sign matrices K for valid σ are collected in the set of sign matrices $\mathcal{K}$, such that:

$$\operatorname{sgn}(K\, \tilde{x}) = \sigma. \tag{6.38}$$

Knowing K from equation (6.27), only valid σ have to be given to provide all valid sign matrices collected in $\mathcal{K}$. With a valid σ a vector $\tilde{x} \in \mathbb{R}^5$ and a matrix $Q \in \mathbb{R}^{3\times 5}$ can be given. If a valid $\tilde{x}$ can be found, such that $Q(\tilde{x})\,\tilde{\lambda}$ has a solution, then a solution for μ can be given by equation (6.12). Thus, steady states satisfying the polynomial system posed by the ordinary differential equations can be given by:

$$\begin{aligned} a_i &= \bar{a}_i \\ b_i &= a_i \exp(\mu_i) \end{aligned}$$

for $i = 1, \ldots, 3n+3$. Here, μ is dependent on $\tilde{x}$ satisfying sign patterns collected in $\mathcal{K}$. Furthermore, the vector of rate constants can be derived again in terms of a and λ according to equation (6.9):

$$k = \operatorname{diag}\left(\Phi(a^{-1})\right) E\, \lambda. \tag{6.39}$$

Recall, certain entries in λ are not independent, compare equation (6.22).

The same overall solution algorithm 6.1, described in detail in this section, can be applied to the remaining network setups. The overall structure of Q and K stays the same in accordance to lemma 6.6. But the size and entries change. General results are given after the next section, detailed ones can be found in appendix B.2 for missing networks (N6.1)+(N6.2).

The solution to the cosed condition is discussed in the next section.

6.2.3 *The Coset Condition*

For steady states to satisfy not only the polynomial condition posed by the ordinary differential equations but also the coset condition, compare section 5.2.2, a sign condition posed by $s = b - a \in \operatorname{im}(N)$ and $\mu = \ln \frac{b}{a}$ arises. Here, μ has to satisfy also conditions posed by $\tilde{x}$. Thus, the following sign conditions have to hold for equations (6.12), (6.38) and (6.6) respectively:

$$\begin{aligned} M\, \tilde{x} - \operatorname{diag}(\delta)\, \zeta_1 &= 0 \\ K\, \tilde{x} - \operatorname{diag}(\sigma)\, \zeta_2 &= 0 \\ W^T \operatorname{diag}(\delta)\, \zeta_3 &= 0 \end{aligned} \tag{6.40}$$

with $\zeta_1, \zeta_2, \zeta_3 > 0$. Valid sign vectors δ and sign patterns σ are referred to as valid sign combinations for the reaction network. The algorithm provided by [58] can be extended to include also the sign patterns collected in $\mathcal{K}$: instead of checking only M, W and δ, the system in equation (6.40) has to be checked. Thus, every possible sign pattern, i. e., all solutions to equation (6.38), are tested in combination with every possible sign vector δ, either 3^{3n+3} for the ternary set of $\delta \in \{+, -, 0\}$ or 2^{3n+3} for the binary set

of $\delta \in \{+, -\}$, yielding not only a desired δ but also valid sign patterns for K via σ, recall equation (6.30) and thus, enabling multistationarity.

Note, one sign pattern σ can be valid for several sign vectors δ. Also, if a certain σ and δ is given, the corresponding sign-inverse $-\sigma$ and $-\delta$ are valid sign combinations as well.

Using the algorithm provided by [58] to test for valid sign combinations, in total 23 sign vectors can be found for network (N6.1)+(N6.2a1). All δ_i for $\delta \in \{+, -, 0\}^9$ are collected in $\Delta \in \{+, -, 0\}^{9\times 23}$, and all σ_i for $\sigma \in \{+, -, 0\}^8$ are collected in $\Sigma \in \{+, -, 0\}^{8\times 23}$:

$$\Delta^T = \begin{bmatrix} -1 & -1 & -1 & -1 & 1 & -1 & 1 & 1 & 1 \\ -1 & 1 & -1 & 1 & 1 & 1 & -1 & -1 & -1 \\ -1 & 1 & -1 & 1 & 1 & 1 & -1 & -1 & -1 \\ -1 & 1 & -1 & 1 & 1 & 1 & -1 & -1 & -1 \\ -1 & 1 & 0 & 1 & 1 & 1 & -1 & -1 & -1 \\ -1 & 1 & 1 & 1 & -1 & 1 & -1 & -1 & -1 \\ -1 & 1 & 1 & 1 & 0 & 1 & -1 & -1 & -1 \\ -1 & 1 & 1 & 1 & 1 & 1 & -1 & -1 & -1 \\ -1 & 1 & 1 & 1 & 1 & 1 & -1 & -1 & -1 \\ -1 & 1 & 1 & 1 & 1 & 1 & -1 & -1 & -1 \\ 0 & -1 & -1 & -1 & 1 & -1 & 1 & 1 & 1 \end{bmatrix} \tag{6.41}$$

Given is only half of the set with the remaining half being the sign inversion of the first and the vector $\delta_{23} = \underline{0}$ being the last valid sign vector. Furthermore, 23 sign patterns σ for K can be found for each sign vector, respectively:

$$\Sigma^T = \begin{bmatrix} -1 & 1 & 1 & -1 & 1 & 1 & -1 & 1 \\ 0 & 1 & -1 & 1 & 1 & -1 & -1 & 1 \\ 1 & 1 & -1 & 1 & 1 & -1 & -1 & 1 \\ -1 & 1 & -1 & 1 & 1 & -1 & -1 & 1 \\ 1 & 1 & -1 & 1 & 1 & -1 & 0 & 0 \\ 1 & -1 & -1 & 1 & -1 & -1 & 1 & -1 \\ 1 & -1 & -1 & 1 & 0 & -1 & 1 & -1 \\ 1 & 0 & -1 & 1 & 1 & -1 & 1 & -1 \\ 1 & 1 & -1 & 1 & 1 & -1 & 1 & -1 \\ 1 & -1 & -1 & 1 & 1 & -1 & 1 & -1 \\ -1 & 1 & 1 & -1 & 1 & 1 & -1 & 1 \end{bmatrix} \tag{6.42}$$

Again, only half of the valid set of σ is given, sign patterns for the inverted half of sign vectors can be computed by $\sigma(\delta) = -\sigma(\delta)$. As the same sign pattern σ can be valid for various δ, some doubling entries can be found. For example the eleventh sign pattern, σ_{11}, corresponds to the first, σ_1.[3]

Each of these 23 sign vectors δ together with its corresponding sign pattern σ can be used to compute steady states a and b. As in section 5.2.2 the sign vector is used to computed cones where $\operatorname{sgn}(s) = \operatorname{sgn}(\mu)$. Here

6.3 Note, additional conditions on choosing $\tilde{\lambda}_l$ might occur, when a certain sign vector is chosen. For example, δ_{15}, as the fifteenth row vector in Δ, yields with $\sigma_{15} = [-1 \quad 1 \quad 1 \quad -1 \quad -1 \quad 1 \quad -1 \quad 1]$ the additional condition $0 < \frac{q_{23}}{q_{13}}$. Other sign vectors do not have to impose additional conditions on λ_l, for example δ_8.

only the corresponding cone E^S to s is used as μ is defined by $\tilde{x}$, recall equation (6.12):

$$\begin{aligned} \mu &= M\,\tilde{x}, \\ s &= E^S\,\beta, \end{aligned} \tag{6.43}$$

where $\tilde{x}$ satisfies equation (6.13) and $\operatorname{sgn}(\mu) = \operatorname{sgn}(s)$. The computation of a and b then follows the same algorithm as in equation (5.50) in section 5.2.2.

$$a_i = \begin{cases} \frac{s_i}{\exp(\mu_i)-1}, & \text{if } \mu_i \neq 0 \\ \bar{a}_i > 0, & \text{if } \mu_i = 0 \end{cases}$$
$$b_i = a_i \exp(\mu_i)$$

for $i = 1, \ldots, 9$. Furthermore, rate constants can be given by

$$k = \operatorname{diag}\left(\Phi(a^{-1})\right)\,\lambda$$

corresponding to equation (5.31) and $\tilde{\lambda}$ restricting some elements of the vector λ, see equation (6.22). An example for steady states is given in the next section.

Results for remaining networks can be found in appendix B.2. Table 6.2 gives an overview on the number of all possible sign vectors $\delta \in \{+, -, 0\}$, and all possible sign patterns $\sigma \in \{+, -, 0\}$, as well as the actual number of valid sign vectors δ and unique valid sign patterns σ. If the number of sign patterns σ is lower than the number of sign vectors δ, then certain σ are valid for several δ, see as well solutions in appendix B.2.

As valid σ and δ can be given for some of the phosphorylation networks in (N6.1)+(N6.2), they can indeed exhibit multiple steady states: They exhibit multiple steady states if and only if the kinase is not synthesized or degraded together with synthesis, but not degradation of the unphosphorylated protein. The two remaining cases, i. e., the kinase is synthesized and degraded, and the unphosphorylated protein is only synthesized, do not yield multiple steady states but only one, see page 167 in appendix B.2. In accordance to table 6.1 all but networks (N6.1)+(N6.2b3) and (N6.1)+(N6.2b4) yield multiple steady states. Additionally to the results given by the CRNT toolbox, a parametrization for the steady states can be given in terms of a, b and k. An example for network (N6.1)+(N6.2a1) will be discussed in the next section.

Remark 6.10. Algorithm 6.1 shifts the nonlinear problem in equation (6.7) in such a way, that solutions to a linear problem in equation (6.12) together with a nonlinear inequality problem in equation (6.13) have to be solved. Lemma 6.6 provides necessary conditions on (6.13), such that a linear problem is provided in equation (6.12) together with sign patterns provided in equation (6.30). This approach is applicable for (bio-) chemical reaction networks of mass action kinetics, and if Remark 6.4 is not valid, the system can be checked for multistationarity and, if present, a parametrization is provided

The Algorithm 6.1 together with Lemma 6.6 does not only confirm results by the *CRNT* toolbox, see table 6.1, but also provides a parametrization of the whole multistationarity region for networks allowing multistationarity.

The next section provides an example for the parametrization. Note, the parametrization of steady states in section 5.4.2 could be applied here, see Remark 5.15, to provide parameters in desired intervals.

Table 6.2: *Overview on number of (valid) sign vectors δ and (valid) sign patterns σ for all synthesis and/or degradation networks in (N6.1)+(N6.2) yielding steady states. The upper blocks provide the maximum number of valid sign vectors and sign patterns. The actual number of valid sign vectors together with valid sign patterns is given in the lower blocks. Note, the zeros in the middle right part indicate systems exhibiting at most one steady state but not multiple steady states. Furthermore, $\delta = \underline{0}$ is neglected in this table as it is a valid result for all twelve networks and results only in systems exhibiting one steady state.*

(N6.1)+	(N6.2a1)	(N6.2a2)	(N6.2a3)	(N6.2a4)
max#(σ)	507	27	117	9
max#(δ)	19683	19683	19683	19683
#σ	20	8	12	2
#δ	22	14	54	2
(N6.1)+	(N6.2b1)	(N6.2b2)	(N6.2b3)	(N6.2b4)
max#(σ)	507	27	117	9
max#(δ)	19683	19683	19683	19683
#σ	2	2	0	0
#δ	2	2	0	0
(N6.1)+	(N6.2c1)	(N6.2c2)	(N6.2c3)	(N6.2c4)
max#(σ)	39	9	9	3
max#(δ)	19683	19683	19683	19683
#σ	2	2	2	2
#δ	2	2	2	2

6.2.4 *Steady States and Bifurcation Analysis*

To compute steady states for network (N6.1)+(N6.2a1) the conditions on $\varkappa_i$ via $\tilde{\varkappa}$ in (6.12) have to be fulfilled. For example, the eighth sign vector δ_8 in (6.41) together with its corresponding sign pattern σ_8 in (6.42) are chosen:

$$\delta_8 = \begin{bmatrix} -1 & 1 & 1 & 1 & 1 & 1 & -1 & -1 & -1 \end{bmatrix}^T,$$
$$\sigma_8 = \begin{bmatrix} 1 & 0 & -1 & 1 & 1 & -1 & 1 & -1 \end{bmatrix}^T.$$

As only the sign itself is specified, different $\varkappa_i$ can be chosen to compute valid μ. All $\varkappa_i$ for σ_8 are arbitrary, but nonzero. They are chosen in a range of $[-1,1]\backslash\{0\}$ and values for each entry are chosen in a basic form according to the condition given, for example:

$$\tilde{\varkappa} = \begin{bmatrix} 0.25 & 0.75 & 0.6 & 0.25 & -0.05 \end{bmatrix}^T.$$

The vector β, equation (6.43), is needed to compute values for s. These are generated as previously in terms of uniformly distributed pseudo random numbers in $(0, 1)$:

$$\beta = [0.995319,\ 0.261444,\ 0.725198,\ 0.342727,\ 0.114304,\ 0.44888,\ 0.376883]^T.$$

Recall, α is not needed, as μ is computed in terms of $\varkappa_i$ via equation (6.43). Thus $\tilde{\varkappa}$ and β yield for δ_8 and σ_8 of network (N6.1)+(N6.2a1)

$$\mu = [-0.35,\ 0.6,\ 0.5,\ 0.25,\ 0.25,\ 0.75,\ -0.1,\ -0.55,\ -0.05]^T,$$
$$s = [-0.0123,\ 0.9867,\ 0.2729,\ 0.4384,\ 0.0625,\ 0.1866,\ -0.4261,\ -0.9145,\ -0.4595]^T.$$

Where $\operatorname{sgn}(\mu) = \operatorname{sgn}(s)$. Furthermore, the vector λ is computed as uniformly distributed pseudo random numbers in $(0, 10)$ besides elements appearing in $\tilde{\lambda}$, see equation (6.22), the free λ_i in $\tilde{\lambda}$ are set to "1", i. e., λ_5 and λ_9:[4]:

$$\lambda = [0.241468,\ 2.19095,\ 2.06396,\ 0.16911,\ 1,\ 2.51463,\ 3.90448,\ 7.06776,\ 1]^T$$

Thus steady states can be computed in the standard way as posed by equation (5.50) on page 53:

$$a = [0.0417865,\ 1.20012,\ 0.420632,\ 1.54353,\ 0.22009,\ 0.167043,\ 4.47721,\ 2.16173,\ 9.42084]^T,$$
$$b = [0.0294465,\ 2.18677,\ 0.693504,\ 1.98194,\ 0.282601,\ 0.353631,\ 4.05115,\ 1.24721,\ 8.96138]^T,$$

with the total concentration given by

$$c = [6.06253,\ 10.0085]^T,$$

and the parameter vector set to:

$$k = [111.607,\ 1.78042,\ 1.84567,\ 111.215,\ 56.5543,\ 5.08165,\ 2.16911,\ 0.140907,\ 4.5436,\ 1292.83,\ 0.853689,\ 1.80196,\ 12.1026,\ 0.417902,\ 0.750226,\ 0.462592]^T.$$

Furthermore the eigenvalues for the steady state a are given by:

$$[-37.1519,\ -21.2114,\ -13.5008,\ -10.8353,\ -2.38677,\ -0.252575 + 0.111824 \cdot i,\ -0.252575 - 0.111824 \cdot i,\ 0,\ 0]$$

Note, two zero eigenvalues occur due to the conservation relation.

Bifurcation analysis for change of total concentration in either $c_1 = [K]_{tot}$ or $c_2 = [P]_{tot}$ yields s-shaped curves with two stable branches and one unstable one in the middle, see figure 6.1 as well as figure 6.2, respectively.

6.4 If there is more than one free λ_i in $\tilde{\lambda}$ but additional conditions occur on remaining λ_j's, the free ones are set to "1" and the other λ_j's are set to a value satisfying the condition posed by Q.

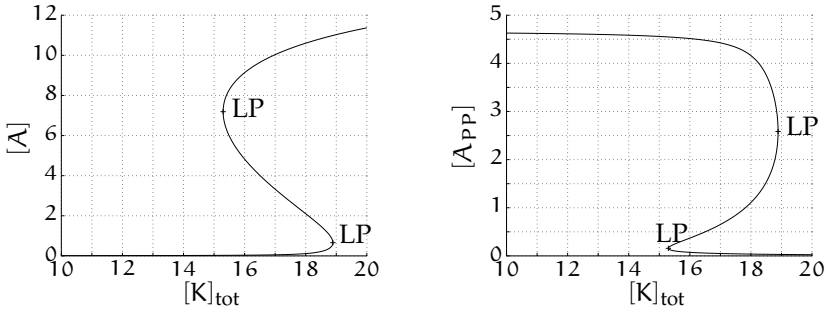

Figure 6.1: *Bifurcation analysis for change of total kinase concentration* c_1*: concentration of unphosphorylated protein,* $x_2 = [A]$ *(left hand side), and double phosphorylated protein,* $x_8 = [A_{PP}]$ *(right hand side), over total concentration of kinase,* $c_1 = [K]_{tot}$*, resulting in two limit points.*

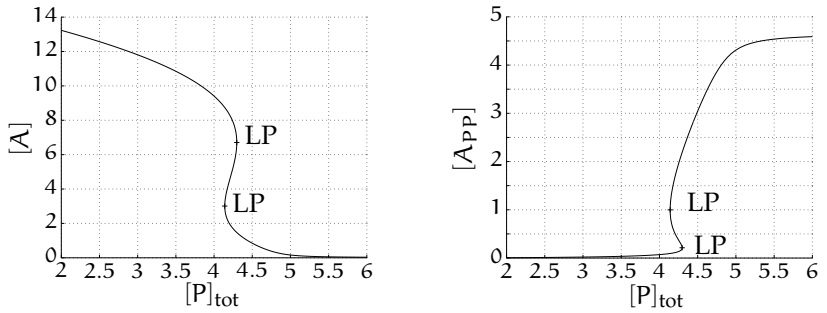

Figure 6.2: *Bifurcation analysis of unphosphorylated protein concentration,* $x_2 = [A]$ *(left hand side), and double phosphorylated protein concentration,* $x_8 = [A_{PP}]$ *(right hand side), over total concentration of phosphatase,* $c_2 = [P]_{tot}$*, resulting in two limit points.*

6.3 AN EXCURSION TOWARDS LARGER NETWORKS

As the protein *Sic1* can actually be phosphorylated on nine sites, where no actual significance of different phosphorylation sites could be distinguished (c. f. see [73]), it is of interest whether the actual number of phosphorylation steps plays an important role. Or if phosphorylation of six sites is enough to trigger degradation of *Sic1* after an ubiquitinase binds to the six times phosphorylated form of *Sic*, see [24]. The following questions arise:

- Why are six phosphorylation sites necessary but also already sufficient to trigger degradation of *Sic1* and not five or seven?
- Why are there nine phosphorylation sites? Which role do the last three phosphorylation sites play?
- Why are there at all that many phosphorylation sites? A phosphorylation network of only two steps could yield similar results, where the binding of the ubiquitinase occurs already at the double phosphorylated form.

Modeling only two phosphorylation steps including synthesis and degradation of proteins and/or enzymes is not sufficient to model the whole mechanism behind *Sic1* and find answers to the questions above. This double phosphorylation describes only a reduced form, where the double phosphorylated form corresponds to the sixth (and higher) phosphorylated protein, the unphosphorylated protein corresponds to the unphosphorylated

protein in the large network, and the single phosphorylated protein corresponds to all in-between proteins, see also section 3.2.2. But, this reduced model describes, in a nice form, phosphorylation and additional synthesis and/or degradation of different proteins. Still, as the number of phosphorylation sites seems to be important, an outlook towards larger networks is given in this section. Here, further cases are considered, containing nine phosphorylation steps of *Sic1* and synthesis and/or degradation of higher phosphorylation forms.

A small remark in advance: matrices M and Q can be computed for these network setups. But, here a matrix K is not provided as Q falls in the range of remark 6.4. And thus, no conclusions on existence of multistationarity can be drawn here. Still, a general discussion is provided, as solutions could be provided for an explicit network using a suitable solver and multistationarity might be established for this explicit system.

Thus, a solution for Algorithm 6.1 is presented here, but no solution to Lemma 6.6, as $Q\tilde{\lambda} = 0$ for $\tilde{\lambda} > 0$ has not been solved at present. Using suitable solvers, solutions to the lemma could be given.

6.3.1 *Modeling of a Large Phosphorylation Network Including Synthesis and Degradation*

While modeling phosphorylation of *Sic1* different scenarios are possible. First, different scenarios for synthesis and/or degradation of the protein and enzymes are possible. Second, there are also various forms for degradation of the different phosphorylation states of the protein. For example only degradation of fully phosphorylated or various combinations of degradation of intermediate phosphorylation forms could be possible.

One focus lays on degradation of all phosphorylation-forms of the protein. This case is modeled as it includes also the remaining cases where, for example, the fully phosphorylated protein can be degraded besides the unphosphorylated one. Of course, if the former algorithm to compute multiple steady states is used, matrix sizes change with the considered network form, e. g., degradation of only the six-times phosphorylated form or all from six to nine. But, considering the maximal case should suffice, general results are given below.

Assume that phosphorylation

$$\begin{aligned} &K + A \rightleftharpoons AK \longrightarrow K + A_P \rightleftharpoons A_PK \longrightarrow K + A_{PP} \rightleftharpoons \cdots \\ &\cdots \rightleftharpoons A_{7P}K \longrightarrow A_{8P} + K \rightleftharpoons A_{8P}K \longrightarrow A_{9P} + K \end{aligned} \tag{$\mathcal{N}$6.3a}$$

and dephosphorylation

$$\begin{aligned} &A_{9P} + P \rightleftharpoons A_{9P}P \longrightarrow A_{8P} + P \rightleftharpoons A_{8P}P \longrightarrow \cdots \\ &\cdots \longrightarrow P + A_{PP} \rightleftharpoons A_{PP}P \longrightarrow P + A_P \rightleftharpoons A_PP \longrightarrow P + A \end{aligned} \tag{$\mathcal{N}$6.3b}$$

follow the standard approach of distributive, sequential phosphorylation.

In a first scenario, synthesis and degradation of enzymes are not allowed. Further network setups can include synthesis and degradation of the enzymes in various forms, see left hand sides of networks ($\mathcal{N}$6.2). Furthermore,

synthesis and degradation of the protein itself are possible in different scenarios with

$$\begin{array}{cccccc} A \longleftarrow 0 & & & & & \\ A_P \longrightarrow 0 & A_{2P} \longrightarrow 0 & \cdots & A_{8P} \longrightarrow 0 & A_{9P} \longrightarrow 0 \end{array} \tag{$\mathcal{N}$6.4}$$

being the maximal one. Other scenarios include degradation of only the fully phosphorylated form or gradually allowing degradation of further phosphorylation forms up to the fully phosphorylated form, for example not allowing degradation of A_P in a second scenario. These would correspond to gradually approaching the actual mechanism of *Sic1*, where only the phosphorylated forms of $n \geqslant 6$ are degraded.

6.3.2 *Network Description*

The network is again labelled in the same ascending manner. The stoichiometric matrix for nine phosphorylation steps can be given by:

$$N = \begin{bmatrix} n_{11} & n_{12} & n_{12} & \cdots & n_{12} & n_{12} \\ n_{21} & n_{22} & 0 & \cdots & & 0 \\ 0 & n_{31} & n_{22} & & & \\ & & n_{31} & \ddots & & \\ & & & \ddots & n_{22} & 0 \\ & & & & n_{31} & n_{22} \\ 0 & & & & 0 & n_{31} \end{bmatrix},$$

with $N \in \mathbb{R}^{30\times 64}$ and

$$n_{11} = \begin{bmatrix} 0 & -1 & 1 & 1 & 0 & 0 & 0 & 0 \\ 1 & -1 & 1 & 0 & 0 & 0 & 1 & 0 \\ 0 & 0 & 0 & 0 & -1 & 1 & 1 & 0 \end{bmatrix},$$

$$n_{12} = \begin{bmatrix} -1 & 1 & 1 & 0 & 0 & 0 & 0 \\ 0 & 0 & 0 & 0 & 0 & 0 & 0 \\ 0 & 0 & 0 & -1 & 1 & 1 & 0 \end{bmatrix},$$

$$n_{21} = \begin{bmatrix} 0 & 1 & -1 & -1 & 0 & 0 & 0 & 0 \\ 0 & 0 & 0 & 1 & -1 & 1 & 0 & -1 \\ 0 & 0 & 0 & 0 & 1 & -1 & -1 & 0 \end{bmatrix},$$

$$n_{22} = \begin{bmatrix} 0 & 0 & 0 & 0 & 0 & 0 & 0 \\ -1 & 1 & 0 & 0 & 0 & 1 & 0 \\ 0 & 0 & 0 & 0 & 0 & 0 & 0 \end{bmatrix},$$

$$n_{31} = \begin{bmatrix} 1 & -1 & -1 & 0 & 0 & 0 & 0 \\ 0 & 0 & 1 & -1 & 1 & 0 & -1 \\ 0 & 0 & 0 & 1 & -1 & -1 & 0 \end{bmatrix}.$$

Submatrices n_{12}, n_{22} and n_{31} appear in total eight times to build the stoichiometric matrix for nine phosphorylation steps.

Furthermore, the rate exponent matrix $Y \in \mathbb{R}^{29\times 54}$ and the educt matrix $\tilde{Y} \in \mathbb{R}^{29\times 48}$ can be given by:

$$
\begin{aligned}
Y = [&0 \;\; e_1+e_2 \;\; e_4 \;\; e_4 \;\; e_3+e_5 \;\; e_6 \;\; e_6 \;\; e_5\\
&e_1+e_5 \;\; e_7 \;\; e_7 \;\; e_3+e_8 \;\; e_9 \;\; e_9 \;\; e_8 \;\; \cdots\\
&e_1+e_{3i-1} \;\; e_{3i+1} \;\; e_{3i+1} \;\; e_3+e_{3i+2} \;\; e_{3i+3} \;\; e_{3i+3} \;\; e_{3i+2} \;\; \cdots\\
&e_1+e_{26} \;\; e_{28} \;\; e_{28} \;\; e_3+e_{29} \;\; e_{30} \;\; e_{30} \;\; e_{29}],\\
\tilde{Y} = [&e_2 \;\; e_1+e_2 \;\; e_4 \;\; e_1+e_5 \;\; e_6 \;\; e_3+e_2 \;\; e_5 \;\; e_7\\
&e_1+e_8 \;\; e_3+e_8 \;\; e_9 \;\; e_8 \;\; \cdots\\
&e_{3i+1} \;\; e_1+e_{3i+2} \;\; e_3+e_{3i+2} \;\; e_{3i+3} \;\; e_{3i+2} \;\; \cdots\\
&e_{28} \;\; e_1+e_{29} \;\; e_3+e_{29} \;\; e_{30} \;\; e_{29}].
\end{aligned}
$$

Considering only the phosphorylation network (N6.3) with synthesis and degradation as in network (N6.4), the total concentration of the two enzymes K and P is constant yielding two conservation relations:

$$
\begin{aligned}
w_1 &= \begin{bmatrix} 1 & 0 & 0 & | & 1 & 0 & 0 & | & \cdots & | & 1 & 0 & 0 \end{bmatrix}^T,\\
w_2 &= \begin{bmatrix} 0 & 0 & 1 & | & 0 & 0 & 1 & | & \cdots & | & 0 & 0 & 1 \end{bmatrix}^T,
\end{aligned}
$$

where both vectors are of length 30.

The given matrices are sufficient to continue with multistationarity analysis following Algorithm 6.1 on page 74.

6.3.3 *Multistationarity Analysis*

To solve for multiple steady states a and b, the Algorithm 6.1 is used to solve equation (6.10), i. e., $Y^T\mu = \ln((E\nu)/(E\lambda))$, for network (N6.4). The solution of this equation is moved to page 181 in appendix B.3. Following the Fredholm alternative, μ can be computed by asking for $U^T Y^T = 0 \to U^T \ln\frac{E\nu}{E\lambda} = 0$. Hence, the following 15 relations occur:

$$
\begin{aligned}
\ln\frac{\nu_{36}}{\lambda_{36}} &= -\ln\frac{\nu_2}{\lambda_2} + \ln\frac{\nu_4}{\lambda_4} + \ln\frac{\nu_{34}}{\lambda_{34}} & \ln\frac{\nu_{33}}{\lambda_{33}} &= -\ln\frac{\nu_2}{\lambda_2} + \ln\frac{\nu_5}{\lambda_5} + \ln\frac{\nu_{30}}{\lambda_{30}}\\
\ln\frac{\nu_{32}}{\lambda_{32}} &= -\ln\frac{\nu_2}{\lambda_2} + \ln\frac{\nu_4}{\lambda_4} + \ln\frac{\nu_{30}}{\lambda_{30}} & \ln\frac{\nu_{29}}{\lambda_{29}} &= -\ln\frac{\nu_2}{\lambda_2} + \ln\frac{\nu_5}{\lambda_5} + \ln\frac{\nu_{26}}{\lambda_{26}}\\
\ln\frac{\nu_{28}}{\lambda_{28}} &= -\ln\frac{\nu_2}{\lambda_2} + \ln\frac{\nu_4}{\lambda_4} + \ln\frac{\nu_{26}}{\lambda_{26}} & \ln\frac{\nu_{25}}{\lambda_{25}} &= -\ln\frac{\nu_2}{\lambda_2} + \ln\frac{\nu_5}{\lambda_5} + \ln\frac{\nu_{22}}{\lambda_{22}}\\
\ln\frac{\nu_{24}}{\lambda_{24}} &= -\ln\frac{\nu_2}{\lambda_2} + \ln\frac{\nu_4}{\lambda_4} + \ln\frac{\nu_{22}}{\lambda_{22}} & \ln\frac{\nu_{21}}{\lambda_{21}} &= -\ln\frac{\nu_2}{\lambda_2} + \ln\frac{\nu_5}{\lambda_5} + \ln\frac{\nu_{18}}{\lambda_{18}}\\
\ln\frac{\nu_{20}}{\lambda_{20}} &= -\ln\frac{\nu_2}{\lambda_2} + \ln\frac{\nu_4}{\lambda_4} + \ln\frac{\nu_{18}}{\lambda_{18}} & \ln\frac{\nu_{17}}{\lambda_{17}} &= -\ln\frac{\nu_2}{\lambda_2} + \ln\frac{\nu_5}{\lambda_5} + \ln\frac{\nu_{14}}{\lambda_{14}}\\
\ln\frac{\nu_{16}}{\lambda_{16}} &= -\ln\frac{\nu_2}{\lambda_2} + \ln\frac{\nu_4}{\lambda_4} + \ln\frac{\nu_{14}}{\lambda_{14}} & \ln\frac{\nu_{13}}{\lambda_{13}} &= -\ln\frac{\nu_2}{\lambda_2} + \ln\frac{\nu_5}{\lambda_5} + \ln\frac{\nu_{10}}{\lambda_{10}}\\
\ln\frac{\nu_{12}}{\lambda_{12}} &= -\ln\frac{\nu_2}{\lambda_2} + \ln\frac{\nu_4}{\lambda_4} + \ln\frac{\nu_{10}}{\lambda_{10}} & \ln\frac{\nu_9}{\lambda_9} &= -\ln\frac{\nu_2}{\lambda_2} + \ln\frac{\nu_5}{\lambda_5} + \ln\frac{\nu_6}{\lambda_6}\\
\ln\frac{\nu_8}{\lambda_8} &= -\ln\frac{\nu_2}{\lambda_2} + \ln\frac{\nu_4}{\lambda_4} + \ln\frac{\nu_6}{\lambda_6}
\end{aligned}
$$

Again, constraints on λ_l occur, thus, $\varkappa_k$ are introduced:

$$\begin{aligned}
&\ln\frac{v_1}{\lambda_1}=\varkappa_1 && \ln\frac{v_2}{\lambda_2}=\varkappa_2 && \ln\frac{v_3}{\lambda_3}=\varkappa_2 && \ln\frac{v_4}{\lambda_4}=\varkappa_3\\
&\ln\frac{v_5}{\lambda_5}=\varkappa_4 && \ln\frac{v_6}{\lambda_6}=\varkappa_5 && \ln\frac{v_7}{\lambda_7}=\varkappa_5 && \ln\frac{v_8}{\lambda_8}=\varkappa_6\\
&\ln\frac{v_9}{\lambda_9}=\varkappa_7 && \ln\frac{v_{10}}{\lambda_{10}}=\varkappa_8 && \ln\frac{v_{11}}{\lambda_{11}}=\varkappa_8 && \ln\frac{v_{12}}{\lambda_{12}}=\varkappa_9\\
&\ln\frac{v_{13}}{\lambda_{13}}=\varkappa_{10} && \ln\frac{v_{14}}{\lambda_{14}}=\varkappa_{11} && \ln\frac{v_{15}}{\lambda_{15}}=\varkappa_{11} && \ln\frac{v_{16}}{\lambda_{16}}=\varkappa_{12}\\
&\ln\frac{v_{17}}{\lambda_{17}}=\varkappa_{13} && \ln\frac{v_{18}}{\lambda_{18}}=\varkappa_{14} && \ln\frac{v_{19}}{\lambda_{19}}=\varkappa_{14} && \ln\frac{v_{20}}{\lambda_{20}}=\varkappa_{15}\\
&\ln\frac{v_{21}}{\lambda_{21}}=\varkappa_{16} && \ln\frac{v_{22}}{\lambda_{22}}=\varkappa_{17} && \ln\frac{v_{23}}{\lambda_{23}}=\varkappa_{17} && \ln\frac{v_{24}}{\lambda_{24}}=\varkappa_{18}\\
&\ln\frac{v_{25}}{\lambda_{25}}=\varkappa_{19} && \ln\frac{v_{26}}{\lambda_{26}}=\varkappa_{20} && \ln\frac{v_{27}}{\lambda_{27}}=\varkappa_{20} && \ln\frac{v_{28}}{\lambda_{28}}=\varkappa_{21}\\
&\ln\frac{v_{29}}{\lambda_{29}}=\varkappa_{22} && \ln\frac{v_{30}}{\lambda_{30}}=\varkappa_{23} && \ln\frac{v_{31}}{\lambda_{31}}=\varkappa_{23} && \ln\frac{v_{32}}{\lambda_{32}}=\varkappa_{24}\\
&\ln\frac{v_{33}}{\lambda_{33}}=\varkappa_{25} && \ln\frac{v_{34}}{\lambda_{34}}=\varkappa_{26} && \ln\frac{v_{35}}{\lambda_{35}}=\varkappa_{26} && \ln\frac{v_{36}}{\lambda_{36}}=\varkappa_{27}.
\end{aligned}$$

Note, only the first ratios of sums are given for reasons of legibility. But terms of sums appear as well in the ln expressions, see appendix B.3 on page 181 for the full list.

The simplifications given above for μ_i also hold for $\varkappa_k$:

$$\begin{aligned}
\varkappa_{27} &= -\varkappa_2+\varkappa_{26}+\varkappa_3, & \varkappa_{25} &= -\varkappa_2+\varkappa_{23}+\varkappa_4,\\
\varkappa_{24} &= -\varkappa_2+\varkappa_{23}+\varkappa_3, & \varkappa_{22} &= -\varkappa_2+\varkappa_{20}+\varkappa_4,\\
\varkappa_{21} &= -\varkappa_2+\varkappa_{20}+\varkappa_3, & \varkappa_{19} &= -\varkappa_2+\varkappa_{17}+\varkappa_4,\\
\varkappa_{18} &= -\varkappa_2+\varkappa_{17}+\varkappa_3, & \varkappa_{16} &= -\varkappa_2+\varkappa_{14}+\varkappa_4,\\
\varkappa_{15} &= -\varkappa_2+\varkappa_{14}+\varkappa_3, & \varkappa_{13} &= -\varkappa_2+\varkappa_{11}+\varkappa_4,\\
\varkappa_{12} &= -\varkappa_2+\varkappa_{11}+\varkappa_3, & \varkappa_{10} &= -\varkappa_2+\varkappa_4+\varkappa_8,\\
\varkappa_9 &= -\varkappa_2+\varkappa_8+\varkappa_3, & \varkappa_7 &= -\varkappa_2+\varkappa_5+\varkappa_4,\\
\varkappa_6 &= -\varkappa_2+\varkappa_5+\varkappa_3.
\end{aligned}$$

As in the previous section for network (N6.2a1) linear constraints between λ_l occur, compare equation (6.20) on page 78. They have been moved to appendix B.3 for reasons of readability. The corresponding $\tilde{\lambda}$ can be given by:

$$\tilde{\lambda} = [\lambda_3,\ \lambda_4,\ \lambda_7,\ \lambda_{11},\ \lambda_{15},\ \lambda_{19},\ \lambda_{23},\ \lambda_{27},\ \lambda_{31},\ \lambda_{35},\ \lambda_8,\ \lambda_{12},\ \lambda_{16},\ \lambda_{20},\ \lambda_{24},\ \lambda_{28},\ \lambda_{32},\ \lambda_{36}]^T,$$

compare equation (6.22) on page 78, and $\tilde{\varkappa}$ by:

$$\tilde{\varkappa} = [\varkappa_1,\ \varkappa_2,\ \varkappa_3,\ \varkappa_4,\ \varkappa_5,\ \varkappa_8,\ \varkappa_{11},\ \varkappa_{14},\ \varkappa_{17},\ \varkappa_{20},\ \varkappa_{23},\ \varkappa_{26}]^T.$$

The matrix Q is then given in analogy to the matrix Q in equation (6.25) for network (N6.2):

$$Q = \begin{bmatrix}
q_{11} & q_{12} & 0 & 0 & 0 & 0 & 0 & 0 & 0 & 0 & q_{13} & q_{14} & q_{15} & q_{16} & q_{17} & q_{18} & q_{19} & q_{19}\\
0 & q_{21} & 0 & 0 & 0 & 0 & 0 & 0 & 0 & 0 & q_{22} & q_{23} & q_{24} & q_{25} & q_{26} & q_{27} & q_{28} & q_{29}\\
0 & 0 & q_{31} & 0 & 0 & 0 & 0 & 0 & 0 & 0 & q_{32} & q_{33} & q_{34} & q_{35} & q_{36} & q_{37} & q_{38} & q_{39}\\
0 & 0 & 0 & q_{41} & 0 & 0 & 0 & 0 & 0 & 0 & 0 & q_{42} & q_{43} & q_{44} & q_{45} & q_{46} & q_{47} & q_{48}\\
0 & 0 & 0 & 0 & q_{51} & 0 & 0 & 0 & 0 & 0 & 0 & 0 & q_{52} & q_{53} & q_{54} & q_{55} & q_{56} & q_{57}\\
0 & 0 & 0 & 0 & 0 & q_{61} & 0 & 0 & 0 & 0 & 0 & 0 & 0 & q_{62} & q_{63} & q_{64} & q_{65} & q_{66}\\
0 & 0 & 0 & 0 & 0 & 0 & q_{71} & 0 & 0 & 0 & 0 & 0 & 0 & 0 & q_{72} & q_{73} & q_{74} & q_{75}\\
0 & 0 & 0 & 0 & 0 & 0 & 0 & q_{81} & 0 & 0 & 0 & 0 & 0 & 0 & 0 & q_{82} & q_{83} & q_{84}\\
0 & 0 & 0 & 0 & 0 & 0 & 0 & 0 & q_{91} & 0 & 0 & 0 & 0 & 0 & 0 & 0 & q_{92} & q_{93}\\
0 & 0 & 0 & 0 & 0 & 0 & 0 & 0 & 0 & q_{101} & 0 & 0 & 0 & 0 & 0 & 0 & 0 & q_{102}
\end{bmatrix}$$

Expressions for elements q_{ij} of Q can be found on page 184 in appendix B.3.

Though the q_{ij} are rather special functions of $\tilde{\varkappa}$, the system $Q\tilde{\lambda} = 0$ for $\tilde{\lambda} > 0$, compare equation (6.25), cannot be solved in general, as more than three unknown q_{ij} are present in the first eight rows of Q, see also the remark in section 6.4 on page 79.

Still, a solution for μ, compare equation (6.12), in terms of the matrix M can be given by:

$$M = \begin{bmatrix}
0 & 0 & -1 & 1 & 0 & 0 & 0 & 0 & 0 & 0 & 0 & 0 \\
1 & 0 & 1 & -1 & 0 & 0 & 0 & 0 & 0 & 0 & 0 & 0 \\
0 & 1 & -1 & 0 & 0 & 0 & 0 & 0 & 0 & 0 & 0 & 0 \\
1 & 0 & 0 & 0 & 0 & 0 & 0 & 0 & 0 & 0 & 0 & 0 \\
0 & 0 & 1 & 0 & 0 & 0 & 0 & 0 & 0 & 0 & 0 & 0 \\
0 & 1 & 0 & 0 & 0 & 0 & 0 & 0 & 0 & 0 & 0 & 0 \\
0 & 0 & 0 & 1 & 0 & 0 & 0 & 0 & 0 & 0 & 0 & 0 \\
0 & -1 & 1 & 0 & 1 & 0 & 0 & 0 & 0 & 0 & 0 & 0 \\
0 & 0 & 0 & 0 & 1 & 0 & 0 & 0 & 0 & 0 & 0 & 0 \\
0 & -1 & 0 & 1 & 1 & 0 & 0 & 0 & 0 & 0 & 0 & 0 \\
0 & -1 & 1 & 0 & 0 & 1 & 0 & 0 & 0 & 0 & 0 & 0 \\
0 & 0 & 0 & 0 & 0 & 1 & 0 & 0 & 0 & 0 & 0 & 0 \\
0 & -1 & 0 & 1 & 0 & 1 & 0 & 0 & 0 & 0 & 0 & 0 \\
0 & -1 & 1 & 0 & 0 & 0 & 1 & 0 & 0 & 0 & 0 & 0 \\
0 & 0 & 0 & 0 & 0 & 0 & 1 & 0 & 0 & 0 & 0 & 0 \\
0 & -1 & 0 & 1 & 0 & 0 & 1 & 0 & 0 & 0 & 0 & 0 \\
0 & -1 & 1 & 0 & 0 & 0 & 0 & 1 & 0 & 0 & 0 & 0 \\
0 & 0 & 0 & 0 & 0 & 0 & 0 & 1 & 0 & 0 & 0 & 0 \\
0 & -1 & 0 & 1 & 0 & 0 & 0 & 1 & 0 & 0 & 0 & 0 \\
0 & -1 & 1 & 0 & 0 & 0 & 0 & 0 & 1 & 0 & 0 & 0 \\
0 & 0 & 0 & 0 & 0 & 0 & 0 & 0 & 1 & 0 & 0 & 0 \\
0 & -1 & 0 & 1 & 0 & 0 & 0 & 0 & 1 & 0 & 0 & 0 \\
0 & -1 & 1 & 0 & 0 & 0 & 0 & 0 & 0 & 1 & 0 & 0 \\
0 & 0 & 0 & 0 & 0 & 0 & 0 & 0 & 0 & 1 & 0 & 0 \\
0 & -1 & 0 & 1 & 0 & 0 & 0 & 0 & 0 & 1 & 0 & 0 \\
0 & -1 & 1 & 0 & 0 & 0 & 0 & 0 & 0 & 0 & 1 & 0 \\
0 & 0 & 0 & 0 & 0 & 0 & 0 & 0 & 0 & 0 & 1 & 0 \\
0 & -1 & 0 & 1 & 0 & 0 & 0 & 0 & 0 & 0 & 1 & 0 \\
0 & -1 & 1 & 0 & 0 & 0 & 0 & 0 & 0 & 0 & 0 & 1 \\
0 & 0 & 0 & 0 & 0 & 0 & 0 & 0 & 0 & 0 & 0 & 1
\end{bmatrix}$$

with $\tilde{\varkappa}$ given above.

As sign restrictions on $\varkappa_i$ cannot be given using the approach introduced in the previous section, valid sign vectors δ and sign patterns σ cannot be computed to find multiple steady states to network (№6.3)+(№6.4). General solutions to equation (6.12) could be computed, yielding a vector μ. Furthermore, sign vectors δ satisfying $\operatorname{sgn}(\mu) = \operatorname{sgn}(s)$ could also be computed. But, μ found in this way, i. e., following equation (5.49) on page 53 rather than equation (6.43) on page 85, do not necessarily imply $\lambda_i > 0$. Thus, no general conclusions can be drawn on the existence of multiple steady states in network (№6.3)+(№6.4). Still, providing solutions for explicit networks might be possible using suitable solvers to compute σ and δ.

As only the synthesis of the protein and degradation of all its phosphorylated forms is considered here, smaller network setups allowing only degradation of higher phosphorylated proteins could be of interest. Comparing the matrix Q for different network setups of the small phosphorylation process from section 6.2 reveals, different reaction mechanisms yield different complex Q matrices. Thus, the number of additional sign restrictions q_{ij} could decrease with different degradation mechanisms, e. g., only degradation of the fully phosphorylated protein. Results here would be of course of interest, especially when comparing results for degradation of six-times and higher phosphorylated proteins with results for degradation of only the fully phosphorylated protein. These different setups could provide an answer to the question, why *Sic1* is phosphorylated on nine sites, when six sites are sufficient for transition to *G1* phase, as stated by [73].

6.4 SUMMARY AND OPEN QUESTIONS

This chapter extends the phosphorylation of a protein in n steps by allowing additional synthesis and/or degradation of the protein, its phosphorylated forms and/or the enzymes. For a small network of $n = 2$ phosphorylation steps, multistationarity can be established for all but two of the arising twelve networks: if both enzymes (phosphatase and kinase) or only the kinase are preserved, multistationarity can be established for all arising networks. If only the phosphatase is conserved, multistationarity can only be established if the unphosphorylated protein is synthesized and degraded. Again, a parametrization for the multistationarity region in the parameter space is provided as well as values for steady states a and b.

This is done using an algorithm, that is also valid in more general terms: the algorithm presented enables to check (bio-) chemical reaction networks of mass action kinetics for multistationarity. If the algorithm, together with the stated lemma on sign patterns, holds, a parametrization for rate constants and steady states is provided.

The network of double phosphorylation corresponds to a reduced version of phosphorylation networks with $n > 2$ containing synthesis and degradation, like phosphorylation of *Sic1*, *Cdc25* or *Wee1*. This lumped network is extended in a network containing nine phosphorylation sites allowing synthesis of the protein and degradation of its phosphorylated forms. Here, multistationarity cannot be guaranteed by the presently chosen approach.

Nonetheless, multiple steady states can indeed be found for networks including synthesis and degradation in a double phosphorylation network, a novel finding.

Concerning Remark 2.3 from page 12, the additional constraints in the vector λ, i. e., the vector $\tilde{\lambda}$, are quite of interest from a biological point of view. Allowing only certain λ_l to be free and restricting others in the presented way should somehow translate to the fluxes in the (bio-) chemical reaction network. If a λ is restricted to certain values, the contribution of the corresponding flux could also be restricted in the reaction network. Thus, the "function" of the (bio-) chemical reaction network could be restricted as well.

On a pu écrire depuis que la voie
la plus courte et la meilleure entre deux vérités du domaine réel
passe souvent par le domaine imaginaire.

— Jacques Hadamard [43]

7 EFFECT OF COMPARTMENTALIZATION IN MULTISITE PHOSPHORYLATION NETWORKS

The phosphorylation introduced in chapter 5 and its extension in chapter 6 are not the only phosphorylation mechanisms that are possible in (bio-) chemical reaction networks. For example, multisite phosphorylation can also occur in networks of information processing. During immune response, the members of the protein family *NFAT* are de-/phosphorylated at many sites in a complex mechanism of compartmentalization of the phosphorylation process. The protein is de-/phosphorylated in different compartments of the cell: in the cytoplasm as well as in the nucleus. This compartmentalization plays an important role for information processing, leading, via the protein *NFAT*, to immune response.

This chapter considers a model of protein phosphorylation including compartmentalization, addressing multistationarity and analysis of the multistationarity region in the cell, taking the phosphorylation of *NFAT* as an example of the underlying principle. The question is, whether phosphorylation networks including compartmentalization can exhibit multiple steady states.

7.1 COMPARTMENTALIZATION AND PHOSPHORYLATION

The protein *NFAT* is fully phosphorylated on at least 21 sites in its inactive form, i. e., if no immune response takes place. During immune response, the protein is dephosphorylated on thirteen of fourteen associated phosphorylation sites. This leads to nuclear translocation, followed by, in a nutshell, gene transcription. Afterwards, the protein is rephosphorylated and transported back into cytoplasm. For a more detailed discussion see chapter 3.2.3. Considering only this short network setup, models are conceivable with various phosphorylation mechanisms:

PM1 The phosphorylation network with a reduced number of fourteen phosphorylation sites: Two kinases phosphorylate in a mutual way all fourteen phosphorylation sites. One phosphatase dephosphorylates thirteen of the fourteen phosphorylation sites. The single phosphorylated protein is transported into nucleus. The fully phosphorylated protein is transported into cytoplasm.

PM2 The phosphorylation network of fourteen phosphorylation steps including only one kinase and one phosphatase: Simplifying the model, both enzymes can attack all phosphorylation sites, i. e., the phosphatase also dephosphorylates all fourteen sites. The single phosphorylated protein is transported into nucleus. The fully phosphorylated protein of fourteen sites is transported back into cytoplasm.

Reactions in cytoplasm can be given by:

$$\begin{aligned}
&\overset{x_1}{K_C} + \overset{x_2}{A} \underset{k_2}{\overset{k_1}{\rightleftharpoons}} \overset{\substack{y_2\\x_4}}{AK_C} \xrightarrow{k_3} K_C + \overset{\substack{y_3\\x_5}}{A_P} \underset{k_8}{\overset{k_7}{\rightleftharpoons}} \overset{\substack{y_7\\x_7}}{A_PK_C} \xrightarrow{k_9} \cdots \xrightarrow{k_{69}} K_C + \overset{\substack{y_{48}\\x_{38}}}{A_{12P}} \underset{k_{74}}{\overset{k_{73}}{\rightleftharpoons}} \overset{\substack{y_{51}\\x_{40}}}{A_{12P}K_C} \xrightarrow{k_{75}} K_C + \overset{\substack{y_{52}\\x_{41}}}{A_{13P}} \\
&P_C + \overset{y_{53}}{A_{13P}} \underset{k_{77}}{\overset{k_{76}}{\rightleftharpoons}} \overset{\substack{y_{54}\\x_{42}}}{A_{13P}P_C} \xrightarrow{k_{78}} P_C + \overset{\substack{y_{49}\\x_{38}}}{A_{12P}} \underset{k_{71}}{\overset{k_{70}}{\rightleftharpoons}} \cdots \underset{k_{11}}{\overset{k_{10}}{\rightleftharpoons}} \overset{\substack{y_{10}\\x_9}}{A_{2P}P_C} \xrightarrow{k_{12}} P_C + \overset{y_4}{A_P} \underset{k_5}{\overset{k_4}{\rightleftharpoons}} \overset{\substack{y_5\\x_6}}{A_PP_C} \xrightarrow{k_6} \overset{\substack{y_6\\x_3}}{P_C} + A,
\end{aligned} \tag{N7.1a}$$

reactions in nucleus by:

$$\begin{aligned}
&\overset{\substack{y_{53}\\x_{43}}}{K_N} + \overset{x_{44}}{B} \underset{k_{80}}{\overset{k_{79}}{\rightleftharpoons}} \overset{\substack{y_{56}\\x_{46}}}{BK_N} \xrightarrow{k_{81}} K_N + \overset{\substack{y_{57}\\x_{47}}}{B_P} \underset{k_{86}}{\overset{k_{85}}{\rightleftharpoons}} \overset{\substack{y_{61}\\x_{49}}}{B_PK_N} \xrightarrow{k_{87}} \cdots \xrightarrow{k_{147}} K_N + \overset{\substack{y_{102}\\x_{80}}}{B_{12P}} \underset{k_{152}}{\overset{k_{151}}{\rightleftharpoons}} \overset{\substack{y_{105}\\x_{82}}}{B_{12P}K_N} \xrightarrow{k_{153}} K_N + \overset{\substack{y_{106}\\x_{83}}}{B_{13P}} \\
&P_N + \overset{y_{107}}{B_{13P}} \underset{k_{155}}{\overset{k_{154}}{\rightleftharpoons}} \overset{\substack{y_{108}\\x_{84}}}{B_{13P}P_N} \xrightarrow{k_{156}} P_N + \overset{y_{103}}{B_{12P}} \underset{k_{147}}{\overset{k_{148}}{\rightleftharpoons}} \cdots \overset{\substack{y_{64}\\x_{51}}}{B_{2P}P_N} \xrightarrow{k_{90}} P_N + \overset{y_{58}}{B_P} \underset{k_{83}}{\overset{k_{82}}{\rightleftharpoons}} \overset{\substack{y_{59}\\x_{48}}}{B_PP_N} \xrightarrow{k_{84}} \overset{\substack{y_{60}\\x_{45}}}{P_N} + B,
\end{aligned} \tag{N7.1b}$$

and reactions for transport for the second phosphorylation mechanism, PM2, can be given by:

$$\overset{\substack{y_{109}\\x_2}}{A} \xrightarrow{k_{157}} \overset{\substack{y_{110}\\x_{44}}}{B} \qquad\qquad \overset{\substack{y_{111}\\x_{83}}}{B_{13P}} \xrightarrow{k_{158}} \overset{\substack{y_{112}\\x_{41}}}{A_{13P}} \tag{N7.1c}$$

PM3 A reduced model of thirteen phosphorylation steps: This model considers again only one kinase and one phosphatase, where both can de-/phosphorylate all proteins. The difference to the first model lies in the transport reaction. Here the unphosphorylated protein is transported into nucleus. And, as there are only thirteen phosphorylation steps, this protein is transported back into cytoplasm. This model corresponds to a shifted version of the first one, as the individual phosphorylated protein forms are just shifted by one. It reduces the reaction network by one order.

PM4 The fully reduced version, comparable to the one in chapter 6: This model considers only two phosphorylation steps, and again one kinase and one phosphatase. Here, the double phosphorylated protein corresponds to the inactive form. The unphosphorylated to the active one, that is transported into nucleus. The double phosphorylated protein is then transported back into cytoplasm. In a reduced approach, the single phosphorylated form represents all intermediate phosphoforms of the protein. This model depicts a reaction network with a drastically reduced number of parameters and states.

In a first attempt to model the phosphorylation of *NFAT* the third mechanism, PM3, is considered. This mechanism already considers a reduced model without too many restrictions on the phosphorylation process.[1]

To model the reaction network, the same assumptions as before hold: the kinases *CK1* and *GSK3* are assumed to operate as one kinase K. The phosphatase *calcineurin* is described by a P. The system in cytoplasm is depicted by an index C and the system in nucleus by an N. To distinguish between the protein being in cytoplasm or nucleus, a variable A is used for the protein in the cytoplasm and a variable B for its presence in the nucleus. A different variable is used instead of an additional index as this would only complicate indexing of the protein.

The standard stepwise notation is kept for each subsystem. The system in cytoplasm is labeled first, then the system in the nucleus. At the end, transport reactions are considered. The concentration of substances is described by $x \in \mathbb{R}^{6n+6}$ and the vector of rate constants by $k \in \mathbb{R}^{12n+2}$ with

$$x = [\underbrace{x_1 \ \cdots \ x_{3n+3}}_{\substack{\text{concentration}\\ \text{in cytoplasm}}} \ \underbrace{x_{3n+4} \ \cdots \ x_{6n+6}}_{\substack{\text{concentration}\\ \text{in nucleus}}}]^T \tag{7.1}$$
$$= \operatorname{col}(x_C, x_N),$$
$$k = [\underbrace{k_1 \ \cdots \ k_{6n}}_{\substack{\text{rate constants}\\ \text{in cytoplasm}}} \ \underbrace{k_{6n+1} \ \cdots \ k_{12n}}_{\substack{\text{rate constants}\\ \text{in nucleus}}} \ \underbrace{k_{12n+1} \ k_{12n+2}}_{\substack{\text{rate constants of}\\ \text{transport reactions}}}]^T \tag{7.2}$$
$$= \operatorname{col}(k_C, k_N, k_T).$$

Vectors and matrices gain a blockwise structure: first elements of the system in cytoplasm (C), then elements of the system in the nucleus (N), and finally elements for the transport reactions (T) appear. The benefit of this notation

7.1 Reducing the system to thirteen phosphorylation steps with a shift of the transported single phosphorylated to the unphosphorylated protein being transported, results only in a shift in final results. If the original system would have been considered, only larger networks due to the higher number of phosphorylation steps would appear, but the results would be comparable. So far, a system including several kinases has not been considered as the actual mechanism of phosphorylation by two kinases is not fully understood up to now, i. e., the order of phosphorylation and the position of actual phosphate groups being attacked are mostly unknown.

lies in the structure of network matrices, as the phosphorylation processes in cytoplasm and nucleus correspond to the standard phosphorylation considered in chapter 5. For these standard phosphorylation processes the network vectors and matrices are already known. The rate vector $v \in \mathbb{R}^{12n+2}$ for the phosphorylation process of *NFAT* can be given in terms of the rate vector of an n-times phosphorylation process, compare equation (5.7) on page 38:

$$\begin{aligned} v_{NFAT} &= \begin{bmatrix} v^{(n)^T} & \hat{v}^{(n)^T} & k_{12n+1} x_2 & k_{12n+2} x_{6n+5} \end{bmatrix}^T \\ &= \operatorname{col}(v_C, v_N, v_T) \end{aligned} \tag{7.3}$$

where $\hat{v}^{(n)}$ corresponds to $v^{(n)}$ by shifting the index of x by $3n+3$ and of k by $6n$:

$$\begin{aligned} v_C = [&k_1 x_2 x_1, \; k_2 x_4, \; k_3 x_4, \; k_4 x_5 x_3, \; k_5 x_6, \; k_6 x_6, \; \ldots, \\ &k_{6i-5} x_{3i-1} x_1, \; k_{6i-4} x_{3i+1}, \; k_{6i-3} x_{3i+1}, \\ &k_{6i-2} x_{3i+2} x_3, \; k_{6i-1} x_{3i+3}, \; k_{6i} x_{3i+3}, \; \ldots \\ &k_{6n-5} x_{3n-1} x_1, \; k_{6n-4} x_{3n+1}, \; k_{6n-3} x_{3n+1}, \\ &k_{6n-2} x_{3n+2} x_3, \; k_{6n-1} x_{3n+3}, \; k_{6n} x_{3n+3}]^T, \\ v_N = [&k_{6n+1} x_{3n+5} x_{3n+4}, \; k_{6n+2} x_{3n+7}, \; k_{6n+3} x_{3n+7}, \\ &k_{6n+4} x_{3n+8} x_{3n+6}, \; k_{6n+5} x_{3n+9}, \; k_{6n+6} x_{3n+9}, \; \ldots, \\ &k_{6n+6i-5} x_{3n+3i+2} x_{3n+4}, \; k_{6n+6i-4} x_{3n+3i+2}, \\ &k_{6n+6i-3} x_{3n+3i+4}, \; k_{6n+6i-2} x_{3n+3i+5} x_{3n+7}, \\ &k_{6n+6i-1} x_{3n+3i+6}, \; k_{6n+6i} x_{3n+3i+6}, \; \ldots \\ &k_{12n-5} x_{6n+2} x_{3n+4}, \; k_{12n-4} x_{6n+4}, \; k_{12n-3} x_{6n+4}, \\ &k_{12n-2} x_{6n+5} x_{3n+6}, \; k_{12n-1} x_{6n+6}, \; k_{12n} x_{6n+6}]^T \\ v_T = [&k_{12n+1} x_2 \; k_{12n+2} x_{6n+5}]^T. \end{aligned}$$

And thus

$$\begin{aligned} v_{NFAT} &= \operatorname{diag}(k_C, k_N, k_T)\, \Phi(x_C, x_N, x_T) \\ &= \operatorname{diag}(k)\, \Phi(x) \end{aligned} \tag{7.4}$$

with

$$\begin{aligned} \Phi(x_C) &= \left[x_C^{y_1}, \ldots, x_C^{y_{6n}}\right]^T, \\ \Phi(x_N) &= \left[x_N^{y_{6n+1}}, \ldots, x_C^{y_{12n}}\right]^T, \\ \Phi(x_T) &= \left[x_2^{y_{12n+1}}, \; x_{6n+5}^{y_{12n+2}}\right]^T. \end{aligned} \tag{7.5}$$

Network matrices can be constructed using matrices of section 5.1 on page 35. The stoichiometric matrix N_{NFAT}, compare equation (5.2) on page 37, for network $\mathcal{N}7.1$ is constructed using two stoichiometric matrices for n-times phosphorylation systems and additional columns for transport reactions. As this matrix is constructed using only ones and zeros, no index shifting has to be done:

$$N_{NFAT} = \begin{bmatrix} N^{(n)} & 0 & \\ 0 & N^{(n)} & N_T \end{bmatrix}, \tag{7.6}$$

$$\text{with } N_T = \begin{bmatrix} -e_2 + e_{3n+5} & e_{3n+2} - e_{6n+5} \end{bmatrix},$$

with $N_{NFAT} \in \mathbb{R}^{2(3n+3)\times(2(6n)+2)}$. A basis for the right nullspace of N_{NFAT} can be given by a matrix $E \in \mathbb{R}^{(12n+2)\times(6n+1)}$. Recall matrix $E^{(1)}$ in equation (5.6) from page 38 and define a matrix $\tilde{E}^{(1)}$:

$$E^{(1)} = \begin{bmatrix} 1 & 0 & 1 \\ 1 & 0 & 0 \\ 0 & 0 & 1 \\ 0 & 1 & 1 \\ 0 & 1 & 0 \\ 0 & 0 & 1 \end{bmatrix}, \qquad \tilde{E}^{(1)} = \begin{bmatrix} 1 & 1 & 0 \\ 1 & 0 & 0 \\ 0 & 1 & 0 \\ 0 & 1 & 1 \\ 0 & 0 & 1 \\ 0 & 1 & 0 \end{bmatrix}.$$

Furthermore, define two column vectors

$$\epsilon_1 = \begin{bmatrix} 0 & 0 & 0 & 1 & 0 & 1 \end{bmatrix}^T, \qquad \epsilon_2 = \begin{bmatrix} 1 & 0 & 1 & 0 & 0 & 0 \end{bmatrix}^T.$$

The matrix E_{NFAT} can then be given by:

$$E_{NFAT} = \begin{bmatrix} \tilde{E}^{(1)} & & & & & 0 & \epsilon_1 \\ & \ddots & & & & & \vdots \\ & & \tilde{E}^{(1)} & & & & \epsilon_1 \\ & & & E^{(1)} & & & \epsilon_2 \\ & & & & \ddots & & \vdots \\ & & & & & E^{(1)} & \epsilon_2 \\ & & & & & & 1 \\ 0 & & & & & & 1 \end{bmatrix}, \tag{7.7}$$

where $E^{(1)}$, $\tilde{E}^{(1)}$, ϵ_1 and ϵ_2 appear in total n-times.

For the rate exponent matrix Y_{NFAT}, compare equation (5.11) on page 39, and the complex matrix $\tilde{Y}_{NFAT}$, compare equation (5.9) on page 39 an index shifting is used with a shift of $3n+3$ for concentrations and $6n$ for rate constants in $\hat{Y}$ and $\hat{\tilde{Y}}$:

$$Y_{NFAT} = \begin{bmatrix} Y^{(n)} & 0 & Y_T \\ 0 & \hat{Y}^{(n)} & \end{bmatrix}, \tag{7.8}$$
$$\text{with } Y_T = \begin{bmatrix} e_2 & e_{6n+5} \end{bmatrix},$$

with $Y_{NFAT} \in \mathbb{R}^{2(3n+3)\times(2(6n)+2)}$ and the complex matrix $\tilde{Y}_{NFAT}$

$$\tilde{Y}_{NFAT} = \begin{bmatrix} \tilde{Y}^{(n)} & 0 & \tilde{Y}_T \\ 0 & \hat{\tilde{Y}}^{(n)} & \end{bmatrix}, \tag{7.9}$$
$$\text{with } \tilde{Y}_T = \begin{bmatrix} e_2 & e_{3n+5} & e_{6n+5} & e_{3n+2} \end{bmatrix},$$

with $\tilde{Y}_{NFAT} \in \mathbb{R}^{2(3n+3)\times(2(4n+2)+4)}$. Remaining entries of the network matrices are only prolonged by blocks of zeros, see for comparison equation (5.3) in section 5.1 on page 35.

Furthermore the conservation relation of the overall network can be given by

$$c_{NFAT} = W_{NFAT}^T x$$

with columns of the weight matrix $W_{NFAT} \in \mathbb{R}^{2(3n+3)\times 5}$ given by:

$$\begin{aligned}
w_{1,NFAT} &= e_1 + \sum_{i=1}^{n} e_{3i+1} \\
w_{2,NFAT} &= e_2 + \sum_{i=1}^{n} e_{3i+1} + e_{3i+2} + e_{3i+3} + e_{3n+5} \\
&\quad + \sum_{i=n+1}^{2n} e_{3i+1} + e_{3i+2} + e_{3i+3} \\
w_{3,NFAT} &= e_3 + \sum_{i=1}^{n} e_{3i+3} \\
w_{4,NFAT} &= e_{3n+4} + \sum_{i=n+1}^{2n} e_{3i+1} \\
w_{5,NFAT} &= e_{3n+6} + \sum_{i=n+1}^{2n} e_{3i+2}
\end{aligned} \tag{7.10}$$

and e_i column vectors of length $6n+6$ with a one at their ith position. This matrix resembles the former weight matrix for a standard phosphorylation in parts. In terms of the old weight matrix $W^{(n)}$ for an n-times phosphorylation network given in equation (5.4) on page 38, the weight matrix W_{NFAT} can be given by:

$$W_{NFAT}^{T} = \begin{bmatrix} w_1^{(n)^T} & 0 \\ w_3^{(n)^T} & w_3^{(n)^T} \\ w_2^{(n)^T} & 0 \\ 0 & \hat{w}_1^{(n)^T} \\ 0 & \hat{w}_2^{(n)^T} \end{bmatrix}, \tag{7.11}$$

where indices in $\hat{w}$ are the indices of w shifted by $3n+3$. For sake of simplicity the subscript $\{\}_{NFAT}$ is omitted.

7.2 MULTISTATIONARITY OF A COMPARTMENTALIZED PHOSPHORYLATION NETWORK

Here, the main question for multisite phosphorylation networks with compartmentalization is, whether they can exhibit multiple steady states. Due to the apparent compartmentalization two setups to achieve multiple steady states are possible. As in the previous chapters, it could be assumed, that the system exhibits multiple steady states. Based on the compartmentalization this would correspond to multiple steady states in cytoplasm but also in nucleus. The overall coupled network should exhibit as well multiple steady states.

But motivated by experimental results, see section 3.2.3, a different approach could be possible as well. If the system in cytoplasm only shows a mono-stable setup, while the system in nucleus exhibits multiple steady states, the overall coupled reaction network could still exhibit multiple steady states.

Both setups could still enable immune response, see figure 7.1. Here, two stable steady states could correspond to immune response taking place at

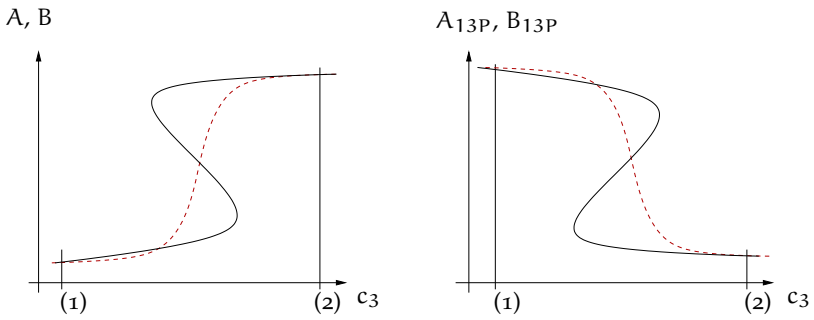

Figure 7.1: *Biological interpretation of the schematic description of a uni-valued setup in the red, dashed line, and a multi-valued setup in the black, solid line. Points (1) and (2) describe two possible concentrations of* $c_3 = [P_C]_{tot}$ *corresponding to no immune response or immune response taking place. (1) With a fixed low concentration* c_3 *the steady state in nucleus is also fixed corresponding to a low steady state concentration of the unphosphorylated protein and a high steady state concentration of the fully phosphorylated protein. (2) Changing the total concentration* c_3 *towards a higher value would switch the behavior with low concentrations for the fully phosphorylated protein forms and high concentrations for unphosphorylated protein forms. The switch corresponds to activation of NFAT and consecutive immune response.*

either a high concentration or a low concentration of the protein. The biological interpretation of two steady states would correspond to an s-shaped response curve, see the solid curves in figure 7.1. Whereas only one steady state or a mono-stable system would correspond to a strictly monotone response curve.

The two setups are given by:

UNI-VALUED RESPONSE CURVE The first setup considers a reaction network showing a different setup in its decoupled and coupled form. If the network is decoupled, the network in cytoplasm exhibits a strictly monotone response curve towards change of the total concentration of an enzyme, e. g., phosphatase concentration. The network in the nucleus exhibits an s-shaped response curve with at least two steady states.

MULTI-VALUED RESPONSE CURVE The second setup considers the same setup in its decoupled and coupled form: an at least s-shaped response curve in cytoplasm and nucleus for the decoupled network should provide a multi-valued coupled reaction network.

To check whether these two setups allow multistationarity in the coupled reaction network, the Algorithm 6.1 introduced in the previous chapter is used in a first step. Besides this algorithm, the approach of subnetwork analysis is used to check whether reaction networks allowing compartmentalization exhibit multistable states. In a second step, one or respectively two steady states are fixed using the toolbox MatCont for MATLAB for the decoupled networks and the two setups given above. The networks are coupled and checked for multistationarity using the toolbox. Either or both of these two approaches, i. e., the mono- and multi-valued setup, might yield multistationarity.

Figure 7.1 describes the response curves of the two setups. While no *calcineurin* intake is happening, the concentration of A_{13P} is constant over time for a certain total concentration of $[P_C]$, see point (1) in figure 7.1. This concentration is associated with a fixed concentration of the unphosphorylated

protein in cytoplasm. Thus the concentration of B in nucleus and the fully phosphorylated form, B_{13P} are constant. This inactive state of the reaction network is associated with no immune response. If Ca^{2+} pores open, the concentration of *calcineurin* changes and A_{13P} is dephosphorylated, point (2), thus the concentration decreases. The unphosphorylated protein A is transported into nucleus for gene transcription and consecutive immune response. In general, the fully phosphorylated form of A in cytoplasm is associated with a high concentration as long as no *calcineurin* is present.

7.2.1 *Multistationarity Using the Solution Algorithm for the Polynomial Condition*

To check for multiple steady states, the Algorithm 6.1 introduced in chapter 6 is followed. The system of ordinary differential equations yields again a polynomial condition. To find a solution for this condition, the rate exponent matrix Y and the arising pointed polyhedral cone E can be used to reduce the nonlinear system:

$$Y^T \mu = \ln \frac{E\,\nu}{E\,\lambda} \tag{7.12}$$

The same algorithm, as in the previous chapter, is used to solve this system. As the number of states and parameters is very high, only a double phosphorylation network is considered in a first step, compare PM4, with results for $n = 14$ provided at the end. The equation from above reduces for $n = 2$ to:

$$\ln \frac{\nu_1 + \nu_2}{\lambda_1 + \lambda_2} = \ln \frac{\nu_1}{\lambda_1}, \qquad \ln \frac{\nu_2}{\lambda_2} = \ln \frac{\nu_1}{\lambda_1}, \tag{7.13a}$$

$$\ln \frac{\nu_{13} + \nu_2 + \nu_3}{\lambda_{13} + \lambda_2 + \lambda_3} = \ln \frac{\nu_3}{\lambda_3}, \qquad \ln \frac{\nu_{13} + \nu_2}{\lambda_{13} + \lambda_2} = \ln \frac{\nu_3}{\lambda_3}, \tag{7.13b}$$

$$\ln \frac{\nu_4 + \nu_5}{\lambda_4 + \lambda_5} = \ln \frac{\nu_4}{\lambda_4}, \qquad \ln \frac{\nu_5}{\lambda_5} = \ln \frac{\nu_4}{\lambda_4}, \tag{7.13c}$$

$$\ln \frac{\nu_{13} + \nu_5 + \nu_6}{\lambda_{13} + \lambda_5 + \lambda_6} = \ln \frac{\nu_6}{\lambda_6}, \qquad \ln \frac{\nu_{13} + \nu_5}{\lambda_{13} + \lambda_5} = \ln \frac{\nu_6}{\lambda_6}, \tag{7.13d}$$

$$\ln \frac{\nu_{13} + \nu_7 + \nu_9}{\lambda_{13} + \lambda_7 + \lambda_9} = \ln \frac{\nu_7}{\lambda_7}, \qquad \ln \frac{\nu_{13} + \nu_9}{\lambda_{13} + \lambda_9} = \ln \frac{\nu_7}{\lambda_7}, \tag{7.13e}$$

$$\ln \frac{\nu_8 + \nu_9}{\lambda_8 + \lambda_9} = \ln \frac{\nu_8}{\lambda_8}, \qquad \ln \frac{\nu_9}{\lambda_9} = \ln \frac{\nu_8}{\lambda_8}, \tag{7.13f}$$

$$\ln \frac{\nu_{10} + \nu_{12} + \nu_{13}}{\lambda_{10} + \lambda_{12} + \lambda_{13}} = \ln \frac{\nu_{10}}{\lambda_{10}}, \qquad \ln \frac{\nu_{12} + \nu_{13}}{\lambda_{12} + \lambda_{13}} = \ln \frac{\nu_{10}}{\lambda_{10}}, \tag{7.13g}$$

$$\ln \frac{\nu_{11} + \nu_{12}}{\lambda_{11} + \lambda_{12}} = \ln \frac{\nu_{11}}{\lambda_{11}}, \qquad \ln \frac{\nu_{12}}{\lambda_{12}} = \ln \frac{\nu_{11}}{\lambda_{11}}. \tag{7.13h}$$

Just like the system in section 6.2.1, these equations exhibit some additional dependencies in λ_l and pose constraints on those. They are addressed by introducing variables $\varkappa_k$ via:

$$\begin{aligned}
\nu_1 &= \exp(\varkappa_1)\lambda_1, & \nu_2 &= \exp(\varkappa_1)\lambda_2,\\
\nu_3 &= \exp(\varkappa_2)\lambda_3, & &\\
\nu_4 &= \exp(\varkappa_3)\lambda_4, & \nu_5 &= \exp(\varkappa_3)\lambda_5,\\
\nu_6 &= \exp(\varkappa_4)\lambda_6, & &\\
\nu_7 &= \exp(\varkappa_5)\lambda_7, & &\\
\nu_8 &= \exp(\varkappa_6)\lambda_8, & \nu_9 &= \exp(\varkappa_6)\lambda_9,\\
\nu_{10} &= \exp(\varkappa_7)\lambda_{10}, & &
\end{aligned}$$

$$\nu_{11} = \exp(\varkappa_8)\lambda_{11}, \qquad \nu_{12} = \exp(\varkappa_8)\lambda_{12},$$
$$\nu_{13} = \exp(\varkappa_9)\lambda_{13}.$$

Following Algorithm 6.1, compare equation (6.20) on page 78, the dependencies in equations (7.13b), (7.13d)(7.13e) and (7.13g) can be rewritten such that, instead of solving the four nonlinear equations arising from equation (7.12), only four nonlinear inequalities have to be solved guaranteeing positivity of λ_l:

$$\begin{aligned}
0 &= (\exp(\varkappa_2) - \exp(\varkappa_1))\ \lambda_2 + (\exp(\varkappa_2) - \exp(\varkappa_9))\ \lambda_{13},\\
0 &= (\exp(\varkappa_4) - \exp(\varkappa_3))\ \lambda_5 + (\exp(\varkappa_4) - \exp(\varkappa_9))\ \lambda_{13},\\
0 &= (\exp(\varkappa_5) - \exp(\varkappa_6))\ \lambda_9 + (\exp(\varkappa_5) - \exp(\varkappa_9))\ \lambda_{13},\\
0 &= (\exp(\varkappa_7) - \exp(\varkappa_8))\ \lambda_{12} + (\exp(\varkappa_7) - \exp(\varkappa_9))\ \lambda_{13}.
\end{aligned} \tag{7.14}$$

Instead of using expressions $\exp() - \exp()$, short forms in terms of q_{ij} are used, compare equation (6.24) on page 78. These q_{ij} are collected in a matrix $Q \in \mathbb{R}^{4\times 5}$, compare equation (6.25). A vector $\tilde{\lambda}$ is introduced, with $Q\tilde{\lambda} = 0$ for $\lambda > 0$:

$$\tilde{\lambda}^{(2)} = \begin{bmatrix}\lambda_2 & \lambda_5 & \lambda_9 & \lambda_{12} & \lambda_{13}\end{bmatrix},$$
$$Q^{(2)} = \begin{bmatrix} q_{11} & & & 0 & q_{12}\\ & q_{21} & & & q_{22}\\ & & q_{31} & & q_{32}\\ 0 & & & q_{41} & q_{42}\end{bmatrix}.$$

To distinguish between matrices for networks of different phosphorylation sizes n, explicit vectors and matrices have a superscript (n). This superscript is omitted during computation and where formulas are given, where possible and applicable. Note, the matrix Q is constructed of only two elements per row in contrast to some matrices in section 6.2.2, i. e., one q_{i1} and one q_{i2} per row. Compare Remark 6.4 and Lemma 6.6 on pp. 79. Note also, no subvector $\tilde{\varkappa}$ with elements of the original vector $\varkappa$ has to be introduced, as no simplifications as in (6.17) on page 77 occur. Thus, equation (6.12) of Algorithm 6.1 holds for $\varkappa$ and not $\tilde{\varkappa}$.

Additional dependencies in λ_k, given in equation (7.14) for $n = 2$, can be found for all $n = 2, \ldots, 14$ for network (N7.1). Thus, the approach is independent of the considered phosphorylation mechanisms PM2–PM4. In contrast to the results in section 6.2.1, the structure of Q stays the same: each step introduces only new terms with the same blockwise structure. This yields only one q_{i1} and one q_{i2} in $Q^{(n)}$ independent of the phosphorylation step n and PM2–PM4:

$$Q^{(n)} = \begin{bmatrix} q_{11} & 0 & 0 & \cdots & 0 & q_{11}\\ 0 & q_{21} & 0 & \cdots & 0 & q_{21}\\ \vdots & \vdots & \ddots & & \vdots & \vdots\\ 0 & 0 & \cdots & q_{(2n-1)1} & 0 & q_{(2n-1)1}\\ 0 & 0 & \cdots & 0 & q_{(2n)1} & q_{(2n)1}\end{bmatrix}.$$

The number of entries in the corresponding equations stays the same, yielding only an increasing number of sign conditions. Table 7.1 gives an overview on the number of additional occurring dependencies, i. e., equations restricting λ_l.

Table 7.1: *Number of additional dependencies (add. dep.) on $\varkappa$ per phosphorylation step for phosphorylation of NFAT. The number of additional restrictions, i. e., number of rows in Q, can be given by $2n$ per phosphorylation step n.*

n	2	3	4	5	6	7	8	9	10	11	12	13
size($\varkappa$)	9	11	13	15	17	19	21	23	25	27	29	31
# of add. dep.	4	6	8	10	12	14	16	18	20	22	24	26

Thus, Remark 6.4 on page 79 does not apply, and the system $Q\,\tilde{\lambda} = 0$ can be solved for $\lambda > 0$. This concludes the second step of Algorithm 6.1, i. e., equation (6.13). This equation states only conditions on λ_l, but does not provide a general solution to equation (7.12), compare equation (6.12). A solution to equation (7.12) in terms of M and $\varkappa = [\varkappa_1, \ldots, \varkappa_9] \in \mathbb{R}^9$ can be given by:

$$\mu = M\,\varkappa$$

with

$$M = \begin{bmatrix} 1 & 0 & 0 & 0 & 0 & 0 & 0 & 0 & -1 \\ 0 & 0 & 0 & 0 & 0 & 0 & 0 & 0 & 1 \\ 1 & 1 & -1 & 0 & 0 & 0 & 0 & 0 & -1 \\ 1 & 0 & 0 & 0 & 0 & 0 & 0 & 0 & 0 \\ -1 & 0 & 1 & 0 & 0 & 0 & 0 & 0 & 1 \\ 0 & 1 & 0 & 0 & 0 & 0 & 0 & 0 & 0 \\ 0 & 0 & 1 & 0 & 0 & 0 & 0 & 0 & 0 \\ -1 & -1 & 1 & 1 & 0 & 0 & 0 & 0 & 1 \\ 0 & 0 & 0 & 1 & 0 & 0 & 0 & 0 & 0 \\ 0 & 0 & 0 & 0 & 0 & -1 & 1 & 1 & -1 \\ 0 & 0 & 0 & 0 & 1 & 1 & -1 & -1 & 1 \\ 0 & 0 & 0 & 0 & 0 & 0 & 0 & 1 & -1 \\ 0 & 0 & 0 & 0 & 1 & 0 & 0 & 0 & 0 \\ 0 & 0 & 0 & 0 & 0 & 1 & 0 & -1 & 1 \\ 0 & 0 & 0 & 0 & 0 & 1 & 0 & 0 & 0 \\ 0 & 0 & 0 & 0 & 0 & 0 & 1 & 0 & 0 \\ 0 & 0 & 0 & 0 & 0 & 0 & 0 & 0 & 1 \\ 0 & 0 & 0 & 0 & 0 & 0 & 0 & 1 & 0 \end{bmatrix}.$$

Thus, a solution to the polynomial condition can be provided, if $Q\,\tilde{\lambda} = 0$ for $\lambda > 0$ is solvable. Recall, equation (7.14) only poses sign conditions on elements q_{ij} as substitutes of expressions $\exp() - \exp()$. Sign patterns guaranteeing positivity of λ are collected in a vector $\sigma = \operatorname{sgn}(q)$, see equation (6.30). If such σ can be found, the polynomial condition is solvable.

To show, that reaction network (N7.1) exhibits multiple steady states, the coset condition has to hold as well, compare Definition 2.4 on page 11. In addition to the sign restrictions posed by $\tilde{\lambda}^{(n)}$ and $Q^{(n)}$, sign vectors δ arising via the coset condition with $s = b - a$ and $\delta = \operatorname{sgn}(s) = \operatorname{sgn}(\mu)$, recall section 6.2.3. Sign restrictions guaranteeing a positive $\tilde{\lambda}$ and sign vectors δ posed by $\operatorname{sgn}(s) = \operatorname{sgn}(\mu)$ have to be checked. The algorithm provided by [58] can be used to check these sign conditions of $\tilde{\lambda}$ and δ, since additional constraints can be implemented. But, as the number of parameters and states is quite large, the performance of the algorithm by [58] is too bad, to be used as a suitable solver. Recall, the algorithm could not be used for sign conditions in chapter 5.3 for networks of size $n = 6$ for the ternary set of $\delta \in \{+, -, 0\}$, and for $n = 7$ for the binary set of $\delta \in \{+, -\}$ due to the computational load.

For the phosphorylation including compartmentalization, each phosphorylation step n introduces 3^{6n+6} or 2^{6n+6} possible sign vectors, dependent on the given sign pattern $\delta \in \{+, -, 0\}$ or $\delta \in \{+, -\}$, respectively. Here, with $2n$ additional sign constraints per step n due to σ, in total $(2^{6n+6} - 1) \cdot 2n \cdot 3$ matrices for the binary set, and $(3^{6n+6}) \cdot 3 \cdot 2n$ matrices for the ternary set

have to be checked for multistationarity.[2] Again, the algorithm is only suited to check small networks and worked for the phosphorylation network described in chapter 5 only up to $n = 5$ with large computation times. For the phosphorylation process here, it is not suited to check even the small system with $n = 2$, as already 3 145 728 matrices have to be checked, which is already larger than the maximal number of sign vectors arising for the phosphorylation process in chapter 5 with $n = 6$ and $\#\delta = 2\,097\,152$ for the binary set.

In addition, the system with fourteen phosphorylation steps is the actual system of interest, where even higher numbers of sign combinations would have to be checked. Thus, this approach is not really applicable to compute valid sign vectors δ together with valid sign patterns σ for multiple steady states of a phosphorylation system as given in network (N7.1). The computational load for higher phosphorylation steps would be too big.

But, as the underlying network (N7.1) corresponds to the phosphorylation network (N5.1) discussed in section 5.1, results of this previous chapter might be applicable to gain some insight on the system: regions of multistationarity for the underlying subnetwork of n-times phosphorylation are known. Extending these regions to the coupled system of network (N7.1) might yield multistationarity for the overall reaction network. This approach will be discussed in the next section.

7.2.2 *Multistationarity Using Subnetwork Analysis*

Conradi et al., [18], introduce an approach, where properties on multistationarity of a subnetwork of a (bio-) chemical reaction can be transferred under certain restrictions to the overall reaction network. As valid sign vectors δ for the underlying subnetwork of multisite phosphorylation are known, some of them might be valid for the overall network under restrictions. Applying this approach does, of course, not yield the whole set of valid sign vectors as would the standard approach, where inequalities have to be solved. But the known valid sign vectors for the underlying phosphorylation might be valid for the coupled network resulting in multistationarity.

The reaction network in (N7.1) is divided into subnetworks of standard multisite phosphorylation and in additional reactions coupling these two reaction networks. The subnetworks of n-times multisite phosphorylations are referred to as the subnetworks, E, consisting of the two n-times phosphorylation networks in cytoplasm and nucleus. The remaining reactions are referred to as the network R, here, the transport reactions. Solutions to the subnetwork E are known. These solutions might be valid in a region around the initial solution for the overall network and are tested throughout this section.

Matrices, introduced before, can as well be used for the analysis here. The structure of the stoichiometric matrix (7.6) is already in such a form that the

7.2 The first factor describes the number of maximal possible sign vectors, $3n + 3$ for the system in cytoplasm, $3n + 3$ for the states in nucleus. The second, $2n$, describes the overall number of sign combinations to be checked, i. e., the number of rows in Q. The third, 3, describes the number of possible sign combinations per row in Q: $\{\binom{+}{-}, \binom{-}{+}, \binom{0}{0}\}$.

subnetwork matrices can be read off easily to generate the stoichiometric matrix off the subnetwork E:

$$N_E = \begin{bmatrix} N^{(n)} & 0 \\ 0 & N^{(n)} \end{bmatrix} \tag{7.15}$$

$$N_R = N_T \tag{7.16}$$

N_E corresponds two the first two column-matrix entries in N, see equation (7.6), with the block of N_T missing. The matrix N_R corresponds to the part of N, where only the transport reactions are present, i. e., the last two columns of N containing N_T, see equation (7.6).

The reaction rates are divided into a part containing only the rate constants of the subnetwork, k_E, and one containing only rate constants of the additional reactions, k_R. Again the stepwise nomenclature allows for an easy description of the respective rate constants

$$k_E = (k_1, \ldots, k_{12n})^T, \tag{7.17}$$

$$k_R = (k_{12n+1}, k_{12n+2})^T \tag{7.18}$$

with $k_E^{(2)} = (k_1, \ldots, k_{24})^T$ and $k_R^{(2)} = (k_{25}, k_{26})^T$. Besides these two vectors, vectors $\hat{k}_E$ and $\hat{k}_R$ of length $12n + 2$ are needed for calculations later on. They correspond to k_E and k_R in a prolonged way by adding zeros at the respective positions, i. e., addition of two zeros at the end of k_E and $12n$ zeros at the beginning of k_R to generate the "hatted" versions.

As the network is divided into a subnetwork and remaining reactions, the reaction rate v changes, too. With k_E and k_R defined, the reaction rate can be given by:

$$\begin{aligned} v_E &= [v_C, v_N]^T, \\ &= \operatorname{diag}(k_C, k_N)\Phi(x_C, x_N), \end{aligned} \tag{7.19}$$

$$\begin{aligned} v_R &= v_T, \\ &= \operatorname{diag}(k_T)\Phi(x_T), \end{aligned} \tag{7.20}$$

with

$$\begin{aligned} \Phi_E &= \Phi(x_C, x_N), \\ \Phi_R &= \Phi(x_T). \end{aligned} \tag{7.21}$$

Recall equation (7.4) and following equations for a definition of v_{NFAT} and $\Phi(x_C, x_N, x_T)$, furthermore, recall equation (7.1) and (7.2) for a definition of the vector of concentrations $x = [x_C, x_N]^T$ and the vector of rate constants $k = [k_C, k_N, k_T]^T$.

The weight matrix poses a more subtle problem. As the subnetwork consists of two standard multisite phosphorylation networks, each of these two has three conservation relations. Thus, the weight for the subnetworks can be given in terms of two decoupled weight matrices of a standard n-times phosphorylation network:

$$W_E = \begin{bmatrix} W^{(n)} & 0 \\ 0 & W^{(n)} \end{bmatrix}.$$

Furthermore, an additional vector w_{add} occurs due to the coupling of the two subnetworks, such that w_{add} complements W, see equation (7.11), in such a way, that they span a basis for the left nullspace of N_E. Choose:[3]

$$w_{\text{add}} = e_2 + \sum_{i=4}^{3n+3} e_i$$

with e unit vectors of length $6n+6$.

Having found an additional weight vector w_{add} and with the monomial vector $\Phi_R(x)$ defined by the educt complexes not contained in the subnetwork, i. e., y_{12n+1} and y_{12n+2}, a positive vector of rate constants k of the overall system resulting in multistationarity of this system can be found by following the algorithm proposed in [18]. Values for k_E are already given by the subnetwork. The algorithm yields values for k_R:

Algorithm 7.1. Adapted from [18], see as well [P6].

(1) For a system with known multiple steady states $x_a^* \neq x_b^*$ for k_E^*, define the Jacobian $J(x,k) = D_x S v(k,x)$ of the overall reaction network and choose an orthonormal basis matrix S_E for $\text{im}(N_E)$. Define further for $i = a, b$

$$A_i^* := S_E^T J(\hat{k}_E^*, x_i^*) S_E,$$

and

$$B_i^* := S_E^T J(\hat{k}_E^*, x_i^*) w_{\text{add}}$$

If both A_i^* are regular, denote the solution to the linear matrix equations $A_i^* X_i + B_i^* = 0$ by X_i.

(2) Choose a vector k_R^* with

$$\begin{bmatrix} w_{\text{add}}^T N_R \operatorname{diag}(\Phi_R(x_a^*)) \\ w_{\text{add}}^T N_R \operatorname{diag}(\Phi_R(x_b^*)) \end{bmatrix} k_R^* = 0. \tag{7.22}$$

for two distinct steady states $x_a^* \neq x_b^*$.

(3) Given a positive vector k_R^* with (7.22), define

$$C_i^* := w_{\text{add}}^T J(\hat{k}_R^*, x_i^*) S_E \tag{7.23}$$
$$D_i^* := w_{\text{add}}^T J(\hat{k}_R^*, x_i^*) w_{\text{add}} \tag{7.24}$$
$$\mathcal{D}_i^* := C_i^* X_i + D_i^*. \tag{7.25}$$

If D_i^* and $\mathcal{D}_i^*$ are regular for $i = a, b$, then there exists a line segment of positive rate constants $k^*(\epsilon) = \hat{k}_E^* + \epsilon \hat{k}_R^*$ and a pair of smooth one-parameter curves of positive steady states $x_a(\epsilon)$ and $x_b(\epsilon)$ with $N x_a = 0 = N x_b$ and $W^T x_a = W^T x_b$ as long as $\epsilon > 0$ is sufficiently small.

Following the algorithm, the condition:

$$w_{\text{add}}^T N_R \operatorname{diag}(\Phi_R(x_i^*)) k_R \overset{!}{=} 0$$

7.3 Of course, the chosen vector is not unique. E. g., $w_{\text{add}} = [0\ 0\ 0\ 0\ 0\ 0\ 0\ 0\ 0\ 1\ 0\ 1\ 1\ 1\ 1\ 1\ 1]^T$ is a valid vector for a double phosphorylation network.

has to be satisfied for $i = a, b$. This condition just poses a condition on the first steady state x_a^*. For sake of simplicity the steady states x_a^* and x_b^* are referred to as a and b, respectively. It can indeed be solved for an arbitrary phosphorylation step n

$$\begin{bmatrix} a_2\, k_{12n+1} - a_{6n+5}\, k_{12n+2} \\ \exp(\mu_2)\, a_2\, k_{12n+1} - \exp(\mu_{6n+5})\, a_{6n+5}\, k_{12n+2} \end{bmatrix} \stackrel{!}{=} 0 \tag{7.26}$$

if

$$\begin{aligned} \mu_2 &= \mu_{6n+5} \\ k_{12n+2} &= \frac{a_2}{a_{6n+5}} k_{12n+1}. \end{aligned} \tag{7.27}$$

If such μ can be found, the second equation provides a solution for transport reactions, such that the overall reaction network exhibits multistationarity, if the subnetwork shows such a behavior.

Recall the two introduced network setups from page 101, i. e., the uni- and multi-valued network setups. To carry on the thought experiment therein, one or two steady states are fixed for the subnetwork and the condition (7.27) is checked.

Furthermore, recall the structure of the sign vectors as a condition on the signs of μ and s from section 5.3.2 for the binary set, $\delta \in \{+, -\}$, and section 5.3.3 for the ternary set, $\delta \in \{+, -, 0\}$, on pages 48 and 51, respectively. The binary set provides steady states a and b for arbitrary $n \geqslant 2$. The ternary set only provides sign vectors for $n = 2, \ldots, 5$. These sign vectors have to be checked for both proposed network setups.

UNI-VALUED RESPONSE CURVE The response curve in cytoplasm shows a uni-valued response curve with $a = b$. Thus, $\mu = 0 \rightarrow \exp(\mu) = 1$. The condition 7.27 reduces to:

$$\begin{aligned} \mu_2 &= 0 \qquad \mu_{6n+5} = 0 \\ k_{12n+2} &= \frac{a_2}{a_{6n+5}} k_{12n+1}, \end{aligned} \tag{7.28}$$

or in terms of the subnetworks:

$$\begin{aligned} \mu_{C,2} &= 0 \\ \mu_{N,3n+2} &= 0 \\ k_{T,2} &= \frac{a_{C,2}}{a_{N,3n+2}} k_{T,1} \end{aligned}$$

Valid sign vectors of the binary set with $\delta \in \{+, -\}$ yielding multistationarity for the subnetwork E naturally do not exhibit a zero element anywhere in their vector. Furthermore sign vectors of the ternary set with $\delta \in \{+, -, 0\}$ are only known up to $n = 5$. These known sign vectors never contain a zero at their second entry or at their second to last entry, compare equations ($5.\Delta_t$) on page 53. It could be possible, that for $n = 6, \ldots, 13$ a sign vector exists, satisfying the condition above. But as these are not known, the sign vectors of the ternary set do not satisfy the condition above for $n \leqslant 5$. Thus, the network setup cannot guarantee existence of multiple steady states via subnetwork analysis. But, the algorithm is only sufficient and not necessary for the existence of multiple steady states. Thus, the network might exhibit multiple steady states with a uni-valued response curve in the cytoplasm subnetwork.

MULTI-VALUED RESPONSE CURVE Having an s-shaped response curve in the decoupled networks in cytoplasm and nucleus, at least two distinct steady sates $a \neq b$ exist in the subnetworks. Thus, the condition (7.26) does not reduce to zero for some μ_i, but can be reduced to (7.27) for a nontrivial:

$$\begin{aligned} \mu_{6n+5} &= \mu_2 \\ k_{12n+2} &= \frac{a_2}{a_{6n+5}} k_{12n+1} \end{aligned}$$

and in terms of the subnetworks:

$$\begin{aligned} \mu_{N,3n+2} &= \mu_{C,2}, \\ k_{T,2} &= \frac{a_{C,2}}{a_{N,3n+2}} k_{T,1}. \end{aligned}$$

The transport rate constant k_{12n+1} is a free parameter. But, multiple steady states can only be exhibited for small variations of the initial chosen vector of rate constants. Only small variations from the initial rate constants of the underlying subnetworks are allowed, a consequence of the Implicit Function theorem being the principle behind the algorithm. Thus small values are chosen for the transport rate constant with $k_{12n+1} = \epsilon$.

Remark 7.2. Choosing a multi-valued response curve as the initial setup of the underlying subnetworks in network (N7.1), the overall reaction network can indeed exhibit multiple steady states.

To compute steady states for the multi-valued setup up in a first approach, one would just chose the same sign vector δ for each standard phosphorylation network, i. e., the same sign vector for the subnetworks:

$$\delta_E = \operatorname{col}\left(\delta^{(n)}, \delta^{(n)}\right).$$

The condition from the subnetwork analysis with $\mu_{6n+5} = \mu_2$ and thus $\operatorname{sgn}(\mu_{6n+5}) = \operatorname{sgn}(\mu_2)$ does not allow for such an approach. Sign vectors cannot be chosen freely due to this condition. But, sign vectors of the binary set are known for arbitrary phosphorylation steps n, see Theorem 5.10 on page 49. Here, the sign of the second to last entry in $\delta^{(n)}$ is always the sign-inverse of the second entry in $\delta^{(n)}$. Thus, with $\operatorname{sgn}(\mu) \overset{!}{=} \operatorname{sgn}(s)$, the choice of sign vectors is

$$\delta_C = -\delta_N$$

to achieve $\operatorname{sgn}(\mu_2) = \operatorname{sgn}(\mu_{6n+5})$. As the vector $\mu = E^{\mathcal{M}}\alpha$, recall equation (5.49), is computed via linear combinations of the extreme rays of $E^{\mathcal{M}}$, the restriction on δ_C and δ_N can be directly translated to restrictions on α. While choosing a certain sign vector, the structure of $E^{\mathcal{M}}$ has to be maintained, restricting thus certain entries in α, see section A.5 on page 147 for an overview on restrictions depending on the chosen sign vector.

Any valid sign vector $\delta \in \{+,-\}$ can be chosen as long as the negative one is chosen for the phosphorylation network in nucleus. The same holds true for $\delta \in \{+,-,0\}$ as long as phosphorylation mechanism PM4 on page 97 is considered, i. e., only two phosphorylation steps take place. But, a different δ imposes different restrictions on α. Thus, a sign vector is chosen, that poses the least restrictions on α. Here, the second δ_2 of $\Delta^{(2)}$ is chosen as

the initial vector with $i_1 = 1$ and $i_2 = n-1$ for larger n, see equation (5.Δ_b2) on page 49, yielding:

$$\begin{aligned} \delta_C^{(n)} &= -\delta_N^{(n)} \\ \alpha_C,\ \alpha_N &> 0 \end{aligned} \tag{7.29}$$

and

$$\alpha_{N,3} = \frac{2}{n-1}(\alpha_{C,1} + \alpha_{C,2}) + \frac{1}{n-1}\alpha_{C,3} - \frac{n-2}{n-1}(\alpha_{N,1} + \alpha_{N,2}). \tag{7.30}$$

See appendix A.5 on page 147 for a more detailed analysis of the restrictions. For arbitrary $n \geqslant 2$ the variable $\alpha_{N,3}$ is fixed. Furthermore, choosing the remaining $\alpha_{C,N}$ and $\beta_{C,N}$ as uniformly distributed pseudo random numbers, compare section 5.4.1, enables computation of steady states, see equation (5.50) on page 53.

Rate constants can be computed by choosing λ, see equation (5.31) on page 42, as either a uniformly distributed pseudo random number or setting each λ_i to a constant value, such that $\sum \lambda_i = 1$. Note that λ is not dependent on $\varkappa$ as only conditions on the subnetworks are of importance as a result of algorithm 7.2.2 being independent on the former section with the algorithm only considering the subnetwork setup. An example for steady states as well as parameters together with bifurcation analysis will be discussed in the next section.

7.3 NUMERICAL ANALYSIS FOR DIFFERENT NETWORK SETUPS

Bifurcation analysis can be done for both network setups, the uni-valued and multi-valued one. For the first setup no δ can be found, see the discussion on page 108. To still test whether the network still can exhibit multiple steady states, a general set of initial conditions motivated by the work of [42] is chosen, see also section 4.1. For the second setup the conditions for δ in equation (7.29) and α in equation (7.30) have to hold.

Bifurcation analysis is done in the same way as before, MATLAB and the toolbox MatCont, version 3p2 and 4p2, are used. Again the number of parameters and network size pose a problem for this toolbox. Only small networks can be analyzed, as the number of parameters in the network becomes too large to generate any data files for bifurcation analysis for $n \geqslant 9$. Thus, results are only given for a double phosphorylation network. PM3, analyzed in the former section, reduces here to PM4. Results from the previous section are applied for $n = 2$.

7.3.1 *Numerical Analysis of Response Curves for the Uni-Valued Setup*

Variables α_C, α_N and β_N are computed as uniformly distributed pseudo random numbers with the dependent $\alpha_{N,3}$ computed by equation (7.30) for a double phosphorylation:

$$\alpha_{N,3} = 2\,\alpha_{C,1} + 2\,\alpha_{C,2} + \alpha_{C,3}.$$

These results are used to compute parameters for the system in nucleus with a uni-valued setup, i. e., equations (5.49) and (5.50) on page 53 hold, yielding for $i = 1, \ldots, 3n+3$

$$\mu_N = E_N^{\mathcal{M}} \alpha_N, \qquad s_N = E_N^{S} \beta_N,$$

$$a_{N,i} = \begin{cases} \frac{s_{N,i}}{\exp(\mu_{N,i})-1}, & \text{if } \mu_{N,i} \neq 0 \\ \bar{a}_{N,i} > 0, & \text{if } \mu_{N,i} = 0 \end{cases} \qquad b_{N,i} = \exp(\mu_{N,i})\ a_{N,i}.$$

The total concentration of the network in nucleus is then given by $c_N = W^{(2)} a_N$. Furthermore λ_N is computed as a normalized vector in the following form, see also section 2.2 for a discussion on λ on page 12: all but the last entry in λ are generated as uniformly distributed pseudo random numbers, the last entry is normalized such that the sum of all entries equals one:

$$\lambda_{N,1:5} = 0.2 \cdot \text{rand}(5) \sim U(0,1)$$

$$\lambda_{N,6} = \sum_{i}^{5} \lambda_{N,i}$$

A value of 0.2 is chosen as a parameter to adjust λ and guarantee a fairly large $\lambda_{N,6}$ with $\sum \lambda_{N,1:5} < 1$. If no such parameter would be chosen, $\lambda_{N,6}$ might be very small or none might be computable at all.

Rate constants in nucleus can then be computed following equation (5.31) on pages 42:

$$k_N = \text{diag}\left(\Phi(a_N)^{-1}\right) E^{(n)} \lambda.$$

Thus, the subnetwork of double phosphorylation in the nucleus exhibits multiple steady states. Next, the steady state in the cytoplasm has to be fixed.

To compute parameters for the uni-valued setup in cytoplasm the approach of [42] is followed, see also section 4.1 on page 29. Thus, rate constants in cytoplasm are set to a constant value, that is scaled by a random (uniformly distributed) number to get several initial setups:

$$k_C = (\text{rand}(1) \sim U(0,1)) \cdot [1\ \ 0.1\ \ 0.1\ \ 1\ \ 0.1\ \ 0.1\ \ 1\ \ 0.1\ \ 0.1\ \ 1\ \ 0.1\ \ 0.1]^T$$

By choosing such values, the network in cytoplasm exhibits a strictly monotone response curve, see for example [85] for a motivation of these values. With k_C given, the concentration in cytoplasm is computed as a function of the rate constant, see equation (5.31):

$$a_C = \begin{bmatrix} \frac{k_{C,6}(\lambda_{C,4}+\lambda_{C,5})(\lambda_{C,5}+\lambda_{C,6})}{k_{C,10}k_{C,7}a_{C,8}(\lambda_{C,(2}+\lambda_{C,3})} \\ \frac{k_{C,10}k_{C,7}a_{C,8}(\lambda_{C,1}+\lambda_{C,3})(\lambda_{C,2}+\lambda_{C,3})}{k_{C,1}k_{C,4}(\lambda_{C,4}+\lambda_{C,6})(\lambda_{C,5}+\lambda_{C,6})} \\ \frac{\lambda_{C,5}+\lambda_{C,6}}{k_{C,10}a_{C,8}} \\ \frac{\lambda_{C,1}}{k_{C,2}} \\ \frac{k_{C,10}a_{C,8}(\lambda_{C,2}+\lambda_{C,3})}{k_{C,4}(\lambda_{C,5}+\lambda_{C,6})} \\ \frac{\lambda_{C,2}}{k_{C,5}} \\ \frac{\lambda_{C,4}}{k_{C,8}} \\ 1 \\ \frac{\lambda_{C,5}}{k_{C,11}} \end{bmatrix},$$

where λ_C is chosen as a uniformly distributed pseudo random number.

The total concentration of the subnetwork in cytoplasm can be given by

$$c_C = W_C^{(2)} a_C,$$

with $W^{(2)}$ defined by equation (5.4), i. e., conservation of all three substances in the subnetwork.

Finally, according to equation (7.28), transport rate constants can be given by

$$k_{T,1} = \epsilon$$
$$k_{T,2} = k_{T,1} \frac{a_{C,2}}{a_{N,8}}$$

with a small, positive number ϵ. When coupling the two systems the total concentration of the overall network is given by

$$c = W^T (a_C, a_N)$$

with W defined by equation (7.11) and (a_C, a_N) a column vector of composed elements of concentrations for substances in cytoplasm and nucleus, respectively, see above. Recall, $W \in \mathbb{R}^{5\times 6n+6}$.

For a numerical test on the response curve of the reaction network, 100 variables are generated in α to compute μ. Furthermore, for each μ, 100 variables in λ are generated to change k. Table (7.2) describes results for bifurcation analysis over three different total concentrations, $c_2 = [A]_{tot} + [B_{tot}]$, $c_3 = [P_C]_{tot}$ and $c_5 = [P_N]_{tot}$ and different ϵ as an influence on the transport rate constant. Each of these systems reveals a similar overall dynamical behavior (over all μ and λ) with hardly any multiple steady states found in accordance to the predictions made in section 7.2.2. Of course, results are only valid in the analyzed range: 900 steps forwards and backwards beginning from the initial value for both network setups. Steady states appearing before or after those steps are not depicted here, but might be present. They could be found by increasing the step size.[4] Thus, the numerical analysis might find only one Hopf bifurcation or one limit point, where several more lay beyond the analyzed range. Besides these results, an increase in the percentage of limit points and Hopf bifurcations can be seen for bifurcation of c_5, last three rows in table 7.2.

Furthermore, changes in c_3 address directly the response curve in the uni-valued subnetwork in cytoplasm and only indirectly the subnetwork in nucleus, as concentrations change in the multi-valued subnetwork due to a change in concentrations in the strictly monotone subnetwork. Thus, changing this total concentration should not have a large influence on the overall response curve of the reaction network, as it is not able to generate switch like behavior in the strictly monotone subnetwork. Consequential, the coupled network does not show limit points or Hopf bifurcations in high percentages, as changes in c_3 only correspond to traversing the strictly monotone curve. On the other hand, changing c_5 directly influences the s-shaped response curve of the subnetwork in nucleus. Thus, the response curve of the overall reaction network should change more significantly. This

7.4 A version update of MatCont from 3 to 4 happened throughout this thesis addressing a derivative error. Not all of the simulations were run again due to computational costs. But results in the first column of table 7.2 might be a consequence of this former error. Furthermore, MatCont is known for showing no convergence for networks with small parameters due to numerical restrictions in the solver step size.

Table 7.2: *Bifurcation analysis for the uni-valued setup and a double phosphorylation network yielding the following results: no con – no convergence, LP – at least two limit points, LP & H: at least two limit points and one Hopf bifurcation, H: at least one Hopf bifurcation, nmss – no multiple steady states could be found in the analyzed region.*

c	ϵ	no con	LP	LP & H	H	nmss
	$1e-7$	–	0.11%	–	0.34%	99.55%
c_2	$1e-6$	–	0.55%	–	0.34%	99.11%
	$1e-5$	0.17%	2.05%	–	0.38%	97.40%
	$1e-7$	–	0.24%	–	0.42%	99.34%
c_3	$1e-6$	–	0.79%	–	0.43%	98.78%
	$1e-5$	0.08%	2.39%	–	0.43%	97.10%
	$1e-7$	0.02%	5.36%	30.69%	58.63%	5.30%
c_5	$1e-6$	0.05%	6.24%	40.78%	48.71%	4.22%
	$1e-5$	0.10%	7.25%	49.35%	39.85%	3.45%

is reflected in the last three rows of table 7.2, where a higher percentage of limit points and Hopf bifurcations can be seen.

Note, the same qualitative results in percentage of limit points and Hopf bifurcations can be seen for change of c_2 as for change of c_3, first three rows in table 7.2. This could be due to the strictly monotone subnetwork having some kind of filter effect on the coupled reaction network decreasing the percentage of limit points and Hopf bifurcations.

Choosing just one example of the set containing two limit points with $\epsilon = 1e-7$ and bifurcation parameter $c_2 = [A]_{tot} + [B]_{tot}$, the values

$$\begin{aligned}
a_C &= [0.3663,\ 1.0000,\ 0.3663,\ 1.8316,\ 1.0000,\ 1.8316,\\
&\quad 1.8316,\ 1.0000,\ 1.8316]^T,\\
c_C &= [4.0295,\ 4.0295,\ 10.3263]^T,\\
a_N &= [0.0431,\ 0.0001,\ 0.0573,\ 1.2881,\ 0.0917,\ 0.1203,,\\
&\quad 0.6474,\ 0.1750,\ 0.04885]^T,\\
b_N &= [3.51e-4,\ 0.0130,\ 0.0419,\ 1.9672,\ 0.1916,\ 0.1837,\\
&\quad 0.0110,\ 0.0041,\ 8.311e-4]^T,\\
c_N &= [1.9786,\ 0.2265,\ 2.3714]^T,
\end{aligned}$$

with

$$c = [4.0295,\ 12.6978,\ 4.0295,\ 1.9786,\ 0.2265]^T,$$

and

$$\begin{aligned}
k_C &= [0.91,\ 0.091,\ 0.091,\ 0.91,\ 0.091,\ 0.091,\\
&\quad 0.91,\ 0.091,\ 0.091,\ 0.91,\ 0.091,\ 0.091]^T,\\
k_N &= [60192.8019,\ 0.0614,\ 0.0778,\ 30.3323,\ 0.4933,\ 0.8331,\\
&\quad 189.6487,\ 0.1354,\ 1.0224,\ 67.1570,\ 0.2416,\ 13.5532]^T,\\
k_T &= 1e-7 \cdot [1,\ 5.7149]^T,
\end{aligned}$$

yield results as given in figure 7.3 for the coupled network setup. Response curve of the decoupled network setup can be found in figure 7.2.

Eigenvalues and concentrations for two arising limit points in the coupled system in figure 7.2 can be given for the first limit point by

$$\begin{aligned} ev_{LP_1} &= [-9\,510.5156,\ -13.9216,\ -8.2888,\ -7.2878,\ 0,\ -3.6914,\\ &\quad 0,\ -3.6867,\ 0,\ -2.7434,\ -1.1712,\ -0.1855,\ -0.1820,\\ &\quad -0.1245,\ -0.0870,\ 0,\ 0,\ 0]^T,\\ x_{LP_1} &= [3.9522,\ 0.00197,\ 3.9522,\ 0.0387,\ -0.0347,\ 0.0387,\ 0.0387,\\ &\quad 0.001957,\ 0.0754,\ 2.9056e-5,\ 0.1574,\ 0.0417,\ 1.9776,\\ &\quad 0.1936,\ 0.1847,\ 9.214e-4,\ 3.4234e-4,\ 6.9515e-5]^T,\\ c_{2,LP_1} &= 2.6751, \end{aligned}$$

and the second limit point:

$$\begin{aligned} ev_{LP_2} &= [-7\,748.12e+3,\ -37.6696,\ -29.4427,\ -2.881+2.1339\,i,\ 0,\\ &\quad -2.8810-2.1339\,i,\ 0,\ -2.8625,\ 0,\ -2.5801,\ -0.4017,\\ &\quad -0.3148,\ -0.182,\ -0.0315,\ -0.0056,\ 0,\ 0,\ 0]^T,\\ x_{LP_2} &= [0.2999,\ 1.2438,\ 0.2999,\ 1.8648,\ 0.6228,\ 1.8648,\ 1.8648,\\ &\quad 1.2438,\ 2.4858,\ 0.1287,\ 1.5513e-5,\ 0.0718,\ 0.8413,\\ &\quad 0.0478,\ 0.0786,\ 1.0086,\ 0.2176,\ 0.0761]^T,\\ c_{2,LP_2} &= 13.4607. \end{aligned}$$

Response curves for both network setups are unstable between the two limit points with one eigenvalue being positive between the limit points and negative otherwise.

7.3.2 *Bifurcation Analysis for a Multi-Valued Setup*

In this section the network setup containing an initial multi-valued setup of the uncoupled subnetworks is considered. Again, only the double phosphorylation network is considered due to computational restrictions in MatCont. As both standard phosphorylation networks in the subnetworks are supposed to exhibit multiple steady states, variables α_C, α_N, β_C and β_N are generated again as uniformly distributed pseudo random numbers with the dependent variable $\alpha_N(3)$ given by

$$\alpha_{N,3} = 2\,\alpha_{C,1} + 2\,\alpha_{C,2} + \alpha_{C,3}$$

as follows from equation (7.30) for $n = 2$.

Furthermore, μ and s are computed for each subsystem according to equation (5.49). As μ_C and μ_N have to have opposing signs due to the condition in equation (7.27), the negative sign vector for the network in nucleus is chosen:

$$\begin{aligned} \mu_C &= E_C^{\mathcal{M}}\,\alpha_C, & \mu_N &= -E_C^{\mathcal{M}}\,\alpha_N,\\ s_C &= E_C^{\mathcal{S}}\,\beta_C, & s_N &= -E^{\mathcal{S}_C,\text{neg}}\,\beta_N. \end{aligned}$$

Note, $\delta_C = -\delta_N$ results in $E_C^{\mathcal{M}} = -E_N^{\mathcal{M}}$. Steady states a and b are then given by (5.50) for each subsystem. The total concentrations of the subsystems are given by

$$c_C = W^{(2)}\,a_C, \qquad c_N = W^{(2)}\,a_N,$$

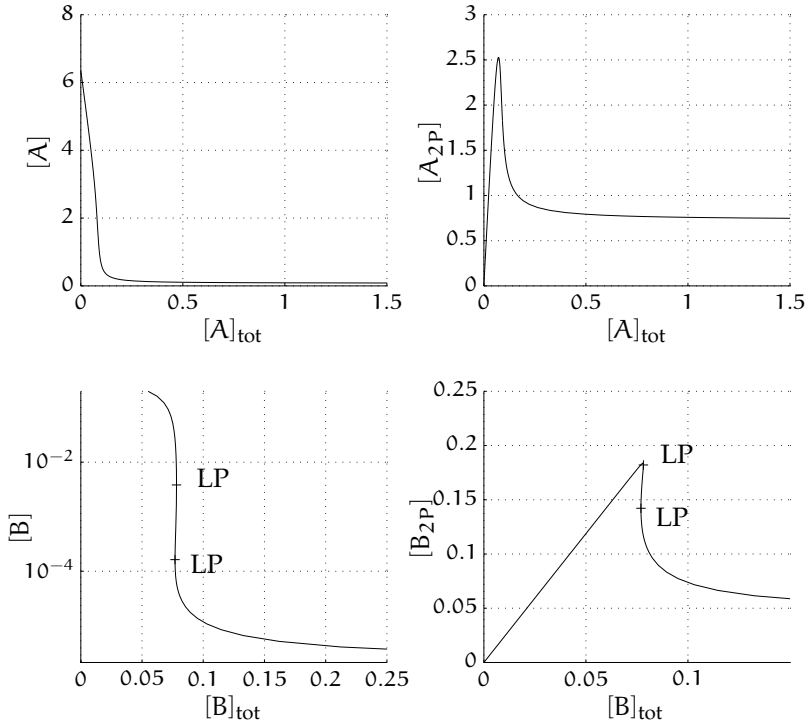

Figure 7.2: *Bifurcation analysis of two decoupled systems for the uni-valued setup. The system in cytoplasm shows a uni-valued response curve, upper two panels, and the system in nucleus shows a multi-valued response curve.*

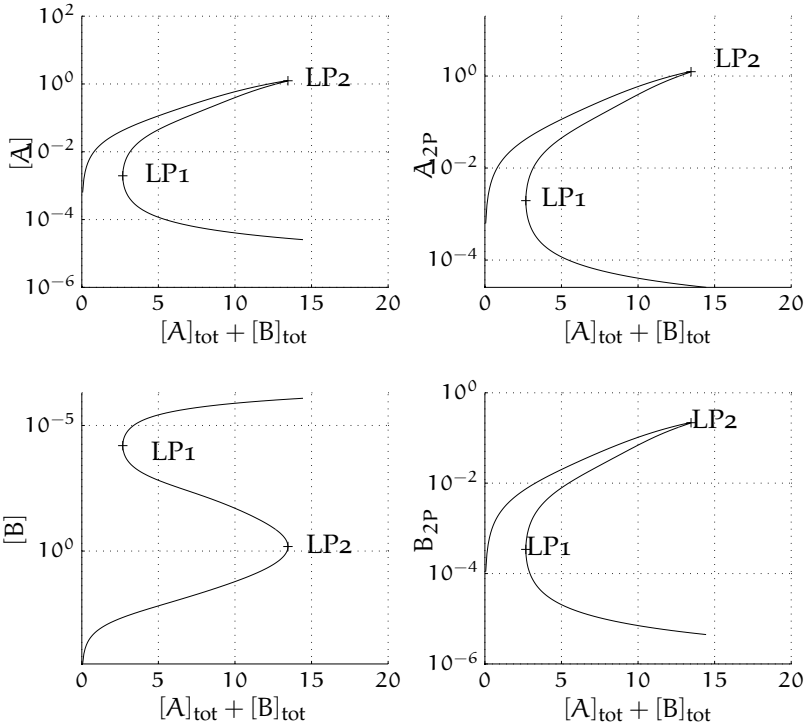

Figure 7.3: *Bifurcation analysis of two coupled systems showing an individual behavior of the decoupled system as illustrated in figure 7.2. The coupled reaction network shows a multi-valued response curve with two limit points arising.*

with $W^{(2)}$ defined by (5.4) for $n = 2$. Note, the total concentration of the whole network has to be computed using the matrix of conservation laws in equation (7.11) for a composed vector of (a_C, a_N) describing the concentration in the overall reaction network.

To compute rate constants k_C and k_N for the subnetwork, the vector λ, see equation (5.31) on page 42, is generated in terms of a scaled, normalized random number: all but the last entry are generated in terms of a scaled uniformly distributed pseudo random number, the last value is normalized such that the sum over all entries in λ equals one:

$$\begin{aligned}
\lambda_{C,1:5} &= 0.2 \cdot \text{rand}(5) \sim U(0,1),\\
\lambda_{N,1:5} &= 0.2 \cdot \text{rand}(5) \sim U(0,1),\\
\lambda_{C,6} &= 1 - \sum_{i}^{5} \lambda_{C,i},\\
\lambda_{N,6}) &= 1 - \sum_{i}^{5} \lambda_{N,i},
\end{aligned}$$

yielding rate constants

$$\begin{aligned}
k_C &= \text{diag}\left(\Phi(a_C)^{-1}\right) E^{(2)} \lambda_C,\\
k_N &= \text{diag}\left(\Phi(a_N)^{-1}\right) E^{(2)} \lambda_N.
\end{aligned}$$

The rate constants of the transport reactions are given by equation (7.27):

$$k_{T,1} = \epsilon, \qquad k_{T,2} = k_{T,1} \frac{a_{C,2}}{a_{N,8}}.$$

For a numerical analysis of the response curve of the coupled reaction networks, 100 values for α and β are generated, yielding a set of 100 parameters μ and s. For each set 100 values for λ are generated. Table 7.3 describes the overall results for numerical analysis via bifurcation of $c_2 = [A]_{tot} + [B]_{tot}$, $c_3 = [P_C]_{tot}$ and $c_5 = [P_N]_{tot}$ and different small, but positive ϵ for 900 steps for- and backwards from the initial values.

Multiple steady states as solutions to the subnetwork are, in the scope of the algorithm 7.2.2, only valid for the overall network in a small region around this initial setup. See table 7.3 for three different ϵ and c_2, c_3 or c_5 as bifurcation parameters. Each of these considered systems shows multistationarity. At the same time, the number of networks without multiple steady states in the analyzed region rises with a rising ϵ due to the restrictions in algorithm 7.2.2, compare also work of [18].

In comparison to the previous case, i. e., a mono-valued response curve, multistationarity can be found in $\approx$ 86% of cases tested for $\epsilon = 1e-7$ and $\approx$ 80% for $\epsilon = 1e-6$ and $\epsilon = 1e-5$. The remaining results, not showing multiple steady states or even no convergence, are probably due to numerical issues, see as well footnote 4 or due to the width of 900 steps forwards and backwards.

Table 7.3: *Bifurcation analysis over different total concentrations* c *for the multi-valued setup of a double phosphorylation network and different transport rate constants via* ϵ*. The coupled system shows: no con – no convergence, LP – at least two limit points, LP & H – at least two limit points and at least one Hopf bifurcation, nmss – no mulitple steady states in the analyzed interval.*

c	ϵ	no con	LP	LP & H	HP	nmss
	$1e-7$	0.01 %	6.35 %	8.97 %	72.13 %	12.54 %
c_2	$1e-6$	0.01 %	9.14 %	16.24 %	64.69 %	9.91 %
	$1e-5$	0.31 %	10.84 %	26.9 %	53.27 %	8.68 %
	$1e-7$	0.02%	5.36%	30.69%	58.63%	5.30
c_3	$1e-6$	0.05%	6.24%	40.78%	48.71%	4.22%
	$1e-5$	0.1%	7.25%	49.35%	39.85%	3.45%
	$1e-7$	0.02%	0.81%	26.83%	68.39%	3.95%
c_5	$1e-6$	0.13%	1.20%	39.57%	55.55%	3.55%
	$1e-5$	0.36%	1.77%	52.70%	42.20%	2.97%

Choosing one example of the set containing limit points as well as Hopf bifurcation, with $\epsilon = 1e-7$ and bifurcation parameter $c_2 = [A]_{tot} + [B]_{tot}$, the values

$$
\begin{aligned}
a_C &= [0.0157,\ 0.4401,\ 0.5015,\ 1.2294,\ 0.1040,\ 2.0918,\\
&\quad\ 0.0272,\ 1.4638,\ 0.0355]^T,\\
b_C &= [0.4695,\ 0.0077,\ 1.3268,\ 0.6425,\ 0.0205,\ 1.0931,\\
&\quad\ 0.1604,\ 3.2587,\ 0.2088]^T,\\
c_C &= [1.2724,\ 2.6288,\ 5.3918]^T,\\
a_N &= [0.2931,\ 0.0009,\ 0.0454,\ 0.4944,\ 0.5109,\ 0.1310,\\
&\quad\ 0.1691,\ 1.7539,\ 0.1075]^T,\\
b_N &= [0.4695,\ 0.0077,\ 1.3268,\ 0.64250.0205,\ 1.0931,\\
&\quad\ 0.1604,\ 3.2587,\ 0.2088]^T,\\
c_N &= [0.9567,\ 0.2839,\ 3.1677]^T,
\end{aligned}
$$

with

$$
c = [1.2724,\ 8.5596,\ 2.6288,\ 0.9567,\ 0.2839]^T,
$$

and

$$
\begin{aligned}
k_C &= [172.3585,\ 0.3180,\ 0.6534,\ 31.3414,\ 0.3974,\ 0.3840,\\
&\quad\ 358.6558,\ 2.2206,\ 19.3479,\ 1.2617,\ 11.2608,\ 14.8601]^T,\\
k_N &= [4\,6024,\ 0.7917,\ 1.6250,\ 70.4185,\ 6.3443,\ 6.1305,\\
&\quad\ 3.9216,\ 0.3576,\ 3.1154,\ 11.6212,\ 3.7155,\ 4.9031]^T,\\
k_T &= 1e-7\ [1.0,\ 0.2509]^T,
\end{aligned}
$$

yield results as given in figure 7.4 for the decoupled and as given in figure 7.5 for the coupled network setup. Eigenvalues and concentrations of the points on the curve can be given by:

$$\begin{aligned}
\mathrm{ev}_{H_1} &= [-2\,758.1,\ -98.0254,\ -35.0978,\ -26.6784,\ 0,\ -29.2774,\\
&\quad 0,\ -20.1976,\ 0,\ -3.5888,\ -2.8405\cdot 10^{-6} - 2.019\cdot 10^{-5}\,\mathrm{i},\\
&\quad 2.8405\cdot 10^{-6} - 2.019\cdot 10^{-5}\,\mathrm{i},\ -0.8052,\ -9.2654,\ -6.5831,\\
&\quad 0,\ -4.4980,\ 0]^{\mathrm{T}},\\
x_{H_1} &= [0.1409,\ 0.0400,\ 0.7560,\ 1.0001,\ 0.0561,\ 1.7016\\
&\quad 0.1315,\ 4.6873,\ 0.1712,\ 0.5988,\ 0.0003,\ 0.1680\\
&\quad 0.3009,\ 0.0841,\ 0.0798,\ 0.0569,\ 0.1595,\ 0.0361]^{\mathrm{T}},\\
c_{2,H_1} &= 8.5054,
\end{aligned}$$

with the first Lyapunov coefficient given by 302.56 for the first Hopf bifurcation, see for example [62].[5] For the first limit point by

$$\begin{aligned}
\mathrm{ev}_{LP_1} &= [-2\,446.7,\ -88.5334,\ -34.8538,\ -20.8221 - 2.3541\,\mathrm{i},\ 0,\\
&\quad -20.8221 + 2.3543\,\mathrm{i},\ 0,\ -30.6582,\ 0,\ -3.7245,\ 0.0642,\\
&\quad 0,\ -0.6799,\ -9.135,\ -6.3736,\ 0,\ -4.5139,\ 0]^{\mathrm{T}},\\
x_{LP_1} &= [0.1059,\ 0.0560,\ 0.6895,\ 1.0525,\ 0.0648,\ 1.7908,\\
&\quad 0.1140,\ 4.4577,\ 0.1485,\ 0.5311,\ 0.0004,\ 0.1456,\\
&\quad 0.3566,\ 0.1150,\ 0.0945,\ 0.0690,\ 0.2232,\ 0.0438]^{\mathrm{T}},\\
c_{2,LP_1} &= 8.5868,
\end{aligned}$$

the second limit point by:

$$\begin{aligned}
\mathrm{ev}_{LP_2} &= [-1\,472.5,\ -93.1079,\ -32.5,\ -50.2162,\ 0,\\
&\quad -16.4112 - 4.0841\,\mathrm{i},\ 0,\ -16.4112 + 4.0841\,\mathrm{i},\ 0,\\
&\quad -9.1931,\ -3.0109,\ 0.1298,\ 0,\ -0.3102,\ -6.1183,\ 0,\\
&\quad -3.7668,\ 0]^{\mathrm{T}},\\
x_{LP_2} &= [0.0302,\ 0.2226,\ 0.5343,\ 1.1945,\ 0.0948,\ 2.0323,\\
&\quad 0.0477,\ 2.4064,\ 0.0621,\ 0.3189,\ 0.0008,\ 0.0677,\\
&\quad 0.5103,\ 0.3539,\ 0.1353,\ 0.1275,\ 0.8870,\ 0.0810]^{\mathrm{T}},\\
c_{2,LP_2} &= 8.1561,
\end{aligned}$$

and the last Hopf bifurcation:

$$\begin{aligned}
\mathrm{ev}_{H_2} &= [-1\,431.3,\ -179.27,\ -90.8973,\ -29.2165,\ 0,\\
&\quad -17.8335 - 2.6058\,\mathrm{i},\ 0,\ -17.8335 + 2.6058\,\mathrm{i},\ 0,\ -9.6928,\\
&\quad -1.671,\ -7.3341,\ -0.261,\ 1.92\cdot 10^{-8} - 7.47\cdot 10^{-5}\,\mathrm{i},\\
&\quad 1.92\cdot 10^{-8} + 7.47\cdot 10^{-5}\,\mathrm{i},\ 0,\ -2.9658,\ 0\Big]^{\mathrm{T}},\\
x_{H_2} &= [0.0092,\ 0.7663,\ 0.4860,\ 1.2467,\ 0.1088,\ 2.1211,\\
&\quad 0.0166,\ 0.9202,\ 0.0216,\ 0.3101,\ 0.0007,\ 0.0331,\\
&\quad 0.4320,\ 0.6127,\ 0.1145,\ 0.2145,\ 3.0537,\ 0.1363]^{\mathrm{T}},\\
c_{2,H_2} &= 9.7658,
\end{aligned}$$

7.5 Note, due to step size restrictions of MatCont only values around the actual limit points and Hopf bifurcations are given. Thus, the real part of the eigenvalues of the Hopf bifurcation is not necessarily zero for the numerical values given by MatCont.

and the first Lyapunov coefficient given by 0.024208. The system is unstable between the two Hopf bifurcations with two positive eigenvalues and stable with no positive eigenvalues left from the first and right from the second Hopf bifurcation.

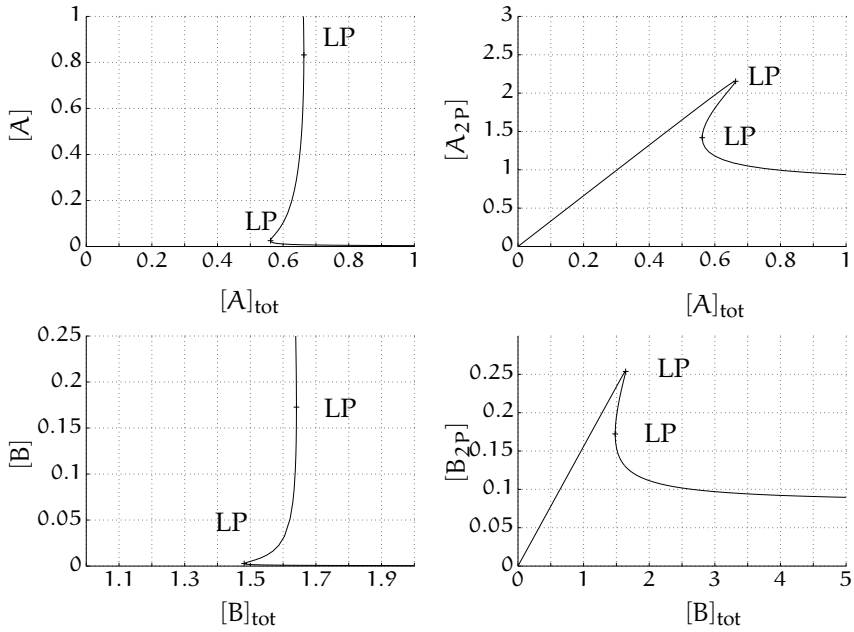

Figure 7.4: *Bifurcation analysis of two decoupled systems using the multi-valued network setup. The response curve of the coupled network setup can be found in figure 7.5.*

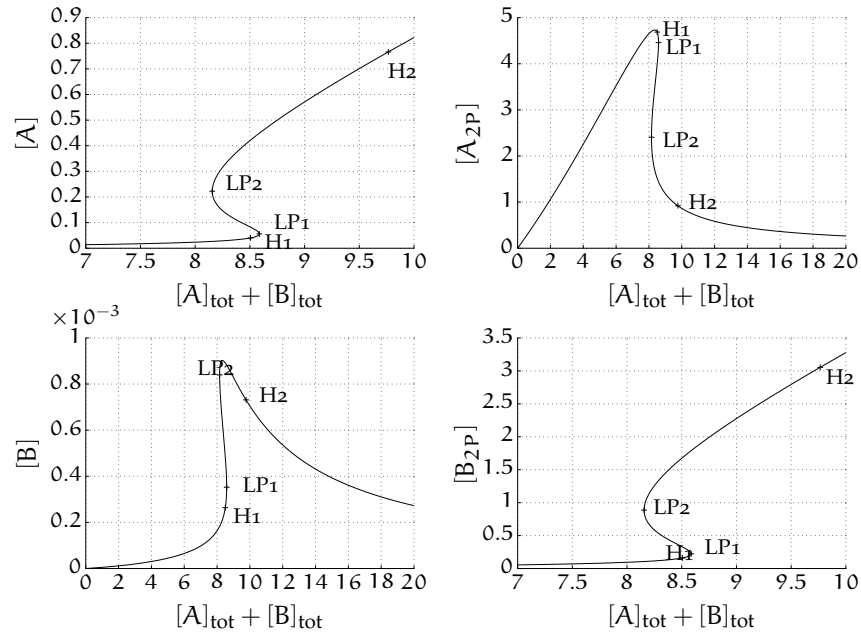

Figure 7.5: *Bifurcation analysis of two coupled system for the multi-valued setup resulting in an overall behavior with two Hopf bifurcations and two limit points. A composed "temporal" course of this figure can be found in figure 7.6.*

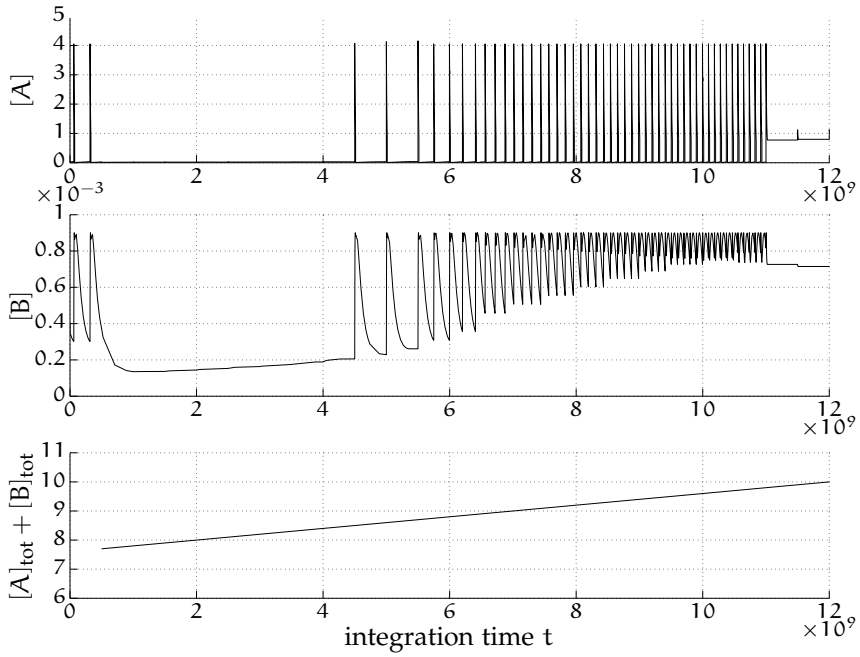

Figure 7.6: *Composed "temporal" course of the dynamical system in figure 7.5 for concentration of the protein in cytoplasm,* [A]*, and in nucleus,* [B]*. The concentration* $c_2 = [A]_{tot} + [B]_{tot}$ *is changed for a fixed integration time* $5 \cdot 10^8$ *by* 0.1 *per integration step as shown in the lower panel. This figure illustrates movement along the curve of figure 7.5. Integration starts below the first Hopf bifurcation, moves on to the upper branch and above the second Hopf bifurcation. Integration time is not long enough for the system to run into a steady state while oscillating.*

Furthermore, a composed "temporal" course of figure 7.5 can be found in figure 7.6. This "temporal" course illustrates movement along the curve in figure 7.5 while varying c_2 stepwise as a dynamical simulation. The total concentration c_2 is changed as a step function for a fixed integration time, such that the system either runs into its steady state or shows other characteristic behavior like oscillations. Note, the resolution for the step size is not large enough for the system to actually run into a steady state, e. g., while its oscillations are decreasing. Step size is chosen such, that c_2 is varied between 7.25 and 9.5 to highlight the behavior.

Recall section 3.2.3 on page 23 and figure 3.6 and the discussion therein. Finding a multivalued region in the phosphorylation network (N7.1) can actually yield response curves as observed in the experiments based on the phosphorylation network itself and is thus not due to oscillations of *calcineurin*.

7.4 SUMMARY AND OPEN QUESTIONS

A large (bio-) chemical reaction network containing two coupled standard phosphorylation networks of size n is considered in this chapter. The underlying subsystem of phosphorylation networks leads to a compartmentalization of the reaction network. In a first approach, the algorithm to solve the polynomial condition of the previous chapters is applied. The algorithm is applicable and yields not only conditions on signs of μ and s but also additional sign restrictions on λ. But, as the network is too big due to the large number of states and parameters, no results for valid sign vectors can

be given. Using a different approach or appropriate solvers to solve sign restrictions in λ and find valid sign vectors δ, it should be possible to provide an explicit answer towards existence of multiple steady states in the considered network. It might be possible to provide solutions following the approach of Lemma 5.9.

As application of this algorithm does not yield solutions, the compartmentalization of the networks is used to check whether the reaction network can exhibit multiple steady states. Known results for the underlying multisite phosphorylation network are used to solve the multistationarity problem in a small area around known solutions of the subnetworks. Conditions on the network are stated to find such solutions. These conditions can actually be satisfied by some sign vectors, such that a region of multistationarity can indeed be found: The n-times phosphorylation network including compartmentalization can exhibit multiple steady states. An example is given, where oscillations arise due to a change in the total protein concentration. This describes a novel finding. The subnetwork analysis could have failed or only stated conditions, that can not be satisfied by the sign vectors of the underlying standard phosphorylation network. But, the phosphorylation process including compartmentalization can actually exhibit multiple steady states. Thus, oscillations observed in experiments can also be found in the considered network. These oscillation need not be a product of oscillating enzyme concentration but can be produced by the reaction network itself. This is a very interesting finding, as the considered reaction network of *NFAT* phosphorylation plays an important role during immune response. Experiments on an enclosed reaction network of *NFAT* phosphorylation could elucidate these findings.

And it's hard to dance
with a devil on your back.
So shake him off, ...

— Florence Welch and Paul Epworth

8 ROBUSTNESS TOWARDS VARIATIONS IN PARAMETER SPACE

Analysis so far has been rather analytical with some excursions to actual values to visualize results. But, existence of multiple steady states, either in general or indeed in biological relevant regions, is not the only interesting topic in (bio-) chemical reaction networks. If multiple stable steady states can be found, it is also of interest, whether these states are still stable if parameter change, as (bio-) chemical reaction networks are often prone to changes. These changes can occur in overall settings, e. g., changes in total concentrations, but also in changes of the temperature, etc., resulting in changes in rate constants. Thus, if the (bio-) chemical reaction network is somewhat robust towards these changes, network properties, like steady states can be preserved if parameters change in small intervals. Otherwise, small environmental changes might have a too drastic impact on the reaction network and the overall organism. This chapter covers some aspects of parameter changes by applying a random walk in parameter space to test robustness of a standard multisite phosphorylation network.

The chapter is based on the robustness analysis done by S. Herold, [45], see also his remarks on different approaches on robustness analysis and on the choice of using a random walk. S. Herold applied a random walk on phosphorylation networks with $n = 2, \ldots, 8$ phosphorylation steps. Analysis therein is extended up to $n = 14$ phosphorylation steps for the binary set of sign vectors $\delta^{(2)} \in \{+, -\}$, see section 5.3 on page 43, for the binary set of sign vectors $\delta^{(3)} \in \{+, -\}$ and $n = 3, \ldots, 15$ phosphorylation steps with $i_1 = 1$ and $i_2 = n - 1$, respectively, compare equation (5.Δ_b). The basic idea is, to change rate constants randomly up to a certain number of times and link robustness to the number of times this change can happen. Preservation of multistationarity in the reaction network is checked via the polynomial and coset condition, compare Definition (2.4) on page 11. In contrast to S. Herold's, see [45, page 19, ff.], this chapter also considers the influence on the robustness of the network of generating the parameters α, β and λ in different ways, i. e.,as uniformly distributed pseudo random numbers or choosing fixed values, compare also section 5.4.

Where S. Herold's focus lies on robustness of multistationarity towards changes in either the individual parameters or the overall parameter vector, this chapter provides results for changes of the whole parameter vector due to the rising number of parameters with larger network sizes n. It also provides results for four different versions of generating parameters α, β and λ, recall Remark 2.5 on page 12.

8.1 GENERATING INITIAL VALUES

To enable robustness analysis initial parameters for rate constants k and steady states a and b have to be generated. The initial concentration of

Table 8.1: *Nomenclature for parameters of different setups for generating* α, β *and* λ. *See also* y*-axis in figure 8.2, C.3 and C.4.*

version/variable	α, β	λ
α, β	random number	fixed parameter
α, β, λ	random number	random number
{}	fixed parameter	fixed parameter
λ	fixed parameter	random number

states a and b are kept constant during the random walk. Following the approach of former chapters, see for example section 5.4.1, different scenarios for generating parameters are possible. Here, parameters are generated in a general form, such that they are not restricted to certain intervals, compare section 5.4.2. Following section 5.4.1, parameters can be generated in two different ways: either parameters are set to a fixed value, for example $1/6$ for all values in $\lambda^{(2)}$, see section 5.4.2 on page 58 but also remark 2.5 on page 12, or chosen as uniformly distributed pseudo random numbers, see table 8.1 for arising combinations of parameters.

Due to the nature of the algorithm, α and β can be chosen freely in the network, recall equation (5.49) on page 53. Thus, choosing uniformly distributed pseudo random variables does not restrict any given network properties. Furthermore, restricting them to a given length might enable better comparison in the random walk analysis between a flexible parameter space or a tight parameter space, respectively. Recall, the α is always of length three for the standard multisite phosphorylation network considered in chapter 5, see also the cone $E^{\mathcal{M}}$ on page 149. Thus, in analogy to Remark 2.5 on page 12 choosing the same value for each entry in α and β would correspond to fixed values in these vectors dependent on the size of their appropriate cones, thus a "fixed" parameter space. Thus, chose for the random setup

$$\alpha \approx \mathcal{U}(0,1) \in \mathbb{R}^{3}_{\delta(n)} \qquad \text{and} \qquad \beta \approx \mathcal{U}(0,1) \in \mathbb{R}^{q}_{\delta(n)},$$

compare equation (5.49) and notation in table 8.1. And, for the fixed setup

$$\alpha = \frac{1}{3} \in \mathbb{R}^{3}_{\delta(n)} \qquad \text{and} \qquad \beta \frac{1}{q} \in \mathbb{R}^{q}_{\delta(n)}.$$

Values for steady states are computed following equation (5.50) on page 53

$$a_i = \begin{cases} \frac{s_i}{\exp(\mu_i)-1}, & \text{if } \mu_i \neq 0 \\ \bar{a}_i > 0, & \text{if } \mu_i = 0 \end{cases}$$
$$b_i = \exp(\mu_i)\ a_i.$$

The same argument holds for the parameter λ and its cone $E^{(n)}$. Furthermore, recall equation (5.31) on page 42, λ can also be interpreted as flux modes in the reaction network, see section 2.2 on page 12. Setting elements of λ to a constant range would correspond to equal influence of every flux mode whereas random values correspond to a biased influence of each elementary mode, e. g., large values correspond to a larger influence of the corresponding reaction. Thus, influence of λ on the reaction network via

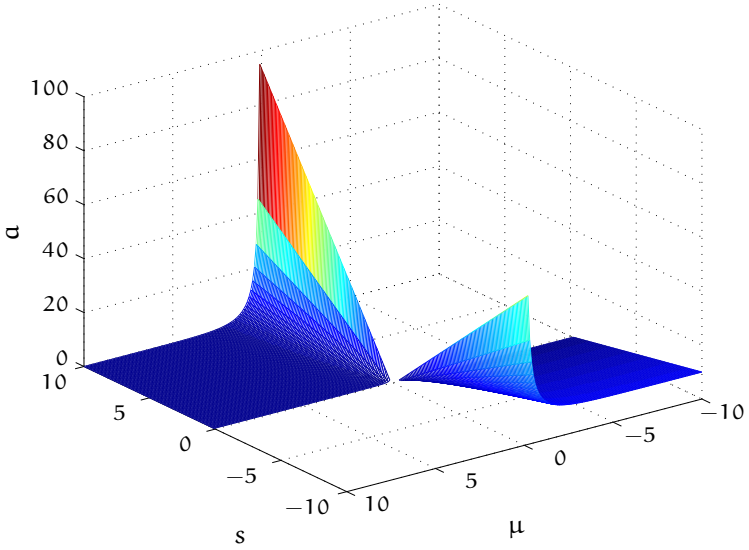

Figure 8.1: *Steady state* a *as a function of* μ *and* s *for* $\operatorname{sgn}(\mu) = \operatorname{sgn}(s)$ *and an interval of* μ, $s \in [-10, 10]$, *compare also figure 5.4 on page 63. Distribution of* a *follows, in an approximation, the slope of a logarithmic function.*

its cone $E^{(n)}$ can be used to interpret results in a biological way. For the random setup

$$\lambda \approx \mathcal{U}(0, 1) \in \mathbb{R}^{3n}_{>0},$$

and the fixed setup

$$\lambda = \frac{1}{3n} \in \mathbb{R}^{3n}_{>0}$$

are chosen. With a given by equation (5.50), a set of initial rate constants $k(0)$ can be computed via equation (5.31) on page 42

$$k(0) = \operatorname{diag}(\Phi(a)^{-1}) E \lambda.$$

To be able to draw conclusions from the random walk, several aspects have to be considered. First of all, the parameter space has to be simply connected or, at least, should not contain holes at unknown positions. The random walk would of course fail reaching boarders or holes. Generating the steady state a via μ and s, the distribution of the steady state seems to follow the slope of a logarithmic function, see figure 8.1, where only $a_i = 0$ is not defined. Thus, the pointed polyhedral cone E, where $\nu(k, a)$ lies, seems to be simply connected minus the origin, without loss of generality due to equation (5.50) and equation (5.31).

The second aspect to be considered is, whether conclusion can be drawn following the random walk itself. The step size is known, given by equation 8.1. A high number of iterations is needed to be able to draw conclusions from the random walk due to the crude approximations on the distribution of generated variables, a and b. In total $R = 1000$ initial steady states are generated and varied in (a maximum of) $m = 100$ steps. These numbers were chosen to guarantee a wide range of initial values even for the tight setup $\{\}$, see table 8.1.

To analyze robustness towards variation in the parameter vector, the vector of rate constants k is varied randomly in each step of the random walk.

This "stochastic process" uses the initial vector $k(0)$ from above, confined to a parameter space dependent on the size of the initial vector of rate constants. The vector $k(j)$ is stepwise varied randomly for $j = 1, \ldots, m$ by a given constant distance $\Delta k(j)$, until the valid parameter region, i. e., the region were the network exhibits multiple steady states, can no longer be sustained:

$$k(j) = k(j-1) + \Delta k(j), \qquad j = 1, 2, \ldots, m \tag{8.1}$$

with

$$\|\Delta k(j)\|_2 = \sqrt{\sum_i^{6n} k_i(0)^2}, \tag{8.2}$$

where the distance $\Delta k(j)$ is not only dependent on the initial vector of rate constants $k(0)$, but also individual values of $k_i(0)$, compare section 3.1.1. Variation of the parameter vector k can either be done individually for specific entries in k, i. e., only one or several entries in k are changed during the random walk, or for the overall vector, i. e., the whole vector changes. This is in contrast to most other sensitivity analysis tools, here variation of certain pairs of k is possible within the random walk, e. g., varying the rate constant of all phosphorylation steps k_{6i-3} or dephosphorylation steps k_{6i} and $i = 1, \ldots, n$, see network (N5.1).

8.1.1 *Variation of the Whole Parameter Vector*

In a first attempt, the whole parameter vector k can be varied to analyze robustness. Choosing a fixed step size independent on actual values in k can yield either too small values for some k_i or too large ones for others, see also [45]. To provide a step size, that takes these differences in the k_i into account, a directed vector $\delta k(j)$ of normally distributed random numbers with mean 0 and standard deviation of 1, $\mathcal{N}(0, 1)$, is generated. The step size is chosen as a function of a biased vector $r \in \mathbb{R}^{6n}_{>0}$:

$$\Delta k(j) = r \cdot \delta k(j) \frac{\|k(0)\|_2}{\|\delta k(j)\|_2} \tag{8.3}$$

to account for differences in the values of the k_i. And thus, parameters $k(j)$ of a step j are dependent on parameters of the former step $j-1$ as well as the initial value $k(0)$. Note, only positive $k_i(j)$ are allowed.

8.1.2 *Variation of Individual Parameters*

A second scenario is possible, where an individual parameter k_i is varied. The influence on the robustness of the network towards a single k_i could be tested in such a way. It would be, for example, of interest whether the property of multistationarity is more robust towards variation of the association rate constants, k_{6i-6} for $i = 1, \ldots, n$, than the phosphorylation rate constants, k_{6i-3}.

Here, single steps j are chosen in such a way, that individual rate constants $k_i(j)$ are only dependent on the initial parameter rate constant $k_i(0)$ and thus, values for the step j are in the same range as the ones of the initial step:

$$\Delta k_i = \delta k_i(j) \cdot \frac{\|k_i(0)\|}{\|k_i(j)\|}$$

and

$$\Delta k_{max,i} = k_i(0),$$

where the step itself is again a normally distributed random number with

$$\delta k_i(j) \approx \mathcal{N}(0,1).$$

Following this approach, all but the i-th rate constants are kept constant. The i-th rate constant is given by equation (8.1) and $k_i(j)$ lies in an interval $k_i(j-1) \pm k_i(0)$. Again, only positive rate constants are admissible.

8.2 THE POLYNOMIAL AND COSET CONDITION

A random walk is applied for network (N5.1) and $n = 2\,(3), \ldots, 14\,(15)$ for variation of the vector of rate constants $k \in \mathbb{R}^{6n}$ and the discussed cases of table 8.1. Preservation of multistationarity by changing the parameter region is guarantied by checking the polynomial condition, see equation (5.14), and the coset condition, see equation (5.15). The polynomial condition has to be fulfilled for every variation step. For validation of the coset condition three scenarios are possible:

RW1 In a biological sense, no external regulation is allowed. The total concentration $c \in \mathbb{R}^3$ of the network is constant with

$$c(0) = c(j) = \text{ const. } \forall j = 1, \ldots, m.$$

The total concentration has to stay constant with each variation step j. New parameters $k(j)$ as well as steady states a, $b \in \mathbb{R}^{3n+3}_{>0}$ have to fulfill

$$0 = \begin{bmatrix} N\,v(k(j),\, a) \\ N\,v(k(j),\, b) \\ c(0) - W^T a \\ c(0) - W^T b \end{bmatrix}$$

such that multistationarity is maintained with $a \neq b$, i. e., steady states for all $k(j)$ have to lay in the same coset.

RW2 External regulation of enzymes in the network is allowed via unmodeled synthesis and/or degradation or inflow via higher network structures. Thus only the total concentration of the protein and its phosphorylated forms is constant for all steps and positive a and b:

$$c_3(0) = c_3(j) = \text{ const. } \forall j = 1, \ldots, m.$$

The following condition has to be fulfilled in each variation step j:

$$0 = \begin{bmatrix} N\,v(k(j),\, a) \\ N\,v(k(j),\, b) \\ \begin{bmatrix} w_1^T \\ w_2^T \end{bmatrix} (b - a) \\ c_3(0) - w_3^T a \\ c_3(0) - w_3^T b \end{bmatrix}$$

to guarantee multistationarity.

RW3 External regulation of all enzymes and the protein is possible. Thus the total concentrations of all substances are allowed to change with each variation step, for positive a and b. To guarantee multistationarity of the network itself, the following condition has to be fulfilled:

$$0 = \begin{bmatrix} N\nu(k(j), a) \\ N\nu(k(j), b) \\ W^T(b-a) \end{bmatrix}.$$

"Robustness" of the network is then defined via the number of possible steps allowed in the current random walk. If the condition in the corresponding setup fails, the current random walk is aborted corresponding to parameters failing to sustain the network property of multistationarity.

Furthermore the different scenarios RW1–RW3 allow to model a degree of freedom for the network, as higher network structures, for example over- and underlying layers in the *MAPK* cascade, are able to intervene with the network and thus increase or decrease the robustness of the network.

8.3 ROBUSTNESS ANALYSIS

To enable robustness analysis, exit conditions, as indicated in RW1–RW3 on page 127, are checked in every variation step j. If they fail, the random walk is aborted and the last valid step is taken as the exit number I of the random walk. By using several cycles of the random walk the mean exit number $\bar{I}$ can be computed

$$\bar{I} = \frac{1}{R}\sum_{i=1}^{R} I(i), \tag{8.4}$$

recall R as being the total number of initial sets being generated,i. e., $R = 1000$ for each phosphorylation step n. And, $m = 100$ as the maximal number of steps taken during the random walk. Furthermore, variables I_{min} and I_{max} are used, to describe the minimal and maximal number of steps a random walk could be performed for all R. Where, in the worst case, $I_{min} = 0$, i. e., the random walk failed in the first step. And at most, $I_{max} = m$.

The mean exit number enables predictions for the actual robustness of the network towards variation of the parameter k for different sign vectors $\delta^{(n)}$: higher values correspond to more robust parameters whereas lower values correspond to more sensitive parameters.

For small phosphorylation networks, the approach of testing the robustness of each individual rate constant is laborious, but feasible. As the number of rate constants rises by 6 per phosphorylation step, the approach is not feasible for larger phosphorylation networks. Consider a simple case of a double phosphorylation: twelve rate constants would have to be varied up to $m = 100$ times. To be able to draw conclusions, about $R = 1000$ initial values would have to be generated, comparable to the former approach for variation of the whole vector. For the small network, this would yield for each sign vector $\delta_i^{(2)} \in \Delta^{(2)}$, see equation (5.51) on page 54, each setup (compare table 8.1) and each scenario, RW1–RW3, in total $4 \times 4 \times 3 = 48$ sets of data for each rate constant. S. Herold followed this approach for phosphorylation networks up to a size $n = 6$ for each scenario and each sign vector, but only one setup, the one corresponding to the first line in table 8.1. He found differences in the robustness of individual rate constants, i. e., certain

rate constants could be varied more often, respective to their initial value, than others, before conditions on multistationarity can no longer be satisfied. But, the computational effort rises of course with a rising network size. For networks of $n > 7$ it is already too large to actually check all rate constants for all $\delta^{(2,3)}$, all setups, compare table 8.1, and scenarios RW1–RW3, under the given conditions. Thus, the approach is not further considered here in favor of testing the influence of generating parameters α, β and λ on the robustness of the reaction network. Robustness analysis is only performed following equation (8.3) for all $\Delta^{(n)}$ of equation ($5.\Delta_b$) with $n = 2, \ldots, 14$ and $n = 3, \ldots, 15$ for $i_1 = 1$ and $i_2 = n - 1$, all four setups of table 8.1 and scenarios RW1–RW3.

8.3.1 *Results for Variation of the Whole Parameter Vector*

A random walk for variation of k for sign vectors $\delta^{(n)}$ of $\Delta^{(n)}$ for $n = 2, \ldots, 14$ and $n = 3, \ldots, 15$ and $i_1 = 1$ and $i_2 = n - 1$ in equation ($5.\Delta_b$) is applied. Selective results for all four setups, $I(\alpha, \beta)$, $I(\alpha, \beta, \lambda)$, $I(\lambda)$ and $I(\{\})$ for RW1–RW3 and $\delta_1^{(2)}$ can be found in figure 8.2. Results for remaining $\delta^{(2)}$ of $\Delta^{(2)}$, and $\Delta^{(3)}$ can be found in appendix C.2 in figure C.3 and C.4, respectively.

Dependent on the scenario, see table 8.1, different "slopes" can be seen. Note, the mean exit number $\bar{I}$ for a given color corresponds to the "same" sign vector for networks of rising n, i. e., sign vectors $\delta^{(2)}$ are only prolonged by δ_1 and δ_3 with $i_1 = 1$ and $i_2 = n - 1$, see equation ($5.\Delta_b 2$) in Theorem 5.10. This excludes of course other sign vectors, i. e., those prolonged by δ_1 and δ_3 but with i_1 and i_2 not fixed in the previous sense, but also all others prolonged by different signs. This approach is used to enable comparability between different phosphorylation steps n. If orthants are prolonged in such a way, ratios between individual concentrations stay the same, see also the discussion in section 5.5 on page 66, in [P1] and the Fact 6.1 in [P2]:

Some scenarios of RW1–RW3 show a constant mean exit number, for some the mean exit number first increases and then decreases, and some scenarios even show a decrease towards a mean exit number of zero, i. e., the random walk fails already in the first step. Comparing the overall slope of the curve of the mean exit number for a fixed scenario, RW1–RW3, but between all four setups, $I(\alpha, \beta)$, $I(\alpha, \beta, \lambda)$, $I(\lambda)$ and $I(\{\})$, the influence of the parameter α and β seems to be higher than the one of λ. The overall appearance stays the same whether λ is chosen fixed or varied randomly, compare curves between left two subplots with those in the right two subplots in figure 8.2. Whereas changes of α and β alter the overall appearance of the mean exit number $\bar{I}$, compare curves in upper two subplots with those in the lower two. The network seems to even lose robustness in parameter variation for larger phosphorylation steps n by setting α and β to fixed values,i. e., the mean exit number is zero and thus no random walk is possible. Overall, the robustness seams to decrease for almost all sign vectors and scenarios for phosphorylation networks of sizes $n > 6$, the only exception being $\delta_1^{(2)}$, compare additional figures C.3-C.4 in appendix C.2.

Besides these influences, the restrictions on the exit conditions, i. e., the cause for violation RW1–RW3, have an influence on the robustness as well. As expected the least restrictive exit condition, RW3, is the most robust one for most of the networks, only in some cases is RW2 better. The mean exit

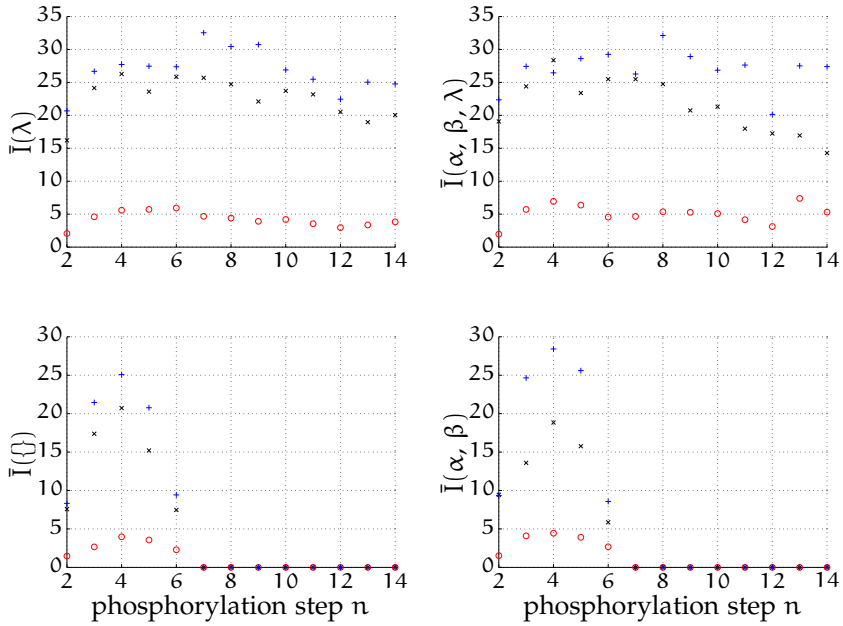

Figure 8.2: *Mean exit number as measure of robustness for perturbation of the parameter vector for sign vectors* $\Delta^{(n)} \in \{+, -\}$ *in equation* (5.Δ_b) *with* $i_1 = 1$ *and* $i_2 = n - 1$. *Different scenarios are coded in the following way: RW1 = red circle, RW2 = black cross, RW3 = blue plus. Note* $\bar{I} = 0$ *for* $n \geqslant 7$ *or* 8 *for fixed* α *and* β *(subplots in lower row).*

number of RW2 lies close by the one of RW3, but is below the one of RW3 in most cases, e. g., exceptions for $\delta^{(2)}_{1,2}$ and $\bar{I}(\alpha, \beta, \lambda)$. With RW1 corresponding to the most restrictive network setup, it shows accordingly the lowest mean exit times and thus, yields the least robust results. On average, only one fifth of the variation steps possible for RW2–RW3 could be achieved for RW1.[1]

8.3.2 *Relaxation of Conservation Relation and Exit Condition*

If the numerical test for the exit condition in each scenario fails, the exit reason is analyzed via the following exit conditions:

#1 Violation of $\langle W, b - a \rangle = 0$.

#2 No positive pair a, b can be found.

#3 No pair a, b can be found at all.

Due to the number of runs and sign vectors, this test is only done for the first four sign vectors of $\Delta^{(2)}$ and their corresponding vectors for $i_1 = 1$, $i_2 = n - 1$ of rules (5.Δ_b).

Figure 8.3 shows the maximum, mean, and minimum exit numbers for $\delta^{(2)}_1$ of $\Delta^{(2)}$ and following $\delta^{(n)}$ of equation (5.Δ_b1) with $i_1 = 1$ and $i_2 = n - 1$ for all three scenarios, RW1–RW3, and four setups from table 8.1, $I(\alpha, \beta)$, $I(\alpha, \beta, \lambda)$, $I(\lambda)$ and $I(\{\})$. Results for remaining sign vectors of $\Delta^{(n)}$

8.1 A Kolmogorov-Smirnov test, see [46], yields the same underlying distribution comparing distribution of mean exit numbers in between the same scenarios, RW1–RW3, in the following sense: distribution of the mean exit numbers of RW1–RW3 of $\bar{I}(\alpha, \beta, \lambda)$ corresponds to the one of $\bar{I}(\alpha, \beta)$, and the distribution of the mean exit numbers of RW1–RW3 of $\bar{I}(\lambda)$ to the one of $\bar{I}(\{\})$.

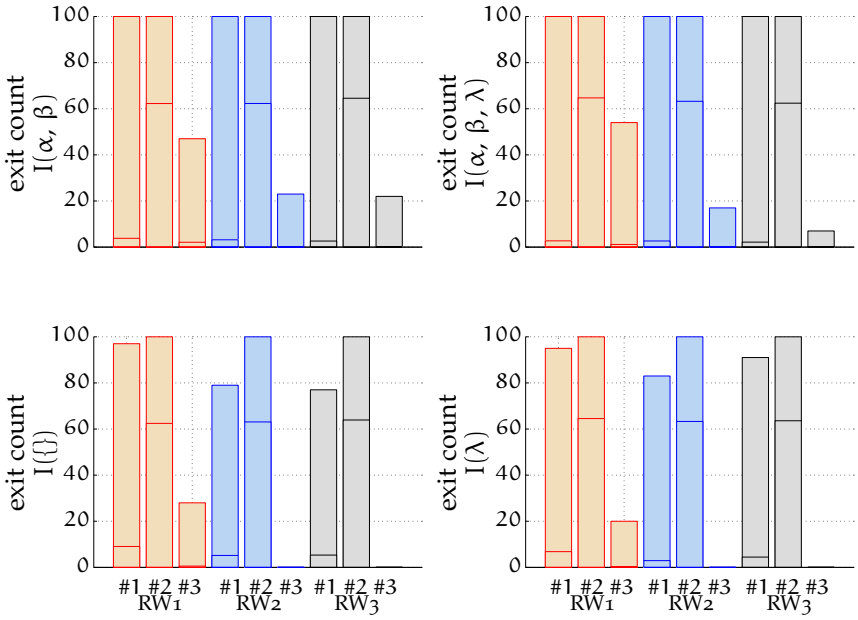

Figure 8.3: *Exit reason for all exit conditions and* $\delta_1^{(2)}$ *of* $\Delta^{(2)}$ *and following* $\delta^{(n)}$ *of equation* (5.Δ_b1) *with* $i_1 = 1$ *and* $i_2 = n - 1$. *Upper (solid red, blue, black) horizontal line describes maximum exit step* I_{max}, *middle horizontal line describes mean exit step* $\bar{I}$ *and lower horizontal line describes minimum exit step* I_{min} *(not visible in all cases as it corresponds to zero, i.e. the first step is already invalid).*

for $n = 2, \ldots, 14$ of equation (5.Δ_b) on page 49 can be found in figures C.5 in appendix C.2 on page 189.

Again, the overall result is similar for all Δ, scenarios, and exit conditions, RW1–RW3: most of the random walks fail due to violation of reason #2. But, small differences can be seen for the different signs $\Delta^{(n)}$. The first sign vector, $\delta_1^{(n)}$, exhibits an overall higher mean value for exit $\bar{I}$ as a consequence of reason #2 for all three RW's than the other three sign vectors. The mean exit number $\bar{I}$ for the other three sign vectors is mostly higher for the second exit reason #2 and RW3. Furthermore, comparing maximum, mean and minimum exit numbers I within a sign vector, all show a similar behavior for different setups from table 8.1: If (only) α and β are chosen randomly, networks might fail as well due to reason #3. But if α and β are fixed, reason #3 never is the cause for violation of the exit condition, except for RW1. Note, I_{min} is zero for all curves in figure 8.3. Thus all random walks fail at least once due to violation of #1, #2 or #3 for all Δ, RW and setups. Interestingly, I_{max} is 100, corresponding to m, only for some scenarios and some Δ. It is always lower than 100 for reason #3, i. e., if reason #3 is violated, the system never reaches its maximum number of steps. But if α and β are fixed, it also hardly reaches the maximum number of steps for RW3.

8.4 SUMMARY AND OPEN QUESTIONS

If a standard phosphorylation network exhibits multiple steady states for $n \geqslant 2$, it is of interest, whether these steady states are robust towards changes in parameter space. Therefore, a random walk in parameter space is applied in this chapter. It is based on work of S. Herold, [45], and ex-

tended in substantial ways. In contrast to work by [45], different forms to generate parameters and their influence on the robustness of the network are considered. Furthermore, different random walk scenarios, RW1–RW3, are considered. The first one corresponds to the polynomial condition and coset condition to hold. The second one allows external regulation of the enzymes, e. g., via synthesis and degradation. The third one allows external regulation of the enzymes and the protein.[2] The different scenarios correspond to network properties, where the reaction network is either operating in a fixed setup or is regulated by external reactions. And thus, might be able to adapt to external influences, e. g., variation in parameters.

Concluding from the results of the different scenarios, RW1–RW3, for different exit conditions for the random walks, the robustness of the multistationarity region in terms of variation of parameters rises with the phosphorylation step n up until four to six phosphorylation steps and then decreases for higher n. These results confirm the findings of [45] for smaller phosphorylation networks. Thus, findings confirm what one would expect from the reaction network: the least restrictive setup is the most robust one as the network is able to adapt to changes imposed by the random walk as long as external regulation via synthesis and degradation is allowed.

Furthermore, generating parameters α, β and λ seems to play an important role. Parameters α and β influence directly steady states a and b and have an indirect influence on k via a. The parameter λ only influences the rate constant k. Robustness analysis indicates, that α and β play a more important role on preservation of multistationarity than the vector λ. While keeping α and β fixed, the random walk fails immediately for $n = 7$ or $n = 8$, depending on the used sign vector δ. Whereas, randomly chosen α and β enable a random walk up to fourteen phosphorylation steps, though the maximum number of possible steps decreases with a rising step n. On the other hand, choosing a fixed or random λ does not seem to have an influence on the random walk itself.

From a biological point of view, this is quite surprising. Here, an interpretation of λ's influence on the reaction network is more intuitive, than the one of α and β. On might expect, that changing λ, i. e., the random setup, should have a more drastic impact on the reaction network, as rate vectors are influenced directly and thus, flux modes in the reaction network. But this does not seem to be the case. Rather, fixing α and β, in terms of their respective cones, seems to impose too strict conditions on the network or move steady states in rather narrow regions of their multistationarity region. Recalling the example provided on the ratios of steady state concentrations, see also [P2], these results are really interesting and more analysis on the influence of parameters α, β and λ in terms of a mathematical but also biological interpretation on the network structure is needed.

Furthermore, the distribution of exit numbers of the random walk over different sign vectors δ is not the same. Dependent on the sign vector used, the random walk fails for some sign vectors already after 20 steps and for others after 60 steps. Again, a biological interpretation of sign vectors is needed to enlighten this phenomenon.

8.2 I. e., the steady state a of an arbitrary random walk step j has to lie in the same coset as the second steady state b for the same step j. But they do not have to lie in the same coset as the initial pair of steady states.

In the end
these things matter most:
How well did you love?
How fully did you live?
How deeply did you let go?

— Siddharta Gautama

9 SUMMARY, OPEN QUESTIONS AND CONCLUSIONS

The thesis discusses the topic of multistationarity in multisite phosphorylation networks. After an introduction of the topic, theoretical and experimental aspects of modeling (bio-) chemical reaction networks are discussed. Experimental results and theoretical findings on the number of steady states of certain reaction networks from literature are given. Multiple steady states have been shown to exist in experimental setups of multisite phosphorylation networks. Furthermore, existence of multiple steady states in a distributive, sequential double phosphorylation network have been shown to exist by [19], where a parametrization of the multistable region is provided for two steady states.

But, nothing could be said so far about existence of multiple steady states in general multisite phosphorylation networks. Thus, a distributive, sequential phosphorylation network with n phosphorylation sites is introduced as the standard phosphorylation network in this thesis. A polynomial and a coset condition are presented as prerequisites for existence of multistationarity. A theorem, together with a proof, is presented to solve the polynomial condition. To solve the coset condition for solutions of the polynomial condition, a lemma is given providing sign vectors. These sign vectors define, in a nutshell, the parametrization of the multistationarity region. Thus, if a sign vector can be given, pairs of steady states can be given as well. As these sign vectors can be found for any $n \geqslant 2$ for distributive, sequential phosphorylation networks of mass action kinetics, a parametrization for at least two steady states can be provided as well. Thus, multisite phosphorylation networks with n phosphorylation sites and a distributive, sequential mechanism indeed exhibit multistable states. A quantitative analysis of the parameter space reveals, that multiple steady states are not only a theoretical result, but can actually be found in biological relevant regions. One result of the sign vectors is, that the ratio of the steady state concentrations of the kinase-substrate complexes is always equal to the ratio of the steady state concentrations phosphatase-substrate complexes.

The distributive, sequential n-times phosphorylation network is extended by additional synthesis and degradation reactions for the enzymes and (phosphorylated) protein to cover a wider set of (bio-) chemical reaction networks. Here, the polynomial condition cannot simply be solved following the theorem for the former reaction network. Still, an algorithm is presented to solve the arising polynomial condition. It results in a system of a linear equation and a system of bilinear inequality. Existence of multistationarity is coupled to existence of sign vectors satisfying not only the polynomial and coset condition, as before, but also the bilinear inequalities. The algorithm is applicable to (bio-) chemical reaction networks, if mass action kinetics are endowed. The distributive, sequential phosphorylation mechanism

from above represents a special case of this algorithm, where no bilinear inequalities arise. For a double phosphorylation network including synthesis and degradation, these sign vectors, and thus, multistationarity, can be established, if either both enzymes or the kinase are preserved. If only the phosphatase is preserved, the unphosphorylated protein has to be synthesized and degradated for the network to exhibit multiple steady states. A parametrization for rate constants and steady states is provided. For larger reaction networks of $n > 2$ multistationarity cannot be established as the arising bilinear inequality set is not tractable.

In a further extension, a reaction network containing two distributive, sequential phosphorylation networks is coupled by two transport reactions. Applying the former algorithm yields a set of linear and bilinear inequalities. In general, it is possible to solve the linear inequalities. Furthermore, the bilinear inequalities are tractable. An explicit solution to the linear equalities and bilinear inequalities cannot be provided, due to the large number of parameters. A different approach is taken. Instead of trying to find sign vectors satisfying the polynomial and coset condition together with solutions for the nonlinear inequalities, the structure of the subnetworks, i. e., compartmentalization in two distributive, sequential phosphorylation networks, is used to provide results. Knowledge of multistationarity of the subnetwork structure can be used to establish multistationarity for certain parameter combinations of the overall reaction network. This approach is successful. It results in a partial parametrization for rate constants and steady states. Furthermore, simulations of the reaction network reveal not only a switch like response curves based on two steady states but also oscillations and limit cycles.

The work is rounded off, by a robustness analysis of the multistationarity region of the distributive, sequential phosphorylation network. Here, robustness is tested towards variation of the parameters. Random walks in parameter space are applied. Multisite phosphorylation networks show distinct results in this robustness analysis dependent on the sign vector: with rising size n the robustness increases up to four to six phosphorylation steps. Then it decreases with rising n.

Thus overall, multisite phosphorylation networks, considered here, are indeed able to generate multiple steady states in a (bio-) chemical reaction network. Furthermore, not only a bistable switch-like behavior can be seen, but also response curves including oscillations. Thus, already a very small network of a multisite phosphorylation can account for certain biological observations, like switching in networks or oscillations. It is thus not necessary to consider higher structures of different feedback loops or even larger setups in (bio-) chemical reaction networks to exhibit multiple steady states. This is quite interesting, as it not only answers questions, for example, whether switching in the cell cycle is already enabled by the underlying phosphorylation mechanism, but also rises new questions. For example, is the exact function and mechanism of the (bio-) chemical reaction network predefined, i. e., does the network structure already define network properties? Is the robustness of the network as well predefined by the size of the phosphorylation network? And if so, why are larger networks apparently more sensitive than smaller ones? And if that is actually the case, why do multisite phosphorylation networks with a high number of phosphorylation sites exist, if they tend to loose robustness for higher numbers of phosphorylation sites, when multistationarity can already be established for small n.

This thesis tries to provide biological interpretations of the solutions provided, where possible. These are discussed in more detail at the end of each of the four main chapters five to eight. Nonetheless, a biological interpretation of the arising sign vectors as a condition for multistationarity is still needed. Also, implications of arising nonlinear inequalities as restrictions on choosing parameters to generate extreme rays of the pointed polyhedral cone, i. e., the solution set where reaction rates in steady state live, cannot be given in a biological sense.

Besides these missing interpretations, this thesis leaves, of course, some open questions. First of all, finding a solution to the problem of the linear equality and nonlinear inequality set polynomial condition together with solutions to the coset condition for phosphorylation networks with compartmentalization should be possible, if either a different approach for the underlying solution algorithm in MATLAB is used, or if better hardware is used.

Furthermore, an expansion to regard also different network setups should be considered. For example, phosphorylation networks including a different number of enzymes would be of interest. And, though only a distributive, sequential reaction mechanism is considered, a random or mixed (random-sequential) mechanism might yield a reaction network, that exhibit multiple steady states. And, with the presented solution algorithm being applicable to (bio-) chemical reaction networks of mass action kinetics, different networks besides phosphorylation networks, should be considered.

Considering the results of the random walk together with the linear inequality set of chapter six, a different question arises. Pairs of steady states can be given in terms of the rate constants and three further variables, e. g., μ_{3n+2}, $\ln \frac{\nu_3}{\lambda_3}$ and $\ln \frac{\nu_6}{\lambda_6}$, compare equation (A.18), independent of the size of the phosphorylation network. It is possible to rewrite the system for any n in terms of three independent variables and all rate constants. Here, a reduced solution set could be considered. The approach so far considered all $3n + 3$ components for the steady state. With the large number of parameters, only the exit time of the random walk could be analyzed. Instead of using the parameter vector for robustness analysis, analysis based on changes the three independent variables, i. e., changing the ratio of a_{3n+2} to b_{3n+2}, λ_3, and λ_6, could be possible as well. This would reduce the number of parameters immensely, and thus, enable robustness analysis up to large n. Besides a reduction of the parameter space for robustness analysis, a completely different approach could be used. Following the work of S. Waldherr, robustness analysis could be done without using explicit parameters by confining the solution space to a region where multiple steady states still can be found based on uncertain parameters, i. e., the method provides a region without local bifurcations and thus, might restrict the region where multiple steady states exist indirectly.

Calvin: "When a kid grows up,
he has to be something.
He can't just stay the way he is.
But a tiger grows up and stays a tiger."
Tiger: "No room for improvement."

— Bill Watterson

A PROOFS AND FURTHER MATHEMATICAL ISSUES

A.1 NULLSPACE OF STOICHIOMETRIC MATRIX FOR STANDARD PHOSPHORYLATION

For a discussion on the nullspace of the stoichiometric matrix, see also [49]. As the stoichiometric matrix $N^{(n)}$ of higher phosphorylation steps can be written in terms of the stoichiometric matrix $N^{(1)}$ of a single phosphorylation step, the nullspace of $N^{(n)}$ can be given in a similar stepwise form. To derive this form, the nullspace of a single phosphorylation process will be considered first. The basis of the nullspace can be given by

$$E^{(1)} = \begin{bmatrix} 1 & 0 & 1 \\ 1 & 0 & 0 \\ 0 & 0 & 1 \\ 0 & 1 & 1 \\ 0 & 1 & 0 \\ 0 & 0 & 1 \end{bmatrix} = \begin{bmatrix} \epsilon_1 & \epsilon_2 & \epsilon_3 \end{bmatrix}. \tag{A.1}$$

The nullspace for higher phosphorylation steps is motivated by the following lemma.

Lemma A.1. *Given the stoichiometric matrix $N^{(n)}$ for the n-th phosphorylation step by equation (5.2) and $E = E^{(1)}$ for a single phosphorylation step by equation (A.1), the following can be stated.*

(i) The basis for the nullspace of $N^{(n)}$ can be given by

$$E^{(n)} = \begin{bmatrix} E & & 0 \\ & \ddots & \\ 0 & & E \end{bmatrix}. \tag{A.2}$$

(ii) The columns of $E^{(n)}$ are generators for $\ker(N^{(n)}) \cap \mathbb{R}^{6n}_{\geqslant 0}$.

(iii) The matrix $N^{(n)}$ is of rank $3n$.

Proof. (i) To show that $\left[E^{(n)}\right] \subseteq \ker(N^{(n)})$ and $\ker(N^{(n)}) \subseteq \left[E^{(n)}\right]$, it is sufficient to proof the condition for n_{11}, n_{12}, n_{21} and n_{22}, by splitting

the stoichiometric matrix $N^{(n)}$ in these elements according to equation (5.2). The nullspace of each element can then be given in terms of ϵ, see equation (A.1), and unit vectors as follows:

$$\ker(n_{11}) = \begin{bmatrix} 1 & 0 & 1 \\ 1 & 0 & 0 \\ 0 & 0 & 1 \\ 0 & 1 & 1 \\ 0 & 1 & 0 \\ 0 & 0 & 1 \end{bmatrix}, \qquad \ker(n_{12}) = \begin{bmatrix} 1 & 1 & 0 & 0 \\ 1 & 0 & 0 & 0 \\ 0 & 1 & 0 & 0 \\ 0 & 0 & 1 & 1 \\ 0 & 0 & 1 & 0 \\ 0 & 0 & 0 & 1 \end{bmatrix},$$

$$\ker(n_{21}) = \begin{bmatrix} 1 & 0 & 1 \\ 1 & 0 & 0 \\ 0 & 0 & 1 \\ 0 & 1 & 1 \\ 0 & 1 & 0 \\ 0 & 0 & 1 \end{bmatrix}, \qquad \ker(n_{22}) = \begin{bmatrix} 1 & 0 & 0 & 0 & 1 \\ 1 & 0 & 0 & 0 & 0 \\ 0 & 1 & 0 & 0 & 0 \\ 0 & 0 & 1 & 0 & 0 \\ 0 & 0 & 0 & 1 & 0 \\ 0 & 0 & 0 & 0 & 1 \end{bmatrix}.$$

with

$$\begin{aligned} \ker(n_{11}) &= \operatorname{span}\left\{ \begin{array}{ccc} \epsilon_1 & \epsilon_2 & \epsilon_3 \end{array} \right\}, \\ \ker(n_{12}) &= \operatorname{span}\left\{ \begin{array}{cccc} \epsilon_1 & \epsilon_2 & e_1 + e_3 & e_4 + e_6 \end{array} \right\}, \\ \ker(n_{21}) &= \operatorname{span}\left\{ \begin{array}{ccc} \epsilon_1 & \epsilon_2 & \epsilon_3 \end{array} \right\}, \\ \ker(n_{22}) &= \operatorname{span}\left\{ \begin{array}{ccccc} \epsilon_1 & e_3 & e_4 & e_5 & e_1 + e_6 \end{array} \right\}. \end{aligned}$$

For $\ker(n_{11}) = \ker(n_{21}) = \ker(N^{(1)})$ holds. Additionally,

$$n_{12}E = 0_{3\times 3} \qquad n_{22}E = 0_{3\times 3}.$$

hold as well with

$$\epsilon_2 = e_4 + e_5 \qquad \text{and} \qquad \epsilon_3 = e_1 + e_3 + e_4 + e_6.$$

(a.) The first condition $\left[E^{(n)}\right] \subseteq \ker(N^{(n)})$ can be satisfied by splitting the two matrices $N^{(n)}$ and $E^{(n)}$ in their elements n_{ij} and E:

$$N^{(n)}E^{(n)} = \begin{bmatrix} n_{11}E & n_{12}E & n_{12}E & \cdots & & n_{12}E \\ n_{21}E & n_{22}E & 0 & & & 0 \\ 0 & n_{21}E & n_{22}E & & & 0 \\ & & \ddots & \ddots & & \vdots \\ \vdots & & \ddots & & n_{22}E & 0 \\ & & & & n_{21}E & n_{22}E \\ 0 & & & & 0 & n_{21}E \end{bmatrix} = 0.$$

(b.) The second one, $\ker(N^{(n)}) \subseteq \left[E^{(n)}\right]$, has to hold as well. To show such, a vector η is introduced, with $\eta \in \ker(N^{(n)})$ and $\eta = \operatorname{col}\left[\begin{array}{ccc} \eta^{(1)} & \dots & \eta^{(n)} \end{array} \right]$, with $\eta^{(i)}$ column vectors of length

six. As $N^{(n)}$ can be rewritten in terms of n_{ij}, we can rewrite $N^{(n)}\eta = 0$ as follows:

$$\begin{aligned} n_{11}\eta^{(1)} + \sum_{i=2}^{n} n_{12}\eta^{(i)} &= 0, \\ n_{21}\eta^{(1)} + n_{22}\eta^{(2)} &= 0, \\ &\vdots \\ n_{21}\eta^{(n-1)} + n_{22}\eta^{(n)} &= 0, \\ n_{21}\eta^{(n)} &= 0. \end{aligned}$$

The last equation yields $\eta^{(n)} \in \ker(n_{21}) = [E] \subseteq \ker(n_{22})$. Consequently $\eta^{(n-1)} \in \ker(n_{21})$ holds as well for the penultimate equation. Substituting stepwise results in $\eta^{(n-2)} \in \ker(n_{21}), \ldots,$ $\eta^{(1)} \in \ker(n_{21})$ for the second equation. And so the first equation has to hold as well with $\ker(n_{11}) = [E]$ and $[E] \in \ker(n_{12})$. Therefore $\ker(N^{(n)}) \subseteq \left[E^{(n)}\right]$.

(ii) By definition, a vector ϵ is a generator of $\ker(N^{(n)}) \cap \mathbb{R}^{6n}_{\geqslant 0}$, if all of the following conditions hold:

$$\epsilon \geqslant 0 \tag{A.3}$$

$$N^{(n)}\epsilon = 0 \tag{A.4}$$

$$\begin{aligned} &\text{If } \epsilon_1 \text{ and } \epsilon_2 \text{ are generators for } \ker(N^{(n)}) \cap \mathbb{R}^{6n}_{\geqslant 0} \text{ and} \\ &\operatorname{supp}(\epsilon_1) \subseteq \operatorname{supp}(\epsilon_2) \text{ holds, then } \epsilon_1 = 0 \text{ or } \epsilon_1 = \alpha\epsilon_2 \\ &\text{has to hold as well, with } \alpha > 0. \end{aligned} \tag{A.5}$$

As the column vectors of E satisfy these three conditions, the columns of $E^{(n)}$ satisfy them as well. Since $E^{(n)}$ is a basis for $\ker(N^{(n)})$, every non negative linear combination of vectors η with $N^{(n)}\eta = 0$ are non negative linear combinations of columns of $E^{(n)}$. Therefore all generators of $\ker(N^{(n)}) \cap \mathbb{R}^{6n}_{\geqslant 0}$ are columns of $E^{(n)}$.

(iii) The matrix E is of rank three. As the matrix $E^{(n)}$ just consists of n matrices E on its main diagonal, its rank can be given by $3n$. Therefore $\operatorname{rank}(N^{(n)}) = 6n - 3n = 3n$.

■

A.2 NULLSPACE OF RATE EXPONENT MATRIX FOR STANDARD PHOSPHORYLATION

A basis for the nullspace U of the rate exponent matrix Y, see equation (5.10) is discussed in this section. For the single phosphorylation process this nullspace can easily be written down at a closer inspection of Y, see equation (5.10) on page 39: As some of the elements in Y just double and the remaining elements do not interfere, the nullspace of this matrix can be given by two vectors

$$u_1 = \begin{bmatrix} 0 & -1 & 1 & 0 & 0 & 0 \end{bmatrix}^T,$$

$$u_2 = \begin{bmatrix} 0 & 0 & 0 & 0 & -1 & 1 \end{bmatrix}^T.$$

With $Y^{(n)}$ described in terms of its predecessor matrices, recall:

$$Y^{(1)} = \begin{bmatrix} e_1+e_2 & e_4 & e_4 & e_3+e_5 & e_6 & e_6 \end{bmatrix},$$

$$Y^{(n)} = \left[\begin{array}{c|ccc} Y^{(n-1)} & e_1+e_{3n-1} & e_{3n+1} & e_{3n+1} \\ \mathbf{0}_{3\times 6(n-1)} & e_3+e_{3n+2} & e_{3n+3} & e_{3n+3} \end{array}\right],$$

compare this rewritten form of Y with entries in equation (5.10), those two vectors $u_{1,2}$ can be found for any n in a corresponding position by simply looking at submatrices. The vectors will therefore be called trivial nullspace vectors. For an arbitrary n these column vectors can be given for $i = 1, \dots, n$ by:

$$\begin{aligned} u_1^{(i)} &= -e_{6i-4} + e_{6i-3}, \\ u_2^{(i)} &= -e_{6i-1} + e_{6i}. \end{aligned} \tag{A.6}$$

Thus, each new phosphorylation step introduces two additional trivial nullspace vectors. Checking for further nullspace vectors for higher phosphorylation steps yields for $n = 3$ and $Y^{(3)} \in \mathbb{R}^{12\times 18}$

$$Y^{(3)} = \begin{bmatrix} e_1+e_2 & e_4 & e_4 & e_3+e_5 & e_6 & e_6 \\ e_1+e_5 & e_7 & e_7 & e_3+e_8 & e_9 & e_9 \\ e_1+e_8 & e_{10} & e_{10} & e_3+e_{11} & e_{12} & e_{12} \end{bmatrix}$$

another nullspace vector:

$$u_3^{(3)} = e_4 - e_7 - e_{10} + e_{13}.$$

It is possible to derive this additional vector again for every phosphorylation step $n \geqslant 3$ by taking a closer inspection of the rate exponent matrix. A description of this vector for higher phosphorylation processes with $i = 3, \dots, n$ can be given by:

$$u_3^{(i)} = e_4 - e_7 - e_{6i-8} + e_{6i-5}. \tag{A.7}$$

Thus, one additional nullspace vector per phosphorylation step n for $n \geqslant 3$ can be found. As these vectors $u_3^{(i)}$ are found by a closer inspection of the matrix Y, they are called non-trivial nullspace vectors. No further vectors can be found for any given n, see also the argument at the end of this section. A basis for the nullspace U of the rate exponent matrix Y contains $2n$ trivial vectors for $n \geqslant 1$ and for $n \geqslant 3$ additionally $n-2$ non-trivial vectors and can be given by:

$$U^{(1)} = \begin{bmatrix} -e_2+e_3 & -e_5+e_6 \end{bmatrix} \tag{A.8}$$

$$U^{(2)} = \left[\begin{array}{c|cc} U^{(1)} & -e_8+e_9 & -e_{11}+e_{12} \\ 0_{6\times 2} & & \end{array}\right] \tag{A.9}$$

$$\begin{aligned} U^{(n)} = \Bigg[\begin{array}{c|cc} U^{(n-1)} & -e_{6n-4}+e_{6n-3} & -e_{6n-1}+e_{6n} \\ 0_{6\times 3n-5} & & \end{array} \\ e_4 - e_7 - e_{6n-8} + e_{6n-5}\Bigg] \end{aligned} \tag{A.10}$$

Thus, the size can be given by $U \in \mathbb{R}^{6\times 2}$ for $n = 1$ and by $U \in \mathbb{R}^{6n\times 3n-2}$ for $n \geqslant 2$.

It remains to be shown, that the basis of the right nullspace of Y is truly given by the $3n-2$ vectors above collected in U. This is done via complete induction by an inspection of the left kernel of Y. The basis of the left kernel is denoted by a matrix $u_l \in \mathbb{R}^{2\times 6}$ for $n = 1$ and by a vector $u_l \in \mathbb{R}^{1\times 3n+3}$ for $n \geqslant 2$:

$$\begin{aligned} u_l^{(1)} &= [-e_1 + e_2,\ -e_3 + e_5] \\ u_l^{(2)} &= [e_1 - e_2 + e_3 - e_5 - e_8] \\ u_l^{(n\geqslant 3)} &= \left[u_l^{(n-1)} - e_{3n+2}\right] = \left[e_1 + e_3 - \sum_1^{n+1} e_{3i-1}\right]. \end{aligned}$$

It can easily be shown that $u_l^{(1)}$ as well as $u_l^{(2)}$ are indeed basis vectors for the left nullspace of matrix $Y(1,2)$, where dimensions of this nullspace is still easily manageable and thus are computable even by hand. Complete induction is used to show that $u_l^{(n\geqslant 3)}$ holds as well for arbitrary $n \geqslant 3$. Recall the former introduced notation for Y, a rewritten form of equation (5.10):

$$Y^{(n)} = \left[\begin{array}{c|ccc} Y^{(n-1)} & e_1 + e_{3n-1} & e_{3n+1} & e_{3n+1} \\ 0_{3\times 6n} & e_3 + e_{3n+2} & e_{3n+3} & e_{3n+3} \end{array}\right].$$

The problem $u_l^{(n)} Y^{(n)}$ is now solved recursively. The first step is given by $u_l^{(2)} Y^{(2)} = \underline{0}_{12}$. Due to the nature of prolonging u_l:

$$u_l^{(n)} Y^{(n)} = \underline{0}_{6n}$$

holds as well, compare elements of $Y^{(n)}$ and $u_l^{(n)}$. Thus for phosphorylation networks of size $n+1$:

$$\begin{aligned} u_l^{(n+1)} &= \left[e_1 + e_3 - \sum_1^{n+1} e_{3i-1}\right] \\ Y^{(n+1)} &= \left[\begin{array}{c|ccc} Y^{(n)} & e_1 + e_{3n+2} & e_{3n+4} & e_{3n+4} \\ 0_{3\times 6(n-1)} & e_3 + e_{3n+5} & e_{3n+6} & e_{3n+6} \end{array}\right]. \end{aligned}$$

This step can be done by a blockwise division of $Y^{(n+1)}$ into three parts: the part of the previous step n in the upper left corner, a block of zeros, in the lower left corner, and a fairly large matrix of six columns on the right hand side (given in this notation by the single line of (sums of) unit vectors e_i). Analyzing individual parts of the rate exponent matrix, the first two blocks (counterclockwise starting at the upper left corner) reduce to:

$$u_l^{(n)} Y^{(n)} + [\ 0\ \ -1\ \ 0]\ 0_{3\times 6n} = \underline{0}_{6n}.$$

This follows stepwise for all n down to $n = 2$. The remaining new part appearing for $n+1$ in the third block has to be analyzed in detail:

$$\begin{aligned}
&\left[\; e_1 + e_3 - \sum_1^{n+2} e_{3i-1} \;\right] \times \left[\; e_1 + e_{3n+2} \quad e_{3n+4} \quad e_{3n+4} \right. \\
&\left. \quad e_3 + e_{3n+5} \quad e_{3n+6} \quad e_{3n+6} \;\right] \\
&= \left[\; e_1 + e_3 - \sum_1^{n} e_{3i-1} - \left(e_{3(n+1)-1} + e_{3(n+2)-1}\right) \;\right] \times \\
&\quad \left[\; e_1 + e_{3n+2} \quad e_{3n+4} \quad e_{3n+4} \quad e_3 + e_{3n+5} \quad e_{3n+6} \quad e_{3n+6} \;\right] \\
&= \left[\; (e_1 - e_{3n+2})^T (e_1 + e_{3n+2}) \quad 0 \quad 0 \quad (e_3 - e_{3n+5})^T (e_3 + e_{3n+5}) \right. \\
&\qquad \left. 0 \quad 0 \;\right] \\
&= \left[\; e_1^T e_1 - e_{3n+2}^T e_{3n+2} \quad 0 \quad 0 \quad e_3^T e_3 - e_{3n+5}^T e_{3n+5} \quad 0 \quad 0 \;\right] \\
&= \left[\; 1-1 \quad 0 \quad 0 \quad 1-1 \quad 0 \quad 0 \;\right] = \underline{0}_6
\end{aligned}$$

Thus recombining these three blocks again, the total system indeed reduces to

$$u_l^{(n+1)} Y^{(n+1)} = \left[\; \underline{0}_{6n} \quad \underline{0}_6 \;\right] = \underline{0}_{6n+6}.$$

As this expression is true for $n = 2$, for n as well as $n+1$, $u_l^{(n)}$ is a basis for the left nullspace of Y yielding $\operatorname{rank}(Y) = 3n+2$ for $n \geqslant 2$. Thus, the right kernel of Y is of dimension $6n \times 3n-2$ for $n \geqslant 2$ yielding U as a basis for the right nullspace of the rate exponent matrix Y.

A.3 SOLVABILITY FOR THE POLYNOMIAL CONDITION

For a proof of the Theorem 5.2 and the argument in section 5.2 on page 39 the following has to be shown, see also [P1]:

$$(A) \to (D) \to (C) \to (B) \to (A) \tag{A.11}$$

To do so, the following matrix is defined:

$$A := \left[\begin{array}{ccc|ccc|ccc|c|ccc} 1 & 0 & 0 & 1 & 1 & 1 & 2 & 2 & 2 & \dots & n & n & n \\ 1 & 0 & 1 & 1 & 0 & 1 & 1 & 0 & 1 & \dots & 1 & 0 & 1 \\ 0 & 1 & 0 & 1 & 1 & 1 & 1 & 1 & 1 & \dots & 1 & 1 & 1 \end{array}\right], \tag{A.12}$$

where A can be computed using M via A^T by the column operations: $(2)+(3)$, $(1)+(2)+(3)$, $(1)+(2)+2\,(3)$, see Theorem 4.3 in [81], where columns of A correspond to the exponents of t_1, t_2, t_3 in the statement of the theorem. The matrix itself is displayed in the corresponding proof in [81]. Furthermore define

$$Q := \begin{bmatrix} n & 0 & 1 \\ 1 & 1 & 1 \\ 2 & 1 & 1 \end{bmatrix}. \tag{A.13}$$

Furthermore, recall definitions in section 5.2.1 for M, ξ the and Π on page 40. With these matrices defined the Theorem 5.2 on page 42 can be proven:

Proof. For reference, see also the proof in [P1].

(A) → (D): For nonsingular Q the following holds:

$$A^T = M^{(n)} Q \tag{A.14}$$

implying $\operatorname{im}\left(M^{(n)}\right) = \operatorname{im}\left(A^T\right)$ with $\mu := \ln b - \ln a$.

(D) → (C): In a first step, $Y^{(n)^T} M^{(n)} = \Pi^{(n)}$ is shown. Recall the stepwise definition of $Y^{(n)^T}$ in equation (5.11) on page 39. Define

$$Y(i) := \begin{bmatrix} e_1 + e_{3i-1} & e_{3i+1} & e_{3i+1} & e_3 + e_{3i+2} & e_{3i+3} & e_{3i+3}, \end{bmatrix}$$

then

$$\begin{aligned} Y_0^{(i)^T} \begin{bmatrix} M(0,n) \\ \vdots \\ M(i,n) \end{bmatrix} &= \begin{bmatrix} \underline{0} & (-i+2)\underline{1} & (i-1)\underline{1} \end{bmatrix} \\ &=: P(i) \in \mathbb{R}^{6\times 3}, \end{aligned} \tag{A.15}$$

where $\underline{1}$ is used to denote a vector of length six filled with ones and, accordingly, $\underline{0}$ to denote a vector of length six filled with zeros. Thus,

$$Y^{(n)^T} M^{(n)} = \begin{bmatrix} P(1) \\ \vdots \\ P(n) \end{bmatrix} \tag{A.16}$$

Recall equation (5.22) for Π and $\xi \in \mathbb{R}^2$ on page 41 and note

$$P(i) \begin{pmatrix} * \\ \xi_1 \\ \xi_2 \end{pmatrix} = \begin{bmatrix} (-i+2)\underline{1} & (i-1)\underline{1} \end{bmatrix} \begin{pmatrix} \xi_1 \\ \xi_2 \end{pmatrix} = \Pi(i) \begin{pmatrix} \xi_1 \\ \xi_2 \end{pmatrix} \tag{A.17}$$

Thus, any nonzero $\mu \in \operatorname{im}(M^{(n)})$

$$\mu = M^{(n)} \begin{pmatrix} * \\ \xi_1 \\ \xi_2 \end{pmatrix} \tag{A.18}$$

yields

$$\begin{aligned} Y^{(n)^T} M^{(n)} \begin{pmatrix} * \\ \xi_1 \\ \xi_2 \end{pmatrix} &= \begin{bmatrix} \Pi_0(1) \\ \vdots \\ \Pi_0(n) \end{bmatrix} \begin{pmatrix} \xi_1 \\ \xi_2 \end{pmatrix} \\ &= \Pi^{(n)} \xi. \end{aligned} \tag{A.19}$$

Recall ν and λ from (5.28a) and (5.28b)–(5.28d). The vector ξ together with any positive λ can be used to compute ν as in (5.28b)–(5.28d). Hence (D) ⇒ (C).

(C) → (B): Let $\mu \in \mathbb{R}^{3n+3}$ with $\mu \neq 0$ and $\xi \in \mathbb{R}^2$ be given, such that (5.27) holds. Further let ν and λ be given satisfying (5.28a) and (5.28b)–(5.28d), that is $\lambda \in \mathbb{R}^{3n}$ and for $i = 1, \ldots, n$

$$\nu_{3i} = \lambda_{3i}\, e^{(2-i)\xi_1 + (i-1)\xi_2}, \tag{A.20a}$$

$$\nu_{3i-1} = \lambda_{3i-1}\, \frac{\nu_{3i}}{\lambda_{3i}} \tag{A.20b}$$

$$\nu_{3i-2} = \lambda_{3i-2}\, \frac{\nu_{3i}}{\lambda_{3i}}. \tag{A.20c}$$

These ν, λ satisfy

$$\ln \frac{\nu_{3i-2}}{\lambda_{3i-2}} = \ln \frac{\nu_{3i-1}}{\lambda_{3i-1}} = \ln \frac{\nu_{3i}}{\lambda_{3i}} = (2-i)\,\xi_1 + (i-1)\xi_2 \tag{A.21}$$

and thus

$$\ln \frac{\nu_{3i-2} + \nu_{3i}}{\lambda_{3i-2} + \lambda_{3i}} = \ln \frac{\nu_{3i}}{\lambda_{3i}} \tag{A.22a}$$

$$\ln \frac{\nu_{3i-1} + \nu_{3i}}{\lambda_{3i-1} + \lambda_{3i}} = \ln \frac{\nu_{3i}}{\lambda_{3i}}. \tag{A.22b}$$

Define

$$\nu_{(i)} := (\nu_{3i-2}, \nu_{3i-1}, \nu_{3i}) \tag{A.23a}$$

$$\lambda_{(i)} := (\lambda_{3i-2}, \lambda_{3i-1}, \lambda_{3i}) \tag{A.23b}$$

with

$$\nu = \operatorname{col}\left(\nu_{(1)}, \ldots, \nu_{(n)}\right) \tag{A.24a}$$

$$\lambda = \operatorname{col}\left(\lambda_{(1)}, \ldots, \lambda_{(n)}\right). \tag{A.24b}$$

Recall the matrices $E^{(n)}$ and E from (5.6) and (5.5) respectively. Note that

$$\ln \frac{E^{(n)}\,\nu}{E^{(n)}\,\lambda} = \left(\ln \frac{E\,\nu_{(1)}}{E\,\lambda_{(1)}}, \ldots, \ln \frac{E\,\nu_{(n)}}{E\,\lambda_{(n)}}\right)$$

and

$$\ln \frac{E\,\nu_{(i)}}{E\,\lambda_{(i)}} = \left(\ln \frac{\nu_{3i-2} + \nu_{3i}}{\lambda_{3i-2} + \lambda_{3i}}, \ln \frac{\nu_{3i-2}}{\lambda_{3i_2}}, \ln \frac{\nu_{3i}}{\lambda_{3i}}, \ln \frac{\nu_{3i-1} + \nu_{3i}}{\lambda_{3i-1} + \lambda_{3i}}, \ln \frac{\nu_{3i-1}}{\lambda_{3i-1}}, \ln \frac{\nu_{3i}}{\lambda_{3i}}\right).$$

Hence the following holds for ν and λ

$$\ln \frac{E\,\nu_{(i)}}{E\,\lambda_{(i)}} = \begin{bmatrix} (2-i)\underline{1} & (i-1)\underline{1} \end{bmatrix} \begin{pmatrix} \xi_1 \\ \xi_2 \end{pmatrix}$$

and

$$\ln \frac{E^{(n)}\,\nu}{E^{(n)}\,\lambda} = \Pi^{(n)}\,\xi.$$

Consequently, if there exist vectors $\mu \in \mathbb{R}^{3n+3}$, $\mu \neq 0$ and $\xi \in \mathbb{R}^2$ satisfying (5.27) and vectors ν, λ satisfying (5.28a), (5.28b)–(5.28d), then μ, ν and λ also satisfy (5.20). Note that ν and λ satisfying (5.28a) and (5.28b)–(5.28d) are positive. Thus, (C) ⇒ (B).

(B) → (A): Finally, assume $\mu \in \mathbb{R}^{3n+3}$ with $\mu \neq 0$ and $\nu, \lambda \in \mathbb{R}^{3n}$ satisfy (5.20). For a fixed $a \in \mathbb{R}^{3n+3}$ define

$$b := \operatorname{diag}(e^{\mu})\, a$$
$$k := \operatorname{diag}\left(\Phi^{(n)}\left(a^{-1}\right)\right) E^{(n)} \lambda.$$

Then

$$\begin{aligned} N^{(n)} \operatorname{diag}(k)\, \Phi^{(n)}(a) &= N^{(n)} \operatorname{diag}\left(\Phi^{(n)}\left(a^{-1}\right)\right) \operatorname{diag}\left(E^{(n)} \lambda\right)\, \Phi^{(n)}(a) \\ &= N^{(n)} E^{(n)} \lambda = 0 \end{aligned}$$

and with equation (5.20)

$$\begin{aligned} N^{(n)} \operatorname{diag}(k)\, \Phi^{(n)}(b) &= N^{(n)} \operatorname{diag}(k) \operatorname{diag}\left(\Phi^{(n)}(a)\right)\, e^{Y^{(n)^T} \mu} \\ &= N^{(n)} E^{(n)} \nu = 0 \end{aligned} \tag{A.25}$$

and thus (B) ⇒ (A).

■

A.4 FEASIBILITY OF SIGN VECTORS FOR STANDARD PHOSPHORYLATION

For a proof of the feasibility of the sign pattern, see also [P1].

Proof. First, the necessity of the sign patterns ($5.\Delta_b$) is shown. Therefore the range of the regular matrix $M(0, n)$ from equation (5.24) is parametrized by

$$w(0) := \begin{bmatrix} y \\ x \\ y - z \end{bmatrix} = \begin{bmatrix} -1 & -n+1 & n \\ 1 & n & -n \\ -1 & -n+2 & n-1 \end{bmatrix} \begin{bmatrix} x + nz \\ x + y \\ x + y + z \end{bmatrix}. \tag{A.26}$$

Thus, one has for $M(i, n)$, $i = 1, \ldots, n$, from eq. (5.25)

$$w(i) = \begin{bmatrix} w_1(i) \\ w_2(i) \\ w_3(i) \end{bmatrix} := \begin{bmatrix} x + iz + y - z \\ x + iz \\ x + iz + y - z \end{bmatrix} = \begin{bmatrix} 0 & -i+2 & i-1 \\ 1 & n-i & -n+i \\ 0 & -i+2 & i-1 \end{bmatrix} \begin{bmatrix} x + nz \\ x + y \\ x + y + z \end{bmatrix}. \tag{A.27}$$

Note that components $w_2(i)$ and $w_1(i) = w_3(i) = w_2(i) + (y - z)$ are affine functions of i, thus sign changes can be easily read off.

Next, necessary conditions for $\operatorname{sgn}(w(0))$ being one of the four sign patterns δ_1, δ_2, δ_4 and δ_7 from (5.40a)–(5.40d) are derived, under the side condition that system (5.43) is not unfeasible. Note, these four sign patterns represent all eight possible sign patterns, as the other half can be easily generated by sign inversion of the first half as they still agree with equations (5.43) and (5.44) with $W(-s) = 0$ and $\operatorname{sgn}(M^{(n)}(-\xi) = -\delta^{(n)}$, respectively.

Indices i_k and j_k given here, will always be $\geqslant 1$.

Regarding the single sign pattern:

1. $\operatorname{sgn}(w(0)) = \delta_1$, i. e., $y > 0$, $x > 0$, $y - z > 0$:
   For $z \geqslant 0$, the components of all the $w(i)$ are of the same sign. By item (1) of Lemma 5.9, $z \geqslant 0$ cannot lead to a feasible sign pattern. For $z < 0$, the $w(i)$ may generate the sign pattern matrices

   $$(\delta_1, [\delta_2]_{i_1}, [\delta_3]_{i_2}), \quad (\delta_1, [\delta_1]_{j_1}, [\delta_2]_{j_2}, [\delta_3]_{j_3})$$

   with $i_1 + i_2 = n$ and $j_1 + j_2 + j_3 = n$ where the δ_3 entries are necessary (otherwise the first rows do not offer a sign change). The direct passage from δ_1 to δ_3 is obviously impossible since $w_2(i) > 0$ implies $w_1(i+1) = w_2(i) + y \geqslant w_2(i) > 0$.

2. $\operatorname{sgn}(w(0)) = \delta_2$, i. e., $y > 0$, $x < 0$, $y - z > 0$:
   For $z \leqslant 0$, the w_{2i} are all negative so that one has $\delta_{20} = \delta_{21} = \cdots = \delta_{2n} = -1$ and $\delta_{10} = \delta_{30} = 1$. By item (3) of Lemma 5.9, $z \leqslant 0$ cannot lead to a feasible sign pattern. For $z > 0$ the possible sign pattern matrices are

   $$(\delta_2, [\delta_3]_{i_1}, [\delta_1]_{i_2}), \quad (\delta_2, [\delta_3]_{j_1}, [\delta_2]_{j_2}, [\delta_1]_{j_3})$$

   for $i_1 + i_2 = n$ and $j_1 + j_2 + j_3 = n$ where the δ_1 entries are necessary by item (3) of Lemma 5.9. Note, the sign pattern $(\delta_2, [\delta_1]_n)$ is unfeasible by item (1) of Lemma 5.9.

3. $\operatorname{sgn}(w(0)) = \delta_4$, i. e., $x < 0$, $0 < y < z$:
   At first, possible sign pattern matrices are

   $$(\delta_4, [\delta_3]_{i_1}, [\delta_1]_{i_2}), \quad (\delta_4, [\delta_5]_{i_1}, [\delta_1]_{i_2}), \quad (\delta_4, [\delta_3]_{j_1}, [\delta_5]_{j_2}, [\delta_1]_{j_3})$$

   for $i_1 + i_2 = n$ and $j_1 + j_2 + j_3 = n$ where the δ_1 entries are necessary by item (2) of Lemma 5.9. Note, the sign pattern $(\delta_4, [\delta_1]_n)$ is unfeasible by item (1) of Lemma 5.9. And note, δ_5 can appear just once because of $w_{1,i+1} = w_{2i} + y \geqslant w_{2i}$.

4. $\operatorname{sgn}(w(0)) = \delta_7$, i. e., $x > 0$, $0 < y < z$:
   Because of $z > 0$, the components w_{1i} are positive for $i = 0, \ldots, n$. By item (1) of Lemma 5.9, δ_7 cannot lead to a feasible sign pattern.

Next, the sufficiency of the sign patterns in equation (5.Δ_b) is discussed, by proving that they are realizable. Thus, a vector for each (δ_k), $k \in \{1, \ldots, 7\}$ is presented by

$$\xi = \operatorname{col}(x, x+y, x+y+z) \in \mathbb{R}^3 \tag{A.28}$$

leading to the sign pattern (δ_k) for $M(i,n)\xi$:

$$\begin{array}{llll}
\text{For } (\delta_1): & x = -n + \frac{1}{4}, & y = n + i_1 - \frac{3}{4}, & z = -1\,. \\
\text{For } (\delta_2): & x = i_2 - \frac{3}{4}, & y = -n + \frac{5}{4}, & z = +1\,. \\
\text{For } (\delta_3): & x = n - \frac{3}{4}, & y = -n + \frac{1}{4}, & z = +1\,. \\
\text{For } (\delta_4): & x = i_2 - \frac{1}{4}, & y = -n + \frac{3}{4}, & z = +1\,. \\
\text{For } (\delta_5): & x = -i_2 - i_3 + \frac{1}{4}, & y = n + i_2 - \frac{3}{4}, & z = -1\,. \\
\text{For } (\delta_6): & x = i_3 - \frac{3}{4}, & y = -n + i_2 + \frac{5}{4}, & z = +1\,. \\
\text{For } (\delta_7): & x = i_2 + \frac{1}{4}, & y = -n + \frac{1}{4}, & z = +1\,.
\end{array} \tag{A.29}$$

■

A.5 RESTRICTIONS ON CHOOSING SIGN VECTORS FOR SYSTEMS WITH COMPARTMENTALIZATION

Restrictions on choosing sign vectors for a double phosphorylation network including compartmentalization describing phosphorylation of the protein *NFAT*, see chapter 7 on page 95, appear. These restriction, following the algorithm described in [18] and in section 7.2.2 on page 105, can be stated as follows:

$$\mu_{C,2} = \mu_{N,8}$$
$$k_{T,2} = \frac{x_{C,2}}{x_{N,8}} k_{T,1}$$

As the vector μ is computed via linear combinations of the rays, α, in $E^{\mathcal{M}}$, the condition in μ can be transformed into a condition in α as $\mu = E^{\mathcal{M}}\,\alpha$. For $\delta_1^{(2)}$ computation is given in detail and results are provided for remaining δ for $n = 2$:

$$E_C^{\mathcal{M},(2)} = \begin{bmatrix} 1 & 0 & 0 \\ 0 & 1 & 0 \\ 2 & 1 & 1 \\ 1 & 1 & 0 \\ -1 & 0 & -1 \\ 1 & 1 & 0 \\ 0 & 0 & -1 \\ -2 & -1 & -2 \\ 0 & 0 & -1 \end{bmatrix}, \qquad E_N^{\mathcal{M},(2)} = \begin{bmatrix} -1 & 0 & 0 \\ 0 & -1 & 0 \\ -2 & -1 & -1 \\ -1 & -1 & 0 \\ 1 & 0 & 1 \\ -1 & -1 & 0 \\ 0 & 0 & 1 \\ 2 & 1 & 2 \\ 0 & 0 & 1 \end{bmatrix}$$

and thus

$$\mu_C = E_C^{\mathcal{M},(2)}\,\alpha_C, \qquad \mu_N = E_N^{\mathcal{M},(2)}\,\alpha_N$$

If $\mu_{N,8} = \mu_{C,2}$ has to hold $\alpha_{C,2} = 2\alpha_{N,1} + \alpha_{N,2} + 2\alpha_{N,3}$ has to hold as well. Thus

$$\alpha_{N,3} = \frac{1}{2}\alpha_{C,2} - \alpha_{N,1} - \frac{1}{2}\alpha_{N,2}.$$

But remaining rows in $E^{\mathcal{M}}$ have to be considered as well, as they restrict α further. Considering as well

$$\begin{aligned} \mu_{N,3} &= -2\alpha_{N,1} - \alpha_{N,2} - \frac{1}{2}\alpha_{C,2} + \alpha_{N,1} + \frac{1}{2}\alpha_{N,2} \\ &\overset{!}{<} 0 \text{ with } \operatorname{sgn}(\mu_{N,3}) = -1 \\ \mu_{N,5} &= \alpha_{N,1} + \frac{1}{2}\alpha_{C,2} - \alpha_{N,1} - \frac{1}{2}\alpha_{N,2} \\ &\overset{!}{>} 0 \text{ with } \operatorname{sgn}(\mu_{N,5}) = 1 \\ \mu_{N,7} &= \mu_{N,9} = \frac{1}{2}\alpha_{C,2} - \alpha_{N,1} - \frac{1}{2}\alpha_{N,2} \\ &\overset{!}{>} 0 \text{ with } \operatorname{sgn}(\mu_{N,7}) = \operatorname{sgn}(\mu_{N,9}) = 1 \end{aligned}$$

yields for $\alpha_i > 0$

$$\begin{aligned} &\alpha_{C,2} > \alpha_{N,2}, \\ &\frac{1}{2}\alpha_{C,2} > \alpha_{N,1} + \frac{1}{2}\alpha_{N,2}. \end{aligned}$$

The same computation can be done for the remaining six δ and yields:

$$
\begin{aligned}
\delta_2: \quad & \alpha_{N,3} = 2\alpha_{C,1} + 2\alpha_{C,2} + \alpha_{C,3} \\
& \alpha > 0 \\
\delta_3: \quad & \alpha_{N,3} = 2\alpha_{C,2} + \alpha_{C,3} \\
& \alpha > 0 \\
& a_3 > 0 \\
\delta_4: \quad & 2\alpha_{N,2} < \alpha_{C,1} + \alpha_{C,3} \\
& 2\alpha_{N,2} < \alpha_{C,1} + \alpha_{C,3} - \alpha_{N,1} \\
& \alpha_{N,3} = -\alpha_{C,1} - \alpha_{C,3} - 2\alpha_{N,2} - \alpha_{N,1} \\
& \alpha > 0 \\
\delta_5: \quad & \alpha_{N,1} < \alpha_{C,1} + \alpha_{C,3} \\
& \alpha_{N,3} = -\alpha_{C,1} - \alpha_{C,3} - \alpha_{N,1} \\
& \alpha > 0 \\
& a_5 > 0 \\
\delta_6: \quad & \alpha_{N,1} < \alpha_{C,1} + 2\alpha_{C,2} + 3\alpha_{C,3} \\
& \alpha_{N,3} = \alpha_{C,1} + 2\alpha_{C,2} + \alpha_{C,3} - \alpha_{N,1} \\
& \alpha > 0 \\
\delta_7: \quad & \alpha_{C,3} > 2\alpha_{N,2} \\
& \alpha_{N,3} = \alpha_{C,3} - 2\alpha_{N,2} \\
& \alpha > 0 \\
& a_1 > 0
\end{aligned}
$$

Results for larger values in n can be computed in a similar way.

"Sometimes", said Pooh,
"the smallest things take up
the most room in your heart."

— Alan Alexander Milne

B

SOME MORE MATRICES AND SOLUTIONS

B.1 CONES OF STANDARD MULTISITE PHOSPHORYLATION

Here, a selected overview on $E^{\mathcal{M}}$ and $E^{\mathcal{S}}$ for $\delta^{(n)}$ is given with $n = 2, \ldots, 14$ and $n = 2, \ldots, 5$, respectively, for δ of (5.Δ_b2) with $i_1 = 1$ and $i_2 = n - 1$ as indicated by the subscript δ_2. Note, $E^{\mathcal{M}}$ is given up to fourteen phosphorylation steps n, where only the $3n + 3$ rows represent the respective rows for the n-th step:

$$E^{\mathcal{M}}_{\delta_2} = \begin{bmatrix}
2 & 1 & 1 \\ -2 & -2 & -1 \\ 1 & 0 & 0 \\ 0 & -1 & 0 \\ -1 & -1 & 0 \\ 0 & -1 & 0 \\ 1 & 0 & 1 \\ 0 & 0 & 1 \\ 1 & 0 & 1 \\ 2 & 1 & 2 \\ 1 & 1 & 2 \\ 2 & 1 & 2 \\ 3 & 2 & 3 \\ 2 & 2 & 3 \\ 3 & 2 & 3 \\ 4 & 3 & 4 \\ 3 & 3 & 4 \\ 4 & 3 & 4 \\ 5 & 4 & 5 \\ 4 & 4 & 5 \\ 5 & 4 & 5 \\ 6 & 5 & 6 \\ 5 & 5 & 6 \\ 6 & 5 & 6 \\ 7 & 6 & 7 \\ 6 & 6 & 7 \\ 7 & 6 & 7 \\ 8 & 7 & 8 \\ 7 & 7 & 8 \\ 8 & 7 & 8 \\ 9 & 8 & 9 \\ 8 & 8 & 9 \\ 9 & 8 & 9 \\ 10 & 9 & 10 \\ 9 & 9 & 10 \\ 10 & 9 & 10 \\ 11 & 10 & 11 \\ 10 & 10 & 11 \\ 11 & 10 & 11 \\ 12 & 11 & 12 \\ 11 & 11 & 12 \\ 12 & 11 & 12 \\ 13 & 12 & 13 \\ 12 & 12 & 13 \\ 13 & 12 & 13
\end{bmatrix} \tag{B.1}$$

$$E^{S}_{\delta_2^{(2)}} = \begin{bmatrix} 1 & 0 & 0 & 0 & 0 & 0 \\ 0 & -1 & 0 & 0 & 0 & 0 \\ 0 & 0 & 1 & 0 & 0 & 0 \\ -1 & 0 & 0 & 0 & -1 & 0 \\ 0 & 0 & 0 & -1 & 0 & 0 \\ 0 & 0 & -1 & 0 & 0 & -1 \\ 0 & 0 & 0 & 0 & 1 & 0 \\ 1 & 1 & 1 & 1 & 0 & 0 \\ 0 & 0 & 0 & 0 & 0 & 1 \end{bmatrix} \quad E^{S}_{\delta_2^{(3)}} = \begin{bmatrix} 0 & 0 & 0 & 0 & 1 & 0 & 0 & 0 & 1 & 0 & 0 & 0 \\ 0 & 0 & 0 & 0 & 0 & -1 & 0 & 0 & 0 & -1 & 0 & 0 \\ 0 & 0 & 0 & 0 & 0 & 0 & 1 & 0 & 0 & 0 & 1 & 0 \\ -1 & 0 & -1 & 0 & -1 & 0 & 0 & 0 & -1 & 0 & 0 & 0 \\ 0 & 0 & 0 & 0 & 0 & 0 & 0 & -1 & 0 & 0 & 0 & -1 \\ 0 & -1 & 0 & -1 & 0 & 0 & -1 & 0 & 0 & 0 & -1 & 0 \\ 1 & 0 & 0 & 0 & 0 & 0 & 0 & 0 & 0 & 0 & 0 & 0 \\ 0 & 0 & 0 & 0 & 0 & 0 & 0 & 0 & 1 & 1 & 1 & 1 \\ 0 & 1 & 0 & 0 & 0 & 0 & 0 & 0 & 0 & 0 & 0 & 0 \\ 0 & 0 & 1 & 0 & 0 & 0 & 0 & 0 & 0 & 0 & 0 & 0 \\ 0 & 0 & 0 & 0 & 1 & 1 & 1 & 1 & 0 & 0 & 0 & 0 \\ 0 & 0 & 0 & 1 & 0 & 0 & 0 & 0 & 0 & 0 & 0 & 0 \end{bmatrix}$$

$$E^{S}_{\delta_2^{(4)}} = \begin{bmatrix} 0 & 0 & 0 & 0 & 0 & 0 & 1 & 0 & 0 & 0 & 1 & 1 & 0 & 0 & 0 & 0 & 0 & 0 \\ 0 & 0 & 0 & 0 & 0 & 0 & 0 & -1 & 0 & 0 & 0 & 0 & -1 & -1 & 0 & 0 & 0 & 0 \\ 0 & 0 & 0 & 0 & 0 & 0 & 0 & 0 & 1 & 0 & 0 & 0 & 0 & 0 & 1 & 1 & 0 & 0 \\ -1 & 0 & -1 & 0 & -1 & 0 & -1 & 0 & 0 & 0 & -1 & -1 & 0 & 0 & 0 & 0 & 0 & 0 \\ 0 & 0 & 0 & 0 & 0 & 0 & 0 & 0 & 0 & -1 & 0 & 0 & 0 & 0 & 0 & 0 & -1 & -1 \\ 0 & -1 & 0 & -1 & 0 & -1 & 0 & 0 & -1 & 0 & 0 & 0 & 0 & 0 & -1 & -1 & 0 & 0 \\ 1 & 0 & 0 & 0 & 0 & 0 & 0 & 0 & 0 & 0 & 0 & 0 & 0 & 0 & 0 & 0 & 0 & 0 \\ 0 & 0 & 0 & 0 & 0 & 0 & 0 & 0 & 0 & 0 & 1 & 0 & 1 & 0 & 1 & 0 & 1 & 0 \\ 0 & 1 & 0 & 0 & 0 & 0 & 0 & 0 & 0 & 0 & 0 & 0 & 0 & 0 & 0 & 0 & 0 & 0 \\ 0 & 0 & 1 & 0 & 0 & 0 & 0 & 0 & 0 & 0 & 0 & 0 & 0 & 0 & 0 & 0 & 0 & 0 \\ 0 & 0 & 0 & 0 & 0 & 0 & 0 & 0 & 0 & 0 & 0 & 1 & 0 & 1 & 0 & 1 & 0 & 1 \\ 0 & 0 & 0 & 1 & 0 & 0 & 0 & 0 & 0 & 0 & 0 & 0 & 0 & 0 & 0 & 0 & 0 & 0 \\ 0 & 0 & 0 & 0 & 1 & 0 & 0 & 0 & 0 & 0 & 0 & 0 & 0 & 0 & 0 & 0 & 0 & 0 \\ 0 & 0 & 0 & 0 & 0 & 0 & 1 & 1 & 1 & 1 & 0 & 0 & 0 & 0 & 0 & 0 & 0 & 0 \\ 0 & 0 & 0 & 0 & 0 & 1 & 0 & 0 & 0 & 0 & 0 & 0 & 0 & 0 & 0 & 0 & 0 & 0 \end{bmatrix}$$

$$E^{S}_{\delta_2^{(5)}} = \begin{bmatrix} 0 & 0 & 0 & 0 & 0 & 0 & 0 & 0 & 1 & 0 & 0 & 0 & 1 & 1 & 1 & 0 & 0 & 0 & 0 & 0 & 0 & 0 & 0 & 0 \\ 0 & 0 & 0 & 0 & 0 & 0 & 0 & 0 & 0 & -1 & 0 & 0 & 0 & 0 & 0 & -1 & -1 & -1 & 0 & 0 & 0 & 0 & 0 & 0 \\ 0 & 0 & 0 & 0 & 0 & 0 & 0 & 0 & 0 & 0 & 1 & 0 & 0 & 0 & 0 & 0 & 0 & 0 & 1 & 1 & 1 & 0 & 0 & 0 \\ -1 & 0 & -1 & 0 & -1 & 0 & -1 & 0 & 0 & 0 & -1 & -1 & -1 & 0 & 0 & 0 & 0 & 0 & 0 & 0 & 0 & 0 & 0 & 0 \\ 0 & 0 & 0 & 0 & 0 & 0 & 0 & 0 & 0 & 0 & 0 & -1 & 0 & 0 & 0 & 0 & 0 & 0 & 0 & 0 & 0 & -1 & -1 & -1 \\ 0 & -1 & 0 & -1 & 0 & -1 & 0 & -1 & 0 & 0 & -1 & 0 & 0 & 0 & 0 & 0 & 0 & 0 & 0 & -1 & -1 & -1 & 0 & 0 & 0 \\ 1 & 0 & 0 & 0 & 0 & 0 & 0 & 0 & 0 & 0 & 0 & 0 & 0 & 0 & 0 & 0 & 0 & 0 & 0 & 0 & 0 & 0 & 0 & 0 \\ 0 & 0 & 0 & 0 & 0 & 0 & 0 & 0 & 0 & 0 & 0 & 0 & 1 & 0 & 0 & 1 & 0 & 0 & 1 & 0 & 0 & 1 & 0 & 0 \\ 0 & 1 & 0 & 0 & 0 & 0 & 0 & 0 & 0 & 0 & 0 & 0 & 0 & 0 & 0 & 0 & 0 & 0 & 0 & 0 & 0 & 0 & 0 & 0 \\ 0 & 0 & 1 & 0 & 0 & 0 & 0 & 0 & 0 & 0 & 0 & 0 & 0 & 0 & 0 & 0 & 0 & 0 & 0 & 0 & 0 & 0 & 0 & 0 \\ 0 & 0 & 0 & 0 & 0 & 0 & 0 & 0 & 0 & 0 & 0 & 0 & 1 & 0 & 0 & 1 & 0 & 0 & 1 & 0 & 0 & 1 & 0 & 0 \\ 0 & 0 & 0 & 1 & 0 & 0 & 0 & 0 & 0 & 0 & 0 & 0 & 0 & 0 & 0 & 0 & 0 & 0 & 0 & 0 & 0 & 0 & 0 & 0 \\ 0 & 0 & 0 & 0 & 1 & 0 & 0 & 0 & 0 & 0 & 0 & 0 & 0 & 0 & 0 & 0 & 0 & 0 & 0 & 0 & 0 & 0 & 0 & 0 \\ 0 & 0 & 0 & 0 & 0 & 0 & 0 & 0 & 0 & 0 & 0 & 0 & 0 & 0 & 1 & 0 & 0 & 1 & 0 & 0 & 1 & 0 & 0 & 1 \\ 0 & 0 & 0 & 0 & 0 & 1 & 0 & 0 & 0 & 0 & 0 & 0 & 0 & 0 & 0 & 0 & 0 & 0 & 0 & 0 & 0 & 0 & 0 & 0 \\ 0 & 0 & 0 & 0 & 0 & 0 & 1 & 0 & 0 & 0 & 0 & 0 & 0 & 0 & 0 & 0 & 0 & 0 & 0 & 0 & 0 & 0 & 0 & 0 \\ 0 & 0 & 0 & 0 & 0 & 0 & 0 & 0 & 1 & 1 & 1 & 1 & 0 & 0 & 0 & 0 & 0 & 0 & 0 & 0 & 0 & 0 & 0 & 0 \\ 0 & 0 & 0 & 0 & 0 & 0 & 0 & 1 & 0 & 0 & 0 & 0 & 0 & 0 & 0 & 0 & 0 & 0 & 0 & 0 & 0 & 0 & 0 & 0 \end{bmatrix}$$

B.2 SOLUTIONS FOR PHOSPHORYLATION NETWORKS OF SIZE 2 INCLUDING SYNTHESIS AND DEGRADATION OF PROTEINS

B.2.1 *Synthesis and Degradation of Protein A*

This section checks existence of multiple steady states in a double phosphorylation network with synthesis and degradation as described in network (N6.2) for remaining subnetworks (N6.2a2)–(N6.2c4). Only solutions to the approach presented in section 6.2 are given. To distinguish between different network setups, each vector and matrix has a subscript denoting the current reaction network, e. g., a2 for network (N6.2a2).

For each subnetwork, $Y\,\mu = \ln(E\,\nu)/(E\,\lambda)$ is given, compare equation (6.14), together with substitutions of $\ln(\nu_i)/(\lambda_i)$ via $\varkappa_k$, see equation (6.16), resulting simplifications, compare equations (6.15) and (6.17), and solutions in M, Q and K, compare equations (6.23), (6.25) and (6.28) respectively, and sign conditions δ and σ, compare equations (6.41) and (6.42). If multiple steady states can be found, an example is given.

Network (N6.2a2)

$$
\begin{aligned}
\mu_1 + \mu_2 &= \ln \frac{\nu_1 + \nu_3 + \nu_8}{\lambda_1 + \lambda_3 + \lambda_8} & \mu_4 &= \ln \frac{\nu_1}{\lambda_1} & \mu_4 &= \ln \frac{\nu_3 + \nu_8}{\lambda_3 + \lambda_8} \\
\mu_3 + \mu_5 &= \ln \frac{\nu_2 + \nu_3}{\lambda_2 + \lambda_3} & \mu_6 &= \ln \frac{\nu_2}{\lambda_2} & \mu_6 &= \ln \frac{\nu_3}{\lambda_3} \\
0 &= \ln \frac{\nu_4 + \nu_8}{\lambda_4 + \lambda_8} & \mu_2 &= \ln \frac{\nu_4}{\lambda_4} & & \\
\mu_1 + \mu_5 &= \ln \frac{\nu_5 + \nu_7 + \nu_8}{\lambda_5 + \lambda_7 + \lambda_8} & \mu_7 &= \ln \frac{\nu_5}{\lambda_5} & \mu_7 &= \ln \frac{\nu_7 + \nu_8}{\lambda_7 + \lambda_8} \\
\mu_3 + \mu_8 &= \ln \frac{\nu_6 + \nu_7}{\lambda_6 + \lambda_7} & \mu_9 &= \ln \frac{\nu_6}{\lambda_6} & \mu_9 &= \ln \frac{\nu_7}{\lambda_7} \\
\mu_8 &= \ln \frac{\nu_8}{\lambda_8} & & & &
\end{aligned}
$$

$$
\begin{aligned}
\varkappa_1 &= \ln \frac{\nu_1 + \nu_3 + \nu_8}{\lambda_1 + \lambda_3 + \lambda_8} = \ln \frac{\nu_1}{\lambda_1} = \ln \frac{\nu_3 + \nu_8}{\lambda_3 + \lambda_8} \\
\varkappa_2 &= \ln \frac{\nu_2 + \nu_3}{\lambda_2 + \lambda_3} = \ln \frac{\nu_2}{\lambda_2} = \ln \frac{\nu_3}{\lambda_3} \\
\varkappa_3 &= \ln \frac{\nu_4}{\lambda_4} \\
\varkappa_4 &= \ln \frac{\nu_5 + \nu_7 + \nu_8}{\lambda_5 + \lambda_7 + \lambda_8} = \ln \frac{\nu_5}{\lambda_5} = \ln \frac{\nu_7 + \nu_8}{\lambda_7 + \lambda_8} \\
\varkappa_5 &= \ln \frac{\nu_6 + \nu_7}{\lambda_6 + \lambda_7} = \ln \frac{\nu_6}{\lambda_6} = \ln \frac{\nu_7}{\lambda_7} \\
\varkappa_6 &= \ln \frac{\nu_8}{\lambda_8}
\end{aligned}
$$

$$
\begin{aligned}
\mu_2 &= \varkappa_3 \\
\mu_4 &= \varkappa_1 \\
\mu_6 &= \varkappa_2 \\
\mu_7 &= \varkappa_4 \\
\mu_8 &= \varkappa_6 \\
\mu_9 &= \varkappa_5
\end{aligned}
$$

$$
\begin{aligned}
\mu_1 + \mu_2 &= \varkappa_1 \\
\mu_3 + \mu_5 &= \varkappa_2 \\
\mu_1 + \mu_5 &= \varkappa_4 \\
\mu_3 + \mu_8 &= \varkappa_5
\end{aligned}
\tag{B.2}
$$

Equation (B.2) yields:

$$\varkappa_6 = -\varkappa_1 - \varkappa_2 + \varkappa_3 + \varkappa_4 + \varkappa_5$$

$$
\begin{aligned}
\nu_1 &= \exp(\varkappa_1)\,\lambda_1 \\
\nu_2 &= \exp(\varkappa_2)\,\lambda_2 & \nu_3 &= \exp(\varkappa_2)\,\lambda_3 \\
\nu_4 &= \exp(\varkappa_3)\,\lambda_4 \\
\nu_5 &= \exp(\varkappa_4)\,\lambda_5 \\
\nu_6 &= \exp(\varkappa_5)\,\lambda_6 & \nu_7 &= \exp(\varkappa_5)\,\lambda_7 \\
\nu_8 &= \exp(\varkappa_6)\,\lambda_8
\end{aligned}
$$

$$
\begin{aligned}
0 &= (\exp(\varkappa_2) - \exp(\varkappa_1))\ \lambda_3 \\
&\quad + (\exp(-\varkappa_1 - \varkappa_2 + \varkappa_3 + \varkappa_4 + \varkappa_5) - \exp(\varkappa_1))\ \lambda_8 \\
0 &= (\exp(\varkappa_3) - 1)\ \lambda_4 + (\exp(-\varkappa_1 - \varkappa_2 + \varkappa_3 + \varkappa_4 + \varkappa_5) - 1)\ \lambda_8 \\
0 &= (\exp(\varkappa_5) - \exp(\varkappa_4))\ \lambda_7 \\
&\quad + (\exp(-\varkappa_1 - \varkappa_2 + \varkappa_3 + \varkappa_4 + \varkappa_5) - \exp(\varkappa_4))\ \lambda_8
\end{aligned}
$$

$$
\begin{aligned}
\tilde{\varkappa}_{a2} &= [\varkappa_1\ \ \varkappa_2\ \ \varkappa_3\ \ \varkappa_4\ \ \varkappa_5]^T \\
\tilde{\lambda}_{a2} &= [\lambda_3\ \ \lambda_4\ \ \lambda_7\ \ \lambda_8]^T
\end{aligned}
$$

$$
M_{a2} = \begin{bmatrix}
1 & 0 & -1 & 0 & 0 \\
0 & 0 & 1 & 0 & 0 \\
1 & 1 & -1 & -1 & 0 \\
1 & 0 & 0 & 0 & 0 \\
-1 & 0 & 1 & 1 & 0 \\
0 & 1 & 0 & 0 & 0 \\
0 & 0 & 0 & 1 & 0 \\
-1 & -1 & 1 & 1 & 1 \\
0 & 0 & 0 & 0 & 1
\end{bmatrix}
$$

$$
Q_{a2} = \begin{bmatrix}
q_{11} & 0 & 0 & q_{12} \\
0 & q_{21} & 0 & q_{22} \\
0 & 0 & q_{31} & q_{31}
\end{bmatrix}
$$

with

$$
\begin{aligned}
q_{11} &= -\exp(\varkappa_1) + \exp(\varkappa_2) \\
q_{12} &= -\exp(\varkappa_1) + \exp(-\varkappa_1 - \varkappa_2 + \varkappa_3 + \varkappa_4 + \varkappa_5) \\
q_{21} &= -1 + \exp(\varkappa_3) \\
q_{22} &= -1 + \exp(-\varkappa_1 - \varkappa_2 + \varkappa_3 + \varkappa_4 + \varkappa_5) \\
q_{31} &= -\exp(\varkappa_4) + \exp(\varkappa_5) \\
q_{32} &= -\exp(\varkappa_4) + \exp(-\varkappa_1 - \varkappa_2 + \varkappa_3 + \varkappa_4 + \varkappa_5)
\end{aligned}
$$

$$K = \begin{bmatrix} -1 & 1 & 0 & 0 & 0 \\ -2 & -1 & 1 & 1 & 1 \\ 0 & 0 & 1 & 0 & 0 \\ -1 & -1 & 1 & 1 & 1 \\ 0 & 0 & 0 & -1 & 1 \\ -1 & -1 & 1 & 0 & 1 \end{bmatrix}$$

Note, only half of the set of valid sign vectors is given from now on. Furthermore the trivial solution is omitted. The same holds true for the sign pattern Σ.

$$\Delta_{a2}^{T} = \begin{bmatrix} -1 & -1 & -1 & -1 & 1 & -1 & 1 & 1 & 1 \\ -1 & 1 & -1 & 1 & 1 & 1 & -1 & -1 & -1 \\ -1 & 1 & 0 & 1 & 1 & 1 & -1 & -1 & -1 \\ -1 & 1 & 1 & 1 & -1 & 1 & -1 & -1 & -1 \\ -1 & 1 & 1 & 1 & 0 & 1 & -1 & -1 & -1 \\ -1 & 1 & 1 & 1 & 1 & 1 & -1 & -1 & -1 \\ 0 & -1 & -1 & -1 & 1 & -1 & 1 & 1 & 1 \end{bmatrix}$$

$$\Sigma_{a2}^{T} = \begin{bmatrix} -1 & 1 & -1 & 1 & -1 & 1 \\ 1 & -1 & 1 & -1 & -1 & 1 \\ 1 & -1 & 1 & -1 & 0 & 0 \\ 1 & -1 & 1 & -1 & 1 & -1 \\ 1 & -1 & 1 & -1 & 1 & -1 \\ 1 & -1 & 1 & -1 & 1 & -1 \\ -1 & 1 & -1 & 1 & -1 & 1 \end{bmatrix}$$

Choosing

$$\tilde{\varkappa}_{a2}^{\delta_1} = [-0.5,\ -0.75,\ -0.25,\ 0.75,\ 0.5]^T$$
$$\beta_{a2}^{\delta_1} = [0.126531,\ 0.863756,\ 0.770589,\ 0.243902,\ 0.636293,\ 0.819782,\ 0.951175]^T$$
$$\lambda_{a2}^{\delta_1} = [0.69805,\ 0.765565,\ 66.1966,\ 38.3715,\ 3.38806,\ 6.65696,\ 15.7401,\ 1]^T$$

yields

$$a_{a2}^{\delta_1} = [0.572022,\ 3.90488,\ 0.932661,\ 0.619876,\ 0.370307,\ 1.5537,\ 0.331632,\ 0.112065,\ 2.45155]^T$$
$$b_{a2}^{\delta_1} = [0.445491,\ 3.04112,\ 0.162072,\ 0.375974,\ 1.0066,\ 0.733914,\ 0.702065,\ 1.06324,\ 4.04192]^T$$
$$c_{a2}^{\delta_1} = [4.9379,\ 1.52353]^T$$
$$k_{a2}^{\delta_1} = [30.3959,\ 1.12611,\ 108.403,\ 193.885,\ 0.492738,\ 42.6059,\ 39.3715,\ 9.82654,\ 95.0228,\ 10.2163,\ 50.4778,\ 214.288,\ 2.71541,\ 6.42046,\ 8.92342]^T$$

Network (N6.2a3)

$$
\begin{aligned}
\mu_1 + \mu_2 &= \ln \frac{\nu_1 + \nu_3 + \nu_4 + \nu_8}{\lambda_1 + \lambda_3 + \lambda_4 + \lambda_8} & \mu_4 &= \ln \frac{\nu_1}{\lambda_1} & \mu_4 &= \ln \frac{\nu_3 + \nu_4 + \nu_8}{\lambda_3 + \lambda_4 + \lambda_8} \\
\mu_2 + \mu_3 &= \ln \frac{\nu_2 + \nu_3}{\lambda_2 + \lambda_3} & \mu_6 &= \ln \frac{\nu_2}{\lambda_2} & \mu_6 &= \ln \frac{\nu_3}{\lambda_3} \\
0 &= \ln \frac{\nu_4 + \nu_8}{\lambda_4 + \lambda_8} & \mu_5 &= \ln \frac{\nu_4}{\lambda_4} & & \\
\mu_1 + \mu_5 &= \ln \frac{\nu_5 + \nu_7 + \nu_8}{\lambda_5 + \lambda_7 + \lambda_8} & \mu_7 &= \ln \frac{\nu_5}{\lambda_5} & \mu_7 &= \ln \frac{\nu_7 + \nu_8}{\lambda_7 + \lambda_8} \\
\mu_3 + \mu_5 &= \ln \frac{\nu_6 + \nu_7}{\lambda_6 + \lambda_7} & \mu_9 &= \ln \frac{\nu_6}{\lambda_6} & \mu_9 &= \ln \frac{\nu_7}{\lambda_7} \\
\mu_8 &= \ln \frac{\nu_8}{\lambda_8} & & & &
\end{aligned}
$$

$$
\begin{aligned}
\varkappa_1 &= \ln \frac{\nu_1 + \nu_3 + \nu_4 + \nu_8}{\lambda_1 + \lambda_3 + \lambda_4 + \lambda_8} = \ln \frac{\nu_1}{\lambda_1} = \ln \frac{\nu_3 + \nu_4 + \nu_8}{\lambda_3 + \lambda_4 + \lambda_8} \\
\varkappa_2 &= \ln \frac{\nu_2 + \nu_3}{\lambda_2 + \lambda_3} = \ln \frac{\nu_2}{\lambda_2} = \ln \frac{\nu_3}{\lambda_3} \\
\varkappa_3 &= \ln \frac{\nu_4}{\lambda_4} \\
\varkappa_4 &= \ln \frac{\nu_5 + \nu_7 + \nu_8}{\lambda_5 + \lambda_7 + \lambda_8} = \ln \frac{\nu_5}{\lambda_5} = \ln \frac{\nu_7 + \nu_8}{\lambda_7 + \lambda_8} \\
\varkappa_5 &= \ln \frac{\nu_6 + \nu_7}{\lambda_6 + \lambda_7} = \ln \frac{\nu_6}{\lambda_6} = \ln \frac{\nu_7}{\lambda_7} \\
\varkappa_6 &= \ln \frac{\nu_8}{\lambda_8}
\end{aligned}
$$

$$
\begin{aligned}
\mu_4 &= \varkappa_1 \\
\mu_5 &= \varkappa_3 \\
\mu_6 &= \varkappa_2 \\
\mu_7 &= \varkappa_4 \\
\mu_8 &= \varkappa_6 \\
\mu_9 &= \varkappa_5
\end{aligned}
$$

$$
\begin{aligned}
\mu_1 + \mu_2 &= \varkappa_1 && \text{(B.3)} \\
\mu_2 + \mu_3 &= \varkappa_2 && \text{(B.4)} \\
\mu_1 + \mu_5 &= \varkappa_4 && \text{(B.5)} \\
\mu_3 + \mu_5 &= \varkappa_5 && \text{(B.6)}
\end{aligned}
$$

Solving equations (B.4)–(B.6) and inserting into (B.3) yields

$$\varkappa_5 = -\varkappa_1 + \varkappa_2 + \varkappa_4.$$

$$
\begin{aligned}
\nu_1 &= \exp(\varkappa_1)\,\lambda_1 & & \\
\nu_2 &= \exp(\varkappa_2)\,\lambda_2 & \nu_3 &= \exp(\varkappa_2)\,\lambda_3 \\
\nu_4 &= \exp(\varkappa_3)\,\lambda_4 & & \\
\nu_5 &= \exp(\varkappa_4)\,\lambda_5 & & \\
\nu_6 &= \exp(\varkappa_5)\,\lambda_6 & \nu_7 &= \exp(\varkappa_5)\,\lambda_7 \\
\nu_8 &= \exp(\varkappa_6)\,\lambda_8 & &
\end{aligned}
$$

$$0 = (\exp(\varkappa_2) - \exp(\varkappa_1))\ \lambda_3 + (\exp(\varkappa_3) - \exp(\varkappa_1))\ \lambda_4 + (\exp(\varkappa_6) - \exp(\varkappa_1))\ \lambda_8 \tag{B.7a}$$

$$0 = (\exp(\varkappa_3) - 1)\ \lambda_4 + (\exp(\varkappa_6) - 1)\ \lambda_8 \tag{B.7b}$$

$$0 = (\exp(-\varkappa_1 + \varkappa_2 + \varkappa_4) - \exp(\varkappa_4))\ \lambda_7 + (\exp(\varkappa_6) - \exp(\varkappa_4))\ \lambda_8 \tag{B.7c}$$

$$\tilde{\varkappa}_{a3} = [\varkappa_1\ \ \varkappa_2\ \ \varkappa_3\ \ \varkappa_4\ \ \varkappa_6]^T$$
$$\tilde{\lambda}_{a3} = [\lambda_3\ \ \lambda_4\ \ \lambda_7\ \ \lambda_8]^T$$

$$M_{a3} = \begin{bmatrix} 0 & 0 & -1 & 1 & 0 \\ 1 & 0 & 1 & -1 & 0 \\ -1 & 1 & -1 & 1 & 0 \\ 1 & 0 & 0 & 0 & 0 \\ 0 & 0 & 1 & 0 & 0 \\ 0 & 1 & 0 & 0 & 0 \\ 0 & 0 & 0 & 1 & 0 \\ 0 & 0 & 0 & 0 & 1 \\ -1 & 1 & 0 & 1 & 0 \end{bmatrix}$$

$$Q_{a3} = \begin{bmatrix} q_{11} & q_{12} & 0 & q_{13} \\ 0 & q_{21} & 0 & q_{22} \\ 0 & 0 & q_{31} & q_{32} \end{bmatrix}$$

with

$$\begin{aligned} q_{11} &= -\exp(\varkappa_1) + \exp(\varkappa_2) \\ q_{12} &= -\exp(\varkappa_1) + \exp(\varkappa_3) \\ q_{13} &= -\exp(\varkappa_1) + \exp(\varkappa_6) \\ q_{21} &= -1 + \exp(\varkappa_3) \\ q_{22} &= -1 + \exp(\varkappa_6) \\ q_{31} &= -\exp(\varkappa_4) + \exp(-\varkappa_1 + \varkappa_2 + \varkappa_4) \\ q_{32} &= -\exp(\varkappa_4) + \exp(\varkappa_6) \end{aligned}$$

$$K_{a3} = \begin{bmatrix} -1 & 1 & 0 & 0 & 0 \\ -1 & 0 & 1 & 0 & 0 \\ -1 & 0 & 0 & 0 & 1 \\ 0 & 0 & 1 & 0 & 0 \\ 0 & 0 & 0 & 0 & 1 \\ -1 & 1 & 0 & 0 & 0 \\ 0 & 0 & 0 & -1 & 1 \end{bmatrix}$$

$$\Delta_{a3}^{T} = \begin{bmatrix}
-1 & -1 & -1 & -1 & 1 & -1 & 1 & -1 & 1 \\
-1 & -1 & 0 & -1 & 1 & -1 & 1 & -1 & 1 \\
-1 & -1 & 1 & -1 & 1 & -1 & 1 & -1 & 1 \\
-1 & 0 & -1 & -1 & 1 & -1 & 1 & -1 & 1 \\
-1 & 1 & -1 & -1 & 1 & -1 & 1 & -1 & 1 \\
-1 & 1 & -1 & -1 & 1 & 0 & 1 & -1 & 1 \\
-1 & 1 & -1 & -1 & 1 & 1 & 1 & -1 & 1 \\
-1 & 1 & -1 & 0 & 1 & 1 & 1 & -1 & 1 \\
-1 & 1 & -1 & 1 & -1 & 1 & -1 & 1 & -1 \\
-1 & 1 & -1 & 1 & 1 & 1 & -1 & -1 & -1 \\
-1 & 1 & -1 & 1 & 1 & 1 & -1 & -1 & -1 \\
-1 & 1 & -1 & 1 & 1 & 1 & -1 & -1 & -1 \\
-1 & 1 & -1 & 1 & 1 & 1 & -1 & -1 & -1 \\
-1 & 1 & -1 & 1 & 1 & 1 & -1 & -1 & 0 \\
-1 & 1 & -1 & 1 & 1 & 1 & -1 & -1 & 0 \\
-1 & 1 & -1 & 1 & 1 & 1 & -1 & -1 & 0 \\
-1 & 1 & -1 & 1 & 1 & 1 & -1 & -1 & 1 \\
-1 & 1 & -1 & 1 & 1 & 1 & -1 & -1 & 1 \\
-1 & 1 & -1 & 1 & 1 & 1 & -1 & -1 & 1 \\
-1 & 1 & -1 & 1 & 1 & 1 & 0 & -1 & 1 \\
-1 & 1 & -1 & 1 & 1 & 1 & 0 & -1 & 1 \\
-1 & 1 & -1 & 1 & 1 & 1 & 0 & -1 & 1 \\
-1 & 1 & -1 & 1 & 1 & 1 & 1 & -1 & 1 \\
-1 & 1 & -1 & 1 & 1 & 1 & 1 & -1 & 1 \\
-1 & 1 & -1 & 1 & 1 & 1 & 1 & -1 & 1 \\
0 & -1 & 1 & -1 & 1 & -1 & 1 & -1 & 1
\end{bmatrix}$$

$$\Sigma_{a3}^{T} = \begin{bmatrix}
1 & 1 & -1 & 1 & -1 & 1 & -1 \\
1 & 1 & -1 & 1 & -1 & 1 & -1 \\
1 & 1 & -1 & 1 & -1 & 1 & -1 \\
1 & 1 & -1 & 1 & -1 & 1 & -1 \\
1 & 1 & -1 & 1 & -1 & 1 & -1 \\
1 & 1 & -1 & 1 & -1 & 1 & -1 \\
1 & 1 & -1 & 1 & -1 & 1 & -1 \\
-1 & -1 & 1 & -1 & 1 & -1 & 1 \\
1 & 0 & -1 & 1 & -1 & 1 & -1 \\
0 & 1 & -1 & 1 & -1 & 0 & 0 \\
1 & 1 & -1 & 1 & -1 & 1 & -1 \\
1 & -1 & -1 & 1 & -1 & 1 & -1 \\
-1 & 1 & -1 & 1 & -1 & -1 & 1 \\
1 & 0 & -1 & 1 & -1 & 1 & -1 \\
1 & 1 & -1 & 1 & -1 & 1 & -1 \\
1 & -1 & -1 & 1 & -1 & 1 & -1 \\
1 & 0 & -1 & 1 & -1 & 1 & -1 \\
1 & 1 & -1 & 1 & -1 & 1 & -1 \\
1 & -1 & -1 & 1 & -1 & 1 & -1 \\
1 & 0 & -1 & 1 & -1 & 1 & -1 \\
1 & 1 & -1 & 1 & -1 & 1 & -1 \\
1 & -1 & -1 & 1 & -1 & 1 & -1 \\
1 & 0 & -1 & 1 & -1 & 1 & -1 \\
1 & 1 & -1 & 1 & -1 & 1 & -1 \\
1 & -1 & -1 & 1 & -1 & 1 & -1 \\
1 & 1 & -1 & 1 & -1 & 1 & -1
\end{bmatrix}$$

This system poses additional conditions on λ_l when certain sign patterns are chosen. E. g., λ_4 poses restrictions in equation (B.7a) but appears also while computing λ_3 in equation (B.7b). For example, if

$$\sigma_{a3} = \begin{bmatrix} 1 & 1 & -1 & 1 & -1 & * & * \end{bmatrix}^{T}$$

is chosen, here $*$ just indicates that the last two signs are arbitrary, as they are not considered right now, additional restrictions occur. This sign vector corresponds to different $\delta(i)_{a3}$, e. g., $\delta(1)_{a3}, \ldots, \delta(8)_{a3}$. Choosing this sign vector yields for entries in Q_{a3}:

$$\frac{q_{22}q_{12}}{q_{21}} > q_{13}.$$

But not all sign vectors impose further restrictions. Choosing for example $\delta(10)_{a3}$ and its corresponding sign pattern in Σ

$$\delta(10)_{a3} = \begin{bmatrix} -1 & 1 & -1 & 1 & 1 & 1 & -1 & -1 & -1 \end{bmatrix}^{T},$$
$$\sigma(10)_{a3} = \begin{bmatrix} 1 & 0 & -1 & 1 & -1 & 1 & -1 \end{bmatrix}^{T}$$

does not pose further conditions, as $\operatorname{sgn}(q_{12}) = 0$. Choosing $\delta(10)_{a3}$ with

$$\tilde{\varkappa}_{a3}^{\delta_{10}} = [0.5,\ 0.75,\ 0.8,\ -0.5,\ -0.75]^T$$
$$\beta_{a3}^{\delta_{10}} = [0.819965,\ 0.765444,\ 0.685297,\ 0.527232,\ 0.794805,\ 0.231815,\ 0.77515]^T$$
$$\lambda_{a3}^{\delta_{10}} = [0.834267,\ 0.916061,\ 1.98176,\ 0.430531,\ 0.2758,\ 0.131831,\ 0.778801,\ 1]^T$$

yields the following steady states:

$$a_{a3}^{\delta_{10}} = [1.12715,\ 0.151584,\ 1.0542,\ 2.48916,\ 0.430204,\ 1.30747,\ 2.01999,\ 0.439348,\ 3.50431]^T$$
$$b_{a3}^{\delta_{10}} = [0.307184,\ 0.917028,\ 0.368905,\ 4.10393,\ 0.957436,\ 2.76792,\ 1.22519,\ 0.207533,\ 2.72916]^T$$
$$c_{a3}^{\delta_{10}} = [5.86598,\ 5.6363]^T$$
$$k_{a3}^{\delta_{10}} = [24.8544,\ 0.33516,\ 1.37086,\ 18.1341,\ 0.700635,\ 1.51572,\ 1.43053,\ 1.00076,\ 4.23713,\ 0.136535,\ 0.880597,\ 2.00791,\ 0.0376196,\ 0.222241,\ 2.2761]^T$$

Network (№6.2a4)

$$\mu_1 + \mu_2 = \ln\frac{\nu_1+\nu_3+\nu_7}{\lambda_1+\lambda_3+\lambda_7} \qquad \mu_4 = \ln\frac{\nu_1}{\lambda_1} \qquad \mu_4 = \ln\frac{\nu_3+\nu_7}{\lambda_3+\lambda_7}$$
$$\mu_3 + \mu_5 = \ln\frac{\nu_2+\nu_3}{\lambda_2+\lambda_3} \qquad \mu_6 = \ln\frac{\nu_2}{\lambda_2} \qquad \mu_6 = \ln\frac{\nu_3}{\lambda_3}$$
$$0 = \ln\frac{\nu_7}{\lambda_7}$$
$$\mu_1 + \mu_5 = \ln\frac{\nu_4+\nu_6+\nu_7}{\lambda_4+\lambda_6+\lambda_7} \qquad \mu_7 = \ln\frac{\nu_4}{\lambda_4} \qquad \mu_7 = \ln\frac{\nu_6+\nu_7}{\lambda_6+\lambda_7}$$
$$\mu_3 + \mu_8 = \ln\frac{\nu_5+\nu_6}{\lambda_5+\lambda_6} \qquad \mu_9 = \ln\frac{\nu_5}{\lambda_5} \qquad \mu_9 = \ln\frac{\nu_6}{\lambda_6}$$
$$\mu_8 = \ln\frac{\nu_7}{\lambda_7}$$

$$\varkappa_1 = \ln\frac{\nu_1+\nu_3+\nu_7}{\lambda_1+\lambda_3+\lambda_7} = \ln\frac{\nu_1}{\lambda_1} = \ln\frac{\nu_3+\nu_7}{\lambda_3+\lambda_7}$$
$$\varkappa_2 = \ln\frac{\nu_2+\nu_3}{\lambda_2+\lambda_3} = \ln\frac{\nu_2}{\lambda_2} = \ln\frac{\nu_3}{\lambda_3}$$
$$\varkappa_3 = \ln\frac{\nu_4+\nu_6+\nu_7}{\lambda_4+\lambda_6+\lambda_7} = \ln\frac{\nu_4}{\lambda_4} = \ln\frac{\nu_6+\nu_7}{\lambda_6+\lambda_7}$$
$$\varkappa_4 = \ln\frac{\nu_5+\nu_6}{\lambda_5+\lambda_6} = \ln\frac{\nu_5}{\lambda_5} = \ln\frac{\nu_6}{\lambda_6}$$
$$\varkappa_5 = \ln\frac{\nu_7}{\lambda_7}$$

$$\mu_4 = \varkappa_1$$
$$\mu_6 = \varkappa_2$$
$$\mu_7 = \varkappa_3$$
$$\mu_8 = 0$$
$$\mu_9 = \varkappa_4$$

$$
\begin{aligned}
\mu_1 + \mu_2 &= \varkappa_1 \\
\mu_3 + \mu_5 &= \varkappa_2 \\
\mu_1 + \mu_5 &= \varkappa_3 \\
\mu_3 + \mu_8 &= \varkappa_4
\end{aligned}
$$

$$
\begin{aligned}
\nu_1 &= \exp(\varkappa_1)\,\lambda_1 \\
\nu_2 &= \exp(\varkappa_2)\,\lambda_2, & \nu_3 &= \exp(\varkappa_2)\,\lambda_3 \\
\nu_4 &= \exp(\varkappa_3)\,\lambda_3 \\
\nu_5 &= \exp(\varkappa_4)\,\lambda_4, & \nu_6 &= \exp(\varkappa_4)\,\lambda_6 \\
\nu_7 &= \lambda_7
\end{aligned}
$$

$$
\begin{aligned}
0 &= (\exp(\varkappa_2) - \exp(\varkappa_1))\ \lambda_3 + (1 - \exp(\varkappa_1))\ \lambda_7 \\
0 &= (\exp(\varkappa_4) - \exp(\varkappa_3))\ \lambda_6 + (1 - \exp(\varkappa_3))\ \lambda_7
\end{aligned}
$$

$$
\begin{aligned}
\tilde{\varkappa}_{a4} &= [\varkappa_1,\ \varkappa_2,\ \varkappa_3,\ \varkappa_4]^T \\
\tilde{\lambda}_{a4} &= [\lambda_3,\ \lambda_6,\ \lambda_7]^T
\end{aligned}
$$

$$
M_{a4} = \begin{bmatrix}
0 & -1 & 1 & 1 \\
1 & 1 & -1 & -1 \\
0 & 0 & 0 & 1 \\
1 & 0 & 0 & 0 \\
0 & 1 & 0 & -1 \\
0 & 1 & 0 & 0 \\
0 & 0 & 1 & 0 \\
0 & 0 & 0 & 0 \\
0 & 0 & 0 & 1
\end{bmatrix}
$$

$$
\begin{aligned}
Q_{a4} &= \begin{bmatrix}
\exp(\varkappa_2) - \exp(\varkappa_1) & 0 & 1 - \exp(\varkappa_1) \\
0 & \exp(\varkappa_4) - \exp(\varkappa_3) & 1 - \exp(\varkappa_3)
\end{bmatrix} \\
&= \begin{bmatrix}
q_{11} & 0 & q_{12} \\
0 & q_{21} & q_{22}
\end{bmatrix}
\end{aligned}
$$

$$
K_{a4} = \begin{bmatrix}
-1 & 1 & 0 & 0 \\
-1 & 0 & 0 & 0 \\
0 & 0 & -1 & 1 \\
0 & 0 & -1 & 0
\end{bmatrix}
$$

The valid sign vector can be given by

$$
\delta_{a4} = \begin{bmatrix} -1 & 1 & -1 & 1 & 1 & 1 & -1 & 0 & -1 \end{bmatrix}^T
$$

with the corresponding sign condition:

$$\sigma_{a4} = \begin{bmatrix} 1 & -1 & -1 & 1 \end{bmatrix}^T$$

Choosing

$$\begin{aligned}
\tilde{\varkappa}_{a4}^{\delta_1} &= [0.5,\ 0.75,\ -0.5,\ -0.75]^T \\
\beta_{a4}^{\delta_1} &= [0.231466,\ 0.935601,\ 0.467326,\ 0.998736,\ 0.182941,\ 0.936059, \\
&\quad 0.973374]^T \\
\lambda_{a4}^{\delta_1} &= [0.96151,\ 5.04049,\ 1.38533,\ 9.30634,\ 8.90458,\ 2.93275\ 1]^T
\end{aligned}$$

yields

$$\begin{aligned}
a_{a4}^{\delta_1} &= [0.267694,\ 0.0836666,\ 0.885702,\ 0.638805,\ 0.286854, \\
&\quad 1.28979,\ 0.464943,\ 1,\ 1.84479]^T \\
b_{a4}^{\delta_1} &= [0.0362285,\ 1.01927,\ 0.418376,\ 1.05321,\ 1.28559, \\
&\quad 2.73049,\ 0.282002,\ 1,\ 0.871418]^T \\
c_{a4} &= [4.02029,\ 1.37144]^T \\
k_{a4}^{\delta_1} &= [149.43217,\ 1.50517,\ 3.73405,\ 25.29184,\ 3.90798, \\
&\quad 1.07407,\ 1,\ 172.40857,\ 20.0161,\ 8.45855, \\
&\quad 13.36493,\ 4.82687,\ 1.58974,\ 1]^T
\end{aligned}$$

Note, a zero in a sign vector $s = \mu$ automatically results in an arbitrary positive value in the corresponding entry of the steady states. A value of '1' is chosen in a_i and b_i, wherever it applies.

B.2.2 *Additional Synthesis and Degradation of Enzyme* E_1

Network (N6.2b1)

$$\begin{aligned}
\mu_1 + \mu_2 &= \ln \frac{\nu_1 + \nu_{10} + \nu_3 + \nu_6}{\lambda_1 + \lambda_{10} + \lambda_3 + \lambda_6} & \mu_4 &= \ln \frac{\nu_1}{\lambda_1} & \mu_4 &= \ln \frac{\nu_{10} + \nu_3 + \nu_6}{\lambda_{10} + \lambda_3 + \lambda_6} \\
\mu_3 + \mu_5 &= \ln \frac{\nu_2 + \nu_3}{\lambda_2 + \lambda_3} & \mu_6 &= \ln \frac{\nu_2}{\lambda_2} & \mu_6 &= \ln \frac{\nu_3}{\lambda_3} \\
\mu_1 &= \ln \frac{\nu_4}{\lambda_4} & 0 &= \ln \frac{\nu_4}{\lambda_4} & \mu_2 &= \ln \frac{\nu_5}{\lambda_5} \\
0 &= \ln \frac{\nu_{10} + \nu_5 + \nu_6}{\lambda_{10} + \lambda_5 + \lambda_6} & \mu_5 &= \ln \frac{\nu_6}{\lambda_6} & & \\
\mu_1 + \mu_5 &= \ln \frac{\nu_{10} + \nu_7 + \nu_9}{\lambda_{10} + \lambda_7 + \lambda_9} & \mu_7 &= \ln \frac{\nu_7}{\lambda_7} & \mu_7 &= \ln \frac{\nu_{10} + \nu_9}{\lambda_{10} + \lambda_9} \\
\mu_3 + \mu_8 &= \ln \frac{\nu_8 + \nu_9}{\lambda_8 + \lambda_9} & \mu_9 &= \ln \frac{\nu_8}{\lambda_8} & \mu_9 &= \ln \frac{\nu_9}{\lambda_9} \\
\mu_8 &= \ln \frac{\nu_{10}}{\lambda_{10}} & & & &
\end{aligned}$$

$$\begin{aligned}
\varkappa_1 &= \ln \frac{\nu_1 + \nu_{10} + \nu_3 + \nu_6}{\lambda_1 + \lambda_{10} + \lambda_3 + \lambda_6} = \ln \frac{\nu_1}{\lambda_1} = \ln \frac{\nu_{10} + \nu_3 + \nu_6}{\lambda_{10} + \lambda_3 + \lambda_6} \\
\varkappa_2 &= \ln \frac{\nu_2 + \nu_3}{\lambda_2 + \lambda_3} = \ln \frac{\nu_2}{\lambda_2} = \ln \frac{\nu_3}{\lambda_3}
\end{aligned}$$

$$
\begin{aligned}
\varkappa_3 &= \ln \frac{\nu_3}{\lambda_3} \\
\varkappa_4 &= \ln \frac{\nu_6}{\lambda_6} \\
\varkappa_5 &= \ln \frac{\nu_{10} + \nu_7 + \nu_9}{\lambda_{10} + \lambda_7 + \lambda_9} = \ln \frac{\nu_7}{\lambda_7} = \ln \frac{\nu_{10} + \nu_9}{\lambda_{10} + \lambda_9} \\
\varkappa_6 &= \ln \frac{\nu_8 + \nu_9}{\lambda_8 + \lambda_9} = \ln \frac{\nu_8}{\lambda_8} = \ln \frac{\nu_9}{\lambda_9} \\
\varkappa_7 &= \ln \frac{\nu_{10}}{\lambda_{10}}
\end{aligned}
$$

$$
\begin{aligned}
\mu_1 &= 0 \\
\mu_2 &= \varkappa_3 \\
\mu_4 &= \varkappa_1 \\
\mu_5 &= \varkappa_4 \\
\mu_6 &= \varkappa_2 \\
\mu_7 &= \varkappa_5 \\
\mu_8 &= \varkappa_7 \\
\mu_9 &= \varkappa_6
\end{aligned}
$$

$$
\begin{aligned}
\mu_1 + \mu_2 &= \varkappa_1 && \text{(B.8)} \\
\mu_3 + \mu_5 &= \varkappa_2 && \text{(B.9)} \\
\mu_1 + \mu_5 &= \varkappa_5 && \text{(B.10)} \\
\mu_3 + \mu_5 &= \varkappa_6 && \text{(B.11)}
\end{aligned}
$$

Using equation (B.9) and (B.11) yields:

$$\varkappa_7 = -\varkappa_2 + \varkappa_4 + \varkappa_6,$$

and equation (B.8) yields

$$\varkappa_3 = \varkappa_1,$$

furthermore equation (B.10) yields

$$\varkappa_5 = \varkappa_4.$$

$$
\begin{aligned}
\nu_1 &= \exp(\varkappa_1)\,\lambda_1 \\
\nu_2 &= \exp(\varkappa_2)\,\lambda_2 && \nu_3 = \exp(\varkappa_2)\,\lambda_3 \\
\nu_4 &= \lambda_4 \\
\nu_5 &= \exp(\varkappa_3)\,\lambda_5 \\
\nu_6 &= \exp(\varkappa_4)\,\lambda_6 \\
\nu_7 &= \exp(\varkappa_5)\,\lambda_7 \\
\nu_8 &= \exp(\varkappa_6)\,\lambda_8 && \nu_9 = \exp(\varkappa_6)\,\lambda_9 \\
\nu_{10} &= \exp(\varkappa_7)\,\lambda_{10}
\end{aligned}
$$

$$
\begin{aligned}
0 &= (\exp(\varkappa_2) - \exp(\varkappa_1))\ \lambda_3 + (\exp(\varkappa_4) - \exp(\varkappa_1))\ \lambda_6 + \\
&\quad (\exp(-\varkappa_2 + \varkappa_4 + \varkappa_6) - \exp(\varkappa_1))\ \lambda_{10} \\
0 &= (\exp(\varkappa_1) - 1)\ \lambda_5 + (\exp(\varkappa_4) - 1)\ \lambda_6 \\
&\quad + (\exp(-\varkappa_2 + \varkappa_4 + \varkappa_6) - 1)\ \lambda_{10} \\
0 &= (\exp(\varkappa_6) - \exp(\varkappa_4))\ \lambda_9 + (\exp(-\varkappa_2 + \varkappa_4 + \varkappa_6) - \exp(\varkappa_4))\ \lambda_{10}
\end{aligned}
$$

$$
\begin{aligned}
\tilde{\varkappa}_{b1} &= [\varkappa_1\ \ \varkappa_2\ \ \varkappa_4\ \ \varkappa_6]^T \\
\tilde{\lambda}_{b1} &= [\lambda_3\ \ \lambda_5\ \ \lambda_6\ \ \lambda_9\ \ \lambda_{10}]^T
\end{aligned}
$$

$$
M_{b1} = \begin{bmatrix}
0 & 0 & 0 & 0 \\
1 & 0 & 0 & 0 \\
0 & 1 & -1 & 0 \\
1 & 0 & 0 & 0 \\
0 & 0 & 1 & 0 \\
0 & 1 & 0 & 0 \\
0 & 0 & 1 & 0 \\
0 & -1 & 1 & 1 \\
0 & 0 & 0 & 1
\end{bmatrix}
$$

$$
Q_{b1} = \begin{bmatrix}
q_{11} & 0 & 0 & q_{12} & q_{13} \\
0 & q_{21} & 0 & q_{22} & q_{23} \\
0 & 0 & q_{31} & 0 & q_{32}
\end{bmatrix}
$$

with

$$
\begin{aligned}
q_{11} &= -\exp(\varkappa_1) + \exp(\varkappa_2) \\
q_{12} &= -\exp(\varkappa_1) + \exp(\varkappa_4) \\
q_{13} &= -\exp(\varkappa_1) + \exp(-\varkappa_2 + \varkappa_4 + \varkappa_6) \\
q_{21} &= -1 + \exp(\varkappa_1) \\
q_{22} &= -1 + \exp(\varkappa_4) \\
q_{23} &= -1 + \exp(-\varkappa_2 + \varkappa_4 + \varkappa_6) \\
q_{31} &= -\exp(\varkappa_4) + \exp(\varkappa_6) \\
q_{32} &= -\exp(\varkappa_4) + \exp(-\varkappa_2 + \varkappa_4 + \varkappa_6)
\end{aligned}
$$

$$
K_{b1} = \begin{bmatrix}
-1 & 1 & 0 & 0 \\
-1 & 0 & 1 & 0 \\
-1 & -1 & 1 & 1 \\
1 & 0 & 0 & 0 \\
0 & 0 & 1 & 0 \\
0 & -1 & 1 & 1 \\
0 & 0 & -1 & 1 \\
0 & -1 & 0 & 1
\end{bmatrix}
$$

$$\delta_{b1} = \begin{bmatrix} 0 & -1 & -1 & -1 & 1 & -1 & 1 & 1 & 1 \end{bmatrix}^T$$

$$\sigma_{b1} = \begin{bmatrix} -1 & 1 & 1 & -1 & 1 & 1 & -1 & 1 \end{bmatrix}^T$$

Choosing

$$\tilde{\varkappa}_{b1}^{\delta_1} = [-0.5,\ -0.75,\ 0.75,\ 0.5]^T$$
$$\beta_{b1}^{\delta_1} = [0.514032,\ 0.026438,\ 0.544385,\ 0.200874,\ 0.201162,\ 0.218151,\ 0.29908,\ 0.690439]^T$$
$$\lambda_{b1}^{\delta_1} = [9.5156,\ 0.965879,\ 61.8123,\ 4.92665,\ 19.0766,\ 1,\ 1.99576,\ 0.42886,\ 11.2584,\ 1]^T$$

yields

$$a_{b1}^{\delta_1} = [1,\ 0.067192,\ 0.700742,\ 0.510519,\ 0.180091,\ 0.413451,\ 0.267753,\ 0.108066,\ 1.17544]^T$$
$$b_{b1}^{\delta_1} = [1,\ 0.040754,\ 0.156357,\ 0.309645,\ 0.381253,\ 0.1953,\ 0.566833,\ 0.798505,\ 1.93798]^T$$
$$c_{b1}^{\delta_1} = 2.28964$$
$$k_{b1}^{\delta_1} = [1091.32,\ 18.6391,\ 124.995,\ 497.46,\ 2.33614,\ 149.503,\ 4.92665,\ 4.92665,\ 283.912,\ 21.0766,\ 5.55274,\ 79.1494,\ 7.45372,\ 45.7824,\ 154.335,\ 0.364849,\ 9.57797,\ 9.25361]^T$$

Network (N6.2b2)

$$\mu_1 + \mu_2 = \ln\frac{\nu_1+\nu_3+\nu_9}{\lambda_1+\lambda_3+\lambda_9} \qquad \mu_4 = \ln\frac{\nu_1}{\lambda_1} \qquad \mu_4 = \ln\frac{\nu_3+\nu_9}{\lambda_3+\lambda_9}$$
$$\mu_3 + \mu_5 = \ln\frac{\nu_2+\nu_3}{\lambda_2+\lambda_3} \qquad \mu_6 = \ln\frac{\nu_2}{\lambda_2} \qquad \mu_6 = \ln\frac{\nu_3}{\lambda_3}$$
$$\mu_1 = \ln\frac{\nu_4}{\lambda_4} \qquad 0 = \ln\frac{\nu_4}{\lambda_4} \qquad \mu_2 = \ln\frac{\nu_5}{\lambda_5}$$
$$0 = \ln\frac{\nu_5+\nu_9}{\lambda_5+\lambda_9}$$
$$\mu_1 + \mu_5 = \ln\frac{\nu_6+\nu_8+\nu_9}{\lambda_6+\lambda_8+\lambda_9} \qquad \mu_7 = \ln\frac{\nu_6}{\lambda_6} \qquad \mu_7 = \ln\frac{\nu_8+\nu_9}{\lambda_8+\lambda_9}$$
$$\mu_3 + \mu_8 = \ln\frac{\nu_7+\nu_8}{\lambda_7+\lambda_8} \qquad \mu_9 = \ln\frac{\nu_7}{\lambda_7} \qquad \mu_9 = \ln\frac{\nu_8}{\lambda_8}$$
$$\mu_8 = \ln\frac{\nu_9}{\lambda_9}$$

$$\varkappa_1 = \ln\frac{\nu_1+\nu_3+\nu_9}{\lambda_1+\lambda_3+\lambda_9} = \ln\frac{\nu_1}{\lambda_1} = \ln\frac{\nu_3+\nu_9}{\lambda_3+\lambda_9}$$
$$\varkappa_2 = \ln\frac{\nu_2+\nu_3}{\lambda_2+\lambda_3} = \ln\frac{\nu_2}{\lambda_2} = \ln\frac{\nu_3}{\lambda_3}$$
$$\varkappa_3 = \ln\frac{\nu_5}{\lambda_5}$$
$$\varkappa_4 = \ln\frac{\nu_6+\nu_8+\nu_9}{\lambda_6+\lambda_8+\lambda_9} = \ln\frac{\nu_6}{\lambda_6} = \ln\frac{\nu_8+\nu_9}{\lambda_8+\lambda_9}$$

$$\varkappa_5 = \ln \frac{\nu_7 + \nu_8}{\lambda_7 + \lambda_8} = \ln \frac{\nu_7}{\lambda_7} = \ln \frac{\nu_8}{\lambda_8}$$
$$\varkappa_6 = \ln \frac{\nu_9}{\lambda_9}$$

$$\mu_1 = 0 \qquad \mu_2 = \varkappa_3$$
$$\mu_4 = \varkappa_1 \qquad \mu_6 = \varkappa_2$$
$$\mu_7 = \varkappa_4 \qquad \mu_8 = \varkappa_6$$
$$\mu_9 = \varkappa_5$$

$$\mu_1 + \mu_2 = \varkappa_1 \tag{B.12}$$
$$\mu_3 + \mu_5 = \varkappa_2 \tag{B.13}$$
$$\mu_1 + \mu_5 = \varkappa_4 \tag{B.14}$$
$$\mu_3 + \mu_8 = \varkappa_5 \tag{B.15}$$

Equations (B.13)–(B.15) yields

$$\varkappa_6 = -\varkappa_2 + \varkappa_4 + \varkappa_5$$

and thus, equation (B.12) yields

$$\varkappa_3 = \varkappa_1$$

$$\nu_1 = \exp(\varkappa_1)\,\lambda_1$$
$$\nu_2 = \exp(\varkappa_2)\,\lambda_2 \qquad \nu_3 = \exp(\varkappa_2)\,\lambda_3$$
$$\nu_4 = \lambda_4$$
$$\nu_5 = \exp(\varkappa_3)\,\lambda_5$$
$$\nu_6 = \exp(\varkappa_4)\,\lambda_6$$
$$\nu_7 = \exp(\varkappa_5)\,\lambda_7 \qquad \nu_8 = \exp(\varkappa_5)\,\lambda_8$$
$$\nu_9 = \exp(\varkappa_6)\,\lambda_9$$

$$0 = (\exp(\varkappa_2) - \exp(\varkappa_1))\ \lambda_3 + (\exp(-\varkappa_2 + \varkappa_4 + \varkappa_5) - \exp(\varkappa_1))\ \lambda_9$$
$$0 = (\exp(\varkappa_1) - 1)\ \lambda_5 + (\exp(-\varkappa_2 + \varkappa_4 + \varkappa_5) - 1)\ \lambda_9$$
$$0 = (\exp(\varkappa_5) - \exp(\varkappa_4))\ \lambda_8 + (\exp(-\varkappa_2 + \varkappa_4 + \varkappa_5) - \exp(\varkappa_4))\ \lambda_9$$

$$\tilde{\varkappa}_{b2} = [\varkappa_1\ \ \varkappa_2\ \ \varkappa_4\ \ \varkappa_5]^T$$
$$\tilde{\lambda}_{b2} = [\lambda_3\ \ \lambda_5\ \ \lambda_8\ \ \lambda_9]^T$$

$$M_{b2} = \begin{bmatrix} 0 & 0 & 0 & 0 \\ 1 & 0 & 0 & 0 \\ 0 & 1 & -1 & 0 \\ 1 & 0 & 0 & 0 \\ 0 & 0 & 1 & 0 \\ 0 & 1 & 0 & 0 \\ 0 & 0 & 1 & 0 \\ 0 & -1 & 1 & 1 \\ 0 & 0 & 0 & 1 \end{bmatrix}$$

$$Q_{b2} = \begin{bmatrix} q_{11} & 0 & 0 & q_{12} \\ 0 & q_{21} & 0 & q_{22} \\ 0 & 0 & q_{31} & q_{32} \end{bmatrix}$$

with

$$\begin{aligned} q_{11} &= -\exp(\varkappa_1) + \exp(\varkappa_2) \\ q_{12} &= -\exp(\varkappa_1) + \exp(-\varkappa_2 + \varkappa_4 + \varkappa_5) \\ q_{21} &= -1 + \exp(\varkappa_1) \\ q_{22} &= -1 + \exp(-\varkappa_2 + \varkappa_4 + \varkappa_5) \\ q_{31} &= -\exp(\varkappa_4) + \exp(\varkappa_5) \\ q_{32} &= -\exp(\varkappa_4) + \exp(-\varkappa_2 + \varkappa_4 + \varkappa_5) \end{aligned}$$

$$K_{b2} = \begin{bmatrix} -1 & 1 & 0 & 0 \\ -1 & -1 & 1 & 1 \\ 1 & 0 & 0 & 0 \\ 0 & -1 & 1 & 1 \\ 0 & 0 & -1 & 1 \\ 0 & -1 & 0 & 1 \end{bmatrix}$$

$$\delta_{b2} = \begin{bmatrix} 0 & -1 & -1 & -1 & 1 & -1 & 1 & 1 & 1 \end{bmatrix}^T$$

$$\sigma_{b2} = \begin{bmatrix} -1 & 1 & -1 & 1 & -1 & 1 \end{bmatrix}^T$$

Choosing

$$\begin{aligned} \tilde{\varkappa}_{b2}^{\delta_1} &= [-0.5,\ -0.75,\ 0.75,\ 0.5]^T \\ \beta_{b2}^{\delta_1} &= [0.1836,\ 0.1189,\ 0.995388,\ 0.297905,\ 0.876835,\ 0.13933, \\ &\quad 0.356146,\ 0.863183]^T \\ \lambda_{b2}^{\delta_1} &= [1.75872,\ 2.69681,\ 50.5539,\ 9.24765,\ 16.2377,\ 5.11683, \\ &\quad 4.91143,\ 11.2584\ 1]^T \end{aligned}$$

yields

$$a_{b2}^{\delta_1} = [1,\ 0.302183,\ 1.28128,\ 0.757124,\ 0.784991,\ 0.264065,\ 0.318842,\ 0.135103,\ 1.74916]^T$$
$$b_{b2}^{\delta_1} = [1,\ 0.183283,\ 0.285892,\ 0.459219,\ 1.66183,\ 0.124736,\ 0.674988,\ 0.998286,\ 2.88388]^T$$
$$c_{b2}^{\delta_1} = 3.2945$$
$$k_{b2}^{\delta_1} = [176.425,\ 2.32289,\ 68.0918,\ 52.944,\ 10.2127,\ 191.445,\ 9.24765,\ 9.24765,\ 53.7349,\ 17.2377,\ 22.1343,\ 16.0482,\ 38.4466,\ 93.4103,\ 2.80788,\ 6.43645,\ 7.40174]^T$$

Networ (N6.2b3)

$$\mu_1 + \mu_2 = \ln\frac{\nu_1+\nu_3+\nu_5+\nu_9}{\lambda_1+\lambda_3+\lambda_5+\lambda_9} \quad \mu_4 = \ln\frac{\nu_1}{\lambda_1} \quad \mu_4 = \ln\frac{\nu_3+\nu_5+\nu_9}{\lambda_3+\lambda_5+\lambda_9}$$
$$\mu_3 + \mu_5 = \ln\frac{\nu_2+\nu_3}{\lambda_2+\lambda_3} \quad \mu_6 = \ln\frac{\nu_2}{\lambda_2} \quad \mu_6 = \ln\frac{\nu_3}{\lambda_3}$$
$$0 = \ln\frac{\nu_4}{\lambda_4} \quad \mu_1 = \ln\frac{\nu_4}{\lambda_4} \quad 0 = \ln\frac{\nu_5+\nu_9}{\lambda_5+\lambda_9}$$
$$\mu_5 = \ln\frac{\nu_5}{\lambda_5}$$
$$\mu_1 + \mu_5 = \ln\frac{\nu_6+\nu_8+\nu_9}{\lambda_6+\lambda_8+\lambda_9} \quad \mu_7 = \ln\frac{\nu_6}{\lambda_6} \quad \mu_7 = \ln\frac{\nu_8+\nu_9}{\lambda_8+\lambda_9}$$
$$\mu_3 + \mu_8 = \ln\frac{\nu_7+\nu_8}{\lambda_7+\lambda_8} \quad \mu_9 = \ln\frac{\nu_7}{\lambda_7} \quad \mu_9 = \ln\frac{\nu_8}{\lambda_8}$$
$$\mu_8 = \ln\frac{\nu_9}{\lambda_9}$$

$$\varkappa_1 = \ln\frac{\nu_1+\nu_3+\nu_5+\nu_9}{\lambda_1+\lambda_3+\lambda_5+\lambda_9} = \ln\frac{\nu_1}{\lambda_1} = \ln\frac{\nu_3+\nu_5+\nu_9}{\lambda_3+\lambda_5+\lambda_9}$$
$$\varkappa_2 = \ln\frac{\nu_2+\nu_3}{\lambda_2+\lambda_3} = \ln\frac{\nu_2}{\lambda_2} = \ln\frac{\nu_3}{\lambda_3}$$
$$\varkappa_3 = \ln\frac{\nu_5}{\lambda_5}$$
$$\varkappa_4 = \ln\frac{\nu_6+\nu_8+\nu_9}{\lambda_6+\lambda_8+\lambda_9} = \ln\frac{\nu_6}{\lambda_6} = \ln\frac{\nu_8+\nu_9}{\lambda_8+\lambda_9}$$
$$\varkappa_5 = \ln\frac{\nu_7+\nu_8}{\lambda_7+\lambda_8} = \ln\frac{\nu_7}{\lambda_7} = \ln\frac{\nu_8}{\lambda_8}$$
$$\varkappa_6 = \ln\frac{\nu_9}{\lambda_9}$$

$$\mu_1 = 0$$
$$\mu_4 = \varkappa_1$$
$$\mu_6 = \varkappa_2$$
$$\mu_7 = \varkappa_4$$
$$\mu_8 = \varkappa_6$$
$$\mu_9 = \varkappa_5$$

$$\mu_1 + \mu_2 = \varkappa_1 \tag{B.16}$$
$$\mu_3 + \mu_5 = \varkappa_2 \tag{B.17}$$
$$\mu_1 + \mu_5 = \varkappa_4 \tag{B.18}$$
$$\mu_3 + \mu_8 = \varkappa_5 \tag{B.19}$$

Equation (B.17)–(B.19) yield

$$\varkappa_6 = -\varkappa_2 + \varkappa_3 + \varkappa_5$$

and thus from (B.16)

$$\varkappa_4 = \varkappa_3$$

$$\begin{aligned}
\nu_1 &= \exp(\varkappa_1)\,\lambda_1 \\
\nu_2 &= \exp(\varkappa_2)\,\lambda_2 \qquad & \nu_3 &= \exp(\varkappa_2)\,\lambda_3 \\
\nu_4 &= \lambda_4 \\
\nu_5 &= \exp(\varkappa_3)\,\lambda_5 \\
\nu_6 &= \exp(\varkappa_4)\,\lambda_6 \\
\nu_7 &= \exp(\varkappa_5)\,\lambda_7 \qquad & \nu_8 &= \exp(\varkappa_5)\,\lambda_8 \\
\nu_9 &= \exp(\varkappa_6)\,\lambda_9
\end{aligned}$$

$$\begin{aligned}
0 &= (\exp(\varkappa_2) - \exp(\varkappa_1))\,\lambda_3 + (\exp(\varkappa_3) - \exp(\varkappa_1))\,\lambda_5 \\
&\quad + (\exp(-\varkappa_2 + \varkappa_3 + \varkappa_5) - \exp(\varkappa_1))\,\lambda_9 \\
0 &= (\exp(\varkappa_3) - 1)\,\lambda_5 + (\exp(-\varkappa_2 + \varkappa_3 + \varkappa_5) - 1)\,\lambda_9 \\
0 &= (\exp(\varkappa_5) - \exp(\varkappa_3))\,\lambda_8 + (\exp(-\varkappa_2 + \varkappa_3 + \varkappa_5) - \exp(\varkappa_3))\,\lambda_9
\end{aligned}$$

$$\tilde{\varkappa}_{b3} = [\varkappa_1 \;\; \varkappa_2 \;\; \varkappa_3 \;\; \varkappa_5]^T$$
$$\tilde{\lambda}_{b3} = [\lambda_3 \;\; \lambda_5 \;\; \lambda_8 \;\; \lambda_9]^T$$

$$M_{b3} = \begin{bmatrix}
0 & 0 & 0 & 0 \\
1 & 0 & 0 & 0 \\
0 & 1 & -1 & 0 \\
1 & 0 & 0 & 0 \\
0 & 0 & 1 & 0 \\
0 & 1 & 0 & 0 \\
0 & 0 & 1 & 0 \\
0 & -1 & 1 & 1 \\
0 & 0 & 0 & 1
\end{bmatrix}$$

$$Q_{b3} = \begin{bmatrix}
q_{11} & 0 & q_{12} & q_{13} \\
0 & 0 & q_{21} & q_{22} \\
0 & q_{31} & 0 & q_{32}
\end{bmatrix}$$

with

$$
\begin{aligned}
q_{11} &= -\exp(\varkappa_1) + \exp(\varkappa_2)\\
q_{12} &= -\exp(\varkappa_1) + \exp(\varkappa_3)\\
q_{13} &= -\exp(\varkappa_1) + \exp(-\varkappa_2 + \varkappa_3 + \varkappa_5)\\
q_{12} &= -1 + \exp(\varkappa_3)\\
q_{22} &= -1 + \exp(-\varkappa_2 + \varkappa_3 + \varkappa_5)\\
q_{31} &= -\exp(\varkappa_3) + \exp(\varkappa_5)\\
q_{32} &= \exp(\varkappa_3)(-1 + \exp(-\varkappa_2 + \varkappa_5))
\end{aligned}
$$

$$
K_{b3} = \begin{bmatrix}
-1 & 1 & 0 & 0\\
-1 & 0 & 1 & 0\\
-1 & -1 & 1 & 1\\
0 & 0 & 1 & 0\\
0 & -1 & 1 & 1\\
0 & 0 & -1 & 1\\
0 & -1 & 0 & 1
\end{bmatrix}
$$

$$
\delta_{b3} = \begin{bmatrix} 0 & 0 & 0 & 0 & 0 & 0 & 0 & 0 & 0 \end{bmatrix}^T
$$

$$
\sigma_{b3} = \begin{bmatrix} 0 & 0 & 0 & 0 & 0 & 0 & 0 \end{bmatrix}^T
$$

Note, if only the zero sign vector is a valid sign vector, no multiple steady states can be found as $\operatorname{sgn}(mu) = \operatorname{sgn}(s) = 0$ and thus $a = b$.

Network (N6.2b4)

$$
\begin{aligned}
\mu_1 + \mu_2 &= \ln\frac{\nu_1 + \nu_3 + \nu_8}{\lambda_1 + \lambda_3 + \lambda_8} & \mu_4 &= \ln\frac{\nu_1}{\lambda_1} & \mu_4 &= \ln\frac{\nu_3 + \nu_8}{\lambda_3 + \lambda_8}\\
\mu_3 + \mu_5 &= \ln\frac{\nu_2 + \nu_3}{\lambda_2 + \lambda_3} & \mu_6 &= \ln\frac{\nu_2}{\lambda_2} & \mu_6 &= \ln\frac{\nu_3}{\lambda_3}\\
0 &= \ln\frac{\nu_4}{\lambda_4} & \mu_1 &= \ln\frac{\nu_4}{\lambda_4} & 0 &= \ln\frac{\nu_8}{\lambda_8}\\
\mu_1 + \mu_5 &= \ln\frac{\nu_5 + \nu_7 + \nu_8}{\lambda_5 + \lambda_7 + \lambda_8} & \mu_7 &= \ln\frac{\nu_5}{\lambda_5} & \mu_7 &= \ln\frac{\nu_7 + \nu_8}{\lambda_7 + \lambda_8}\\
\mu_3 + \mu_8 &= \ln\frac{\nu_6 + \nu_7}{\lambda_6 + \lambda_7} & \mu_9 &= \ln\frac{\nu_6}{\lambda_6} & \mu_9 &= \ln\frac{\nu_7}{\lambda_7}\\
\mu_8 &= \ln\frac{\nu_8}{\lambda_8}
\end{aligned}
$$

$$
\begin{aligned}
\varkappa_1 &= \ln\frac{\nu_1 + \nu_3 + \nu_8}{\lambda_1 + \lambda_3 + \lambda_8} = \ln\frac{\nu_1}{\lambda_1} = \ln\frac{\nu_3 + \nu_8}{\lambda_3 + \lambda_8}\\
\varkappa_2 &= \ln\frac{\nu_2 + \nu_3}{\lambda_2 + \lambda_3} = \ln\frac{\nu_2}{\lambda_2} = \ln\frac{\nu_3}{\lambda_3}\\
\varkappa_3 &= \ln\frac{\nu_5 + \nu_7 + \nu_8}{\lambda_5 + \lambda_7 + \lambda_8} = \ln\frac{\nu_5}{\lambda_5} = \ln\frac{\nu_7 + \nu_8}{\lambda_7 + \lambda_8}\\
\varkappa_4 &= \ln\frac{\nu_6 + \nu_7}{\lambda_6 + \lambda_7} = \ln\frac{\nu_6}{\lambda_6} = \ln\frac{\nu_7}{\lambda_7}
\end{aligned}
$$

$$
\begin{aligned}
\mu_1 &= 0 \\
\mu_4 &= \varkappa_1 \\
\mu_6 &= \varkappa_2 \\
\mu_7 &= \varkappa_3 \\
\mu_8 &= 0 \\
\mu_9 &= \varkappa_4
\end{aligned}
$$

$$
\begin{aligned}
\mu_1 + \mu_2 &= \varkappa_1 \\
\mu_3 + \mu_5 &= \varkappa_2 \\
\mu_1 + \mu_5 &= \varkappa_3 \\
\mu_3 + \mu_8 &= \varkappa_4
\end{aligned}
\tag{B.20}
$$

Equation (B.20) then yields

$$\varkappa_4 = \varkappa_2 - \varkappa_3.$$

$$
\begin{aligned}
\nu_1 &= \exp(\varkappa_1)\,\lambda_1 \\
\nu_2 &= \exp(\varkappa_2)\,\lambda_2 & \nu_3 &= \exp(\varkappa_2)\,\lambda_3 \\
\nu_4 &= \lambda_4 \\
\nu_5 &= \exp(\varkappa_3)\,\lambda_5 \\
\nu_6 &= \exp(\varkappa_4)\,\lambda_6 & \nu_7 &= \exp(\varkappa_4)\,\lambda_7 \\
\nu_8 &= \lambda_8
\end{aligned}
$$

$$
\begin{aligned}
0 &= (\exp(\varkappa_2) - \exp(\varkappa_1))\ \lambda_3 + (1 - \exp(\varkappa_1))\ \lambda_8 \\
0 &= (\exp(\varkappa_2 - \varkappa_3) - \exp(\varkappa_3))\ \lambda_7 + (1 - \exp(\varkappa_3))\ \lambda_8
\end{aligned}
$$

$$
\begin{aligned}
\tilde{\varkappa}_{b4} &= [\varkappa_1 \ \ \varkappa_2 \ \ \varkappa_3]^T \\
\tilde{\lambda}_{b4} &= [\lambda_3 \ \ \lambda_7 \ \ \lambda_8]^T
\end{aligned}
$$

$$
M_{b4} = \begin{bmatrix}
0 & 0 & 0 \\
1 & 0 & 0 \\
0 & 1 & -1 \\
1 & 0 & 0 \\
0 & 0 & 1 \\
0 & 1 & 0 \\
0 & 0 & 1 \\
0 & 0 & 0 \\
0 & 1 & -1
\end{bmatrix}
$$

$$Q_{b4} = \begin{bmatrix} -\exp(\varkappa_1) + \exp(\varkappa_2) & 0 & 1 - \exp(\varkappa_1) \\ 0 & \exp(\varkappa_2 - \varkappa_3) - \exp(\varkappa_3) & 1 - \exp(\varkappa_3) \end{bmatrix}$$
$$= \begin{bmatrix} q_{11} & 0 & q_{12} \\ 0 & q_{21} & q_{22} \end{bmatrix}$$

$$K_{b4} = \begin{bmatrix} -1 & 1 & 0 \\ -1 & 0 & 0 \\ 0 & 1 & -2 \\ 0 & 0 & -1 \end{bmatrix}$$

$$\delta_{b4} = \begin{bmatrix} 0 & 0 & 0 & 0 & 0 & 0 & 0 & 0 & 0 \end{bmatrix}^T$$

$$\sigma_{b4} = \begin{bmatrix} 0 & 0 & 0 & 0 \end{bmatrix}^T$$

Same results as for network (N6.2b3) apply here, as only $\delta = \underline{0}$ is a valid sign vector to the system.

B.2.3 *Additional Synthesis and Degradation of Enzyme* E_2

Network (N6.2c1)

$$\begin{aligned}
\mu_1 + \mu_2 &= \ln \frac{\nu_1 + \nu_{10} + \nu_3 + \nu_6}{\lambda_1 + \lambda_{10} + \lambda_3 + \lambda_6} & \mu_4 &= \ln \frac{\nu_1}{\lambda_1} & \mu_4 &= \ln \frac{\nu_{10} + \nu_3 + \nu_6}{\lambda_{10} + \lambda_3 + \lambda_6} \\
\mu_3 + \mu_5 &= \ln \frac{\nu_2 + \nu_3}{\lambda_2 + \lambda_3} & \mu_6 &= \ln \frac{\nu_2}{\lambda_2} & \mu_6 &= \ln \frac{\nu_3}{\lambda_3} \\
\mu_2 &= \ln \frac{\nu_4}{\lambda_4} \\
0 &= \ln \frac{\nu_{10} + \nu_4 + \nu_6}{\lambda_{10} + \lambda_4 + \lambda_6} \\
\mu_3 &= \ln \frac{\nu_5}{\lambda_5} \\
0 &= \ln \frac{\nu_5}{\lambda_5} \\
\mu_5 &= \ln \frac{\nu_6}{\lambda_6} \\
\mu_1 + \mu_5 &= \ln \frac{\nu_{10} + \nu_7 + \nu_9}{\lambda_{10} + \lambda_7 + \lambda_9} & \mu_7 &= \ln \frac{\nu_7}{\lambda_7} & \mu_7 &= \ln \frac{\nu_{10} + \nu_9}{\lambda_{10} + \lambda_9} \\
\mu_3 + \mu_8 &= \ln \frac{\nu_8 + \nu_9}{\lambda_8 + \lambda_9} & \mu_9 &= \ln \frac{\nu_8}{\lambda_8} & \mu_9 &= \ln \frac{\nu_9}{\lambda_9} \\
\mu_8 &= \ln \frac{\nu_{10}}{\lambda_{10}}
\end{aligned} \tag{B.21}$$

$$
\begin{aligned}
\varkappa_1 &= \ln \frac{\nu_1 + \nu_{10} + \nu_3 + \nu_6}{\lambda_1 + \lambda_{10} + \lambda_3 + \lambda_6} = \ln \frac{\nu_1}{\lambda_1} = \ln \frac{\nu_{10} + \nu_3 + \nu_6}{\lambda_{10} + \lambda_3 + \lambda_6} \\
\varkappa_2 &= \ln \frac{\nu_2 + \nu_3}{\lambda_2 + \lambda_3} = \ln \frac{\nu_2}{\lambda_2} = \ln \frac{\nu_3}{\lambda_3} \\
\varkappa_3 &= \ln \frac{\nu_4}{\lambda_4} \\
\varkappa_4 &= \ln \frac{\nu_6}{\lambda_6} \\
\varkappa_5 &= \ln \frac{\nu_{10} + \nu_7 + \nu_9}{\lambda_{10} + \lambda_7 + \lambda_9} = \ln \frac{\nu_7}{\lambda_7} = \ln \frac{\nu_{10} + \nu_9}{\lambda_{10} + \lambda_9} \\
\varkappa_6 &= \ln \frac{\nu_8 + \nu_9}{\lambda_8 + \lambda_9} = \ln \frac{\nu_8}{\lambda_8} = \ln \frac{\nu_9}{\lambda_9} \\
\varkappa_7 &= \ln \frac{\nu_{10}}{\lambda_{10}}
\end{aligned}
$$

$$
\begin{aligned}
\mu_2 &= \varkappa_3 & \mu_3 &= 0 \\
\mu_4 &= \varkappa_1 & \mu_5 &= \varkappa_4 \\
\mu_6 &= \varkappa_2 & \mu_7 &= \varkappa_5 \\
\mu_8 &= \varkappa_7 & \mu_9 &= \varkappa_6
\end{aligned}
$$

$$\mu_1 + \mu_2 = \varkappa_1 \tag{B.22}$$
$$\mu_3 + \mu_5 = \varkappa_2 \tag{B.23}$$
$$\mu_1 + \mu_5 = \varkappa_5 \tag{B.24}$$
$$\mu_3 + \mu_8 = \varkappa_6 \tag{B.25}$$

Combining equation (B.22) and (B.24) yields

$$\varkappa_5 = \varkappa_1 + \varkappa_2 - \varkappa_3,$$

furthermore equation (B.23) yields

$$\varkappa_4 = \varkappa_2,$$

and equation (B.25) yields

$$\varkappa_6 = \varkappa_7.$$

Furthermore equation (B.21) yields

$$\varkappa_6 = \varkappa_5$$

$$
\begin{aligned}
\nu_1 &= \exp(\varkappa_1)\,\lambda_1 & & \\
\nu_2 &= \exp(\varkappa_2)\,\lambda_2 & \nu_3 &= \exp(\varkappa_2)\,\lambda_3 \\
\nu_4 &= \exp(\varkappa_3)\,\lambda_4 & & \\
\nu_5 &= \lambda_5 & & \\
\nu_6 &= \exp(\varkappa_4)\,\lambda_6 & & \\
\nu_7 &= \exp(\varkappa_5)\,\lambda_7 & & \\
\nu_8 &= \exp(\varkappa_6)\,\lambda_8 & \nu_9 &= \exp(\varkappa_6)\,\lambda_9 \\
\nu_{10} &= \exp(\varkappa_7)\,\lambda_{10} & &
\end{aligned}
$$

$$
\begin{aligned}
0 &= (\exp(\varkappa_2) - \exp(\varkappa_1))\ \lambda_3 + (\exp(\varkappa_2) - \exp(\varkappa_1))\ \lambda_6 \\
&\quad + (\exp(\varkappa_1 + \varkappa_2 - \varkappa_3) - \exp(\varkappa_1))\ \lambda_{10} \\
0 &= (\exp(\varkappa_3) - 1)\ \lambda_4 + (\exp(\varkappa_2) - 1)\ \lambda_6 + (\exp(\varkappa_1 + \varkappa_2 - \varkappa_3) - 1)\ \lambda_{10}
\end{aligned}
$$

$$
\begin{aligned}
\tilde{\varkappa}_{c1} &= [\varkappa_1 \ \ \varkappa_2 \ \ \varkappa_3]^T \\
\tilde{\lambda}_{c1} &= [\lambda_3 \ \ \lambda_4 \ \ \lambda_6 \ \ \lambda_{10}]^T
\end{aligned}
$$

$$
M_{c1} = \begin{bmatrix}
1 & 0 & -1 \\
0 & 0 & 1 \\
0 & 0 & 0 \\
1 & 0 & 0 \\
0 & 1 & 0 \\
0 & 1 & 0 \\
1 & 1 & -1 \\
1 & 1 & -1 \\
1 & 1 & -1
\end{bmatrix}
$$

$$
Q_{c1} = \begin{bmatrix}
q_{11} & 0 & q_{11} & q_{13} \\
0 & q_{21} & q_{22} & q_{32}
\end{bmatrix}
$$

with

$$
\begin{aligned}
q_{11} &= -\exp(\varkappa_1) + \exp(\varkappa_2) \\
q_{12} &= -\exp(\varkappa_1) + \exp(\varkappa_2) \\
q_{13} &= -\exp(\varkappa_1) + \exp(\varkappa_1 + \varkappa_2 - \varkappa_3) \\
q_{21} &= -1 + \exp(\varkappa_3) \\
q_{22} &= -1 + \exp(\varkappa_2) \\
q_{23} &= -1 + \exp(\varkappa_1 + \varkappa_2 - \varkappa_3)
\end{aligned}
$$

$$
K_{c1} = \begin{bmatrix}
-1 & 1 & 0 \\
-1 & 1 & 0 \\
0 & 1 & -1 \\
0 & 0 & 1 \\
0 & 1 & 0 \\
1 & 1 & -1
\end{bmatrix}
$$

$$
\delta_{c1} = \begin{bmatrix} -1 & 1 & 0 & 1 & 1 & 1 & -1 & -1 & -1 \end{bmatrix}^T
$$

$$
\sigma_{c1} = \begin{bmatrix} 1 & 1 & -1 & 1 & 1 & -1 \end{bmatrix}^T
$$

Choosing

$$\tilde{\varkappa}_{c1}^{\delta_1} = [0.2,\ 0.5,\ 0.8]^T$$
$$\beta_{c1}^{\delta_1} = [0.842524,\ 0.283754,\ 0.568224,\ 0.904543,\ 0.629725,\ 0.313306,\ 0.852005,\ 0.984639]^T$$

with an additional condition of

$$\lambda_{10} > 6.81698\,\lambda_6$$

and thus

$$\lambda_{c1}^{\delta_1} = [0.243565,\ 5.39844,\ 6.40818,\ 0.24716,\ 6.38347,\ 1,\ 7.04565,\ 0.211258,\ 4.51445\ 10]^T$$

the following steady states and parameter can be given

$$a_{c1}^{\delta_1} = [1.86734,\ 0.231534,\ 1,\ 5.22048,\ 1.39435,\ 0.970718,\ 3.29232,\ 8.95315,\ 10.3469]^T$$
$$b_{c1}^{\delta_1} = [1.02482,\ 0.515288,\ 1,\ 6.37631,\ 2.29889,\ 1.60044,\ 2.97901,\ 8.10115,\ 9.36227]^T$$
$$c_{c1}^{\delta_1} = 10.3801$$
$$k_{c1}^{\delta_1} = [40.8272,\ 0.0466556,\ 3.33459,\ 8.46749,\ 5.56129,\ 6.60149,\ 1.06749,\ 11.2472,\ 6.38347,\ 6.38347,\ 0.717181,\ 8.28048,\ 2.14003,\ 4.40858,\ 0.527827,\ 0.0204175,\ 0.436309,\ 1.11692]^T$$

Network (№6.2c2)

$$\begin{aligned}
\mu_1 + \mu_2 &= \ln\frac{\nu_1+\nu_3+\nu_9}{\lambda_1+\lambda_3+\lambda_9} & \mu_4 &= \ln\frac{\nu_1}{\lambda_1} & \mu_4 &= \ln\frac{\nu_3+\nu_9}{\lambda_3+\lambda_9}\\
\mu_3 + \mu_5 &= \ln\frac{\nu_2+\nu_3}{\lambda_2+\lambda_3} & \mu_6 &= \ln\frac{\nu_2}{\lambda_2} & \mu_6 &= \ln\frac{\nu_3}{\lambda_3}\\
\mu_2 &= \ln\frac{\nu_4}{\lambda_4} & & & & \\
0 &= \ln\frac{\nu_4+\nu_9}{\lambda_4+\lambda_9} & & & & \\
\mu_3 &= \ln\frac{\nu_5}{\lambda_5} & 0 &= \ln\frac{\nu_5}{\lambda_5} & & \\
\mu_1 + \mu_5 &= \ln\frac{\nu_6+\nu_8+\nu_9}{\lambda_6+\lambda_8+\lambda_9} & \mu_7 &= \ln\frac{\nu_6}{\lambda_6} & \mu_7 &= \ln\frac{\nu_8+\nu_9}{\lambda_8+\lambda_9}\\
\mu_3 + \mu_8 &= \ln\frac{\nu_7+\nu_8}{\lambda_7+\lambda_8} & \mu_9 &= \ln\frac{\nu_7}{\lambda_7} & \mu_9 &= \ln\frac{\nu_8}{\lambda_8}\\
\mu_8 &= \ln\frac{\nu_9}{\lambda_9} & & & &
\end{aligned} \tag{B.26}$$

$$\varkappa_1 = \ln \frac{\nu_1 + \nu_3 + \nu_9}{\lambda_1 + \lambda_3 + \lambda_9} = \ln \frac{\nu_1}{\lambda_1} = \ln \frac{\nu_3 + \nu_9}{\lambda_3 + \lambda_9}$$
$$\varkappa_2 = \ln \frac{\nu_2 + \nu_3}{\lambda_2 + \lambda_3} = \ln \frac{\nu_2}{\lambda_2} = \ln \frac{\nu_3}{\lambda_3}$$
$$\varkappa_3 = \ln \frac{\nu_4}{\lambda_4}$$
$$\varkappa_4 = \ln \frac{\nu_6 + \nu_8 + \nu_9}{\lambda_6 + \lambda_8 + \lambda_9} = \ln \frac{\nu_6}{\lambda_6} = \ln \frac{\nu_8 + \nu_9}{\lambda_8 + \lambda_9}$$
$$\varkappa_5 = \ln \frac{\nu_7 + \nu_8}{\lambda_7 + \lambda_8} = \ln \frac{\nu_7}{\lambda_7} = \ln \frac{\nu_8}{\lambda_8}$$
$$\varkappa_6 = \ln \frac{\nu_9}{\lambda_9}$$

$$\mu_2 = \varkappa_3 \qquad \mu_3 = 0$$
$$\mu_4 = \varkappa_1 \qquad \mu_6 = \varkappa_2$$
$$\mu_7 = \varkappa_4 \qquad \mu_8 = \varkappa_6$$
$$\mu_9 = \varkappa_5$$

$$\mu_1 + \mu_2 = \varkappa_1 \tag{B.27}$$
$$\mu_3 + \mu_5 = \varkappa_2 \tag{B.28}$$
$$\mu_1 + \mu_5 = \varkappa_4 \tag{B.29}$$
$$\mu_3 + \mu_8 = \varkappa_5 \tag{B.30}$$

Equation (B.30) yields

$$\varkappa_5 = \varkappa_6,$$

and equation (B.27) and (B.29) yield

$$\varkappa_4 = \varkappa_1 + \varkappa_2 - \varkappa_3.$$

Furthermore equation (B.26) yields

$$\varkappa_5 = \varkappa_1 + \varkappa_2 - \varkappa_3$$

$$\nu_1 = \exp(\varkappa_1)\,\lambda_1$$
$$\nu_2 = \exp(\varkappa_2)\,\lambda_2 \qquad \nu_3 = \exp(\varkappa_2)\,\lambda_3$$
$$\nu_4 = \exp(\varkappa_3)\,\lambda_4$$
$$\nu_5 = \lambda_5$$
$$\nu_6 = \exp(\varkappa_4)\,\lambda_6$$
$$\nu_7 = \exp(\varkappa_5)\,\lambda_7 \qquad \nu_8 = \exp(\varkappa_5)\,\lambda_8$$
$$\nu_9 = \exp(\varkappa_6)\,\lambda_9$$

$$0 = (\exp(\varkappa_2 - \exp(\varkappa_1)))\,\lambda_3 + (\exp(\varkappa_1 + \varkappa_2 - \varkappa_3) - \exp(\varkappa_1))\,\lambda_9$$
$$0 = (\exp(\varkappa_3 - 1))\,\lambda_4 + (\exp(\varkappa_1 + \varkappa_2 - \varkappa_3) - 1)\,\lambda_9$$

$$\tilde{\varkappa}_{c2} = [\varkappa_1 \;\; \varkappa_2 \;\; \varkappa_3]^T$$
$$\tilde{\lambda}_{c2} = [\lambda_3 \;\; \lambda_4 \;\; \lambda_9]^T$$

$$M_{c2} = \begin{bmatrix} 1 & 0 & -1 \\ 0 & 0 & 1 \\ 0 & 0 & 0 \\ 1 & 0 & 0 \\ 0 & 1 & 0 \\ 0 & 1 & 0 \\ 1 & 1 & -1 \\ 1 & 1 & -1 \\ 1 & 1 & -1 \end{bmatrix}$$

$$Q_{c2} = \begin{bmatrix} q_{11} & 0 & q_{12} \\ 0 & q_{21} & q_{22} \end{bmatrix}$$

with

$$q_{11} = -\exp(\varkappa_1) + \exp(\varkappa_2)$$
$$q_{12} = -\exp(\varkappa_1) + \exp(\varkappa_1 + \varkappa_2 - \varkappa_3)$$
$$q_{21} = -1 + \exp(\varkappa_3)$$
$$q_{22} = -1 + \exp(\varkappa_1 + \varkappa_2 - \varkappa_3)$$

$$K_{c2} = \begin{bmatrix} -1 & 1 & 0 \\ 0 & 1 & -1 \\ 0 & 0 & 1 \\ 1 & 1 & -1 \end{bmatrix}$$

$$\delta_{c2} = \begin{bmatrix} -1 & 1 & 0 & 1 & 1 & 1 & -1 & -1 & -1 \end{bmatrix}^T$$

$$\sigma_{c2} = \begin{bmatrix} 1 & -1 & 1 & -1 \end{bmatrix}^T$$

Choosing

$$\tilde{\varkappa}_{c2}^{\delta_1} = [0.2,\; 0.5,\; 0.8]^T$$
$$\beta_{c2}^{\delta_1} = [0.116211,\; 0.586789,\; 0.897889,\; 0.909449,\; 0.410328,\; 0.917537,\; 0.647233,\; 0.822854]^T$$
$$\lambda_{c2}^{\delta_1} = [2.89629,\; 5.89607,\; 0.74082,\; 0.07765,\; 2.32315,\; 4.41779,\; 4.94928,\; 8.24542,\; 1]^T$$

yields

$$
\begin{aligned}
a_{c2}^{\delta_1} &= [0.257567,\ 0.4788,\ 1,\ 4.66909,\ 1.40191,\ 0.632519,\ 9.64179,\\
&\quad 6.80134,\ 8.64682]^T\\
b_{c2}^{\delta_1} &= [0.141356,\ 1.06559,\ 1,\ 5.70284,\ 2.31136,\ 1.04285,\ 8.72425,\\
&\quad 6.15411,\ 7.82397]^T\\
c_{c2}^{\delta_1} &= 14.5684\\
k_{c2}^{\delta_1} &= [37.6013,\ 0.620312,\ 0.372839,\ 4.73417, 9.32157, 1.17122,\\
&\quad 0.162175,\ 1.07765,\ 2.32315,\ 2.32315,\ 37.8392,\ 0.458193,\\
&\quad 0.95889,\ 1.94001,\ 0.572381,\ 0.953577,\ 0.14703]^T
\end{aligned}
$$

Network (N6.2c3)

$$
\begin{aligned}
\mu_1 + \mu_2 &= \ln\frac{\nu_1+\nu_3+\nu_5+\nu_9}{\lambda_1+\lambda_3+\lambda_5+\lambda_9} & \mu_4 &= \ln\frac{\nu_1}{\lambda_1} & \mu_4 &= \ln\frac{\nu_3+\nu_5+\nu_9}{\lambda_3+\lambda_5+\lambda_9}\\
\mu_3 + \mu_5 &= \ln\frac{\nu_2+\nu_3}{\lambda_2+\lambda_3} & \mu_6 &= \ln\frac{\nu_2}{\lambda_2} & \mu_6 &= \ln\frac{\nu_3}{\lambda_3}\\
0 &= \ln\frac{\nu_5+\nu_9}{\lambda_5+\lambda_9} & & & & \qquad\qquad (B.31)\\
\mu_3 &= \ln\frac{\nu_4}{\lambda_4} & 0 &= \ln\frac{\nu_4}{\lambda_4} & \mu_5 &= \ln\frac{\nu_5}{\lambda_5}\\
\mu_1 + \mu_5 &= \ln\frac{\nu_6+\nu_8+\nu_9}{\lambda_6+\lambda_8+\lambda_9} & \mu_7 &= \ln\frac{\nu_6}{\lambda_6} & \mu_7 &= \ln\frac{\nu_8+\nu_9}{\lambda_8+\lambda_9}\\
\mu_3 + \mu_8 &= \ln\frac{\nu_7+\nu_8}{\lambda_7+\lambda_8} & \mu_9 &= \ln\frac{\nu_7}{\lambda_7} & \mu_9 &= \ln\frac{\nu_8}{\lambda_8}\\
\mu_8 &= \ln\frac{\nu_9}{\lambda_9}
\end{aligned}
$$

$$
\begin{aligned}
\varkappa_1 &= \ln\frac{\nu_1+\nu_3+\nu_5+\nu_9}{\lambda_1+\lambda_3+\lambda_5+\lambda_9} = \ln\frac{\nu_1}{\lambda_1} = \ln\frac{\nu_3+\nu_5+\nu_9}{\lambda_3+\lambda_5+\lambda_9}\\
\varkappa_2 &= \ln\frac{\nu_2+\nu_3}{\lambda_2+\lambda_3} = \ln\frac{\nu_2}{\lambda_2} = \ln\frac{\nu_3}{\lambda_3}\\
\varkappa_3 &= \ln\frac{\nu_5}{\lambda_5}\\
\varkappa_4 &= \ln\frac{\nu_6+\nu_8+\nu_9}{\lambda_6+\lambda_8+\lambda_9} = \ln\frac{\nu_6}{\lambda_6} = \ln\frac{\nu_8+\nu_9}{\lambda_8+\lambda_9}\\
\varkappa_5 &= \ln\frac{\nu_7+\nu_8}{\lambda_7+\lambda_8} = \ln\frac{\nu_7}{\lambda_7} = \ln\frac{\nu_8}{\lambda_8}\\
\varkappa_6 &= \ln\frac{\nu_9}{\lambda_9}
\end{aligned}
$$

$$
\begin{aligned}
\mu_3 &= 0 & \mu_4 &= \varkappa_1\\
\mu_5 &= \varkappa_3 & \mu_6 &= \varkappa_2\\
\mu_7 &= \varkappa_4 & \mu_8 &= \varkappa_6\\
\mu_9 &= \varkappa_5
\end{aligned}
$$

$$\mu_1 + \mu_2 = \varkappa_1$$
$$\mu_3 + \mu_5 = \varkappa_2 \tag{B.32}$$
$$\mu_1 + \mu_5 = \varkappa_4$$
$$\mu_3 + \mu_8 = \varkappa_5 \tag{B.33}$$

Equation (B.32)

$$\varkappa_3 = \varkappa_2,$$

and (B.33) yields

$$\varkappa_6 = \varkappa_4,$$

furthermore equation (B.31) yields

$$\varkappa_5 = \varkappa_4.$$

$$\begin{aligned}
\nu_1 &= \exp(\varkappa_1)\,\lambda_1 \\
\nu_2 &= \exp(\varkappa_2)\,\lambda_2 & \nu_3 &= \exp(\varkappa_2)\,\lambda_3 \\
\nu_4 &= \lambda_4 \\
\nu_5 &= \exp(\varkappa_3)\,\lambda_5 \\
\nu_6 &= \exp(\varkappa_4)\,\lambda_6 \\
\nu_7 &= \exp(\varkappa_5)\,\lambda_7 & \nu_8 &= \exp(\varkappa_5)\,\lambda_8 \\
\nu_9 &= \exp(\varkappa_6)\,\lambda_9
\end{aligned}$$

$$\begin{aligned}
0 &= (\exp(\varkappa_2) - \exp(\varkappa_1))\ \lambda_3 + (\exp(\varkappa_2) - \exp(\varkappa_1))\ \lambda_5 \\
&\quad + (\exp(\varkappa_4) - \exp(\varkappa_1))\ \lambda_9 \\
0 &= (\exp(\varkappa_2) - 1)\ \lambda_5 + (\exp(\varkappa_4) - 1)\ \lambda_9
\end{aligned}$$

$$\begin{aligned}
\tilde{\varkappa}_{c3} &= [\varkappa_1 \ \ \varkappa_2 \ \ \varkappa_4]^T \\
\tilde{\lambda}_{c3} &= [\lambda_3 \ \ \lambda_5 \ \ \lambda_9]^T
\end{aligned}$$

$$M_{c3} = \begin{bmatrix}
0 & -1 & 1 \\
1 & 1 & -1 \\
0 & 0 & 0 \\
1 & 0 & 0 \\
0 & 1 & 0 \\
0 & 1 & 0 \\
0 & 0 & 1 \\
0 & 0 & 1 \\
0 & 0 & 1
\end{bmatrix}$$

$$Q_{c3} = \begin{bmatrix} q_{11} & q_{11} & q_{12} \\ 0 & q_{21} & q_{22} \end{bmatrix}$$

with

$$q_{11} = -\exp(\varkappa_1) + \exp(\varkappa_2) \qquad q_{12} = -\exp(\varkappa_1) + \exp(\varkappa_4)$$
$$q_{21} = -1 + \exp(\varkappa_2) \qquad q_{22} = -1 + \exp(\varkappa_4)$$

$$K_{c3} = \begin{bmatrix} -1 & 1 & 0 \\ -1 & 1 & 0 \\ -1 & 0 & 1 \\ 0 & 1 & 0 \\ 0 & 0 & 1 \end{bmatrix}$$

$$\delta_{c3} = \begin{bmatrix} -1 & 1 & 0 & 1 & 1 & 1 & -1 & -1 & -1 \end{bmatrix}^T$$

$$\sigma_{c3} = \begin{bmatrix} 1 & 1 & -1 & 1 & -1 \end{bmatrix}^T$$

Choosing

$$\tilde{\varkappa}_{c3}^{\delta_1} = [0.5,\ 0.75,\ -0.5]^T$$
$$\beta_{c3}^{\delta_1} = [0.858816,\ 0.0459736,\ 0.816562,\ 0.245334,\ 0.974303,\ 0.878165,\ 0.163494,\ 0.6968261]^T$$
$$\lambda_{c3}^{\delta_1} = [7.21801,\ 6.62893,\ 1.87332,\ 3.58024,\ 0.35226,\ 7.07666,,\ 5.71935,\ 0.961662,\ 1]^T$$

yields

$$a_{c3}^{\delta_1} = [0.54762,\ 0.144533,\ 1,\ 0.883383,\ 0.0857965,\ 0.794956,\ 0.463429,\ 1.85948,\ 2.00634]^T$$
$$b_{c3}^{\delta_1} = [0.156896,\ 0.831732,\ 1, 1.45645,\ 0.181631,\ 1.68292,\ 0.281084,\ 1.12783,\ 1.21691]^T$$
$$c_{c3}^{\delta_1} = 1.89443$$
$$k_{c3}^{\delta_1} = [118.76,\ 6.98925,\ 3.65139,\ 111.407,\ 9.66726,\ 2.35651,\ 1.35226,\ 0.205306,\ 0.205306,\ 4.10571,\ 318.876,\ 14.6554,\ 17.6733,\ 7.32318,\ 3.20335,\ 3.58379,\ 0.537785]^T$$

Network (N6.2c4)

$$
\begin{aligned}
\mu_1+\mu_2 &= \ln\frac{\nu_1+\nu_3+\nu_8}{\lambda_1+\lambda_3+\lambda_8} & \mu_4 &= \ln\frac{\nu_1}{\lambda_1} & \mu_4 &= \ln\frac{\nu_3+\nu_8}{\lambda_3+\lambda_8}\\
\mu_3+\mu_5 &= \ln\frac{\nu_2+\nu_3}{\lambda_2+\lambda_3} & \mu_6 &= \ln\frac{\nu_2}{\lambda_2} & \mu_6 &= \ln\frac{\nu_3}{\lambda_3}\\
0 &= \ln\frac{\nu_8}{\lambda_8} & \mu_3 &= \ln\frac{\nu_4}{\lambda_4} & 0 &= \ln\frac{\nu_4}{\lambda_4}\\
\mu_1+\mu_5 &= \ln\frac{\nu_5+\nu_7+\nu_8}{\lambda_5+\lambda_7+\lambda_8} & \mu_7 &= \ln\frac{\nu_5}{\lambda_5}\\
\mu_7 &= \ln\frac{\nu_7+\nu_8}{\lambda_7+\lambda_8}\\
\mu_3+\mu_8 &= \ln\frac{\nu_6+\nu_7}{\lambda_6+\lambda_7} & \mu_9 &= \ln\frac{\nu_6}{\lambda_6} & \mu_9 &= \ln\frac{\nu_7}{\lambda_7}\\
\mu_8 &= \ln\frac{\nu_8}{\lambda_8}
\end{aligned}
\tag{B.34}
$$

$$
\begin{aligned}
\varkappa_1 &= \ln\frac{\nu_1+\nu_3+\nu_8}{\lambda_1+\lambda_3+\lambda_8} = \ln\frac{\nu_1}{\lambda_1} = \ln\frac{\nu_3+\nu_8}{\lambda_3+\lambda_8}\\
\varkappa_2 &= \ln\frac{\nu_2+\nu_3}{\lambda_2+\lambda_3} = \ln\frac{\nu_2}{\lambda_2} = \ln\frac{\nu_3}{\lambda_3}\\
\varkappa_3 &= \ln\frac{\nu_5+\nu_7+\nu_8}{\lambda_5+\lambda_7+\lambda_8} = \ln\frac{\nu_5}{\lambda_5} = \ln\frac{\nu_7+\nu_8}{\lambda_7+\lambda_8}\\
\varkappa_4 &= \ln\frac{\nu_6+\nu_7}{\lambda_6+\lambda_7} = \ln\frac{\nu_6}{\lambda_6} = \ln\frac{\nu_7}{\lambda_7}
\end{aligned}
$$

$$
\begin{aligned}
\mu_3 &= 0 & \mu_4 &= \varkappa_1\\
\mu_6 &= \varkappa_2 & \mu_7 &= \varkappa_3\\
\mu_8 &= 0 & \mu_9 &= \varkappa_4
\end{aligned}
$$

$$
\begin{aligned}
\mu_1+\mu_2 &= \varkappa_1\\
\mu_3+\mu_5 &= \varkappa_2\\
\mu_1+\mu_5 &= \varkappa_3\\
\mu_3+\mu_8 &= \varkappa_4
\end{aligned}
\tag{B.35}
$$

Equation (B.35) yields

$$\varkappa_4 = 0,$$

and equation (B.34) yields

$$\varkappa_3 = 0.$$

$$
\begin{aligned}
\nu_1 &= \exp(\varkappa_1)\,\lambda_1\\
\nu_2 &= \exp(\varkappa_2)\,\lambda_2 & \nu_3 &= \exp(\varkappa_2)\,\lambda_3\\
\nu_4 &= \lambda_4\\
\nu_5 &= \exp(\varkappa_3)\,\lambda_5\\
\nu_6 &= \exp(\varkappa_4)\,\lambda_6 & \nu_7 &= \exp(\varkappa_4)\,\lambda_7\\
\nu_8 &= \lambda_8
\end{aligned}
$$

$$0 = (\exp(\varkappa_2) - \exp(\varkappa_1))\ \lambda_3 + (\exp(\varkappa_1) - 1)\ \lambda_8$$

$$\tilde{\varkappa}_{c4} = [\varkappa_1 \ \ \varkappa_2]^T$$
$$\tilde{\lambda}_{c4} = [\lambda_3 \ \ \lambda_8]^T$$

$$M_{c4} = \begin{bmatrix} 0 & -1 \\ 1 & 1 \\ 0 & 0 \\ 1 & 0 \\ 0 & 1 \\ 0 & 1 \\ 0 & 0 \\ 0 & 0 \\ 0 & 0 \end{bmatrix}$$

$$\begin{aligned} Q_{c4} &= \begin{bmatrix} -\exp(\varkappa_1) + \exp(\varkappa_2) & 1 - \exp(\varkappa_1) \end{bmatrix} \\ &= \begin{bmatrix} q_{11} & q_{12} \end{bmatrix} \end{aligned}$$

$$K_{c4} = \begin{bmatrix} -1 & 1 \\ -1 & 0 \end{bmatrix}$$

Results for the system can be given by:

$$\delta_{c4} = \begin{bmatrix} -1 & 1 & 0 & 1 & 1 & 1 & 0 & 0 & 0 \end{bmatrix}^T$$

$$\sigma_{c4} = \begin{bmatrix} 1 & -1 \end{bmatrix}^T$$

Choosing

$$\begin{aligned} \tilde{\varkappa}_{c4}^{\delta_1} &= [0.5,\ 0.75]^T \\ \beta_{c4}^{\delta_1} &= [0.0164385,\ 0.17352,\ 0.734814,\ 0.702408,\ 0.207469,\ 0.11047, \\ &\quad 0.749789,\ 0.452581]^T \\ \lambda_{c4}^{\delta_1} &= [7.42513,\ 0.293478,\ 1.38533,\ 2.24759,\ 8.93328,\ 5.1864, \\ &\quad 0.325866,\ 1]^T \end{aligned}$$

yields

$$
\begin{aligned}
a_{c4}^{\delta_1} &= [0.0311552,\ 0.0696773,\ 1,\ 0.0253399,\ 0.628835,\ 0.185738,\\
&\quad 1,\ 1,\ 1]^T\\
b_{c4}^{\delta_1} &= [0.0147167,\ 0.243198,\ 1,\ 0.0417784,\ 1.33124,\ 0.393207,\\
&\quad 1,\ 1,\ 1]^T\\
c_{c4}^{\delta_1} &= 1.0565\\
k_{c4}^{\delta_1} &= [4519.27,\ 293.022,\ 94.1335,\ 2.66972,\ 1.58007,\ 7.45853,\\
&\quad 1,\ 2.24759,\ 2.24759,\ 523.654,\ 8.93328,\ 1.32587,\\
&\quad 5.51227,\ 5.1864,\ 0.325866,\ 1]^T
\end{aligned}
$$

B.2.4 *Synthesis and Degradation of Proteins and Enzymes*

Additional versions for synthesis and degradation of proteins and enzymes to network (N6.1) are possible. The following version includes synthesis and/or degradation of the protein A together with both enzymes:

$$A \rightleftharpoons 0 \qquad K \rightleftharpoons 0 \qquad P \rightleftharpoons 0 \qquad\qquad\qquad (\mathcal{N}A.1a)$$

$$A \rightleftharpoons 0 \qquad K \rightleftharpoons 0 \qquad P \rightleftharpoons 0 \qquad A_P \longrightarrow 0 \longleftarrow A_{2P} \qquad (\mathcal{N}A.1b)$$

$$A \rightleftharpoons 0 \qquad K \rightleftharpoons 0 \qquad P \rightleftharpoons 0 \qquad 0 \longleftarrow A_{2P} \qquad (\mathcal{N}A.1c)$$

$$A \longleftarrow 0 \qquad K \rightleftharpoons 0 \qquad P \rightleftharpoons 0 \qquad A_P \longrightarrow 0 \longleftarrow A_{2P} \qquad (\mathcal{N}A.1d)$$

$$A \longleftarrow 0 \qquad K \rightleftharpoons 0 \qquad P \rightleftharpoons 0 \qquad 0 \longleftarrow A_{2P} \qquad (\mathcal{N}A.1e)$$

The network itself is completely open without any conservation relation. The first scenario ($\mathcal{N}A.1a$) results in

$$\mu_{10a} = \underline{0}$$

thus yielding only one steady state $a = b$. With an open network any state of the system corresponds to the steady state, compare also (5.50) on page 53.

B.2.5 *Synthesis and Degradation of Enzymes*

A scenario considering only synthesis and degradation of the enzymes but not the unphosphorylated form of the protein with

$$K \rightleftharpoons 0 \qquad P \rightleftharpoons 0 \qquad\qquad\qquad (\mathcal{N}A.2a)$$

$$K \rightleftharpoons 0 \qquad P \rightleftharpoons 0 \qquad A_P \longrightarrow 0 \longleftarrow A_{2P} \qquad (\mathcal{N}A.2b)$$

$$K \rightleftharpoons 0 \qquad P \rightleftharpoons 0 \qquad 0 \longleftarrow A_{2P} \qquad (\mathcal{N}A.2c)$$

can be used to describe possible network setups in chemical reaction networks.

The first network setup yields a weight vector for the conservation relation of the total concentration of A and its phosphorylated form. The second and third one are open systems towards conservation of the substances.

The first network setup (NA.2a) yields

$$\mu_{11a} = \begin{bmatrix} 0 & 1 & 0 & 1 & 1 & 1 & 1 & 1 & 1 \end{bmatrix}^T \ln \frac{\nu_3}{\lambda_3}$$

Conservation of substances in system (NA.2) happens only for substrate A and its phosphorylated forms. This yields only one weight vector $w_{11a} = \mu_{11a}$. Thus $s \perp \mu$ resulting in no steady states at all.

The second and third network setups, (NA.2b) and (NA.2c) respectively, yield only $\mu_{11b/c} = \underline{0}$. Only $a = b$ is valid for any μ and s and thus exactly one steady state can be found for these two network setups.

B.3 AN EXCURSION TOWARDS LARGER NETWORKS WITH SYNTHESIS AND DEGRADATION

Provided are the solutions to $Y^T \mu = \ln \frac{E\nu}{E\lambda}$ for a nine-times phosphorylation network including synthesis and degradation of the (phosphorylated) protein, compare section 6.3 on page 88:

$$0 = \ln \frac{\nu_{12}+\nu_{16}+\nu_{20}+\nu_{24}+\nu_{28}+\nu_{32}+\nu_{36}+\nu_4+\nu_8}{\lambda_{12}+\lambda_{16}+\lambda_{20}+\lambda_{24}+\lambda_{28}+\lambda_{32}+\lambda_{36}+\lambda_4+\lambda_8}$$

$$\mu_1+\mu_2 = \ln \frac{\nu_1+\nu_{12}+\nu_{16}+\nu_{20}+\nu_{24}+\nu_{28}+\nu_3+\nu_{32}+\nu_{36}+\nu_4+\nu_8}{\lambda_1+\lambda_{12}+\lambda_{16}+\lambda_{20}+\lambda_{24}+\lambda_{28}+\lambda_3+\lambda_{32}+\lambda_{36}+\lambda_4+\lambda_8}$$

$$\mu_3+\mu_5 = \ln \frac{\nu_2+\nu_3}{\lambda_2+\lambda_3}$$

$$\mu_4 = \ln \frac{\nu_1}{\lambda_1} \qquad \mu_6 = \ln \frac{\nu_2}{\lambda_2}$$

$$\mu_4 = \ln \frac{\nu_{12}+\nu_{16}+\nu_{20}+\nu_{24}+\nu_{28}+\nu_3+\nu_{32}+\nu_{36}+\nu_4+\nu_8}{\lambda_{12}+\lambda_{16}+\lambda_{20}+\lambda_{24}+\lambda_{28}+\lambda_3+\lambda_{32}+\lambda_{36}+\lambda_4+\lambda_8}$$

$$\mu_6 = \ln \frac{\nu_3}{\lambda_3} \qquad \mu_5 = \ln \frac{\nu_4}{\lambda_4}$$

$$\mu_1+\mu_5 = \ln \frac{\nu_{12}+\nu_{16}+\nu_{20}+\nu_{24}+\nu_{28}+\nu_{32}+\nu_{36}+\nu_5+\nu_7+\nu_8}{\lambda_{12}+\lambda_{16}+\lambda_{20}+\lambda_{24}+\lambda_{28}+\lambda_{32}+\lambda_{36}+\lambda_5+\lambda_7+\lambda_8}$$

$$\mu_3+\mu_8 = \ln \frac{\nu_6+\nu_7}{\lambda_6+\lambda_7}$$

$$\mu_7 = \ln \frac{\nu_5}{\lambda_5} \qquad \mu_9 = \ln \frac{\nu_6}{\lambda_6}$$

$$\mu_7 = \ln \frac{\nu_{12}+\nu_{16}+\nu_{20}+\nu_{24}+\nu_{28}+\nu_{32}+\nu_{36}+\nu_7+\nu_8}{\lambda_{12}+\lambda_{16}+\lambda_{20}+\lambda_{24}+\lambda_{28}+\lambda_{32}+\lambda_{36}+\lambda_7+\lambda_8}$$

$$\mu_9 = \ln \frac{\nu_7}{\lambda_7} \qquad \mu_8 = \ln \frac{\nu_8}{\lambda_8}$$

$$\mu_1+\mu_8 = \ln \frac{\nu_{11}+\nu_{12}+\nu_{16}+\nu_{20}+\nu_{24}+\nu_{28}+\nu_{32}+\nu_{36}+\nu_9}{\lambda_{11}+\lambda_{12}+\lambda_{16}+\lambda_{20}+\lambda_{24}+\lambda_{28}+\lambda_{32}+\lambda_{36}+\lambda_9}$$

$$\mu_{11}+\mu_3 = \ln \frac{\nu_{10}+\nu_{11}}{\lambda_{10}+\lambda_{11}}$$

$$\mu_{10} = \ln \frac{\nu_9}{\lambda_9} \qquad \mu_{12} = \ln \frac{\nu_{10}}{\lambda_{10}}$$

$$\mu_{10} = \ln \frac{\nu_{11}+\nu_{12}+\nu_{16}+\nu_{20}+\nu_{24}+\nu_{28}+\nu_{32}+\nu_{36}}{\lambda_{11}+\lambda_{12}+\lambda_{16}+\lambda_{20}+\lambda_{24}+\lambda_{28}+\lambda_{32}+\lambda_{36}}$$

$$\mu_{12} = \ln \frac{\nu_{11}}{\lambda_{11}} \qquad \mu_{11} = \ln \frac{\nu_{12}}{\lambda_{12}}$$

$$\mu_1+\mu_{11} = \ln \frac{\nu_{13}+\nu_{15}+\nu_{16}+\nu_{20}+\nu_{24}+\nu_{28}+\nu_{32}+\nu_{36}}{\lambda_{13}+\lambda_{15}+\lambda_{16}+\lambda_{20}+\lambda_{24}+\lambda_{28}+\lambda_{32}+\lambda_{36}}$$

$$\mu_{14}+\mu_3=\ln\frac{\nu_{14}+\nu_{15}}{\lambda_{14}+\lambda_{15}}$$
$$\mu_{13}=\ln\frac{\nu_{13}}{\lambda_{13}}\qquad\mu_{15}=\ln\frac{\nu_{14}}{\lambda_{14}}$$
$$\mu_{13}=\ln\frac{\nu_{15}+\nu_{16}+\nu_{20}+\nu_{24}+\nu_{28}+\nu_{32}+\nu_{36}}{\lambda_{15}+\lambda_{16}+\lambda_{20}+\lambda_{24}+\lambda_{28}+\lambda_{32}+\lambda_{36}}$$
$$\mu_{15}=\ln\frac{\nu_{15}}{\lambda_{15}}\qquad\mu_{14}=\ln\frac{\nu_{16}}{\lambda_{16}}$$
$$\mu_1+\mu_{14}=\ln\frac{\nu_{17}+\nu_{19}+\nu_{20}+\nu_{24}+\nu_{28}+\nu_{32}+\nu_{36}}{\lambda_{17}+\lambda_{19}+\lambda_{20}+\lambda_{24}+\lambda_{28}+\lambda_{32}+\lambda_{36}}$$
$$\mu_{17}+\mu_3=\ln\frac{\nu_{18}+\nu_{19}}{\lambda_{18}+\lambda_{19}}$$
$$\mu_{16}=\ln\frac{\nu_{17}}{\lambda_{17}}\qquad\mu_{18}=\ln\frac{\nu_{18}}{\lambda_{18}}$$
$$\mu_{16}=\ln\frac{\nu_{19}+\nu_{20}+\nu_{24}+\nu_{28}+\nu_{32}+\nu_{36}}{\lambda_{19}+\lambda_{20}+\lambda_{24}+\lambda_{28}+\lambda_{32}+\lambda_{36}}$$
$$\mu_{18}=\ln\frac{\nu_{19}}{\lambda_{19}}\qquad\mu_{17}=\ln\frac{\nu_{20}}{\lambda_{20}}$$
$$\mu_1+\mu_{17}=\ln\frac{\nu_{21}+\nu_{23}+\nu_{24}+\nu_{28}+\nu_{32}+\nu_{36}}{\lambda_{21}+\lambda_{23}+\lambda_{24}+\lambda_{28}+\lambda_{32}+\lambda_{36}}$$
$$\mu_{20}+\mu_3=\ln\frac{\nu_{22}+\nu_{23}}{\lambda_{22}+\lambda_{23}}$$
$$\mu_{19}=\ln\frac{\nu_{21}}{\lambda_{21}}\qquad\mu_{21}=\ln\frac{\nu_{22}}{\lambda_{22}}$$
$$\mu_{19}=\ln\frac{\nu_{23}+\nu_{24}+\nu_{28}+\nu_{32}+\nu_{36}}{\lambda_{23}+\lambda_{24}+\lambda_{28}+\lambda_{32}+\lambda_{36}}$$
$$\mu_{21}=\ln\frac{\nu_{23}}{\lambda_{23}}\qquad\mu_{20}=\ln\frac{\nu_{24}}{\lambda_{24}}$$

$$\mu_1+\mu_{20}=\ln\frac{\nu_{25}+\nu_{27}+\nu_{28}+\nu_{32}+\nu_{36}}{\lambda_{25}+\lambda_{27}+\lambda_{28}+\lambda_{32}+\lambda_{36}}\qquad\mu_{23}+\mu_3=\ln\frac{\nu_{26}+\nu_{27}}{\lambda_{26}+\lambda_{27}}$$
$$\mu_{22}=\ln\frac{\nu_{25}}{\lambda_{25}}\qquad\mu_{24}=\ln\frac{\nu_{26}}{\lambda_{26}}$$
$$\mu_{22}=\ln\frac{\nu_{27}+\nu_{28}+\nu_{32}+\nu_{36}}{\lambda_{27}+\lambda_{28}+\lambda_{32}+\lambda_{36}}\qquad\mu_{24}=\ln\frac{\nu_{27}}{\lambda_{27}}$$
$$\mu_{23}=\ln\frac{\nu_{28}}{\lambda_{28}}$$
$$\mu_1+\mu_{23}=\ln\frac{\nu_{29}+\nu_{31}+\nu_{32}+\nu_{36}}{\lambda_{29}+\lambda_{31}+\lambda_{32}+\lambda_{36}}\qquad\mu_{26}+\mu_3=\ln\frac{\nu_{30}+\nu_{31}}{\lambda_{30}+\lambda_{31}}$$
$$\mu_{25}=\ln\frac{\nu_{29}}{\lambda_{29}}\qquad\mu_{27}=\ln\frac{\nu_{30}}{\lambda_{30}}$$
$$\mu_{25}=\ln\frac{\nu_{31}+\nu_{32}+\nu_{36}}{\lambda_{31}+\lambda_{32}+\lambda_{36}}\qquad\mu_{27}=\ln\frac{\nu_{31}}{\lambda_{31}}$$
$$\mu_{26}=\ln\frac{\nu_{32}}{\lambda_{32}}$$
$$\mu_1+\mu_{26}=\ln\frac{\nu_{33}+\nu_{35}+\nu_{36}}{\lambda_{33}+\lambda_{35}+\lambda_{36}}\qquad\mu_{29}+\mu_3=\ln\frac{\nu_{34}+\nu_{35}}{\lambda_{34}+\lambda_{35}}$$
$$\mu_{28}=\ln\frac{\nu_{33}}{\lambda_{33}}\qquad\mu_{30}=\ln\frac{\nu_{34}}{\lambda_{34}}$$
$$\mu_{28}=\ln\frac{\nu_{35}+\nu_{36}}{\lambda_{35}+\lambda_{36}}\qquad\mu_{30}=\ln\frac{\nu_{35}}{\lambda_{35}}$$
$$\mu_{29}=\ln\frac{\nu_{36}}{\lambda_{36}}$$

The following dependencies occur due to the structure of the terms in the logarithms:

$$\begin{aligned}
\ln\frac{\nu_1}{\lambda_1} &= \ln\frac{\nu_{12}+\nu_{16}+\nu_{20}+\nu_{24}+\nu_{28}+\nu_3+\nu_{32}+\nu_{36}+\nu_4+\nu_8}{\lambda_{12}+\lambda_{16}+\lambda_{20}+\lambda_{24}+\lambda_{28}+\lambda_3+\lambda_{32}+\lambda_{36}+\lambda_4+\lambda_8}\\
&= \ln\frac{\nu_1+\nu_{12}+\nu_{16}+\nu_{20}+\nu_{24}+\nu_{28}+\nu_3+\nu_{32}+\nu_{36}+\nu_4+\nu_8}{\lambda_1+\lambda_{12}+\lambda_{16}+\lambda_{20}+\lambda_{24}+\lambda_{28}+\lambda_3+\lambda_{32}+\lambda_{36}+\lambda_4+\lambda_8}\\
\ln\frac{\nu_2}{\lambda_2} &= \ln\frac{\nu_3}{\lambda_3} = \ln\frac{\nu_2+\nu_3}{\lambda_2+\lambda_3}\\
\ln\frac{\nu_5}{\lambda_5} &= \ln\frac{\nu_{12}+\nu_{16}+\nu_{20}+\nu_{24}+\nu_{28}+\nu_{32}+\nu_{36}+\nu_7+\nu_8}{\lambda_{12}+\lambda_{16}+\lambda_{20}+\lambda_{24}+\lambda_{28}+\lambda_{32}+\lambda_{36}+\lambda_7+\lambda_8}\\
&= \ln\frac{\nu_{12}+\nu_{16}+\nu_{20}+\nu_{24}+\nu_{28}+\nu_{32}+\nu_{36}+\nu_5+\nu_7+\nu_8}{\lambda_{12}+\lambda_{16}+\lambda_{20}+\lambda_{24}+\lambda_{28}+\lambda_{32}+\lambda_{36}+\lambda_5+\lambda_7+\lambda_8}\\
\ln\frac{\nu_6}{\lambda_6} &= \ln\frac{\nu_7}{\lambda_7} = \ln\frac{\nu_6+\nu_7}{\lambda_6+\lambda_7}\\
\ln\frac{\nu_9}{\lambda_9} &= \ln\frac{\nu_{11}+\nu_{12}+\nu_{16}+\nu_{20}+\nu_{24}+\nu_{28}+\nu_{32}+\nu_{36}}{\lambda_{11}+\lambda_{12}+\lambda_{16}+\lambda_{20}+\lambda_{24}+\lambda_{28}+\lambda_{32}+\lambda_{36}}\\
&= \ln\frac{\nu_{11}+\nu_{12}+\nu_{16}+\nu_{20}+\nu_{24}+\nu_{28}+\nu_{32}+\nu_{36}+\nu_9}{\lambda_{11}+\lambda_{12}+\lambda_{16}+\lambda_{20}+\lambda_{24}+\lambda_{28}+\lambda_{32}+\lambda_{36}+\lambda_9}\\
\ln\frac{\nu_{10}}{\lambda_{10}} &= \ln\frac{\nu_{11}}{\lambda_{11}} = \ln\frac{\nu_{10}+\nu_{11}}{\lambda_{10}+\lambda_{11}}\\
\ln\frac{\nu_{13}}{\lambda_{13}} &= \ln\frac{\nu_{15}+\nu_{16}+\nu_{20}+\nu_{24}+\nu_{28}+\nu_{32}+\nu_{36}}{\lambda_{15}+\lambda_{16}+\lambda_{20}+\lambda_{24}+\lambda_{28}+\lambda_{32}+\lambda_{36}}\\
&= \ln\frac{\nu_{13}+\nu_{15}+\nu_{16}+\nu_{20}+\nu_{24}+\nu_{28}+\nu_{32}+\nu_{36}}{\lambda_{13}+\lambda_{15}+\lambda_{16}+\lambda_{20}+\lambda_{24}+\lambda_{28}+\lambda_{32}+\lambda_{36}}\\
\ln\frac{\nu_{14}}{\lambda_{14}} &= \ln\frac{\nu_{15}}{\lambda_{15}} = \ln\frac{\nu_{14}+\nu_{15}}{\lambda_{14}+\lambda_{15}}\\
\ln\frac{\nu_{17}}{\lambda_{17}} &= \ln\frac{\nu_{19}+\nu_{20}+\nu_{24}+\nu_{28}+\nu_{32}+\nu_{36}}{\lambda_{19}+\lambda_{20}+\lambda_{24}+\lambda_{28}+\lambda_{32}+\lambda_{36}}\\
&= \ln\frac{\nu_{17}+\nu_{19}+\nu_{20}+\nu_{24}+\nu_{28}+\nu_{32}+\nu_{36}}{\lambda_{17}+\lambda_{19}+\lambda_{20}+\lambda_{24}+\lambda_{28}+\lambda_{32}+\lambda_{36}}\\
\ln\frac{\nu_{18}}{\lambda_{18}} &= \ln\frac{\nu_{19}}{\lambda_{19}} = \ln\frac{\nu_{18}+\nu_{19}}{\lambda_{18}+\lambda_{19}}\\
\ln\frac{\nu_{21}}{\lambda_{21}} &= \ln\frac{\nu_{23}+\nu_{24}+\nu_{28}+\nu_{32}+\nu_{36}}{\lambda_{23}+\lambda_{24}+\lambda_{28}+\lambda_{32}+\lambda_{36}}\\
&= \ln\frac{\nu_{21}+\nu_{23}+\nu_{24}+\nu_{28}+\nu_{32}+\nu_{36}}{\lambda_{21}+\lambda_{23}+\lambda_{24}+\lambda_{28}+\lambda_{32}+\lambda_{36}}\\
\ln\frac{\nu_{22}}{\lambda_{22}} &= \ln\frac{\nu_{23}}{\lambda_{23}} = \ln\frac{\nu_{22}+\nu_{23}}{\lambda_{22}+\lambda_{23}}\\
\ln\frac{\nu_{25}}{\lambda_{25}} &= \ln\frac{\nu_{27}+\nu_{28}+\nu_{32}+\nu_{36}}{\lambda_{27}+\lambda_{28}+\lambda_{32}+\lambda_{36}}\\
&= \ln\frac{\nu_{25}+\nu_{27}+\nu_{28}+\nu_{32}+\nu_{36}}{\lambda_{25}+\lambda_{27}+\lambda_{28}+\lambda_{32}+\lambda_{36}}\\
\ln\frac{\nu_{26}}{\lambda_{26}} &= \ln\frac{\nu_{27}}{\lambda_{27}} = \ln\frac{\nu_{26}+\nu_{27}}{\lambda_{26}+\lambda_{27}}\\
\ln\frac{\nu_{29}}{\lambda_{29}} &= \ln\frac{\nu_{31}+\nu_{32}+\nu_{36}}{\lambda_{31}+\lambda_{32}+\lambda_{36}}\\
&= \ln\frac{\nu_{29}+\nu_{31}+\nu_{32}+\nu_{36}}{\lambda_{29}+\lambda_{31}+\lambda_{32}+\lambda_{36}}
\end{aligned}$$

$$\ln\frac{\nu_{30}}{\lambda_{30}} = \ln\frac{\nu_{31}}{\lambda_{31}} = \ln\frac{\nu_{30}+\nu_{31}}{\lambda_{30}+\lambda_{31}}$$
$$\ln\frac{\nu_{33}}{\lambda_{33}} = \ln\frac{\nu_{35}+\nu_{36}}{\lambda_{35}+\lambda_{36}} = \ln\frac{\nu_{33}+\nu_{35}+\nu_{36}}{\lambda_{33}+\lambda_{35}+\lambda_{36}}$$
$$\ln\frac{\nu_{34}}{\lambda_{34}} = \ln\frac{\nu_{35}}{\lambda_{35}} = \ln\frac{\nu_{34}+\nu_{35}}{\lambda_{34}+\lambda_{35}}$$

Thus dependencies between λ_l in terms of $\varkappa$ can be given by:

$$\begin{aligned}
0 &= (\exp(c_1)-\exp(\varkappa_1))\,\lambda_{36} + (\exp(c_2)-\exp(\varkappa_1))\,\lambda_{32}\\
&\quad + (\exp(c_3)-\exp(\varkappa_1))\,\lambda_{28} + (\exp(c_4)-\exp(\varkappa_1))\,\lambda_{24}\\
&\quad + (\exp(c_5)-\exp(\varkappa_1))\,\lambda_{20} + (\exp(c_6)-\exp(\varkappa_1))\,\lambda_{16}\\
&\quad + (\exp(c_7)-\exp(\varkappa_1))\,\lambda_{12} + (\exp(c_8)-\exp(\varkappa_1))\,\lambda_{8}\\
&\quad + (\exp(\varkappa_3)-\exp(\varkappa_1))\,\lambda_{4} + (\exp(\varkappa_2)-\exp(\varkappa_1))\,\lambda_{3},\\
0 &= (\exp(c_1)-1)\,\lambda_{36} + (\exp(c_2)-1)\,\lambda_{32} + (\exp(c_3)-1)\,\lambda_{28}\\
&\quad + (\exp(c_4)-1)\,\lambda_{24} + (\exp(c_5)-1)\,\lambda_{20} + (\exp(c_6)-1)\,\lambda_{16}\\
&\quad + (\exp(c_7)-1)\,\lambda_{12} + (\exp(c_8)-1)\,\lambda_{8} + (\exp(\varkappa_3)-1)\,\lambda_{4},\\
0 &= (\exp(c_1)-\exp(\varkappa_4))\,\lambda_{36} + (\exp(c_2)-\exp(\varkappa_4))\,\lambda_{32}\\
&\quad + (\exp(c_3)-\exp(\varkappa_4))\,\lambda_{28} + (\exp(c_4)-\exp(\varkappa_4))\,\lambda_{24}\\
&\quad + (\exp(c_5)-\exp(\varkappa_4))\,\lambda_{20} + (\exp(c_6)-\exp(\varkappa_4))\,\lambda_{16}\\
&\quad + (\exp(c_7)-\exp(\varkappa_4))\,\lambda_{12} + (\exp(c_8)-\exp(\varkappa_4))\,\lambda_{8}\\
&\quad + (\exp(\varkappa_5)-\exp(\varkappa_4))\,\lambda_{7},\\
0 &= (\exp(c_1)-\exp(d_1))\,\lambda_{36} + (\exp(c_2)-\exp(d_1))\,\lambda_{32}\\
&\quad + (\exp(c_3)-\exp(d_1))\,\lambda_{28} + (\exp(c_4)-\exp(d_1))\,\lambda_{24}\\
&\quad + (\exp(c_5)-\exp(d_1))\,\lambda_{20} + (\exp(c_6)-\exp(d_1))\,\lambda_{16}\\
&\quad + (\exp(c_7)-\exp(d_1))\,\lambda_{12} + (\exp(\varkappa_8)-\exp(d_1))\,\lambda_{11},\\
0 &= (\exp(c_1)-\exp(d_2))\,\lambda_{36} + (\exp(c_2)-\exp(d_2))\,\lambda_{32}\\
&\quad + (\exp(c_3)-\exp(d_2))\,\lambda_{28} + (\exp(c_4)-\exp(d_2))\,\lambda_{24}\\
&\quad + (\exp(c_5)-\exp(d_2))\,\lambda_{20} + (\exp(c_6)-\exp(d_2))\,\lambda_{16}\\
&\quad + (\exp(\varkappa_{11})-\exp(d_2))\,\lambda_{15},\\
0 &= (\exp(c_1)-\exp(d_3))\,\lambda_{36} + (\exp(c_2)-\exp(d_3))\,\lambda_{32}\\
&\quad + (\exp(c_3)-\exp(d_3))\,\lambda_{28} + (\exp(c_4)-\exp(d_3))\,\lambda_{24}\\
&\quad + (\exp(c_5)-\exp(d_3))\,\lambda_{20} + (\exp(\varkappa_{14})-\exp(d_3))\,\lambda_{19},\\
0 &= (\exp(c_1)-\exp(d_4))\,\lambda_{36} + (\exp(c_2)-\exp(d_4))\,\lambda_{32}\\
&\quad + (\exp(c_3)-\exp(d_4))\,\lambda_{28} + (\exp(c_4)-\exp(d_4))\,\lambda_{24}\\
&\quad + (\exp(\exp(d_4))\,\lambda_{23},\\
0 &= (\exp(c_1)-\exp(d_5))\,\lambda_{36} + (\exp(c_2)-\exp(d_5))\,\lambda_{32}\\
&\quad (\exp(c_3)-\exp(d_5))\,\lambda_{28} + (\exp(\varkappa_{20})-\exp(d_5))\,\lambda_{27},\\
0 &= (\exp(c_1)-\exp())\,\lambda_{36} + (\exp(c_2)-\exp(d_6))\,\lambda_{32}\\
&\quad + (\exp(\varkappa_{23})-\exp(d_6))\,\lambda_{31},\\
0 &= (\exp(c_1)-\exp(d_7))\,\lambda_{36} + (\exp(\varkappa_{26})-\exp(d_7))\,\lambda_{35}
\end{aligned}$$

with

$$c_1 = -\varkappa_2 + \varkappa_3 + \varkappa_{26} \qquad c_2 = -\varkappa_2 + \varkappa_3 + \varkappa_{23}$$
$$c_3 = -\varkappa_2 + \varkappa_3 + \varkappa_{20} \qquad c_4 = -\varkappa_2 + \varkappa_3 + \varkappa_{17}$$
$$c_5 = -\varkappa_2 + \varkappa_3 + \varkappa_{14} \qquad c_6 = -\varkappa_2 + \varkappa_3 + \varkappa_{11}$$
$$c_7 = -\varkappa_2 + \varkappa_3 + \varkappa_8 \qquad c_8 = -\varkappa_2 + \varkappa_3 + \varkappa_5$$
$$d_1 = -\varkappa_2 + \varkappa_4 + \varkappa_5 \qquad d_2 = -\varkappa_2 + \varkappa_4 + \varkappa_8$$
$$d_3 = -\varkappa_2 + \varkappa_4 + \varkappa_{11} \qquad d_4 = -\varkappa_2 + \varkappa_4 + \varkappa_{14}$$
$$d_5 = -\varkappa_2 + \varkappa_4 + \varkappa_{17} \qquad d_6 = -\varkappa_2 + \varkappa_4 + \varkappa_{20}$$
$$d_7 = -\varkappa_2 + \varkappa_4 + \varkappa_{23}$$

Some people are old at 18
and some are young at 90.
Time is a concept
that humans created.

— Yoko Ono

C

SOME MORE TABLES AND FIGURES

C.1 FURTHER FIGURES FOR NETWORKS WITH COMPARTMENTALIZATION

The reaction network including compartmentalization by two coupled standard phosphorylation networks for the multi-valued setup can also yield further interesting response curves, e. g., closed loops in the bifurcation diagrams:

$$
\begin{aligned}
x_C &= [0.0239,\ 0.6736,\ 0.1762,\ 0.7982,\ 0.9263,\ 0.8435,\\
&\quad 0.0101,\ 1.7460,\ 0.0881]^T,\\
x_N &= [0.7781,\ 0.0084,\ 5.5190,\ 2.1990,\ 0.8094,\ 1.5128,\\
&\quad 0.4575,\ 2.2992,\ 0.6636]^T,\\
c_C &= [0.8322,\ 1.1077,\ 5.0857]^T,\\
c_N &= [3.4346,\ 7.6954,\ 7.9497]^T,\\
k_C &= [54.0889,\ 0.0578,\ 1.0317,\ 5.6395,\ 0.1152,\ 0.9763,\\
&\quad 74.4054,\ 68.6440,\ 93.8750,\ 4.1188,\ 3.6011,\ 10.7911]^T,\\
c &= [0.8322,\ 13.0354,\ 1.1077,\ 3.4346,\ 7.6954]^T,\\
k_N &= [133.2642,\ 0.0210,\ 0.3745,\ 0.2061,\ 0.0642,\ 0.5443,\\
&\quad 2.6121,\ 1.5189,\ 2.0771,\ 0.0999,\ 0.4779,\ 1.4320]^T,\\
k_T &= 1e-07 \cdot [1,\ 0.29307]^T,
\end{aligned}
$$

see figure C.1 for the uncoupled response curve and figure C.2 for the coupled one. Bifurcation analysis starts at $a = f(x_C, x_N)$.

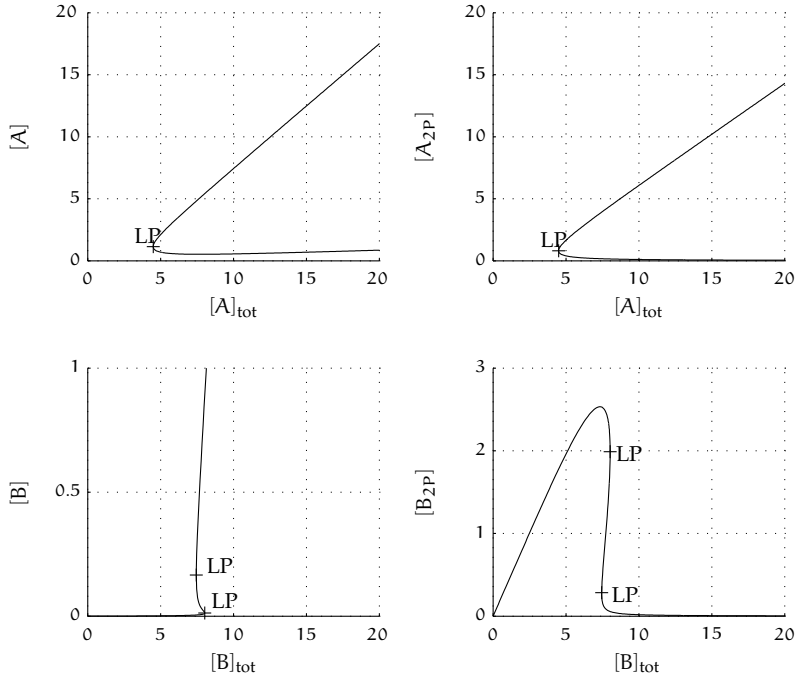

Figure C.1: *Bifurcation analysis for the multi-valued setup of two decoupled systems. Results for coupling these two systems can be found in figure C.2.*

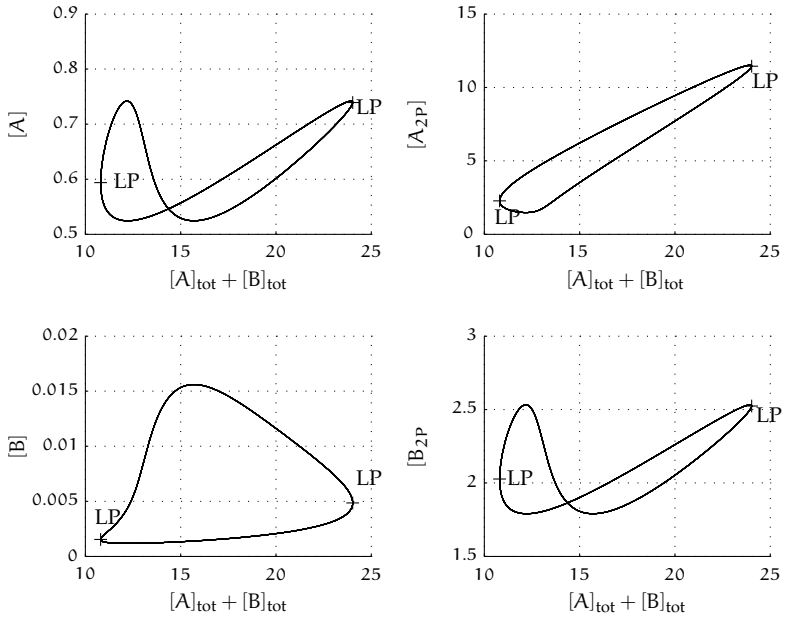

Figure C.2: *Bifurcation analysis of coupling two systems of the multi-valued setup with multiple steady states as given in figure C.1. Here closed loops can be seen.*

C.2 FURTHER FIGURES FOR ROBUSTNESS ANALYSIS TOWARDS PARAMETER VARIATION

Results for mean exit number $\bar{I}$ of remaining sign vectors for robustness analysis are given for $\delta^{(2)}_{2,3,4}$ and following $\Delta^{(n)}$ for $n = 2, \ldots, 14$ and $n = 3, \ldots, 15$, of equation (5.Δ_b2)–(5.Δ_b4) for $i_1 = 1$ and $i_2 = n-1$.

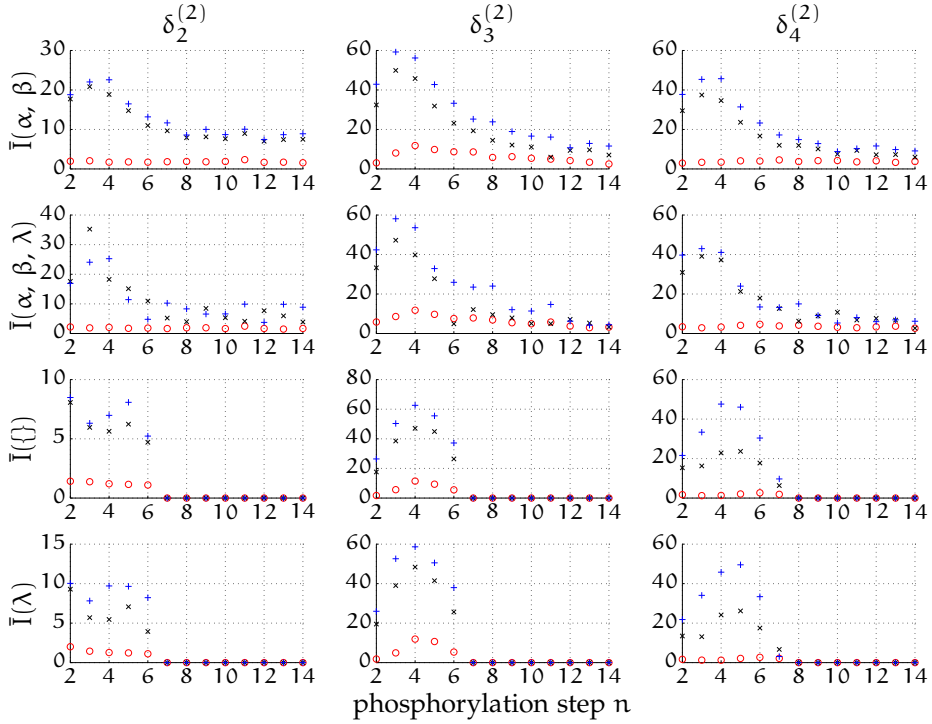

Figure C.3: *Mean exit number* $\bar{I}$ *as measure of robustness for perturbation of the parameter vector for sign vectors* $\delta \in \{+, -\}$ *for missing* $\delta^{(2)}_{2,3,4}$ *and higher* n *with* $i_1 = 1$ *and* $i_2 = n - 1$ *for equations* (5.Δ_b2)–(5.Δ_b4). *Different exit conditions are coded in the following way: RW1 = red circle, RW2 = black cross, RW3 = blue plus. Note,* $\bar{I} = 0$ *for* $n \geqslant 7$ *or 8 for fixed* α *and* β *(last two rows).*

C.3 VALUES FOR RATE CONSTANTS AND CONCENTRATIONS

Given here is an overview on rate constants and concentrations in multi-site phosphorylation networks from literature for section 3.1.1 in table C.1 and C.2.

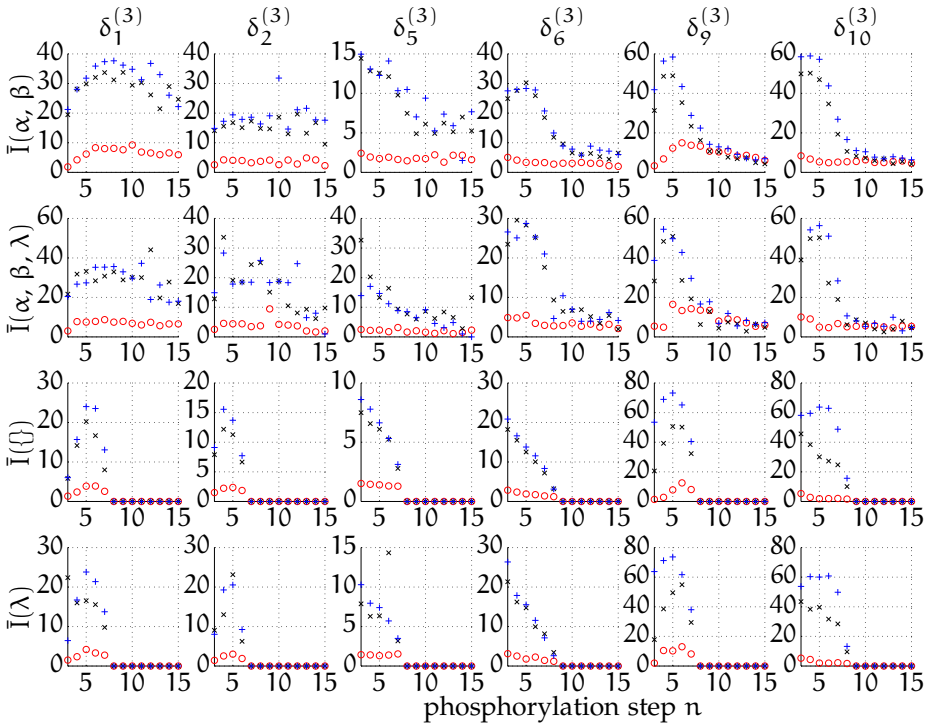

Figure C.4: *Mean exit number* $\bar{I}$ *as measure for robustness for sign vectors* $\delta_i \in \{+, -\}$ *with* $i = 1, 2, 5, 6, 9$ *and* 10 *of* $\Delta^{(3)}$ *and higher* n *with* $i_1 = 1$ *and* $i_2 = n - 1$, *see equations* (5.Δ_b). *Here, remaining sign vectors in* $n = 3, \ldots, 15$ *are shown, missing four sign vectors of* $\delta^{(3)}$ *are those in figure 8.2 and C.3 for* $n = 2$. *Exit conditions are coded by: RW1 = red circle, RW2 = black cross, RW3 = blue plus. Note again,* $\bar{I} = 0$ *for* $n \geqslant 7$ *or 8 for fixed* α *and* β *(last two rows).*

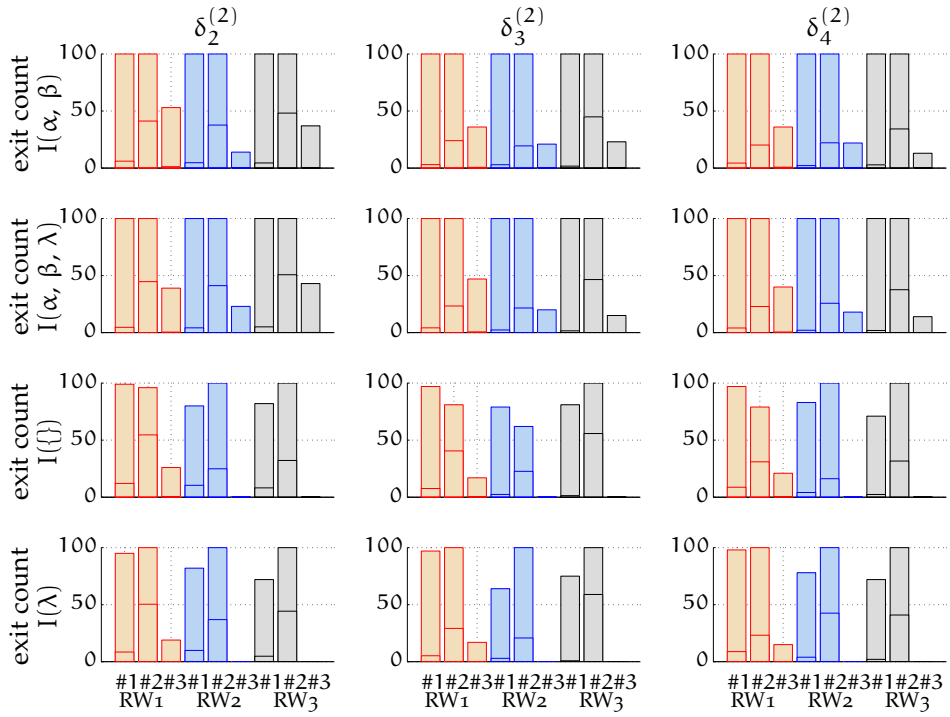

Figure C.5: *Exit reason, see section 8.3.2 for all exit conditions, RW1–RW3. Upper (solid red, blue, black) horizontal line describes maximum exit step* I_{max}*, middle horizontal line describes mean exit step* $\bar{I}$ *and lower horizontal line describes minimum exit step* I_{min} *(not seen as it corresponds to zero, i.e. the first step is already invalid). Given are exit times for* $\Delta^{(n)}$ *for sign vectors* $\delta \in \{+, -\}$ *for missing* $\delta^{(2)}_{2,3,4}$ *and higher* n *with* $i_1 = 1$ *and* $i_2 = n - 1$ *for equations* (5.Δ_b2)–(5.Δ_b4).

Table C.1: *Examples for rate constants and concentrations from literature for various protein phosphorylation processes.*

protein	kinase	# sites	concentration: protein in $^{mol}/_{l}$	kinase in $^{mol}/_{l}$	rate constants: k_M in $^{mol}/_{l}$	k_1 in $^{l}/_{(mol\,s)}$	k_2 in $^{1}/_{s}$	k_3 in $^{1}/_{s}$	n_H	ref.
IκBα	*IKK*	2	$[0.5-10]\cdot10^{-6}$	$0.1\cdot10^{-6}$	$1.7\cdot10^{-6}$	$22.5\cdot10^{3}$	$1.25\cdot10^{-3}$	$3.7\cdot10^{-2}$		[44]
ERK		2	$[1-10]\cdot10^{-6}$	$1\cdot10^{-3}$	$22.9\cdot10^{-6}$	nd	nd	$7.28\cdot10^{-4}$		[123]
→*ERK2/pY*	*MEK1*		$[1-10]\cdot10^{-6}$	$1\cdot10^{-3}$	$15.5\cdot10^{-6}$	nd	nd	0.165		
→*ERK2/pT*	*MEK1*		$[1-10]\cdot10^{-6}$	$1\cdot10^{-3}$	$15.2\cdot10^{-6}$	nd	nd	0.451		
→*ERK2/pTpY*	*MEK1*		$[1-10]\cdot10^{-6}$	$1\cdot10^{-3}$	$10.0\cdot10^{-6}$	nd	nd	6.51		
Sic1	*CK2α*	9	$[0-1.5]\cdot10^{-6}$	$[0.1-1]\cdot10^{-6}$	$460\cdot10^{-9}$	$5.85\cdot10^{3}$	$2.09\cdot10^{-3}$	nd		[4]
	CK2β		$[0-1.5]\cdot10^{-6}$	$[0.1-1]\cdot10^{-6}$	$460\cdot10^{-9}$	$9.42\cdot10^{4}$	$3.56\cdot10^{-3}$	nd		
Cdc25	*Cdk1*	$\geqslant 14$	$150\cdot10^{-9}$	$100\cdot10^{-9}$		nd	nd	nd	11	[106]
Wee1	*Cdk1*	$\geqslant 5$	$[10-120]\cdot10^{-9}$	$200\cdot10^{-9}$	$566\cdot10^{-9}$	nd	nd	nd	3.5	[55]
ATP	*Cdk1*	3	10^{-3}	$1\cdot10^{-3}$	$35\cdot10^{-6}$	nd	nd	2.2		[113]

Table C.2: *Examples for rate constants and concentrations from literature for various protein dephosphorylation processes.*

protein	phosphatase	# sites	concentration of protein in $^{mol}/_{l}$	phosphatase in $^{mol}/_{l}$	rate constants k_M in M	k_1 in $^{l}/_{(mol\,s)}$	k_2 in $^{1}/_{s}$	k_3 in $^{1}/_{s}$	n_H	ref.
ERK	*MKP3*	2	$[0-20]\cdot10^{-3}$	$200\cdot10^{-9}$	$1.5\cdot10^{-3}$	nd	nd	0.45		[56]
	VHR		$[0-20]\cdot10^{-3}$	$200\cdot10^{-9}$	$2.32\cdot10^{-3}$	nd	nd	6.2		
Cdc25	(*PP2A*)	$6-13$	$150\cdot10^{-9}$			nd	nd	nd	32	[106]
Wee1	(*PP2A*)	$(\geqslant 5)$	$[10-120]\cdot10^{-9}$		$97\cdot10^{-9}$	nd	nd	nd	1.5	[55]

BIBLIOGRAPHY

[1] R. Alsallaq and H.-X. Zhou. Prediction of protein-protein association rates from a transition-state theory. *Structure*, 15:215–224, 2007. (Cited on page 18.)

[2] R. S. Annan, M. J. Huddleston, R. Verma, R. J. Deshaies, and S. A. Carr. A multidimensional electrospray ms-based approach to phosphopeptide mapping. *Analytical Chemistry*, 73(3):393–404, 2001. (Cited on page 22.)

[3] M. Barberis. Sic1 as a timer of Clb cyclin waves in the yeast cell cycle — design principle of not just an inhibitor. *FEBS Journal*, 279(18):3386–3410, 2012. (Cited on pages 20 und 21.)

[4] M. Barberis, M. A. Pagano, L. De Gioia, O. Marin, M. Vanoni, P. A. Pinna, and L. Alberghina. CK2 regulates in vitro the activity of the yeast cyclin-dependent kinase inhibitor Sic1. *Biochemical and Biophysical Research Communications*, 336:1040–1048, 2005. (Cited on page 192.)

[5] M. Barberis, C. Linke, M. À. Adrover, A. González-Novo, H. Lehrach, S. Krobitsch, F. Posas, and E. Klipp. Sic1 plays a role in timing and oscillatory behavior of B-type cyclins. *Biotechnology Advances*, 30:108–130, 2012. (Cited on page 22.)

[6] S. Barry. *The secret scripture*. Faber & Faber, 2008. (Cited on page 13.)

[7] J. Birge and F. Louveaux. *Introduction to stochastic programming*. Springer, New York, 1997. (Cited on page 5.)

[8] B. Boros. Notes on the deficiency-one theorem: Multiple linkage classes. *Mathematical Biosciences*, 235:110–122, 2012. (Cited on page 33.)

[9] R. Bringhurst. *The elements of typographic style*. Version 3.2. Hartley & Marks Publishers, Point Roberts, WA, USA, 2008. (Cited on page 203.)

[10] C. Bukowski. *Love is a dog from hell*. Ecco, 2002. (Cited on page 29.)

[11] J. Chancellor. Lateralus, February, 2002. (Cited on page 5.)

[12] C. W. Chow, M. Rincón, and R. J. Davis. Requirement for transcription factor NFAT in interleukin-2 expression. *Molecular and Cellular Biology*, 19(3):2300–2307, 1999. (Cited on page 24.)

[13] M. H. Cobb. MAP kinase pathways. *Progress in Biophysics and Molecular Biology*, 71:479–500, 1999. Elsevier. (Cited on page 13.)

[14] P. Coccetti, V. Zinzalla, G. Tedeschi, G. L. Russo, S. Fantinato, O. Marin, A. L. Pinna, M. Vanoni, and L. Alberghina. Sic1 is phosphorylated by CK2 on Ser201 in budding yeast cells. *Biochemical and Biophysical Research Communications*, 346:786–793, 2006. (Cited on pages 21 und 22.)

[15] C. Conradi. *Multistationarity in (bio)chemical reaction networks with mass action kinetics: model discrimination, robustness and beyond*. PhD thesis,

Forschungberichte aus dem Max-Planck-Institut für Dynamik komplexer technischer Systeme, Shaker Verlag, 2008. (Cited on pages 1, 33 und 35.)

[16] C. Conradi and D. Flockerzi. Multistationarity in mass action networks with applications to ERK activation. *Mathematical Biosciences*, 65:107–156, 2012. (Cited on pages 1 und 32.)

[17] C. Conradi, J. Saez-Rodriguez, E. D. Gilles, and J. Raisch. Using chemical reaction network theory to discard a kinetic mechanism hypothesis. *Systems Biology, IEE Proceedings (now IET Systems Biology)*, 152(4): 243–248, 2005. (Cited on page 14.)

[18] C. Conradi, D. Flockerzi, J. Raisch, and J. Stelling. Subnetwork analysis reveals dynamic features of complex (bio)chemical networks. *Proceedings of the National Academy of Sciences*, 104(49):19175–19180, 2007. (Cited on pages 105, 107, 116 und 147.)

[19] C. Conradi, D. Flockerzi, and J. Raisch. Multistationarity in the activation of a MAPK: Parametrizing the relevant region in parameter space. *Mathematical Biosciences*, 211:05–131, 2008. (Cited on pages 31, 43, 55, 74 und 133.)

[20] M. T. Cooling, P. Hunter, and E. J. Crampin. Sensitivity of NFAT cycling to cytosolic calcium concentration: Implications for hypertrophic signals in cardiac myocytes. *Biophysical Journal*, 96:2095–2104, 2009. (Cited on pages 18, 23, 24, 26, 58, 63 und 65.)

[21] A. Cornish-Bowden. *Fundamentals of enzyme kinetics*. Portland Press, 3rd edition edition, 2004. (Cited on pages 5 und 15.)

[22] G. Craciun, Y. Tang, and M. Feinberg. Understanding bistability in complex enzyme-driven reaction networks. *Proceedings of the National Academy of Sciences*, 103(23):8697–8702, 2006. (Cited on pages 1 und 32.)

[23] Frederick R. Cross. Two redundant oscillatory mechanisms in the yeast cell cycle. *Developmental Cell*, 4:741–752, 2003. (Cited on page 22.)

[24] R. J. Deshaies and J. E. Ferrell Jr. Multisite phosphorylation and the countdown to S phase. *Cell Press*, 107:819–822, 2001. (Cited on pages 2, 13, 21, 22 und 88.)

[25] R. E. Dolmetsch and R. S. Lewis. Signaling between intracellular Ca^{2+} stores and depletion-activated Ca^{2+} channels generates $[Ca^{2+}]_i$ oscillations in T lymphocytes. *The Journal of General Physiology*, 103:365–388, 1994. (Cited on page 24.)

[26] R. E. Dolmetsch, R. S. Lewis, C. C. Goodnow, and J. I. Healy. Differential activation of transcription factors induced by Ca^{2+} response amplitude and duration. *Letters to Nature*, 386:855–858, 1997. (Cited on pages 25 und 26.)

[27] P. R. Ellison. *The advanced deficiency algorithm and its application to mechanism discrimination*. PhD thesis, University of Rochester, New York, 1998. (Cited on pages 32 und 33.)

[28] I. Famili and B. Palsson. The convex basis of the left null space of the stoichiometric matrix leads to the definition of metabolically meaningful pools. *Biophysical Journal*, 85:16–26, 2003. (Cited on page 10.)

[29] M. Feinberg. Lectures on chemical reaction networks, 1980. Archive for Rational Mechanics and Analysis. (Cited on page 73.)

[30] M. Feinberg. Chemical reaction network structure and the stability of complex isothermal reactors – I. The deficiency zero and deficiency one theorems. *Chemical Engineering Sciences*, 42(10):2229–2268, 1987. (Cited on pages 1, 7, 29, 32, 43 und 73.)

[31] M. Feinberg. Chemical reaction network structure and the stability of complex isothermal reactors – II. Multiple steady states for networks of deficiency one. *Chemical Engineering Sciences*, 43(1):1–25, 1988. (Cited on pages 1 und 32.)

[32] M. Feinberg. The existence and uniqueness of steady states for a class of chemical reaction networks. *Archive for Rational Mechanics and Analysis*, 132:311–370, 1995. (Cited on page 32.)

[33] M. Feinberg. Multiple steady states for chemical reaction networks of deficiency one. *Archive for Rational Mechanics and Analysis*, 132:371–406, 1995. (Cited on pages 32 und 43.)

[34] M. Feinberg. *The Chemical Reaction Network Theory Toolbox*. The Ohio State University, last checked April, 3rd, 2014. URL `http://www.chbmeng.ohio-state.edu/~feinberg/crntwin/`. (Cited on pages 33 und 73.)

[35] M. Feinberg and F. J. M. Horn. Chemical mechanism structure and the coincidence of the stoichiometric and kinetic subspaces. *Archive for Rational Mechanics and Analysis*, 66:83–97, 1977. (Cited on page 32.)

[36] J. E. Ferrell Jr. and Ch.-Y. F. Huang. Ultrasensitivity in the mitogen-activated protein kinase cascade. *Proceedings of the National Academy of Sciences*, 93:10078–10083, 1996. (Cited on page 13.)

[37] S. Feske, H. Okamura, P. G. Hogan, and A. Rao. Ca^{2+}/calcineurin signaling in cells of the immune system. *Biochemical and Biophysical Research Communications*, 311:1117–1132, 2003. (Cited on pages 23 und 25.)

[38] D. Fisher, L. Krasinska, D. Coudreuse, and B. Novák. Phosphorylation network dynamics in the control of cell cycle transitions. *Journal of Cell Science*, 125(20):4703–4711, 2012. (Cited on pages 2, 22 und 69.)

[39] W. G. Fisher, P.-C. Yang, R. K. Medikonduri, and M. S. Jafri. NFAT and NFκB activation in T lymphocytes: A model of differential activation of gene expression. *Annals of Biomedical Engineering*, 34(11):1712–1728, 2006. (Cited on pages 2, 23, 24 und 26.)

[40] A. Goldbeter and D. E. Koshland Jr. An amplified sensitivity arising from covalend modification in biological systems. *Proceedings of the National Academy of Sciences*, 78(11):6840–6844, 1981. (Cited on page 16.)

[41] J. Guckenheimer and P. Holmes. *Nonlinear Oscillations, Dynamical Systems, and Bifurcations of Vector Fields*. Applied mathematical sciences, 42, Springer, 1983. (Cited on page 5.)

[42] J. Gunawardena. Multisite protein phosphorylation makes a good threshold but can be a poor switch. *Proceedings of the National Academy of Sciences*, 102(41):14617–14622, 2005. (Cited on pages 1, 22, 29, 31, 63, 67, 110 und 111.)

[43] J. Hadamard. *Analyse des travaux scientifiques*. Reprinted in Librairie Scientifique et Technique, Albert Blanchard. Painlevé, P., Gauthier-Villars, Paris, 1967, pp. 1–2, 1900. (Cited on page 95.)

[44] R. Heilker, F. Freuler, M. Vanek, R. Pulfer, T. Kobel, J. Peter, H.-G. Zerwes, H. Hofstetter, and J. Eder. The kinetics of association and phosphorylation of IκB isoforms by IκB kinase correlate with their cellular regulation in human endothelial cells. *Biochemistry*, 38(19): 6231–6238, 1999. (Cited on pages 18 und 192.)

[45] S. Herold. Analyse der Robustheit mehrfach stationärer Zustände bei der n-fach Phosphorylierung eines Proteins. Diploma's thesis, Otto-von-Guericke Universität Magdeburg, 2008. (Cited on pages 3, 123, 126, 128, 131 und 132.)

[46] W. H. Hines, D. C. Montgomery, D. M. Goldsman, and C. M. Borror. *Probability and statistics in engineering*. Wiley, 4 edition, 2003. (Cited on pages 5 und 130.)

[47] P. G. Hogan, L. Chen, J. Nardone, and A. Rao. Transcriptional regulation by Calcium, Calcineurin, and NFAT. *Genes and Development*, 17: 2205–2232, 2003. (Cited on pages 24 und 25.)

[48] C. I. Holmberg, S. E. F. Tran, J. E. Eriksson, and L. Sistonen. Multisite phosphorylation provides sophisticated regulation of transcription factors. *Trends in Biochemical Sciences*, 27(12):619–627, 2002. (Cited on page 23.)

[49] K. Holstein. Mathematische Analyse der n-fach Phosphorylierung eines Proteins: Existenz mehrfach stationärer Zustände. Diploma's thesis, Otto-von-Guericke Universität Magdeburg, 2008. (Cited on pages 2, 35, 74 und 137.)

[50] L. Jaulin, M. Kieffer, O. Didrit, and É. Walter. *Applied interval analysis*. Springer, 2001. (Cited on page 59.)

[51] M. Kõivomägi, E. Valk, R. Venta, A. Iofik, M. Lepiku, E. R. Balog, S. M. Rubin, D. O. Morgan, and M. Loog. Cascades of multisite phosphorylation control Sic1 destruction at the onset of S phase. *Nature*, 12(480): 128–31, 2011. (Cited on page 22.)

[52] O. Kapuy, D. Barik, R. M. Domingo Sananes, J. J. Tyson, and B. Novák. Bistability by multiple phosphorylation of regulatory proteins. *Progress in Biophysics and Molecular Biology*, 100:47–56, 2009. (Cited on page 20.)

[53] O. Kapuy, E. He, S. López-Avilés, F. Uhlmann, J. J. Tyson, and B. Novák. System level feedbacks control cell cycle progression. *Progress in Biophysics and Molecular Biology*, 100:47–56, 2009. (Cited on page 20.)

[54] O. A. Karlsson, C. N. Chi, Å. Engström, and P. Jemth. The transition state of coupled folding and binding for a flexible β-finger. *Journal of Molecular Biology*, 417(213):253–261, 2012. (Cited on page 18.)

[55] S. Y. Kim and J. E. Ferrell Jr. Substrate competition as a source of ultrasensitivity in the inactivation of Wee1. *Cell*, 128(6):1133–1145, 2007. (Cited on page 192.)

[56] Y. Kim, A. E. Rice, and J. M. Denu. Intramolecular dephosphorylation of ERK by MKP3. *Biochemistry*, 42(51):15197–15207, 2003. (Cited on pages 18 und 192.)

[57] S. Klamt. *Strukturelle Analyse von Stoffwechselnetzen illustriert am bakteriellen Redox- und Zentralstoffwechsel*. PhD thesis, Forschungberichte aus dem Max-Planck-Institut für Dynamik tomplexer technischer Systeme, Shaker Verlag, 2005. (Cited on pages 11 und 12.)

[58] S. Klamt and J. Gagneur. Computation of elementary modes: a unifying framework and the new binary approach. *BMC Bioinformatics*, 175 (5), 2004. (Cited on pages 10, 44, 45, 83, 84 und 104.)

[59] E. Klipp, W. Liebermeister, C. Wierling, A. Kowald, H. Lehrach, and R. Herwig. *Systems biology*. Wiley-Blackwell, Weinheim, 1st edition, 2010. (Cited on pages 5 und 15.)

[60] R. Koren and G. G. Hammes. A kinetic study of protein-protein interactions. *Biochemstry*, 15(5):1165–1711, 1976. (Cited on page 18.)

[61] I. A. Kurnaz. Kinetic analysis of RSK2 and ELK-1 interaction on the serum response element and implications for cellular engineering. *Biotechnology and Bioengineering*, 88(7):890–900, 2004. (Cited on page 18.)

[62] Y. A. Kuznetsov. *Elements of Applied Bifurcation Theory*. Springer-Verlag, 2004. (Cited on pages 5 und 118.)

[63] F. Llaneras and J. Picó. Stoichiometric modeling of cell metabolism. *Journal of Bioscience and Bioengineering*, 105(1):1–11, 2008.

[64] C. Loh, J. A. Carew, J. Kim, P. G. Hogan, and A. Rao. T-cell receptor stimulation elicits an early phase of activation and a late phase of deactivation of the transcription factor NFAT1. *Molecular and Cellular Biology*, 16(7):3945–3954, 1996. (Cited on pages 1, 24 und 26.)

[65] C. Loh, K. T.-Y. Shaw, J. A. Carew, J. P. B. Viola, C. Luo, B. A. Perrino, and A. Rao. Calcineurin binds the transcription factor NFAT1 and reversibly regulates its activity. *Journal of Biological Chemistry*, 271(18): 10884–10891, 1996. (Cited on page 24.)

[66] D. G. Luenberger. *Introduction to dynamic systems*. Wiley, 1st edition, 1979. (Cited on page 5.)

[67] F. Macian. NFAT proteins: key regulators of T-cell development and function. *Nature Reviews — Immunology*, 5:472–483, 2005. (Cited on pages 23 und 26.)

[68] D. Mack. *Kabuki: The alchemy*. Marvel Publishing, 2008. (Cited on page v.)

[69] N. I. Markevich, J. B. Hoek, and B. N. Kholodenko. Signaling switches and bistability arising from multisite phosphorylation in protein kinase cascades. *Journal of Cell Biology*, 164(3):353–359, 2004. (Cited on pages 1, 11, 18, 19, 20, 58 und 65.)

[70] M. Medyouf and J. Ghysdael. The calcineurin/NFAT signaling pathway. *Cell Cycle*, 7(3):297–303, 2008. (Cited on page 23.)

[71] A. A. Milne. *The complete tales of Winnie-The-Pooh*. Dutton Juvenile, 1996. (Cited on page 149.)

[72] R. Motwani and P. Raghavan. *Randomized algorithms*. Cambridge University Press, 1995. (Cited on page 5.)

[73] P. Nash, X. Tang, S. Orlicky, Q. Chen, F. B. Gertler, M. D. Mendenhall, F. Sicheri, T. Pawson, and M. Tyers. Multisite phosphorylation of a CDK inhibitor sets a threshold for the onset of DNA replication. *Nature*, 414:514–521, 2001. (Cited on pages 22, 88 und 93.)

[74] F. Nietsche. *Also sprach Zarathustra*. Fischer Klassik, 4th edition, 2010. (Cited on page 69.)

[75] S. H. Northrup and H. P. Erickson. Kinetics of protein-protein association explained by Brownian dynamics computer simulation. *Proceedings of the National Academy of Science*, 89(8):3338–3342, 1992. (Cited on page 18.)

[76] H. Okamura, J. Aramburu, C. García-Rodríguez, J. P. B. Viola, A. Raghavan, M. Tahiliani, X. Zhang, J. Qin, P. G. Hogan, and A. Rao. Concerted dephosphorylation of the transcription factor NFAT1 induces a conformational switch that regulates transcriptional activity. *Molecular Cell*, 6:539–550, 2000. (Cited on page 26.)

[77] H. Okamura, C. García-Rodrǵuez, H. Martinson, J. Qin, D. M. Virshup, and A. Rao. A conserved docking motif for CK1 binding controls nuclear localization of NFAT1. *Molecular and Cellular Biology*, 24(10): 4184–4195, 2004. (Cited on page 24.)

[78] J. Papin, N. Price, and B. Palsson. Extreme pathway lengths and reaction participation in genome-scale metabolic networks. *Genome Research*, 12:1889–1900, 2002. Cold Spring Harbor Laboratory Press. (Cited on page 10.)

[79] J. Papin, N. Price, S. Wiback, D. Fell, and B. Palsson. Metabolic pathways in the post-genome era. *Trends in Biochemical Science*, 28(5):250–258, 2003. Elsevier. (Cited on page 11.)

[80] G. Pearson, F. Robinson, T. Beers Gibson, B. Xu, M. Karandikar, K. Berman, and M. H. Cobb. Mitogen-activated protein (MAP) kinase pathways: Regulation and physiological functions. *Endocrine Reviews*, 22:153–183, 2001. (Cited on page 13.)

[81] M. PérezÂ Millán, A. Dickenstein, A. Shiu, and C. Conradi. Chemical reaction systems with toric steady states. *Bulletin of Mathematical Biology*, 74(5):1027–1065, 2012. (Cited on pages 32 und 142.)

[82] J. A. Perry and S. Kornbluth. Cdc25 and Wee1: Analogous opposites? *Cell Division*, 2(12):1–12, 2007. (Cited on page 1.)

[83] T. Pratchett. *Hogfather*. Corgi Books, 1998. (Cited on page xi.)

[84] C. Salazar and T. Höfer. Activation of the transcription factor NFAT1: Concerted or modular regulation? *FEBS Letters*, 579:621–626, 2005. (Cited on page 24.)

[85] C. Salazar and T. Höfer. Versatile regulation of multisite protein phosphorylation by order of phosphate processing and protein-protein interactions. *Federation of European Biochemical Societies*, 274:1046–1061, 2007. (Cited on pages 15, 22, 29, 67 und 111.)

[86] C. Salazar and T. Höfer. Multisite protein phosphorylation — from molecular mechanisms to kinetic models. *Federation of European Biochemical Societies*, 276:3177–3198, 2009. (Cited on page 15.)

[87] C. H. Schilling, D. Letscher, and B. Palsson. Theory for the systemic definition of metabolic pathways and their use in interpreting metabolic function from a pathway-oriented perspective. *Journal of Theoretical Biology*, 203(3):229–248, 2000. (Cited on page 11.)

[88] M. Schlosshauer and D. Baker. Realistic protein-protein association rates from a simple diffusional model neglecting long-range interactions, free energy barriers, and landscape ruggedness. *Protein Science*, 13:1660–1669, 2004. (Cited on page 18.)

[89] S. Schuster, T. Dandekar, and D. A. Fell. Detection of elementary flux modes in biochemical networks: A promising tool for pathway analysis and metabolic engineering. *Tibtech*, 17:53–60, 1999. (Cited on page 11.)

[90] S. Schuster, D. A. Fell, and T. Dandekar. A general definition of metabolic pathways useful for systematic organization and analysis of complex metabolic networks. *Nature Biotechnology*, 18:326–332, 2000.

[91] J.-M. Schwartz and M. Kanehisa. Quantitative elementary mode analysis of metabolic pathways: the example of yeast glycolysis. *BMC Bioinformatics*, 186(7), 2006. (Cited on page 12.)

[92] E. G. Seger, R.and Krebs. The MAPK signaling cascade. *Federation of American Societies For Experimental Biology Journal*, 9:726–735, 1995. (Cited on page 35.)

[93] K. T.-Y. Shaw, A. M. Ho, A. Raghavan, J. Kim, J. Jain, J. Park, S. Sharma, A. Rao, and P. G. Hogan. Immunosuppresive drugs prevent a rapid dephosphorylation of transcription factor NFAT1 in stimulated immune cells. *Proceedings of the National Academy of Sciences*, 92:11205–11209, 2005. (Cited on page 25.)

[94] T. Shen, Z. Cseresnyés, Y. Liu, W. P. Randall, and M. Schneider. Regulation of the nuclear export of the transcription factor NFATc1 by protein kinases after slow fibre type electrical stimulation of adult mouse skeletal muscle fibres. *The Journal of Physiology*, 579:535–551, 2007. (Cited on page 24.)

[95] F. Shibasaki, E. R. Price, D. Milan, and F. McKeon. Role of kinases and the phosphatase calcineurin in the nuclear shuttling of transcription factor NF-AT4. *Nature*, 382:370–373, 1996. (Cited on page 24.)

[96] S.-Y. Shin, H.-W. Yang, J.-R. Kim, W. D. Heo, and K.-H. Cho. A hidden incoherent switch regulates RCAN1 in the calcineurin-NFAT signaling network. *Journal of Cell Science*, 124:82–90, 2011. (Cited on page 26.)

[97] W. Shou, R. Verma, R. S. Annan, M. J. Huddleston, S. L. Chen, S. A. Carr, and R. J. Deshaies. Mapping phosphorylation sites in proteins by

mass spectrometry. *Methods in Enzymology*, 351:279–296, 2002. (Cited on pages 11 und 22.)

[98] M. V. Smoluchowski. Versuch einer mathematischen Theorie der Koagulationskinetik kolloider Lösungen. *Zeitschrift für Physikalische Chemie*, 92:129–168, 1917. (Cited on page 18.)

[99] J. Stelling, S. Klamt, K. Bettenbrock, S. Schuster, and E. D. Gilles. Metabolic network structure determines key aspects of functionality and regulation. *Nature*, 420:190–193, 2002. (Cited on page 40.)

[100] P. Tavi, S. Pikkarainen, J. Ronkainen, P. Niemelä, M. Ilves, M. Weckström, O. Vuolteenaho, J. Bruton, H. Westerblad, and H. Ruskoaho. Pacing-induced calcineurin activation controls cardiac Ca^{2+} signaling and gene expression. *The Journal of Physiology*, 554:309–320, 2003. (Cited on page 24.)

[101] M. Thomson and J. Gunawardena. Unlimited multistability in multisite phosphorylation systems. *Nature*, 460(7252):274–277, 2009. (Cited on page 1.)

[102] T. M. Thomson, K. R. Benjamin, A. Bush, T. Love, D. Pincus, O. Resnekov, R. C. Yu, A. Gordon, A. Colman-Lerner, D. Endy, and R. Brent. Scaffold number in yeast signaling system sets tradeoff between system output and dynamic range. *Proceedings of the National Academy of Sciences*, 108(50):20265–20270, 2011. (Cited on page 18.)

[103] L. A. Tibbles and J. R. Woodgett. The stress-activated protein kinase pathways. *Cellular and Molecular Life Sciences*, 55:1230–1254, 1999. (Cited on page 13.)

[104] T. Tomida, K. Hirose, A. Takizawa, F. Shibasaki, and M. Iino. NFAT functions as a working memory of Ca^{+2} signals in decoding Ca^{+2} oscillation. *The European Molecular Biology Organization Journal*, 22(15): 3825–3832, 2003. (Cited on pages 1 und 25.)

[105] C. T. Trinh, A. Wlaschin, and F. Scrienc. Elementary mode analysis: A useful metabolic pathway analysis tool for characterizing cellular metabolism. *Applied Microbiology and Biotechnology*, 81:813–826, 2009. (Cited on page 11.)

[106] N. B. Trunnell, A. C. Poon, S. Y. Kim, and J. E. Ferrell Jr. Ultrasensitivity in the regulation of Cdc25C by Cdk1. *Molecular Cell*, 41(3):263–274, 2011. (Cited on pages 1, 22 und 192.)

[107] J. J. Tyson. Temporal organization of the eukariyotic cell cycle. Kolloquium at Max-Planck-Institut für Dynamik komplexer technischer Systeme, July 2009. (Cited on page 21.)

[108] J. J. Tyson. *Computational Cell Biology*. Virginia Tech, last checked April, 3rd, 2014. URL `http://mpf.biol.vt.edu/lab_website/`. (Cited on pages 20, 22 und 23.)

[109] J. J. Tyson and B. Novák. *Irreversible Transitions, Bistability and Checkpoint Controls in the Eukaryotic Cell Cycle: A Systems-level Understanding*. To be published. (Cited on page 11.)

[110] J. J. Tyson and B. Novák. Temporal organization of the cell cycle. *Current Biology*, 18:R759–R768, 2008. (Cited on pages 11 und 21.)

[111] J. J. Tyson, K. C. Chen, and B. Novák. *Cell Cycle Vignettes*. Springer Verlag, 2011. (Cited on page 21.)

[112] Ch. Überhuber. *Computer-Numerik*. Springer, Berlin, 1995. (Cited on page 5.)

[113] J. A. Ubersax, E. L. Woodbury, P. N. Quang, M. Paraz, J. D. Blethrow, K. Shah, K. M. Shokat, and D. O. Morgan. Targets of the cyclin-dependent kinase Cdk1. *Letters to Nature*, 425:859–864, 2003. (Cited on pages 18 und 192.)

[114] M. Uhr. *Structural Analysis of Inference Problems Arising in Systems Biology*. PhD thesis, ETH Zurich, 2012. (Cited on pages 44 und 45.)

[115] K. S. M. Varedi, A. C. Ventura, S. D. Merajver, and X. N. Lin. Multisite phosphorylation provides an effective and flexible mechanism for switch-like protein degradation. *Public Library of Science One*, 5(12): 1–18, 2010. (Cited on pages 2 und 22.)

[116] R. Venta, E. Valk, M. Kõivomägi, and M. Loog. Double-negative feedback between S-phase cyclin-CDK and CKI generates abruptness in the G1/S switch. *Frontiers in Physiology*, 3(459):1–15, 2012. (Cited on page 22.)

[117] R. Verma, R. S. Annan, M. J. Huddleston, S. A. Carr, G. Reynard, and R. J. Deshaies. Phosphorylation of Sic1p by G1 Cdk required for its degradation and entry into S phase. *Science*, 278(455):455–460, 1997. (Cited on page 22.)

[118] S. Waldherr and F. Allgöwer. Robust stability and instability of biochemical networks with parametric uncertainty. *Automatica*, 47:1139–1146, 2011. (Cited on page 135.)

[119] L. Wang and E. D. Sontag. A remark on the number of steady states in a multiple futile cycle. *Journal of Mathematical Biology*, 57:29–52, 2008. (Cited on pages 1, 29, 33, 34 und 67.)

[120] B. Watterson. *The complete Calvin and Hobbes*. Andrews McMeel Publishing, 2005. (Cited on page 137.)

[121] F. Welch and P. Epworth. Shake it out, September, 14th, 2011. (Cited on page 123.)

[122] S.-H. Yang, A. D. Sharrocks, and A. J. Whitmarsh. Transcriptional regulation by the MAP kinase signaling cascades. *Gene*, 320:3–21, 2003. (Cited on page 19.)

[123] B. Zhou and Z.-Y. Zhang. The activity of the extracellular signal-regulated kinase 2 is regulated by differential phosphorylation in the activation loop. *Journal of Biological Chemistry*, 277(16):13889–13899, 2002. (Cited on pages 18 und 192.)

[124] H.-Z. Zhou. Rate theories for biologists. *Quarterly Reviews for Biophysics*, 43(2):219–293, 2010. (Cited on pages 17, 18 und 63.)

COLOPHON

Computer algebra systems Mathematica 8, DIVA 3.9, as well as MATLAB 18 (R2007b, 7.5.0) were used. Various toolboxes were used together with MATLAB. As one of the non-standard but free toolboxes MaTCont version 3p2 as well as 4p2 was used.

This thesis was typeset with LaTeX 2ε using the beautiful work of André Miede, based on Hermann Zapf's *Palatino* and *Euler* type faces (Type 1 PostScript fonts *URW Palladio L* and *FPL* were used).

The typographic style was inspired by Robert Bringhurst's genius as presented in *The Elements of Typographic Style*. It is available for LaTeX via CTAN as "`classicthesis`".

Final Version as of July 10, 2014 (`classicthesis` version 4.1).

CURRICULUM VITÆ

PERSONAL INFORMATION

Katharina Holstein

Ackerstraße 17c
39112 Magdeburg

Born in Burg, Germany, January, 30th, 1984

k_holstein@posteo.de

+49 (0) 172 2165090

EDUCATION

2008–present	Ph. d. with International Max Planck Research School, Magdeburg; as presented by this thesis Advisor: Dr.-Ing. Carsten Conradi, Prof. Dietrich Flockerzi & Assoc. Prof. Rolf Findeisen, as handed in with this thesis
2003–2008	Diploma in systems theory and technical cybernetics, Otto-von-Guericke University, Magdeburg, Institute: Automation Engineering, Focus: Automation, Systems Biology
2003	A level at Bismarck Gymnasium, Genthin

July 10, 2014

DECLARATION

I hereby declare that this thesis and the work reported herein has been composed by myself, besides where explicitly stated in the text. Information derived from the published and unpublished work of others is acknowledged in the text, and a list of references is given in the bibliography. Work herein has not been submitted for any other degree or professional qualification besides in the stated publications, some of them still ongoing. No commercial consultant concerning graduation has been used, neither did a third party receive any non monetary perquisites directly or indirectly for activities which are connected with the contents of the presented thesis.

In particular, I have not consciously:

- fabricated data or rejected undesired results,
- misused statistical methods with the aim of drawing other conclusions than those warranted by the available data,
- plagiarized data or publications,
- presented the results of other researchers in a distorted way.

I do know that violations of copyright may lead to injunction and damage claims of the author and also to prosecution by the law enforcement authorities. I hereby agree that the thesis may need to be reviewed with an electronic data processing for plagiarism.

This work has not yet been submitted as a doctoral thesis in the same or a similar form in Germany or in any other country. It has not yet been published as a whole.

Magdeburg, July 10, 2014

Katharina Holstein